COPY 2

Report No. FAA-RD-74-203
NA-74-172

FAA WJH Technical Center
00090811

NAFEC
LIBRARY
MAR 11 1975
RECEIVED

SIMULATION MODEL FOR NEW YORK AIR TRAFFIC CONTROL COMMUNICATIONS

J. S. Hunter
D.-A. Hsu

FEBRUARY 1975

INTERIM REPORT

Document is available to the public through the
National Technical Information Service,
Springfield, Virginia 22151

Prepared for

U.S. DEPARTMENT OF TRANSPORTATION
FEDERAL AVIATION ADMINISTRATION
Systems Research & Development Service
Washington, D. C. 20590

NOTICE

This document is disseminated under the sponsorship of the Department of Transportation in the interest of information exchange. The United States Government assumes no liability for its contents or use thereof.

Princeton University., School of Engineering
Simulation Model for New York Air Traffic Control Communications, by J.S. Hunter and D.-A. Hsu. Interim report. Princeton, N.J., February 1975.

240 p. (RD-74-203)
(NA-74-172)
Contract No. FA72NA-741

1. New York ATC Metroplex 2. Communications. 3. Air Traffic Control-- Communications. 4. Simulation. I. Hunter, J.S.

PREFACE

This interim report is part of a continuing study on "Modeling Air Traffic Performance Measures" being conducted at Princeton University as a joint activity of the Transportation Program, Department of Civil Engineering and the Department of Statistics. This publication, Volume III of the study, describes the construction, validation and exercise of a simulation model descriptive of air traffic communications.

The simulation model for ATC communications is based upon voice communications data gathered over the NY area in July 1969, as reported upon in Volumes I and II of this investigation. The model can be used to simulate individual sectors or a sector function. Following validation, the simulation model was exercised in an experimental program to determine the consequences of altering incoming aircraft density for each sector function. Although this experimental program was modest, the results clearly demonstrated the value of the model. Of particular interest was the estimation of the traffic density that produced an explosive growth in the number of aircraft in the sector, and the determination of the length of communications queues. The communications queue responses are not available in the historical record. The authors expect the simulation model to prove of great value in exploring the consequences of changes in sector operations.

The simulation model is straight-forward. Many hours were spent in adapting this model to the realities of the historical data, and many additional hours to programming and testing. Much work was also spent on re-characterizing the distributions of several of the input variables, and in efforts to get the output responses succinctly analyzed and plotted.

It is a pleasure to acknowledge the work of several individuals who have brought this phase of the study to its conclusion. Recognition is first due Dr. Der-Ann Hsu for his contributions. Of very special note are two statistical procedures developed by Dr. Hsu as part of this investigation. The first is a new statistic for comparing the structure of an historical response time series with that of a simulated response time series. The second is a novel method for determining the probability of the onset of response instability within a sector. Both methodologies have proved of great value. Mr. Neil Polhemus, a graduate student in the Transportation Program at Princeton, also deserves special recognition for his work on the GPSS program and simulation model. Further, it is a pleasure to report that Mr. Polhemus won first prize in the national student paper competition of the Transportation Research Forum of the Operations Research Society. His paper "Modeling Aircraft Flow in Air Traffic Control Systems", was stimulated by this FAA study.

Dr. Dennis Blumenfeld, Research Associate, directed the efforts of Miss Linda J. Lamort '74, whose senior thesis "Simulation Modeling and the Theory of Queues" forms part of Chapter V, and of Mr. Graham A. Harrison '74, whose senior thesis "Fitting Truncated Asymmetric Distributions to Discrete Frequency Data" is also reported on in Chapter V. Other individuals who

have contributed to this present work are

Leroy Adler
Peter Bloomfield
Robert Greenberg
William M. Hunter
Roderick Montgomery
Charles B. Reynolds
Marc N. Terziev
John C. Turner
J. Douglas Van Ness

Special acknowledgment is also due our secretary, Mrs. Jeanne L. Carlucci, and her aide, Mrs. Pat Halliday, for their patience with the authors. Finally, Mr. Allen C. Busch of the FAA has continued to give the Princeton group most valuable advice throughout the entire year.

J. Stuart Hunter
Principal Investigator

TABLE OF CONTENTS

		Page
1.	ANALYSES OF COMMUNICATIONS DATA	
1.1	Introduction	1-1
1.2	Aircraft Arrivals	1-3
1.3	Number of Communications Transactions per Aircraft	1-6
1.4	Intercommunication Gap Lengths	1-12
1.5	Communications Transaction Lengths	1-16
1.6	Channel Utilization	1-21
1.7	Aircraft Loading	1-21
1.8	Communications Queuing	1-21
1.9	Network Analyses	1-25
1.10	Preview of the Following Chapters	1-25
2.	CONSTRUCTION OF THE SIMULATION MODEL	
2.1	Introduction	2-1
2.2	Structure of the Simulation Model	2-2
2.3	GPSS Computer Programs for the ATC Communications	2-5
2.4	Simulations of the Intercommunication Gap Lengths	2-12
2.5	Summary and Remarks	2-18
3.	VALIDATION OF THE SIMULATION MODEL	
3.1	Introduction	3-1
3.2	A Testing Scheme for Autoregressive Parameters and Error Variance	3-3
3.3	Comparison of the Means of Two Autoregressive Time Series	3-11

TABLE OF CONTENTS (Cont'd)

		Page
3.4	Validation of Sector Simulations	3-13
3.5	The Validation of Sector Function Simulations	3-20
3.6	Summary and Remarks	3-21
4.	APPLICATIONS OF THE SIMULATION MODEL	
4.1	Introduction	4-1
4.2	An Experiment in Changing Traffic Density	4-2
4.3	Stochastic Stationarity and the Operational Stability of a Communication Sector	4-3
4.4	The Highest Posterior Density (HPD) Contours of the Autoregressive Parameters	4-13
4.5	A Test Statistic for Stationarity	4-14
4.6	Studies of the Simulated Queuing	4-19
4.7	Summary and Remarks	4-25
5.	FURTHER RELATED STUDIES	
5.1	Introduction	5-1
5.2	Analysis of the Response Coupling	5-1
5.3	Studies of Air Traffic Control Network Capacities	5-16
5.4	The Sequential Structure of Intercommunication Gap Lengths	5-29
5.5	A Basic Queuing Theory Model	5-44
5.6	Further Distributions for Number of TR per CT	5-53

LIST OF ILLUSTRATIONS

Figure	Title	Page
1.1	Air Traffic Communications Performance	1-4
1.2	Decomposition of a Communications Transaction	1-5
1.3	Probability Density Functions for a Poisson Process	1-7
1.4	Distributions of Numbers of Gaps per Aircraft	1-8
1.5	Mean Gap Length vs. Number of Gaps for Aircraft in a Sector	1-13
1.6	Co-plot of Regression Coefficients a_o and a_1 for 101 Sectors	1-15
1.7	Observed Distribution of Gap Lengths in a Sector	1-17
1.8	Observed Distribution of Number of TR's per CT for Sector Function DP	1-18
1.9	Gamma Distribution Fitted to Observed Frequencies of TR Lengths for Sector Function DP	1-20
1.10	Determination of Channel Utilization from Composite Communications Record	1-22
1.11	Historical Time Series of Channel Utilization in Sector HI 475	1-23
1.12	Historical Time Series of Aircraft Loading in Sector HI 475	1-24
1.13	Schematic Diagram Showing Numbers of Transitions between High Altitude Sectors	1-27
2.1	Flow-Chart Block Diagram for the Communication Simulation Model	2-3
2.2	Block Diagram for the GPSS V Simulation Program	2-7
2.3	Histogram of Aircraft Interarrival Times from GPSS V Simulation	2-27

LIST OF ILLUSTRATIONS (cont'd)

Figure	Title	Page
2.4	Histogram of the Number of Transactions per Aircraft from GPSS V Simulation	2-28
2.5	Histogram of the Number of Transmissions per Transaction from GPSS V Simulation	2-29
2.6	Histogram of Transmission Lengths from GPSS V Simulation	2-30
2.7	Histogram of Transaction Lengths from GPSS V Simulation	2-31
2.8	Histogram of Intercommunication Gap Lengths from GPSS V Simulation	2-32
2.9	Histogram of Aircraft Times in Sector from GPSS V Simulation	2-33
2.10	Histogram of Aircraft Interdeparture Times from GPSS V Simulation	2-34
2.11	Histogram of Channel Queuing Times from GPSS V Simulation	2-35
2.12	Histogram of the Number of Aircraft in the Sector per Second from GPSS V Simulation	2-36
2.13	Histogram of the Number of Aircraft in the Queue per Second from GPSS V Simulation	2-37
2.14	Histogram of the Durations of Non-Zero Queuing from GPSS V Simulation	2-38
2.15	Plot of Arrivals and Departures from GPSS V Simulation	2-39
2.16	Plot of the Number of Aircraft in the Sector from GPSS V Simulation	2-40
2.17	Plot of Sixty-Second Average Aircraft Loadings from GPSS V Simulation	2-41

LIST OF ILLUSTRATION (cont'd)

Figure	Title	Page
2.18	Sample Autocorrelation Function for the Aircraft Loading Series from GPSS V Simulation	2-42
2.19	Sample Partial Autocorrelation Function for the Aircraft Loading Series from GPSS V Simulation	2-43
2.20	Plot of the Number of Aircraft in the Queue from GPSS V Simulation	2-44
2.21	Plot of Sixty-Second Average Queue Lengths from GPSS V Simulation	2-45
2.22	Sample Autocorrelation Function for the Queue Length Series from GPSS V Simulation	2-46
2.23	Sample Partial Autocorrelation Function for the Queue Length Series from GPSS V Simulation	2-47
2.24	Plot of Sixty-Second Average Queue Transforms from GPSS V Simulation	2-48
2.25	Sample Autocorrelation Function for the Queue Transform Series from GPSS V Simulation	2-49
2.26	Sample Partial Autocorrelation Function for the Queue Transform Series from GPSS V Simulation	2-50
2.27	Plot of the Channel Status per Second from GPSS V Simulation	2-51
2.28	Plot of Sixty-Second Average Channel Utilizations from GPSS V Simulation	2-52
2.29	Sample Autocorrelation Function for the Channel Utilization Series from GPSS V Simulation	2-53
2.30	Sample Partial Autocorrelation Function for the Channel Utilization Series from GPSS V Simulation	2-54
2.31	Two Different Simulation Schemes for Intercommunication Gap Lengths	2-14

LIST OF ILLUSTRATIONS (cont'd)

Figure	Title	Page
2.32	Simulated Distributions of Gap Lengths and the Number of Gaps per Aircraft	2-15
2.33	Comparison of Historical versus Simulated Mean Gap Length per Aircraft	2-17
2.34	Comparison of Historical versus Simulated Gap Lengths	2-19
3.1	Two Time Series Recorded from the Same Real System	3-2
3.2	HPD Contours of $(\underset{\sim}{\psi},\gamma)$ for p=1 under Four Cases	3-10
3.3	HPD Contours of $(\underset{\sim}{\psi},\gamma)$ for p=2 under Four Cases	3-10
3.4	Historical Time Series of Aircraft Loading in Sector 453 LT	3-15
3.5	Simulated Time Series of Aircraft Loading in Sector 453 LT at 100% of Historical Traffic Density	3-16
3.6	Autocorrelation Function of Historical Aircraft Loading Series (Sector 453)	3-17
3.7	Autocorrelation Function of Simulated Aircraft Loading Series (Sector 453)	3-17
3.8	Historical Time Series of Channel Utilization in Sector 453 LT	3-22
3.9	Simulated Time Series of Channel Utilization in Sector 453 LT at 100% of Historical Traffic Density	3-23
3.10	Historical Time Series of Aircraft Loading in Sector 475 HI	3-24
3.11	Simulated Time Series of Aircraft Loading in Sector 475 HI at 100% of Historical Traffic Density	3-25
3.12	Historical Time Series of Channel Utilization in Sector 475 HI	3-26

LIST OF ILLUSTRATIONS (cont'd)

Figure	Title	Page
3.13	Simulated Time Series of Channel Utilization in Sector 475 HI at 100% of Historical Traffic Density	3-27
3.14	Historical Time Series of Aircraft Loading in Sector 504 GN	3-28
3.15	Simulated Time Series of Aircraft Loading in Sector 504 GN at 100% of Historical Traffic Density	3-29
3.16	Historical Time Series of Channel Utilization in Sector 504 GN	3-30
3.17	Simulated Time Series of Channel Utilization in Sector 504 GN at 100% of Historical Traffic Density	3-31
3.18	Historical Time Series of Aircraft Loading in Sector 510 LC	3-32
3.19	Simulated Time Series of Aircraft Loading in Sector 510 LC at 100% of Historical Traffic Density	3-33
3.20	Historical Time Series of Channel Utilization in Sector 510 LC	3-34
3.21	Simulated Time Series of Channel Utilization in Sector 510 LC at 100% of Historical Traffic Density	3-35
3.22	Historical Time Series of Aircraft Loading in Sector 524 LG	3-36
3.23	Simulated Time Series of Aircraft Loading in Sector 524 LG at 100% of Historical Traffic Density	3-37
3.24	Historical Time Series of Channel Utilization in Sector 524 LG	3-38
3.25	Simulated Time Series of Channel Utilization in Sector 524 LG at 100% of Historical Traffic Density	3-39
3.26	Historical Time Series of Aircraft Loading in Sector 534 DP	3-40

LIST OF ILLUSTRATIONS (cont'd)

Figure	Title	Page
3.27	Simulated Time Series of Aircraft Loading in Sector 534 DP at 100% of Historical Traffic Density	3-41
3.28	Historical Time Series of Channel Utilization in Sector 534 DP	3-42
3.29	Simulated Time Series of Channel Utilization in Sector 534 DP at 100% of Historical Traffic Density	3-43
3.30	Historical Time Series of Aircraft Loading in Sector 534 AD	3-44
3.31	Simulated Time Series of Aircraft Loading in Sector 534 AD at 100% of Historical Traffic Density	3-45
3.32	Historical Time Series of Channel Utilization in Sector 543 AD	3-46
3.33	Simulated Time Series of Channel Utilization in Sector 543 AD at 100% of Historical Traffic Density	3-47
3.34	Historical Time Series of Aircraft Loading in Sector 553 AR	3-48
3.35	Simulated Time Series of Aircraft Loading in Sector 553 AR at 100% of Historical Traffic Density	3-49
3.36	Historical Time Series of Channel Utilization in Sector 553 AR	3-50
3.37	Simulated Time Series of Channel Utilization in Sector 553 AR at 100% of Historical Traffic Density	3-51
4.1	Simulated Time Series of Aircraft Loading in Sector 475 HI at 100% of Historical Traffic Density	4-4
4.2	Simulated Time Series of Channel Utilization in Sector 475 HI at 100% of Historical Traffic Density	4-5
4.3	Simulated Time Series of Queue Length in Sector 475 HI at 100% of Historical Traffic Density	4-6
4.4	Simulated Time Series of Aircraft Loading in Sector 475 HI at 125% of Historical Traffic Density	4-7

LIST OF ILLUSTRATIONS (cont'd)

Figure	Title	Page
4.5	Simulated Time Series of Channel Utilization in Sector 475 HI at 125% of Historical Traffic Density	4-8
4.6	Simulated Time Series of Queue Length in Sector 475 HI at 125% of Historical Traffic Density	4-9
4.7	Simulated Time Series of Aircraft Loading in Sector 475 HI at 150% of Historical Traffic Density	4-10
4.8	Simulated Time Series of Channel Utilization in Sector 475 HI at 150% of Historical Traffic Density	4-11
4.9	Simulated Time Series of Queue Length in Sector 475 HI at 150% of Historical Traffic Density	4-12
4.10	Confidence Regions of (ϕ_1, ϕ_2) Based on Historical Aircraft Loading Time Series for Sector 475	4-15
4.11	Confidence Regions of (ϕ_1, ϕ_2) Based on Simulated Aircraft Loading Time Series for Sector 475 at 100% of Historical Traffic Density	4-16
4.12	Confidence Regions of (ϕ_1, ϕ_2) Based on Simulated Aircraft Loading Time Series at 125% of Historical Traffic Density (Sector 475)	4-17
4.13	Confidence Regions of (ϕ_1, ϕ_2) Based on Simulated Aircraft Loading Time Series at 150% of Historical Traffic Density (Sector 475)	4-18
4.14	Average Queuing Time per Aircraft versus Traffic Density	4-21
4.15	Average Queue Length versus Traffic Density	4-21
4.16	Average Aircraft Loading versus Traffic Density	4-22
4.17	Average Channel Utilization versus Traffic Density	4-22
4.18	$Pr(\xi>1\|\gamma)$ versus Traffic Density	4-23
5.1	Simulated Time Series of Queue Transforms in Sector 475 HI at 100% of Historical Traffic Density	5-4

LIST OF ILLUSTRATIONS (cont'd)

Figure	Title	Page
5.2	Simulated Time Series of Queue Transforms in Sector 475 HI at 125% of Historical Traffic Density	5-5
5.3	Simulated Time Series of Queue Transforms in Sector 475 HI at 150% of Historical Traffic Density	5-6
5.4	Simulated Time Series of Queue Transforms in Sector 453 LT at 100% of Historical Traffic Density	5-7
5.5	Simulated Time Series of Queue Length in Sector 453 LT at 100% of Historical Traffic Density	5-8
5.6	Simulated Time Series of Queue Transforms in Sector 524 LG at 100% of Historical Traffic Density	5-9
5.7	Simulated Time Series of Queue Length in Sector 524 LG at 100% of Historical Traffic Density	5-10
5.8	Simulated Time Series of Queue Transforms in Sector 553 AR at 100% of Historical Traffic Density	5-11
5.9	Simulated Time Series of Queue Length in Sector 553 AR at 100% of Historical Traffic Density	5-12
5.10	A Heuristic Model for Communication Responses Using a Triple-Tank Water System	5-17
5.11	ATC Network at LaGuardia Airport	5-18
5.12	Modified ATC Network	5-23
5.13	Schematic Diagram of Customers' Arrivals and Service Times	5-47
5.14	Flow Chart for Simulation of a Simple Queue	5-48
5.15	Average Waiting Time as a Function of Arrival Rate	5-49
5.16	Standard Deviation of Waiting Time as a Function of Arrival Rate	5-50
5.17	Average Queue Length as a Function of Arrival Rate	5-51
5.18	Probability of No Wait as a Function of Arrival Rate	5-52

LIST OF ILLUSTRATIONS (cont'd)

Figure	Title	Page
5.19	Distribution of Interval between Beginning of Service	5-54
5.20	Fitting the Gamma Distribution to the Observed Number of Transmissions per Transaction for Sector Function HI	5-62
5.21	Fitting the Lognormal Distribution to the Observed Number of Transmissions per Transaction for Sector Function HI	5-64

LIST OF TABLES

Table	Title	Page
1.1	Sector Function Identification for New York Metrolplex	1-2
1.2	Fit of Negative Binomial Distribution to Number of Intercommunication Gaps per Aircraft	1-10
1.3	Fit of Shifted Negative Binomial Distribution to Number of Intercommunication Gaps per Aircraft for Enroute Sector Functions	1-11
1.4	Average Values of Regression Estimates a_o, a_1 for Gap Lengths in Each Sector Function	1-14
1.5	Transition Matrix from New York Sample Data	1-26
2.1	Listing of GPSS Input Statements	2-22
2.2	Summary of Input Parameters and System Responses	2-10
2.3	Comparisons of Historical versus Simulated Gap Length Statistics	2-20
3.1	Comparison of Historical versus Simulated Aircraft Loading Series	3-18
3.2	Comparison of Historical versus Simulated Channel Utilization Series	3-19
3.3	Comparisons of Historical versus Simulated Data (General HI Simulation)	3-21
4.1	Results of Simulations for Sector 475 at Four Different Traffic Densities	4-20
4.2	Average Queuing Time per Aircraft	4-24
5.1	Estimates of the Transfer Function Parameters Comprising the Impulse Response Function of (C_t, n_t)	5-13
5.2	Estimates of the Transfer Function Parameters Comprising the Impulse Response Function of (q_t, n_t)	5-14
5.3	Estimates of the Transfer Function Parameters Comprising the Impulse Response Function of (q_t, C_t)	5-15

LIST OF TABLES (Cont'd)

Table	Title	Page
5.4	ATC Sector Parameters for Network Analysis	5-20
5.5	Assignment of Maximum Feasible Flow to Free-Flow Network	5-25
5.6	Assignment of Maximum Feasible Flow to Constrained-Flow Network	5-27
5.7	Results of the Rank Test	5-30
5.8	Intercommunication Gap Length Statistics for Sector Function LT	5-32
5.9	Intercommunication Gap Length Statistics for Sector Function LE	5-33
5.10	Intercommunication Gap Length Statistics for Sector Function HI	5-34
5.11	Intercommunication Gap Length Statistics for Sector Function CD	5-35
5.12	Intercommunication Gap Length Statistics for Sector Function GN	5-36
5.13	Intercommunication Gap Length Statistics for Sector Function LC	5-37
5.14	Intercommunication Gap Length Statistics for Sector Function LG	5-38
5.15	Intercommunication Gap Length Statistics for Sector Function AP	5-39
5.16	Intercommunication Gap Length Statistics for Sector Function DP	5-40
5.17	Intercommunication Gap Length Statistics for Sector Function AD	5-41
5.18	Intercommunication Gap Length Statistics for Sector Function AR	5-42
5.19	Intercommunication Gap Length Statistics for Sector Function RA	5-43

LIST OF TABLES (cont'd)

Table	Title	Page
5.20	Results of Fitting the Truncated Negative Binomial Distribution to the Observed Number of TR per CT for the 12 Sector Functions	5-56
5.21	Results of Fitting the Truncated Sichel Distribution to the Observed No. of TR per CT for the 12 Sector Functions	5-58
5.22	Results of Fitting the Gamma Distribution to the Observed No. of TR per CT for the HI and RA Sector Functions	5-61
5.23	Results of Fitting the Log-Normal Distribution to the Observed No. of TR per CT for the HI and GN Sector Functions	5-63

CHAPTER 1

ANALYSES OF COMMUNICATIONS DATA

1.1 Introduction

The development of the simulation model presented in this report is based on results of the analyses of data described in detail in the reports

Modeling Air Traffic Performance Measures

Volume I: Message Element Analyses and Dictionaries

Volume II: Initial Data Analyses and Simulations

Report No. DOT FA72NA-741.

The data were obtained from tape recordings of voice communications between controller and pilot and from corresponding aircraft information collected by the National Aviation Facilities Experimental Center (NAFEC) of the Federal Aviation Administration (FAA). The conversations contained in the data cover a busy two-hour period (20/00/00 to 22/00/00 GMT) on April 30, 1969, for all 101 sectors comprising the greater New York ATC metroplex.

The first volume is concerned specifically with statistics of the different messages contained in communications between pilot and controller. Volume II describes the data file and presents statistical analyses of the components of the whole voice communications system. The initial stages of the construction of a simulation model are also given in Volume II.

This report (Volume III) presents the continued development of the simulation model into its present form and indicates its applications to the ATC communications system. It should be emphasized that although the construction of the simulation model uses data collected in the New York ARTCC, the framework of the model has been kept general in order to be applicable to other airport regions using the ATC communications system.

Although details are given in the earlier report (Volume II), it is appropriate to describe briefly the characteristics of the ATC communications system. The air space within the airport region is divided into a number of "sectors", each with its own controller. The New York ARTCC contains 101 separate sectors. These sectors are divided into twelve different sector functions as shown in Table 1.1. The sector functions are partitioned into three distinct groups: enroute sectors, tower cab sectors and IFR room sectors. The numbers of sectors in each sector function are given on the right of Table 1.1.

Within a sector, a number of communications are made between the controller and each aircraft within that sector's jurisdiction. A completed

FAA WJH Technical Center
00090811

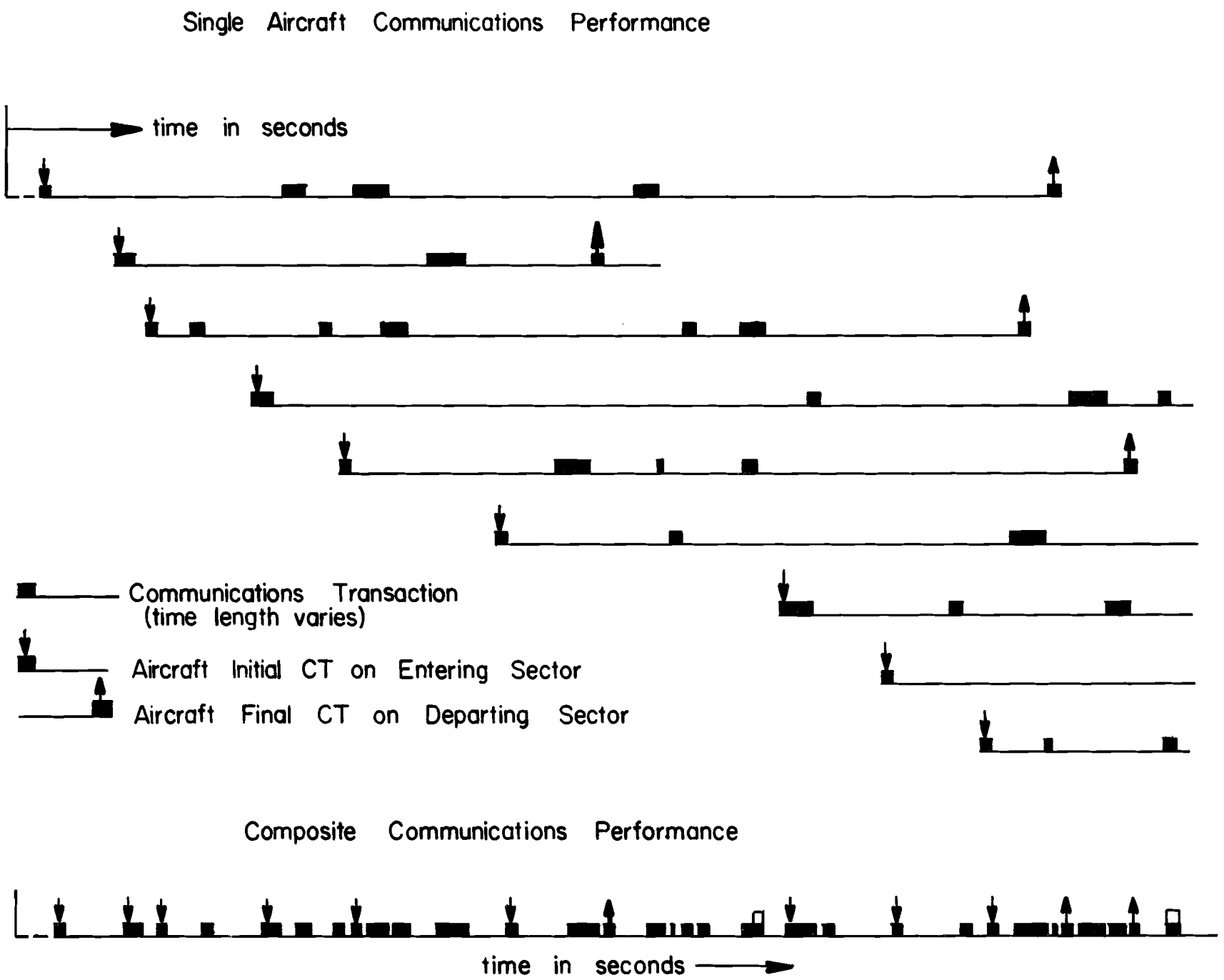

Figure 1.1 Air Traffic Communications Performance

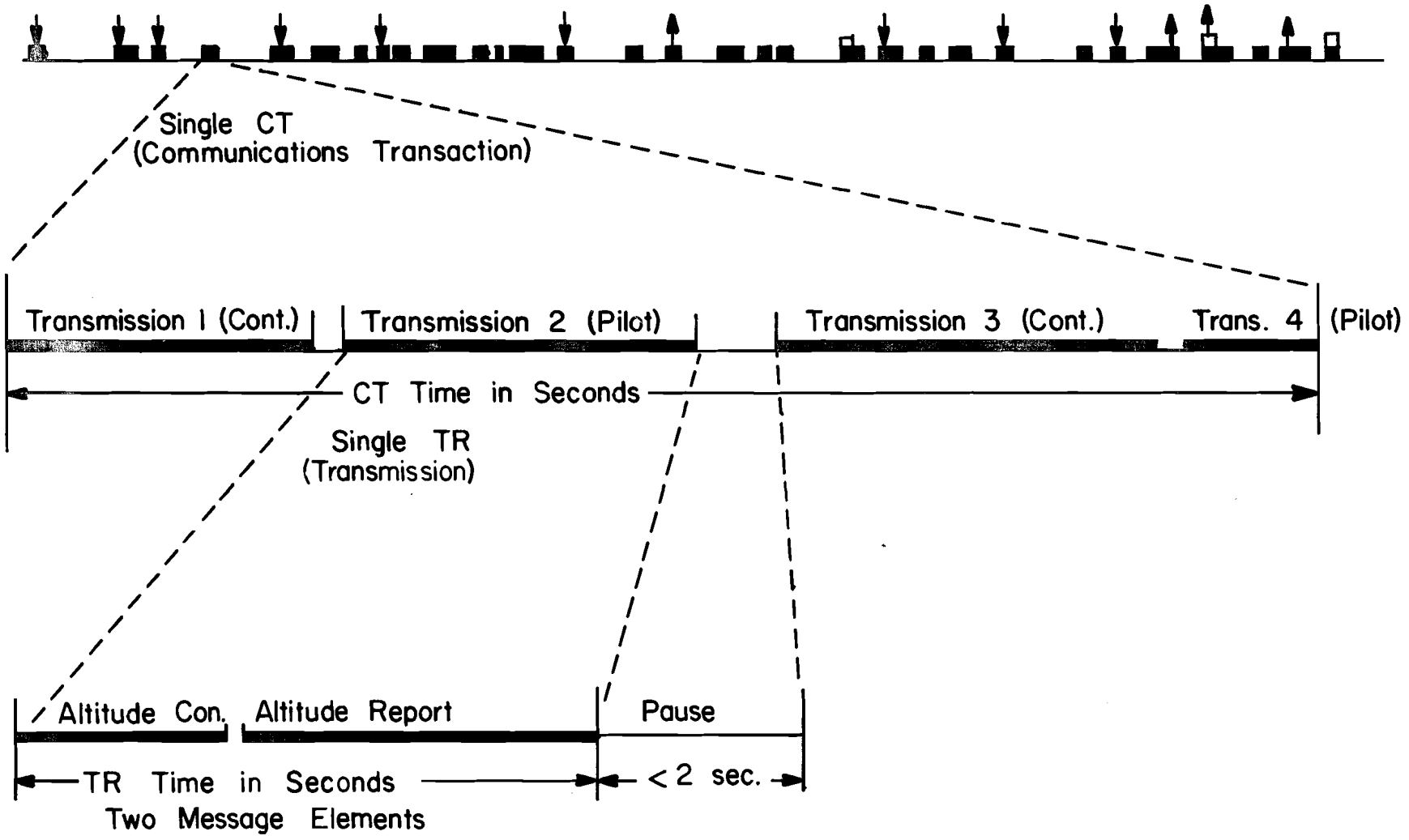

Figure 1.2 Decomposition of a Communications Transaction

Poisson process the times between successive arrivals are independently distributed as an exponential distribution so that the probability of a time interval between t_1 and t_2 is given by $\int_{t_1}^{t_2} \rho e^{-\rho t} dt$. An illustration of the Poisson distribution and the associated exponential distribution for a Poisson process with arrival rate $\rho = 0.5$ aircraft per minute is shown in Figure 1.3.

The Poisson process has been incorporated into the simulation model for ATC communications performance. There are a few sectors, however, for which the Poisson process is not a sufficiently accurate description of the arrival pattern, particularly for ground control (GN) sectors. For such sectors, arrivals are more likely to be scheduled than independently random. The problem of finding an appropriate mathematical model for such sectors and sector functions continues under study. Actual arrival rate data can, of course, be used in any simulation if required.

In analyzing arrival data it is the time of the first communications transaction (CT) with the controller that is recorded, and not the time the aircraft actually arrives in a sector. For most sectors, particularly enroute sectors, these two times are likely to be approximately coincidental and in the simulation model are taken to be the same. But for sectors such as ground control sectors the arrival of an aircraft may well be much earlier than the time of its first CT, especially if the controller is very busy. Some preliminary studies have been made to discover the relationship between the distribution of the interarrival times of aircraft and the "inter-enter" times, i.e. the intervals between the starting times of the first CT of aircraft sequentially entering a sector. This topic requires further analysis and is discussed at the end of this report.

1.3 Number of Communications Transactions per Aircraft

Each aircraft in a sector has a certain number of communications transactions (CT's) with the controller, and this number will vary from aircraft to aircraft. The CT's are displayed schematically over time in Figure 1.1. The distribution of the number of CT's per aircraft will, in general, vary from sector to sector.

In analyzing the number of CT's per aircraft, it is more convenient to consider the gaps between CT's observed for the same aircraft. The number of such intercommunication gaps per aircraft is simply one less than the number of CT's. The relative frequencies of the different number of intercommunication gaps per aircraft have been calculated for each sector in the New York ATC data and are grouped for the twelve sector functions in Figure 1.4. For most of the sectors, the distribution of number of intercommunication gaps per aircraft, r, was found to be adequately represented

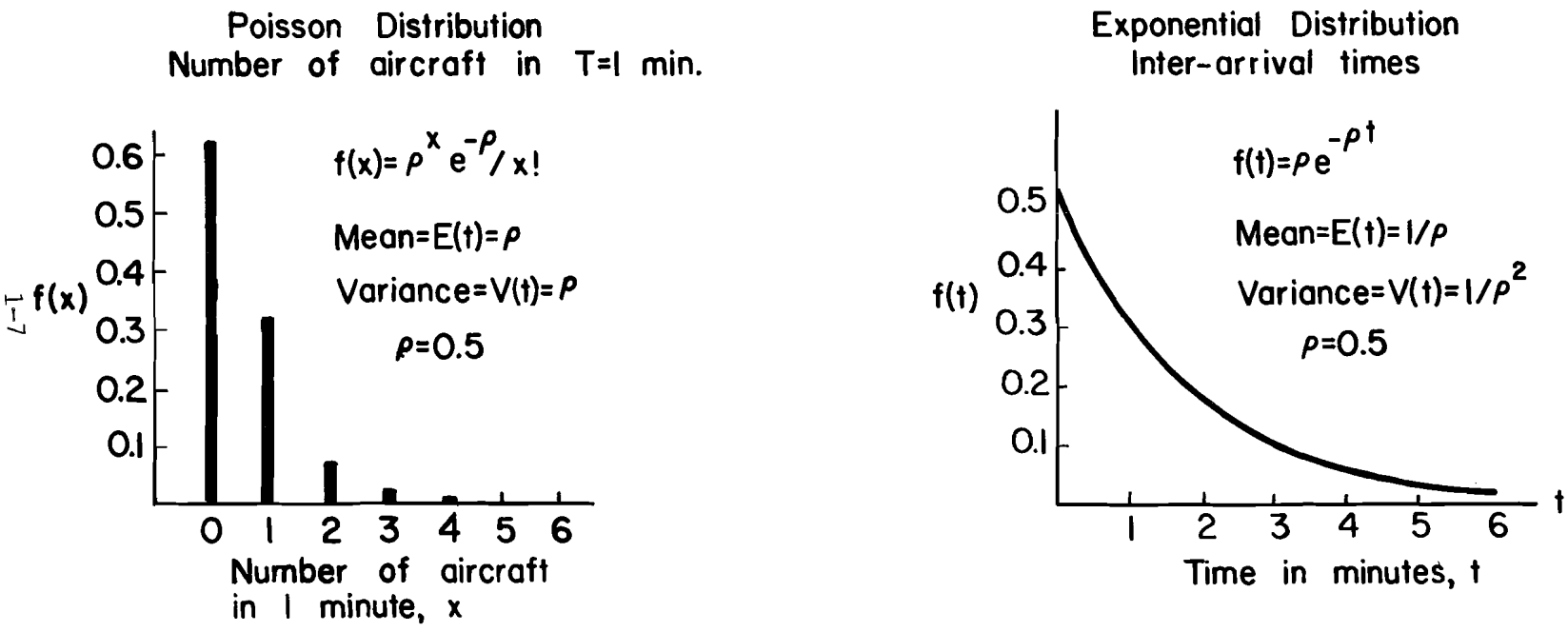

Figure 1.3 Probability Density Functions for a Poisson Process

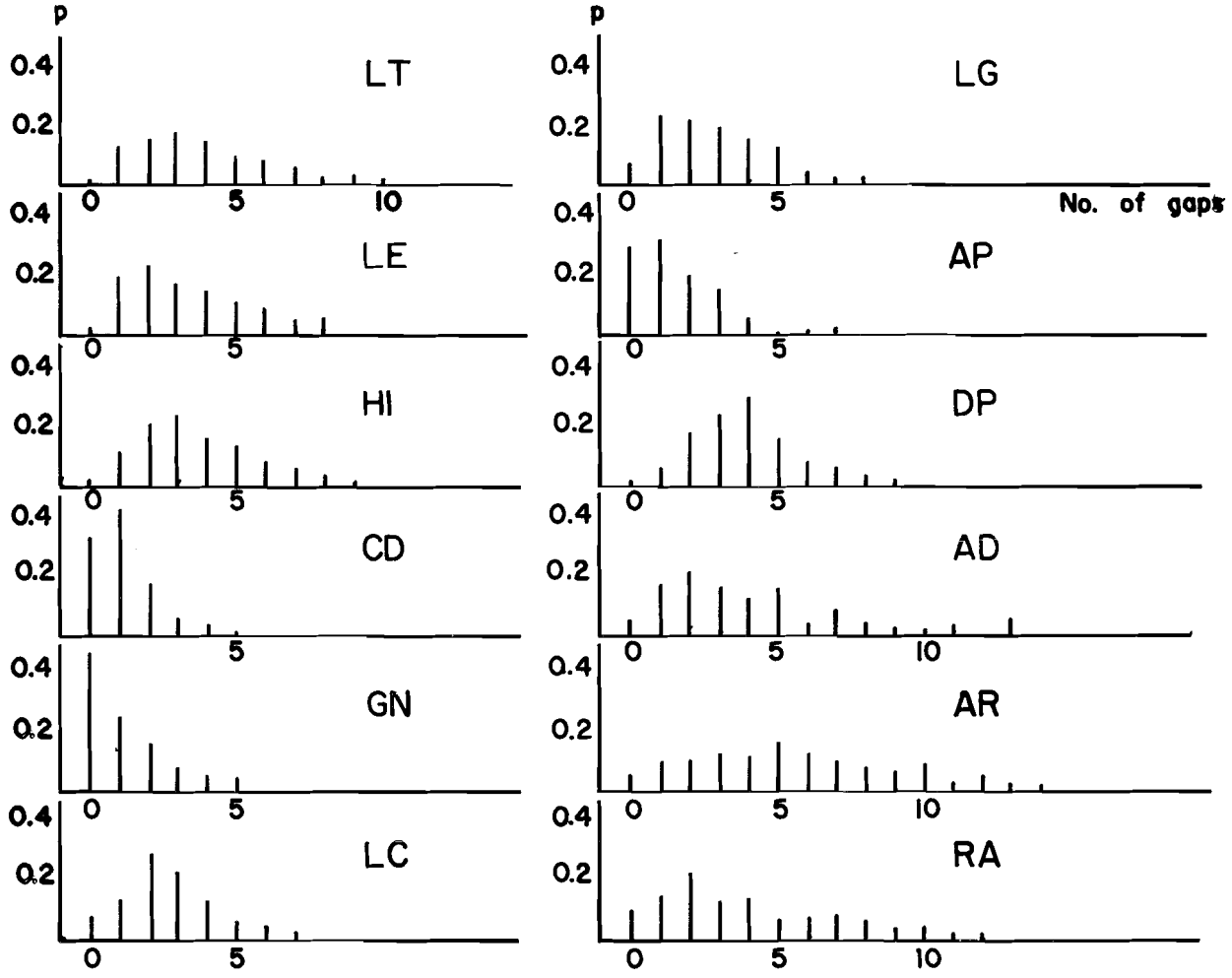

Figure i.4 Distributions of Numbers of Gaps per Aircraft

by the negative binomial distribution, given by

$$P(r) = \binom{k+r-1}{k-1} p^k (1 - p)^r \qquad r = 0, 1, 2, \ldots \ (0 < p < 1) \qquad (1.1)$$

where p and k are parameters and P(r) is the probability of r gaps per aircraft. This probability distribution was also found to fit the data grouped into sector functions (Figure 1.4) for eight of the twelve sector functions. The estimates $\hat{p}$ and $\hat{k}$ of the parameters p and k and the χ^2 goodness-of-fit test for the twelve sector functions are given in Table 1.2.

Since the number of gaps is one less than the number of CT's per aircraft, the resulting theoretical probability distribution for the number of CT's per aircraft is a shifted negative binomial distribution, valid over the range 1, 2, ... and with a mean equal to one more than the distribution of number of gaps per aircraft. The shifted negative binomial distribution is used to generate the number of CT's per aircraft in the simulation model.

The χ^2 values in Table 1.2 indicate a significant difference between the observed distribution of number of gaps per aircraft and the negative binomial distribution in the LT, LE, LC and AR sector functions. For the LT and LE sector functions, it can be seen from Figure 1.4 that the relative frequency of zero gaps per aircraft is very small. In these two sector functions and in the other enroute sector function (HI), there are generally at least two CT's per aircraft (one for the entry of an aircraft to the sector and one for the exit), so that the number of gaps per aircraft is generally at least one. By ignoring the very small probability of zero gaps per aircraft and fitting a shifted negative binomial distribution to the number of gaps per aircraft, considering 1 as 0 and 2 as 1 and so on, a much closer agreement was obtained for the enroute sector functions LT, LE and HI, as shown in Table 1.3. The χ^2 values in Table 1.3 for the LT and LE sector functions are then not significant and in the case of the HI sector function which provided a good fit before "shifting" the χ^2 value is also reduced. It should be noted that if the number of gaps per aircraft is fitted by a shifted negative binomial distribution, the corresponding distribution for the number of CT's per aircraft is a doubly shifted negative binomial distribution valid over the range 2, 3,...

For the LC sector function, the poor fit of the negative binomial distribution appears to be due to the very long tail of the observed distribution with occurences of up to 32 gaps per aircraft. Analyses of the AR sector function show a non-homogeneity between the separate sectors which would explain the poor fit of a single theoretical distribution. In particular, the analyses show different average numbers of gaps per aircraft for AR sectors within the major airports. It is clear from

Table 1.2 Fit of Negative Binomial Distribution to Number of Intercommunication Gaps per Aircraft

Sector Function	No. Obs.	$\hat{p}$	$\hat{k}$	Degrees of Freedom	χ^2
LT	521	0.51	4.58	15	67.21*
LE	501	0.62	6.07	12	43.00*
HI	383	0.76	12.13	11	15.56
CD	200	0.94	15.87	4	8.30
GN	905	0.41	0.88	10	16.15
LC	1075	0.71	6.83	11	125.49*
LG	128	0.69	6.83	8	10.78
AP	49	0.63	2.63	5	7.02
DP	252	0.88	30.45	10	7.27
AD	88	0.58	4.85	9	8.28
AR	225	0.43	4.54	16	33.46*
RA	95	0.46	3.01	10	7.72

* significant lack of fit at the 0.01 level.

Table 1.3 Fit of Shifted Negative Binomial Distribution to Number of Intercommunication Gaps per Aircraft for Enroute Sector Functions

Sector Function	No. Obs.	$\hat{p}$	$\hat{k}$	Degrees of Freedom	χ^2
LT	514	0.41	2.36	14	21.07
LE	498	0.46	2.30	12	13.89
HI	379	0.58	4.03	11	4.14

this analysis that, within a major airport containing several AR sectors, the sectors now classified in the AR function should be separated further into mutually supporting sub-functions.

The parameter estimates $\hat{p}$ and $\hat{k}$ listed in Table 1.2 and 1.3 are computed based upon the data of sector functions and are used in the construction of a general simulation for sector types. From these tables, henceforth called "master tables", one can determine the appropriate parameter values for the type of sector to be simulated.

1.4 Intercommunication Gap Lengths

The number of CT's per aircraft has an effect on the time between consecutuve CT's of an aircraft, i.e. on the intercommunication gap lengths. For example, for a given time spent by an aircraft in a sector the more CT's the aircraft has, the shorter the gap lengths must be on the average. The relationship between the mean gap length for an aircraft in a sector and the number of gaps it has (one less than the number of CT's) has been examined for all sectors in the New York data. An example of the plot of these variables is shown in Figure 1.5 for a given sector (HI 475), each point in the figure representing the statistics for one aircraft.

To remove the skewness of the gap length distributions and to stabilize the gap length variance, a logarithmic transformation was performed on the gap length data for each sector. A least squares regression line of the form

$$y = a_0 + a_1 x \quad , \tag{1.2}$$

where y is the log of mean gap length per aircraft, x is the number of gaps, and a_0, a_1 are parameters, was then fitted to the transformed data for all New York sectors. For a given number of gaps per aircraft x, the log of mean gap length per aircraft is assumed to be Normally distributed about a mean y. (Note that y is the <u>mean</u> of the log of mean gap length per aircraft).

Since the object of this study is to develop a simulation model appropriate for ATC communication in general, the data on the 101 sectors required summarization. Fortunately a great deal of similarity was noted amongst the coefficients a_0 and a_1. A complete tabulation of these coefficients is given in Table 4.6 of Volume II. The average values of a_0 and a_1 for each sector function are given in Table 1.4. Further on plotting a_0 versus a_1 for the 101 sectors, the plotted data were clearly negatively correlated as shown in Figure 1.6. A linear regression of a_0 on a_1 gave the following statistically significant equation:

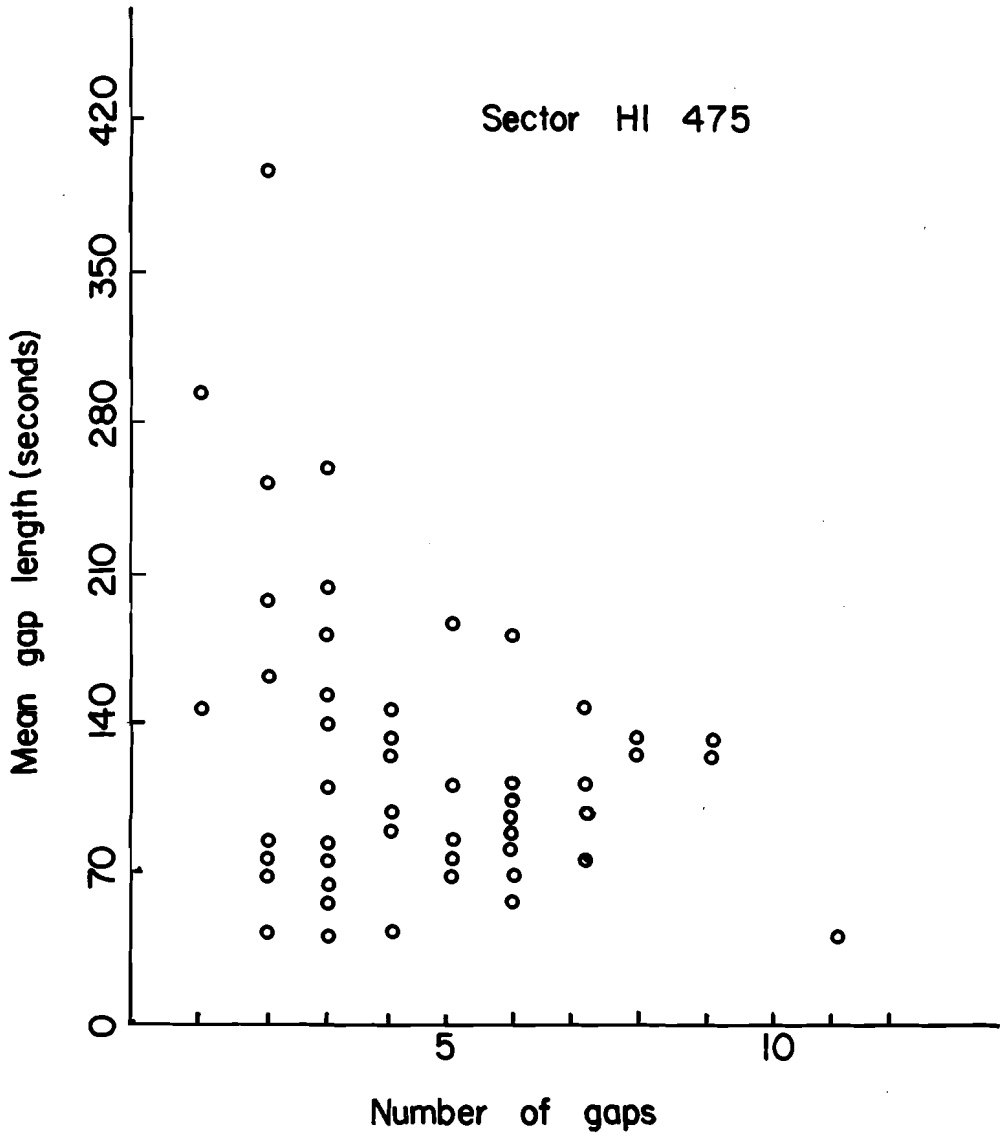

Figure 1.5 Mean Gap Length vs. Number of Gaps for Aircraft in a Sector

Table 1.4 Average Values of Regression Estimates a_o, a_1 for Gap Lengths in Each Sector Function

Sector Function	$\bar{a}_o$	$\bar{a}_1$	Sector Function	$\bar{a}_o$	$\bar{a}_1$
LT (12)	4.903	-0.109	LG (5)	4.919	-0.028
LE (11)	5.579	-0.164	AP (4)	4.671	0.069
HI (9)	5.1841	-0.083	DP (6)	4.415	-0.046
CD (4)	5.600	-0.171	AD (12)	4.646	-0.048
GN (13)	4.180	0.162	AR (6)	4.583	-0.065
LC (16)	4.673	-0.024	RA (3)	4.902	-0.048

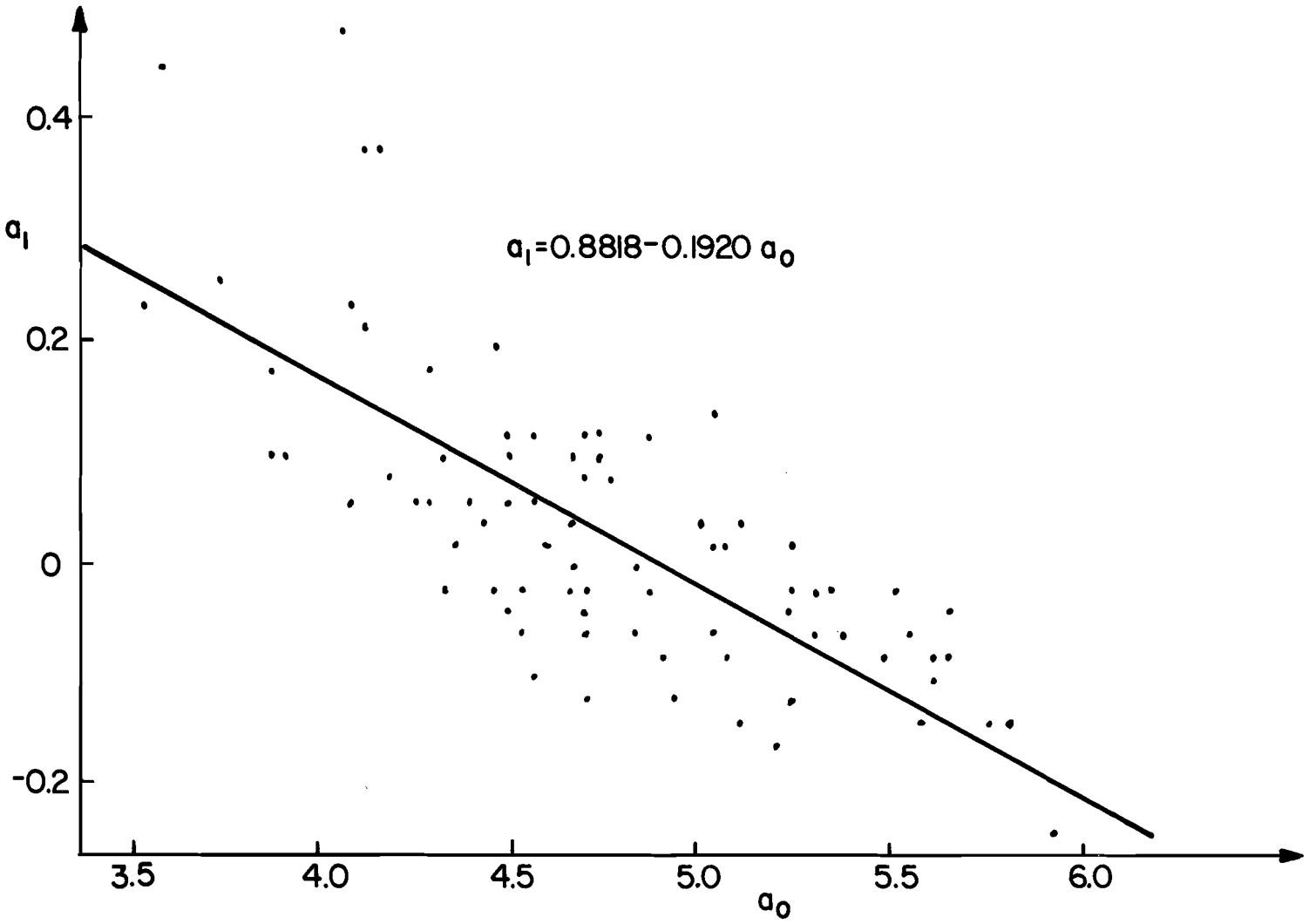

Figure 1.6 Co-plot of Regression Coefficients a_0 and a_1 for 101 Sectors

$$a_1 = 0.882 - 0.192a_o \ . \tag{1.3}$$

This equation, henceforth termed a "master equation", is employed in the simulation in the following fashion. Given the sector function to be simulated, the appropriate a_o is obtained from Table 1.4, and then a_1 is determined, using the above master equation. The number of gaps x for the aircraft is obtained by a random sample of the appropriate sector function negative binomial distribution, or when necessary, from the appropriate sector function empirical distribution. The equation $y = a_o + a_1 x$ then gives the estimated mean of the log mean gap legnth for all aircraft with x gaps. The log mean gap length for one aircraft, log z, is obtained by generating a random variate from a Normal distribution with mean y. Finally the individual gap lengths for an aircraft are obtained by randomly sampling from an exponential distribution with mean z.

The exponential distribution was taken to be an appropriate distribution for the individual gap lengths for an aircraft, based on analyses of the data. The sample of gap lengths for a single aircraft is too small to indicate a distribution, but the gap lengths for all aircraft in a sector provided a sufficiently large sample for analysis. An example of the observed distribution of gap lengths for all aircraft in a sector is given in Figure 1.7, which shows the shape of the distribution to be of exponential form.

1.5 Communications Transaction Lengths

In addition to the characterization of gaps between CT's, it is important to represent adequately the times taken by the CT's themselves, i.e. the CT time lengths. Since each CT is made up of separate TR's, the CT lengths are influenced by two quantities: the number of TR's in a CT, and the time lengths of the separate TR's.

The manner in which the number of TR's per CT varies in each sector was examined for the New York data. The frequencies of number of TR's per CT for the separate sectors were also grouped by sector function. An example of a histogram for a sector function showing the observed distribution of number of TR's per CT is given in Figure 1.8. For most sectors, the variance of the distribution was found to be greater than the mean, indicating that a suitable discrete distribution to fit the data might be the negative binomial distribution. Since the number of TR's per CT cannot be zero, the data were fitted by the truncated negative binomial distribution given by

$$f(x) = \left[\frac{1}{1 - (1+\Theta)^{-n}}\right] \binom{n+x-1}{n-1} \left[\frac{\Theta}{1+\Theta}\right]^x \left[1 - \frac{\Theta}{1+\Theta}\right]^n \ ; \ x = 1, 2, \ldots , \tag{1.4}$$

where f(x) is the probability of x TR's per CT, and n and Θ are parameters to be estimated from the data. This distribution fits the data fairly well

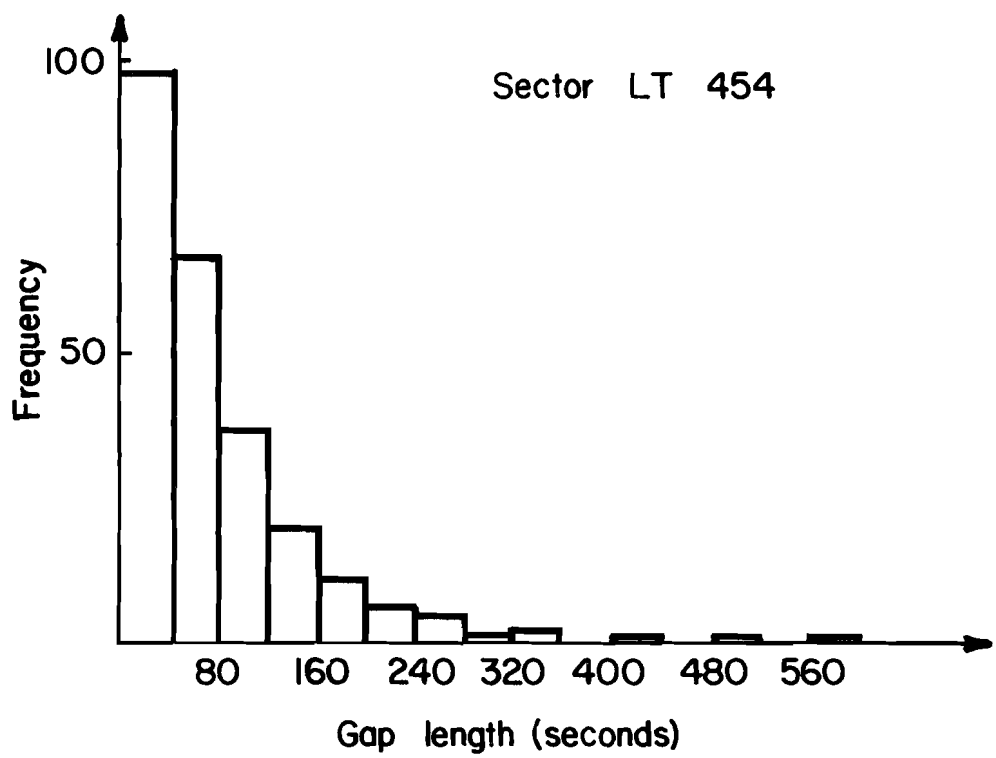

Figure 1.7 Observed Distribution of Gap Lengths in a Sector

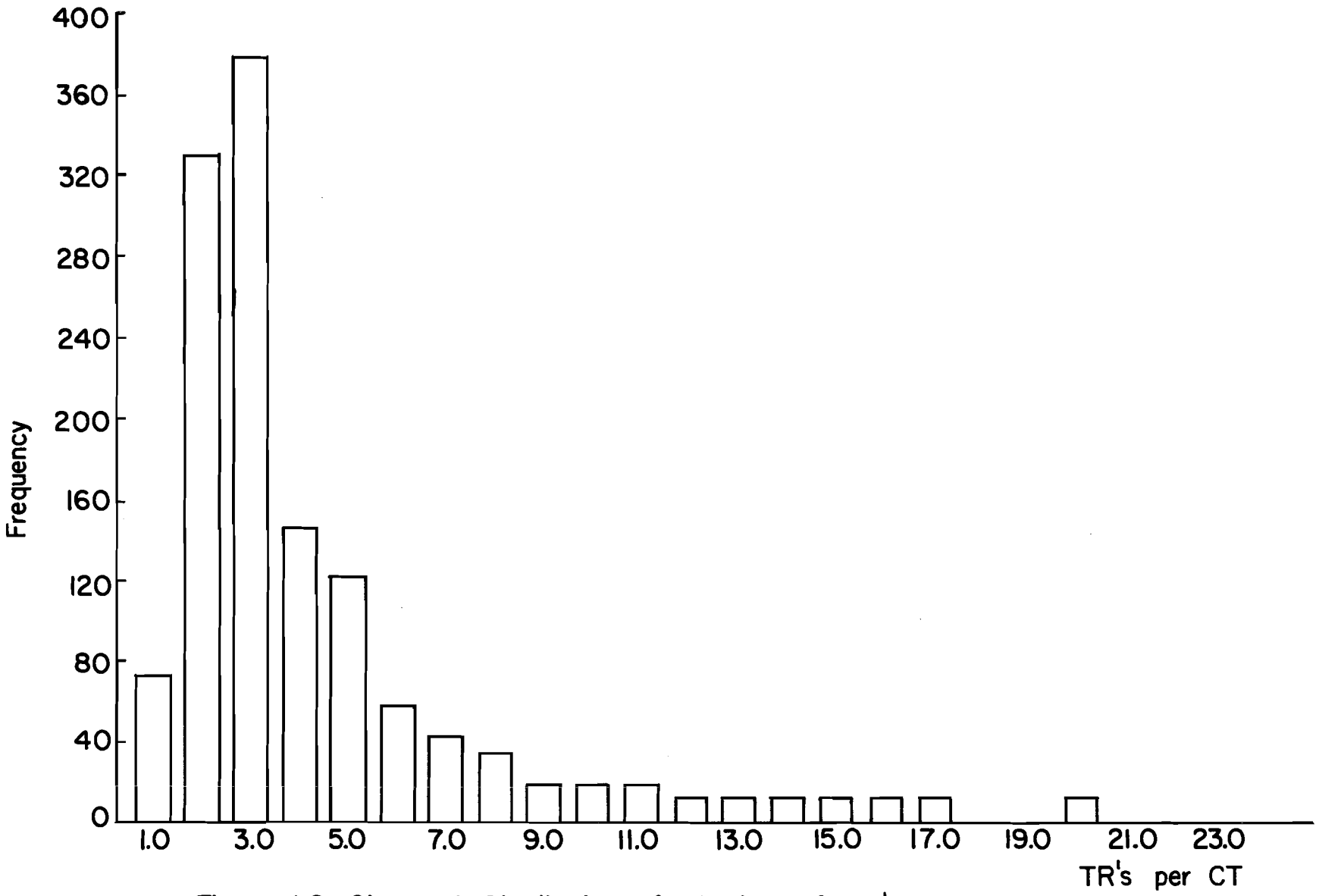

Figure 1.8 Observed Distribution of Number of TR's per CT for Sector Function DP

for the different sector functions. Further analyses indicate that a close agreement is also provided by the truncated Sichel distribution, discussed in the last chapter of this report.

Analyses of the histograms of TR length for separate sectors and for sector functions showed that the observed distributions of TR lengths could be adequately represented by the gamma distribution. The probability density function (p.d.f.), f(t), for the gamma distribution is given by

$$f(t) = \frac{1}{\lambda^{\alpha}\Gamma(\alpha)} t^{\alpha-1} e^{-t/\lambda}; \qquad 0 < t < \infty, \quad \alpha > 0,\ \lambda > 0 \tag{1.5}$$

where t is the TR length, α and λ are parameters, and $\Gamma(\alpha)$ is a gamma function. Figure 1.9 shows an example of the fit of the gamma distribution to TR lengths in a sector function. In addition to fitting the gamma distribution for sectors and sector functions, estimates of the parameters α and λ have also been estimated for the lengths of TR's for each observed combination of message elements. Details of the message element combinations and associated gamma distribution parameter estimates are provided in "dictionaries" in the first of these reports (Volume I).

A CT length is obtained by first generating a random value of x, the number of TR's per CT, from the appropriate distribution (such as the truncated negative binomial distribution or an empirical distribution), and generating x TR lengths $t_1, t_2, \ldots, t_x$ from a gamma distribution. The generated CT length is then $t_1 + t_2 + \ldots + t_x$.

As in the case of the study of intercommunication gaps, a great deal of similarity and association was evident among the estimated parameters α and λ for TR length. Two master equations were determined for these two parameters. With the CD, AF and RA sector functions as exceptions due to their small numbers and unique behavior, the following two equations apply to all sectors except as otherwise specified:

(i) $\alpha \cdot \lambda = 3.70 - 0.0079X$ (General)
$\alpha \cdot \lambda = 2.97 - 0.0021X$ (LC)

(ii) $(\alpha - 1)\lambda = 20$ (General)
$(\alpha - 1)\lambda = 1.7$ (GN)
$(\alpha - 0.14)\lambda = 3.0$ (DP)
$(\alpha - 1.5)\lambda = 1.0$ (AD) (1.6)

where X is the expected number of aircraft arrivals in a two-hour period. A pair of parameter values α and λ can be obtained, given X, by solving these two equations.

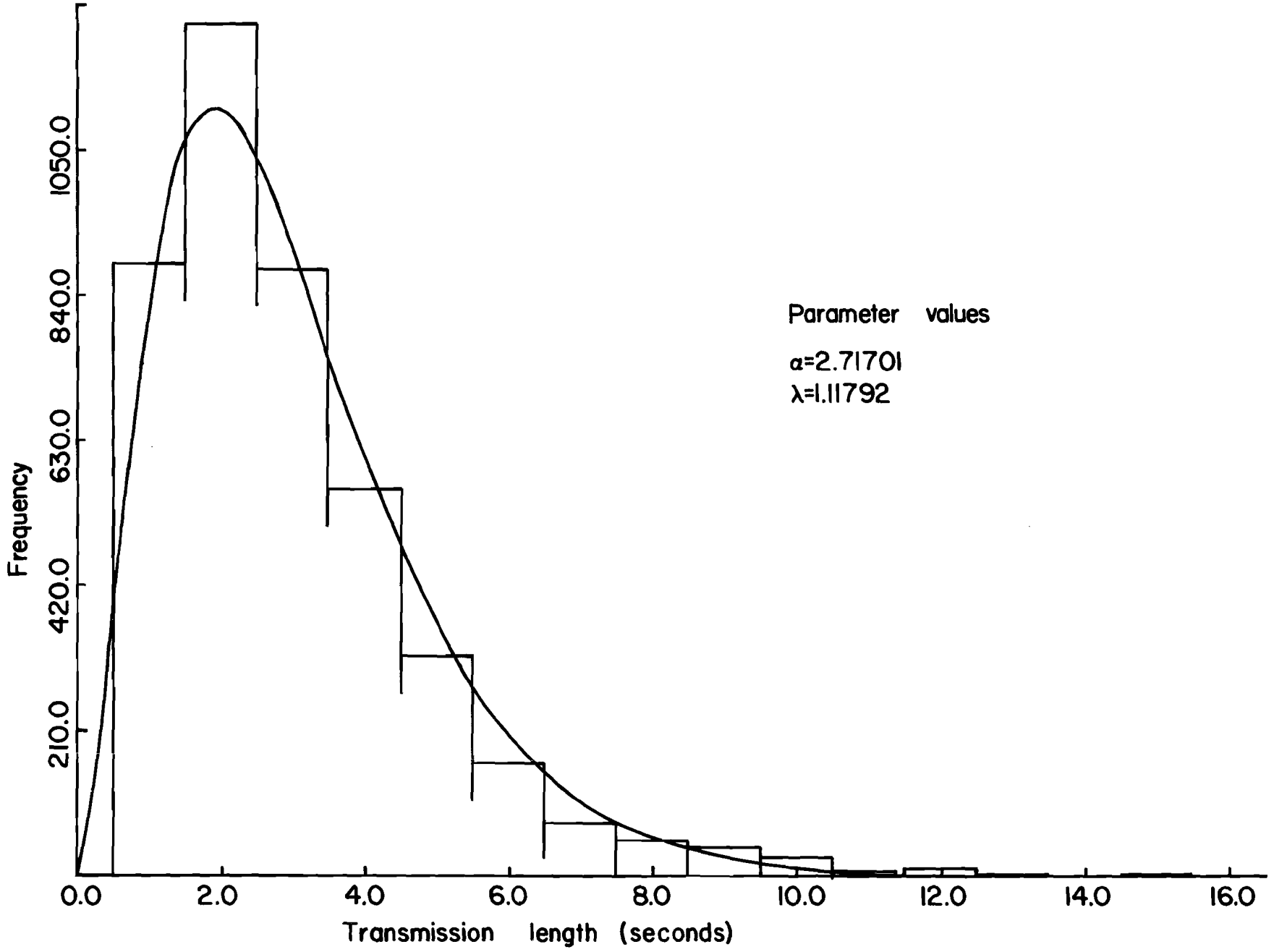

Figure 1.9 Gamma Distribution Fitted to Observed Frequencies of TR Lengths for Sector Function DP

1.6 Channel Utilization

One of the most important responses to be examined in the ATC communication system is the Channel Utilization or CU defined by

$$CU = \frac{\text{Time used in communication}}{\text{Total time available for communication}} \quad . \qquad (1.7)$$

This quantity gives a measure of how busy the controller is over a time period. For example, in the composite communications record displayed along the bottom of Figure 1.1, the channel utilization for the time period shown is estimated to be 0.4215 i.e. about 42% of the available time was used in communication as illustrated in Figure 1.10.

The historical record (and the simulation model) is recorded on a per second basis. Thus we know each second whether or not the communication channel is being used. The average channel utilization over 60 seconds has been calculated for each of the New York sectors, and these averages have been plotted for consecutive 60-second intervals. Since a minimum gap length of approximately one second has been observed between consecutive CT's, the effective maximum channel utilization is somewhat less than 100%. An example of the observed resulting time series plot is shown in Figure 1.11. Analyses of the observed time series show them to be an autoregressive process of the first order, i.e., an AR(1) process. Such time series plots of channel utilization are used to validate the simulation model. This is accomplished by generating the equivalent series from the simulation model, and then comparing the simulated time series with the observed time series.

1.7 Aircraft Loading

Another important response in the ATC communications system is the number of aircraft in a sector at any given point in time, i.e. the aircraft loading. In the same way as for channel utilization, average values of aircraft loading over 60-second intervals have been calculated from the New York data for each of the sectors. Figure 1.12 shows an example of the observed time series of consecutive 60-second average values n_t of aircraft loading in a sector. Time series analyses of the observed aircraft loading series indicate an autoregressive process of the second order, i.e. an AR(2) process, described in Chapter 7 of Volume II and in the later chapters of this report. Simulated time series of aircraft loading are also compared with the observed time series for aircraft loading in validating the simulation model.

1.8 Communications Queuing

When the aircraft loading in a sector is heavy, the controller is

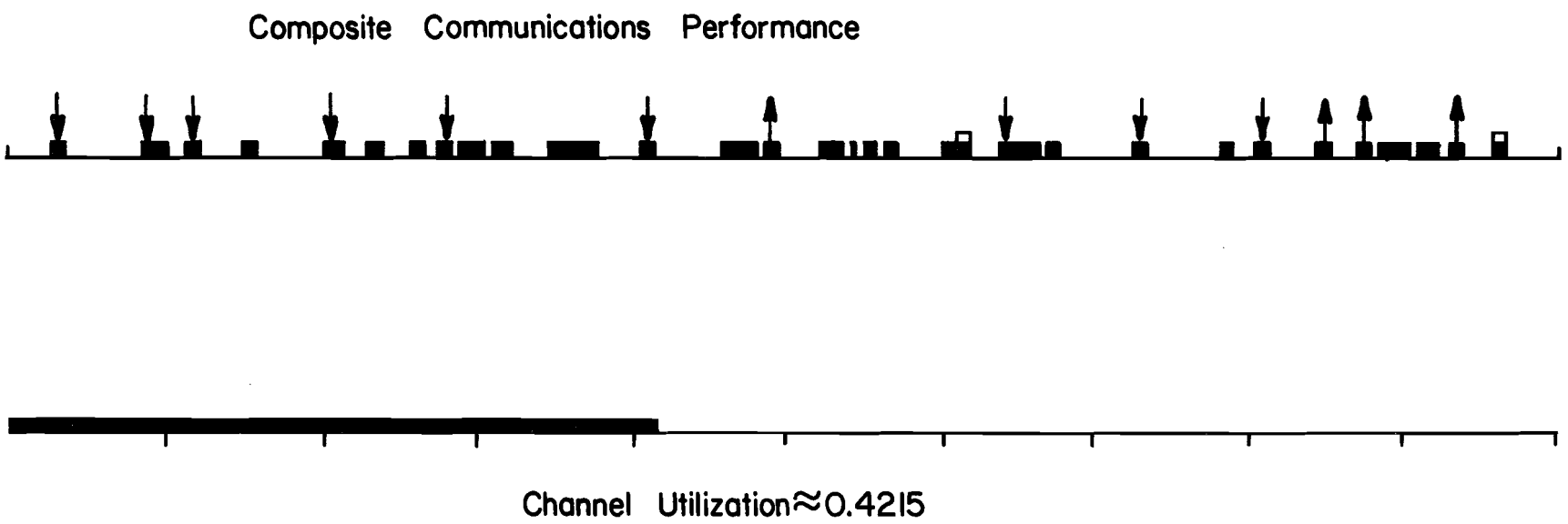

Figure 1.10 Determination of Channel Utilization from Composite Communications Record

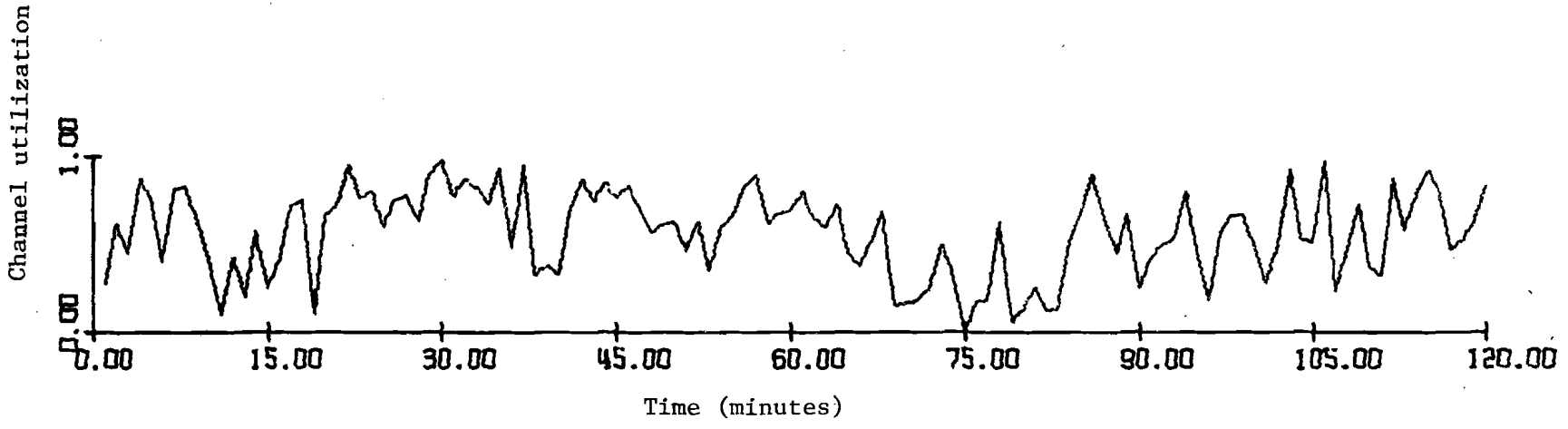

Figure 1.11 Historical Time Series of Channel Utilization in Sector HI 475

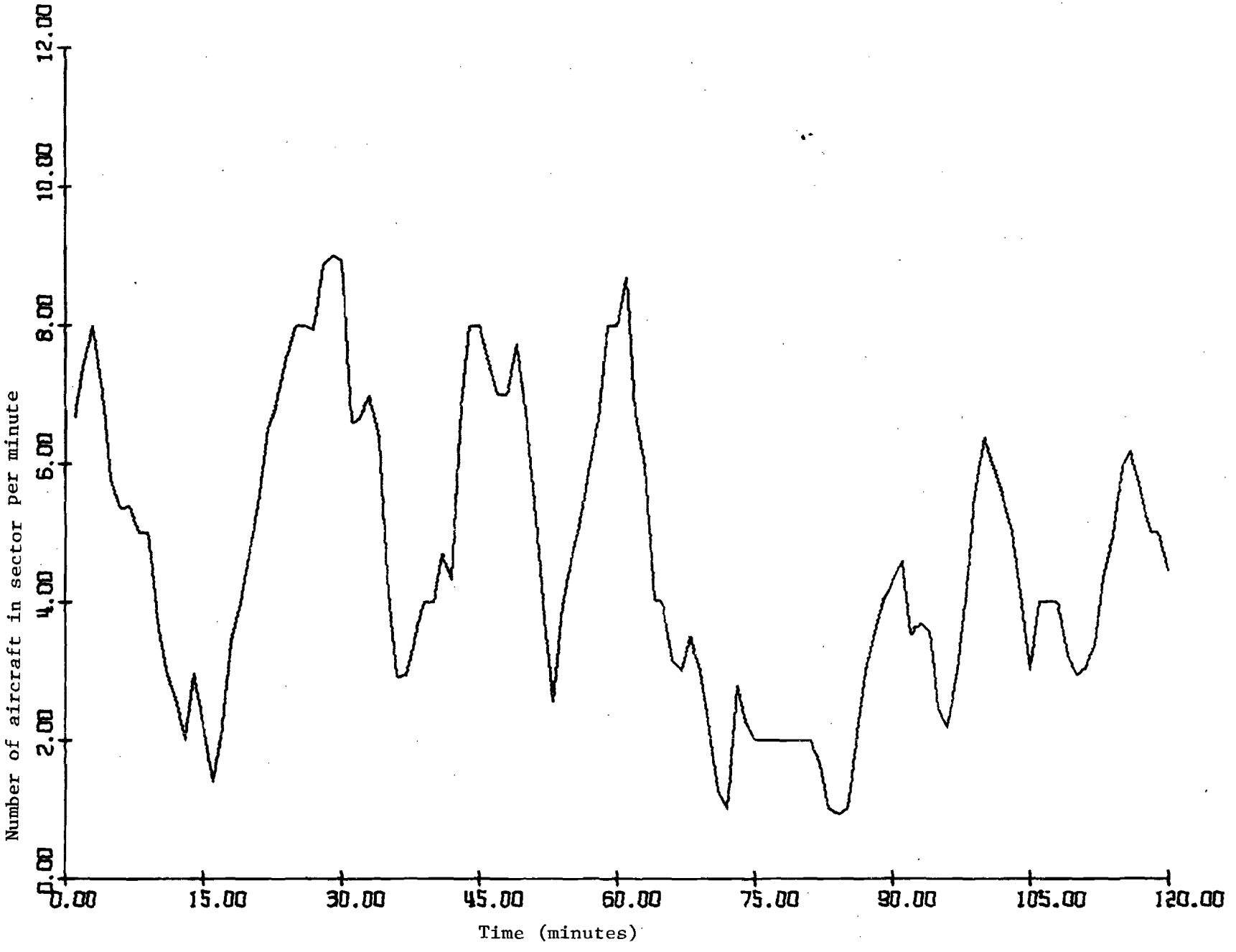

Figure 1.12 Historical Time Series of Aircraft Loading in Sector HI 475

likely to be busy and aircraft may have to wait to communicate with the controller. The number of aircraft waiting each second is a response not available in the historical record. However, it is a response that can be monitored on a per second basis with a simulation model. Simulated time series for Q_t, the average number of aircraft in the queue over a sixty-second period, are generated and examined in later chapters of this report. A critical aspect of the communications system is the relationship between the aircraft loading, the channel utilization and the queue length.

1.9 Network Analyses

In order to construct a simulation model that is applicable to a whole airport region, it is necessary to examine the patterns of transfer of aircraft from one sector to another in addition to the within-sector characteristics. The movements of aircraft between sectors were followed through on the New York data and the numbers of aircraft transfering between all pairs of sectors determined. These observed transitions were also summarized by sector function and are shown in a transition matrix in Table 1.5.

More detailed information on the patterns of movement of aircraft between separate sectors was presented in a number of schematic diagrams obtained from further analyses of the data. Figure 1.13 shows an example of one of the schematic diagrams of transitions between various sectors. These studies and others on the networks of routes between sectors are reported in Chapter 7 of Volume II.

An important network problem presented by the study of sector transitions is the determination of system capacity given the structure of individual sectors. An initial formulation of the ATC system in network terminology is discussed in the final chapter of this report, and maximum flow algorithms are applied to a sample network.

1.10 Preview of the Following Chapters

The following chapters of this report describe the development and use of the simulation model for ATC communications, based on the data analyses presented in detail in Volumes I and II and summarized in the previous sections of this chapter. A simulation model was considered to be the most appropriate way of representing the communications system, rather than the use of a purely analytical approach. An analytical study making use of queuing theory would have required a number of over-simplifying assumptions in order to formulate a model, and much of the diverse characteristics of the system would have been lost. In addition, the mathematics resulting from a study of even such over-simplified models would be quite

Table 1.5 Transition Matrix from New York Sample Data

	Enroute			Tower Cab					IFR Room			
From \ To	LT	LE	HI	CD	GN	LC	LG	AP	DP	AD	AR	RA
LT	184	88	72	0	0	0	0	0	0	7	162	0
LE	31	159	53	0	0	0	2	17	0	16	60	0
HI	79	79	104	0	0	0	0	0	0	0	0	0
CD	0	0	0	0	151	22	0	0	0	0	0	0
GN	0	0	0	40	7	354	0	0	0	0	0	0
LC	11	0	1	0	351	11	0	3	192	25	5	21
LG	0	13	0	0	0	0	2	3	0	10	0	0
AP	4	3	0	0	0	12	10	0	0	0	1	0
DP	159	48	0	0	0	3	0	0	0	1	5	1
AD	4	22	0	0	0	19	9	2	6	1	2	0
AR	1	1	0	0	0	289	0	0	6	2	167	8
RA	1	0	0	0	0	44	0	0	0	0	2	7

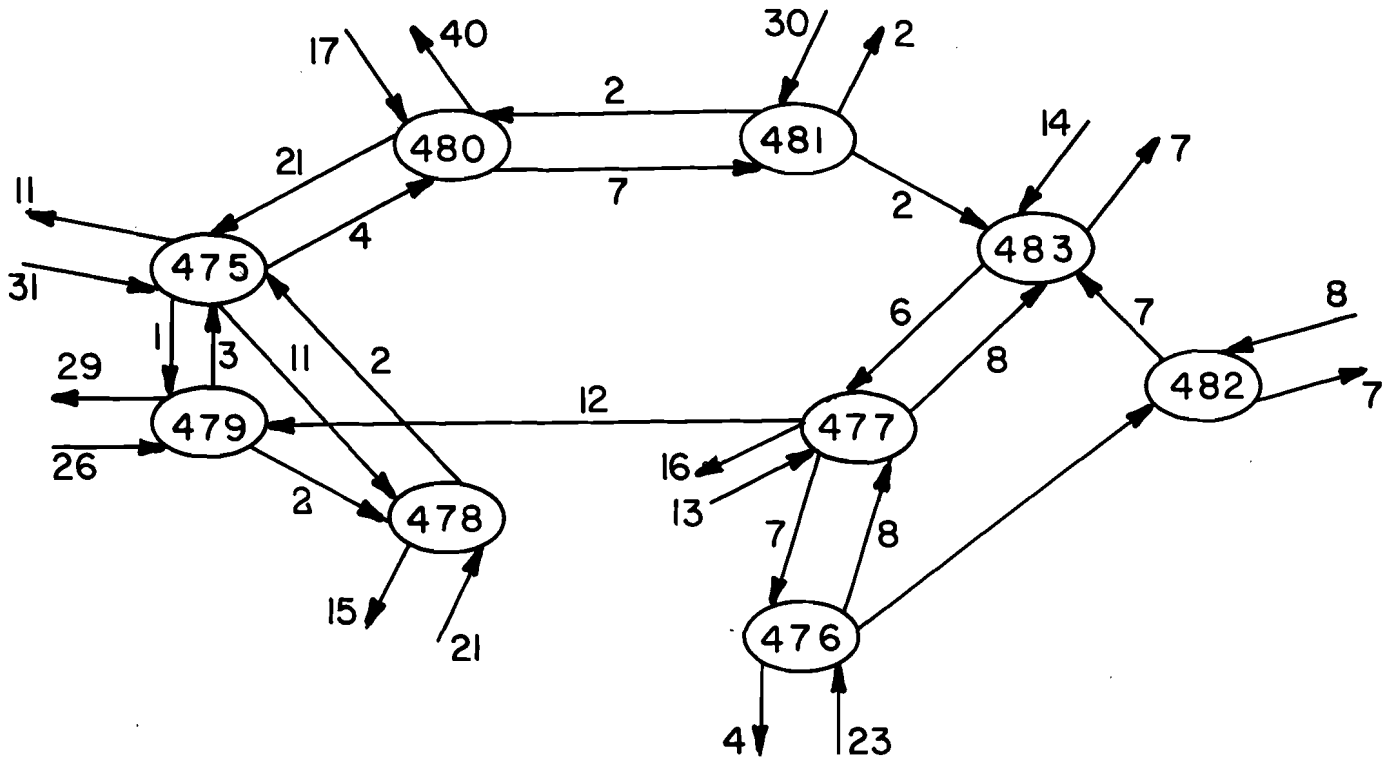

Figure 1.13 Schematic Diagram Showing Numbers of Transitions between High Altitude Sectors

formidable. In the development of a simulation model, a balance can be maintained between simplifying the complexity of the communications process and keeping the essential characteristics of the real system, while the problem of intractable mathematics is avoided.

The construction of the simulation model is described in Chapter 2, in which the basic flow chart for the communications system is shown. The computer simulation is executed through a General Purpose Simulation System GPSS V program. Incorporated into the program are the three main responses of interest: channel utilization, aircraft loading and queue length.

Chapter 3 is concerned with the validation of the simulation model. Results from simulation runs are checked against the historical data, so that the final model is consistent and can be reliably applied to new communication conditions. Channel utilization and aircraft loading functions are the responses tested in the validation of the model, comparing simulated results with observed time series.

The applications of the simulation model are presented in Chapter 4. The model is exercised for different traffic densities, and the main responses are analysed. The results are used to determine the communications capacity of a sector. The last section of Chapter 4 contains a special study on communications queuing. Various aspects of the queuing status deduced from the GPSS V program are examined, such as the average and standard deviation of waiting time and of queue length, and the channel utilization. The effect of traffic density on the queuing situations is also explored.

Chapter 5 presents some further studies related to the main simulation project. These include an examination of the dynamic relationship between the three main responses: channel utilization, aircraft loading and queue length. Transfer function models are constructed to describe and explore the relationship. Another section presents an algorithm for obtaining the maximum flow of aircraft through a sequence of sectors. The final sections include a study of a basic queuing theory model and a study of distributions to fit more closely the observed numbers of transmissions per communications transaction.

CHAPTER 2

CONSTRUCTION OF THE SIMULATION MODEL

2.1 Introduction

As noted in the previous chapter, a considerable effort has been spent in investigating the varied aspects of ATC communications in the N.Y. ARTCC. The available data have been digested in many ways, and where ever possible mathematical models have been postulated and fitted to these historical events. For example, the Normal, Poisson, binomial, negative binomial and gamma distributions, both truncated and shifted, have all been used along with more esoteric functions. Parametric time series have been fitted, and various data transformations attempted. These mathematical models have been developed for the individual sectors, and by sector function, and a great many consistencies observed. Master equations have been constructed which, by sector function, relate the distributions and model parameters to traffic density (expected number of aircraft arrivals in a one-hour period of time). All these models are, of course, abstractions of various elements in the historical data, and as each mathematical relationship has been derived, it has been tested to determine its adequacy as a replacement for the data.

Our objective now is to gather together these many detailed abstractions into a single system description of ATC communications. However, the construction of this general system in pure mathematical terms seems intractable. Those aspects of the problem that are amenable to direct mathematical treatment often provide ornate results of little practical value. Some of the mathematical questions raised have, to the best of our knowledge, no known answers. To appreciate the kinds of problems, one has only to contemplate the analytical solution to a queuing model excited by random events from a gamma distribution convoluted with a negative binomial distribution. In brief, a useful analytical model of an ATC communications system appears unattainable.

We have therefore decided to construct a simulation model of the ATC communications system. In simplest terms, we have attempted to reproduce what goes on in the actual system using the GPSS V simulation language with a 360/91 computer facility. This task is vastly simplified through the use of the master equations and master tables already found useful in describing the historical data.

The next portions of this chapter describe the structure of the model for the general ATC communications simulation. This is followed by a more

detailed description of the key terminology and elements of the General Purpose Simulation System GPSS V computer program. In addition, the character of the simulation inputs and responses along with a sample of the computer input and output is provided. An investigation on the simulation of intercommunication gap lengths is finally presented and the similarity between observed and simulated data illustrated.

2.2 Structure of the Simulation Model

The structure of the simulation model for ATC communications is best described by the flow-chart block diagram shown in Figure 2.1. Details of each of the blocks are listed below in the order of their assigned numbers (1), (2), ..., (12).

(1) The aircraft arrival rates are generated from a Poisson process with parameter ρ.

(2) The number of CT per aircraft is based on the number of intercommunication gaps which is generated from a negative binomial distribution with shifted origin, with parameters p and k. The value of p and k can be determined from an appropriate master table (Table 1.2 and/or 1.3) constructed for sector functions.

(3) The message types and combinations are selected with appropriate probabilities from the message dictionaries (see Volume I: Message Element Analyses and Dictionaries). The parameters α and λ of the transmission length distributions are also obtained from the dictionaries.

(4) Specific transmission lengths are generated based on the value of α and λ parameters assigned at (3). To reduce the complexity at the current stage of simulation, we use only a pair of α and λ for each sector, based upon two simultaneous equations specified in Equation (1.6).

(5) The number of TR/CT is obtained from empirical histograms. (Strenuous efforts have been made to use the truncated negative binomial distributions, log Normal and Sichel's distributions).

(6) Combining all information found from (3) to (5), a CT is constructed.

(7) The intercommunication gaplengths are obtained by using a regression model, based upon the results from (2), with parameters a_0 and a_1. Again, the values of a_0 and a_1 have been grouped for each sector function and listed in Table 1.4.

(8) All values generated are then placed into the GPSS computer program to derive (9) - (12).

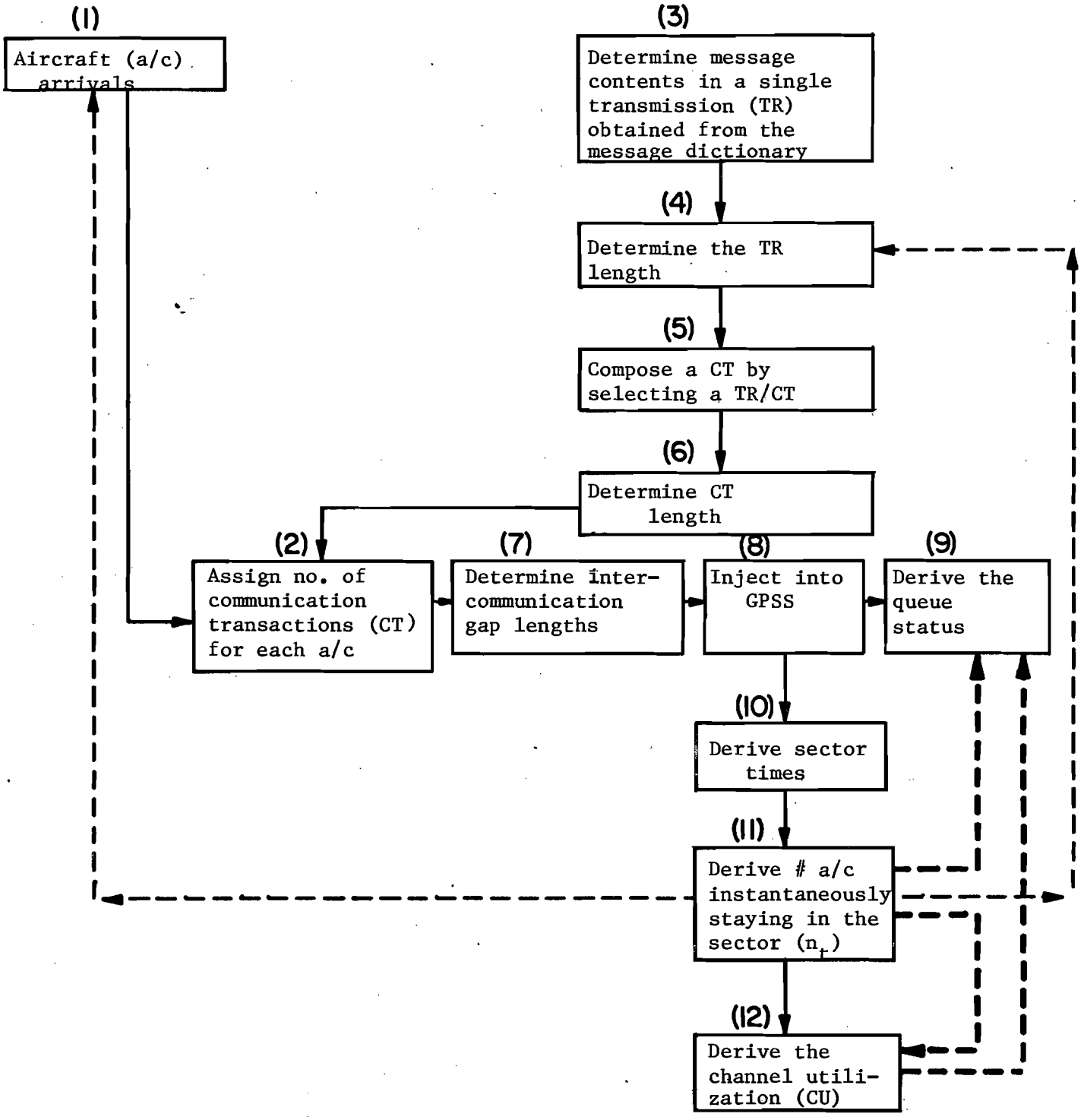

Figure 2.1 Flow-Chart Block Diagram for the Communication Simulation Model

(9) The queue status is based on the first-come first-served rule.

(10) Sector times are the time lengths during which an aircraft stays in the sector.

(11) The average number of aircraft staying in a sector instantaneously, per minute, is used as the index of aircraft loading.

(12) The channel utilization per minute is considered as a response variable.

The model contains two feedback loops indicated by the thin dashed lines in Figure 2.1. Both feedback loops employ regression equations constructed from the NY ARTCC data. These equations reflect interactions between various sector variables found to be statistically significant in the earlier data analysis. In order to reduce complexity, and to reduce the burden of output, both feedback loops have been omitted in our initial studies. Instead, the feedback effects are specified in the model by the first of the two master equations listed in Equation (1.6) which relates the traffic density to the parameters of the distributions of transmission lengths. This is an equivalent feedback procedure without transient aspects.

With the simulation framework given above, it has been found adequate for the large majority of sectors to simulate the aircraft loading and channel utilization responses using only seven initiating parameters:

ρ, the aircraft arrival rate;

p and k, the parameters of the number of intercommunication gaps per aircraft distribution;

α and λ, the parameters of the transmission length distribution;

a_o and a_1, the parameters relating the CT length with the number of CT per aircraft.

In addition, the number of TR/CT must be randomly sampled from the sector histograms.

However, as noted in Chapter 1, there exists a great deal of similarity and association between these parameters, especially among sectors having the same function. This has led to the establishment of "master" tables and equations for the sector functions. In fact, as a consequence of these master relationships, the successful simulation of a sector need depend only upon ρ (the aircraft arrival rate) and the identification of the sector function. Used in this fashion the simulation block diagram given above becomes a general simulation model for ATC communications.

The major responses to be simulated by the model are:

(i) aircraft loading, n_t;

(ii) channel utilization, C_t;

(iii) number of aircraft in queue waiting to communicate, Q_t.

Each of these responses is a time series reflecting the ebb and flow of air traffic through a sector and the resulting burden of communications. They have been characterized by parametric time series models. The resulting models are listed below:

(i) for n_t, the second order autoregressive model

$$n_t = \mu + \phi_1(n_{t-1} - \mu) + \phi_2(n_{t-2} - \mu) + a_t$$

where ϕ_1 and ϕ_2 are parameters, $a_t \sim N(0, \sigma^2)$ and μ is the expected value of n_t;

(ii) for CU (denoted by C_t), the first order autoregressive model

$$C_t = \Theta + \phi_1^*(C_{t-1} - \Theta) + b_t$$

where ϕ_1^* is a parameter, $b_t \sim N(0, \sigma_*^2)$ and Θ is the expected level of C_t;

(iii) for Q_t (after a negative exponential transformation, denoted by a_t), the second order autoregressive model

$$q_t = \omega + \phi_1^{**}(q_{t-1} - \omega) + \phi_2^{**}(q_{t-2} - \omega) + e_t$$

where ϕ_1^{**} and ϕ_2^{**} are parameters, $e_t \sim N(0, \sigma_{**}^2)$ and ω is the mean level of q_t.

Furthermore, these dynamic responses are interdependent. The thick dashed lines in the flow chart of Figure 2.1 indicate the dynamic responses linked by transfer function models. The estimation of the parameters of the different transfer functions is also discussed in Section 5.1. The final result is a single dynamic multi-response model.

2.3 GPSS Computer Programs for the ATC Communications

Several different computer programs are available for simulation modeling. The system chosen for this study is the General Purpose Simulation System V (GPSS V) copyrighted by IBM. The program consists of a generalized computer language coupled with FORTRAN linkages to external mathematical functions and operations. GPSS V permits the user to employ both deterministic and stochastic data to compile statistics, histo-

grams, information on queues, and to record time-sequenced histories of both input and output data.

The type of simulation model developed for the ATC communications system is a discrete-event model, implying that events can occur only at a multiple of some base unit of simulated time (here selected to represent one second of real time). Aircraft are generated at a specified rate and moved through a sequence of blocks as represented in Figure 2.2. Communication requirements are assigned as an aircraft enters, and when all CT's are completed, the aircraft departs from the sector and is removed from the system. The entire system is constantly monitored, and the simulation ends after a specified length of simulated time has elapsed (here two hours).

The flow of aircraft through the model corresponds to the behavior observed in the data base. Aircraft are generated as a Poisson stream, entering the sector at exponentially distributed interarrival times with a specified mean. A HELP block is used to access a FORTRAN subroutine SUBNB1 which generates the number of transactions for the calling aircraft from a shifted negative binomial distribution. A second FORTRAN subroutine GAPM uses the generated number of CT's to determine the mean intercommunication gap length for the calling aircraft (the details of this determination will be discussed in the next section of this chapter). The aircraft then immediately attempts to make its first transaction.

The simulation of voice communications is handled by defining a "facility" to represent the communications channel. Access to the channel is controlled by a queue, which operates in a "first-in, first-out" mode. The length of a transaction is determined by adding together gamma-distributed transmission lengths (from FORTRAN subroutine MSSG), with the number of TR's per CT generated by sampling from the empirical distribution function for the appropriate sector function. The channel is held until the simulation clock has been advanced the required number of seconds, during which time the channel cannot be seized. In addition, a minimum of one second is imposed between the end of one CT and the start of another.

When an aircraft has completed its CT, a test is made to determine whether all of its required transactions have been completed. If not, a FORTRAN subroutine EXPON is called to generate an intercommunications gap length from an exponential distribution using the mean which was determined when the aircraft entered the system. After the clock has been advanced to the end of the gap, the aircraft loops back and reenters the queue for the channel. The same procedure is repeated until the last CT has been completed, at which time the aircraft leaves the sector and is removed from the system.

The flow of aircraft as represented in Figure 2.2 was coded in IBM's General Purpose System Simulation V (GPSS V) language. A listing of the input statements used to simulate a particular low altitude transitional sector (LT) is given in Table 2.1 at the end of this chapter. Other sector functions can be modeled by simply changing the parameters and functions

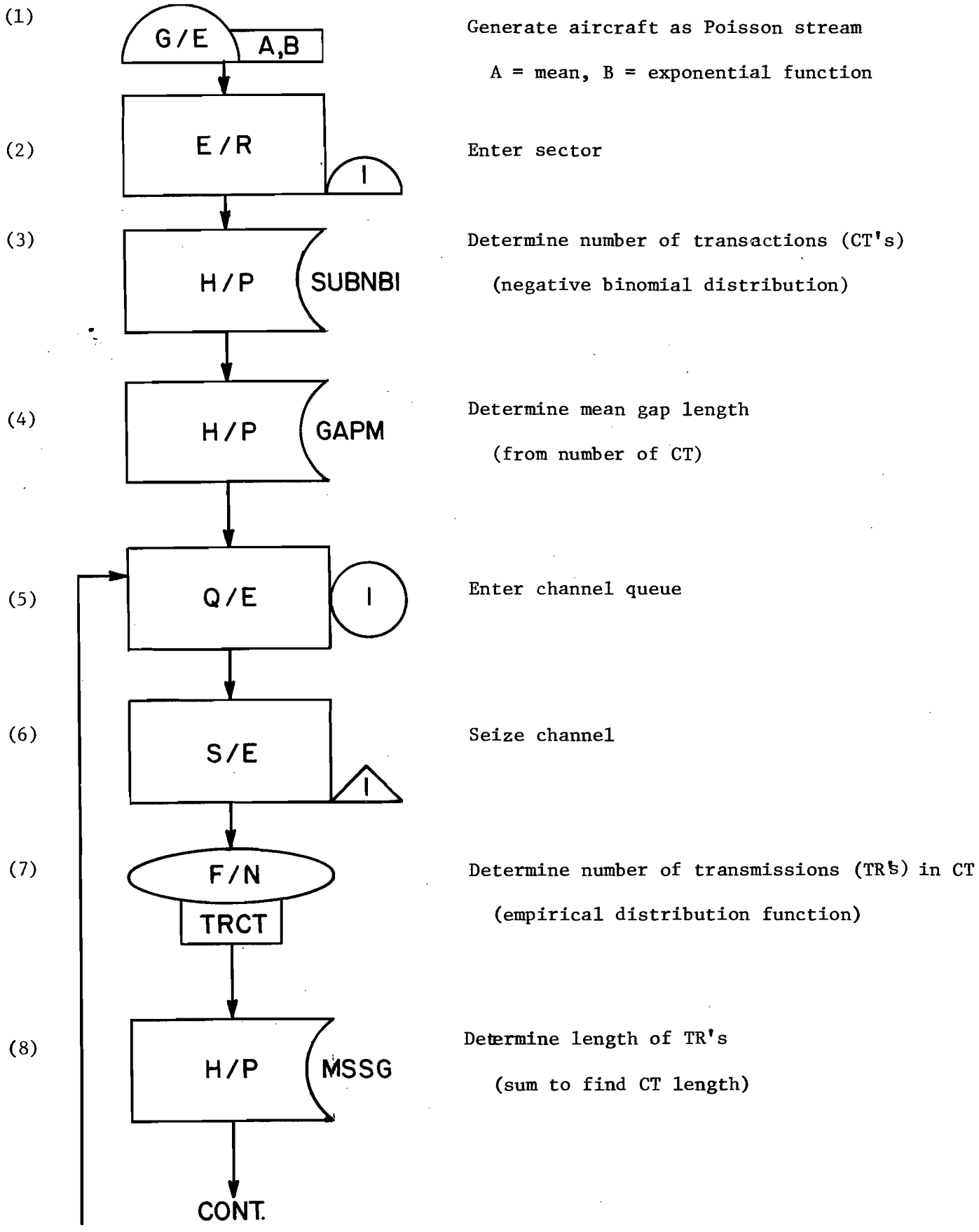

Figure 2.2 Block Diagram for the GPSS V Simulation Program

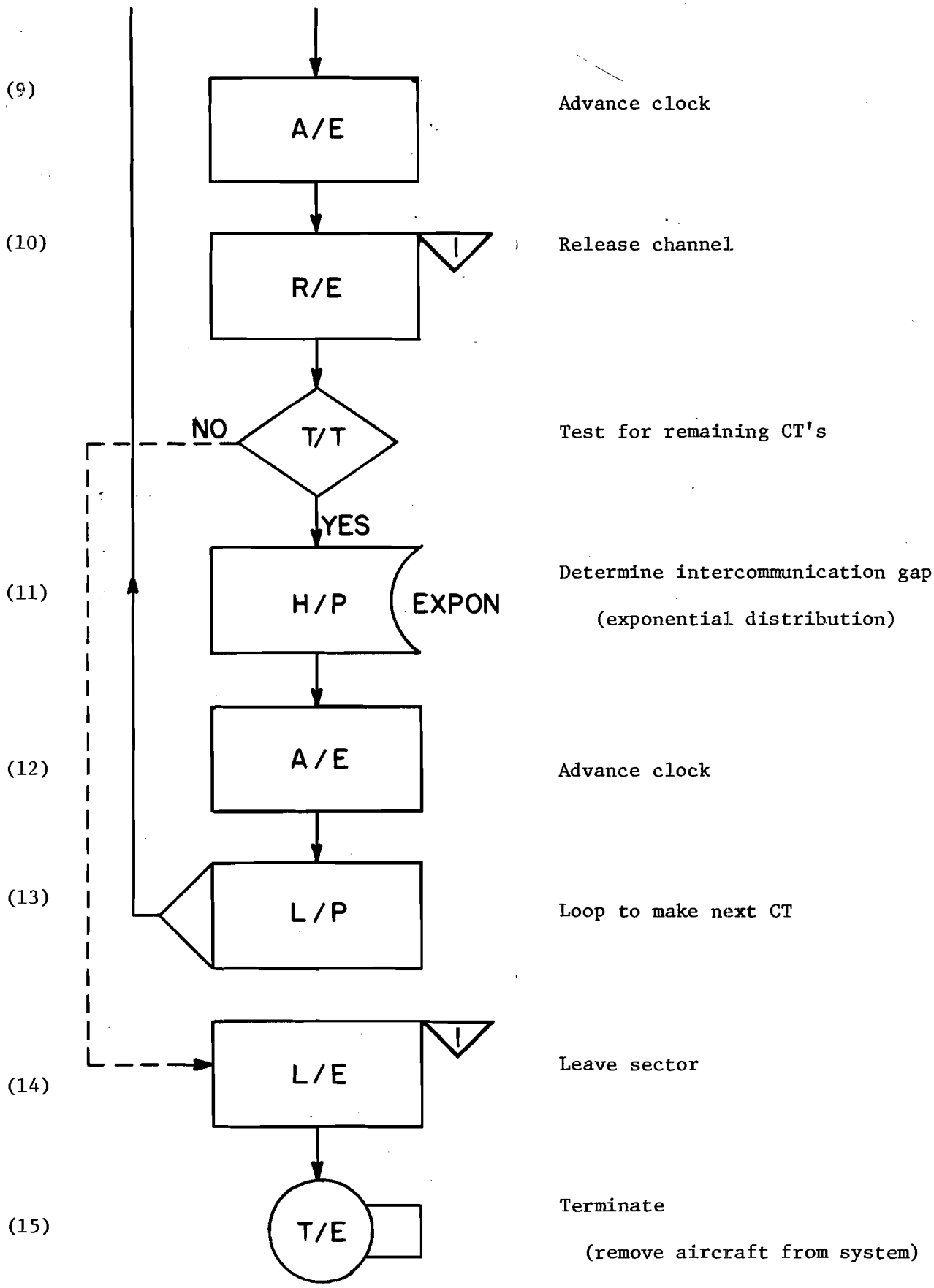

Figure 2.2 Block Diagram for the GPSS V Simulation Program (continued)

specified in statement numbers 3, 4, 5, 22, 23, 25, 26, 27, and 28.

The coding of GPSS can be grouped into five sections:

[A] specification of parameters and functions and initialization of GPSS entities;

[B] coding of the block diagram for the movement of aircraft;

[C] monitoring of the system and collection of data;

[D] timing;

and [E] formatting of output.

For the example given, the parameters and functions supplied were determined from an analysis of LT sector 453. The mean interarrival time was specified to be 125.48 as estimated from the historical data. Seven random number generators were used for needed sampling distributions.

In section [B], the statements corresponding to the block diagram in Figure 2.2 are identifiable by the comments and command names. Most of the additional statements are merely used for bookkeeping. The timer in Section [D] asks that one hour of real time should be simulated without collecting any data (to allow the system to approach steady state), then two hours are simulated over which data is collected.

The output produced by the simulation includes a summary of the input parameters, tabulation of system responses, histograms of important variables, and plots of system behavior over time. Time series identification routines are also called to analyze the dynamic behavior of the model. All responses are saved on disk for any subsequent analysis.

As a part of the standard output from the simulation program, Table 2.2 lists the input distributions and parameters driving the model and summarizes the response of aircraft loading, communications, and channel queuing. Of particular importance in analyzing the congestion of the sector is the channel utilization (.529), average queuing time (9.397 seconds), and maximum number of aircraft in the queue (5).

Twelve histograms of driving variables and system response variables are included at the end of this chapter as Figures 2.3 ∿ 2.14. They consist of:

(1) aircraft interarrival times;

(2) number of transactions per aircraft;

Table 2.2 Summary of Input Parameters and System Responses

```
***** GPSS SIMULATION MODEL FOR ATC VERBAL COMMUNICATIONS SYSTEM *****
                    TRANSPORTATION PROGRAM
                  DEPT. OF CIVIL ENGINEERING
                     PRINCETON UNIVERSITY
                         MARCH, 1974


INPUT PARAMETERS - SECTOR 453

   (1) AIRCRAFT INTERARRIVAL TIMES: EXPONENTIAL WITH MEAN =  125.479 SECONDS
   (2) TRANSACTIONS PER AIRCRAFT: SHIFTED NEGATIVE BINOMIAL WITH K =   2.509 AND P =   0.379
   (3) TRANSMISSIONS PER TRANSACTION: EMPIRICAL DISTRIBUTION
   (4) TRANSMISSIONS LENGTHS: GAMMA WITH P =   0.8021 AND ALPHA =   2.6042
          (NOTE: GAMMA PARAMETERS DETERMINED FROM EXPECTED ARRIVAL RATE)
   (5) INTERCOMMUNICATION GAP LENGTHS ARE A FUNCTION OF TRANSACTIONS PER AIRCRAFT


     SIMULATION RESPONSE - 2 HOUR ANALYSIS

   (1) SECTOR AIRCRAFT LOADING
        NUMBER OF AIRCRAFT IDENTIFIED IN SECTOR =   64
        AVERAGE NUMBER OF AIRCRAFT PER SECOND =   5.006
        MAXIMUM NUMBER OF AIRCRAFT PER SECOND =  10

   (2) COMMUNICATIONS CHANNEL LOADING
        AVERAGE CHANNEL UTILIZATION =  .529
        TOTAL NUMBER OF TRANSACTIONS =  318
        AVERAGE LENGTH OF TRANSACTIONS =  12.000 SECONDS

   (3) CHANNEL QUEUEING EFFECTS
        AVERAGE TIME IN QUEUE =    9.397 SECONDS
        AVERAGE TIME EXCLUDING ZERO ENTRIES =   17.319 SECONDS
        TOTAL ENTRIES INTO QUEUE =  317
        NUMBER OF ZERO ENTRIES (NON-WAITING) =  145
        PERCENT OF ZERO ENTRIES =  45.7
        AVERAGE NUMBER OF AIRCRAFT IN QUEUE =    .413
        MAXIMUM NUMBER OF AIRCRAFT IN QUEUE =   5
```

(3) number of transmissions per transaction;

(4) transmission lengths;

(5) transaction lengths;

(6) intercommunication gap lengths;

(7) aircraft time in sector;

(8) aircraft interdeparture times;

(9) channel queuing times;

(10) number of aircraft in sector per second;

(11) number of aircraft in queue per second;

(12) duration of non-zero queuing.

The histograms of driving variables are reviewed to ensure that the simulation is behaving properly. The system responses are studied by watching their behavior as the various driving variables are manipulated.

The simulation output also includes a study of the system behavior over time. Figure 2.15 is a plot of the times at which aircraft entered and left the simulated sector. A comparison of the arrival stream with the departure stream could suggest whether the sector significantly modified the Poisson nature of the traffic stream. Using the variables for LT Sector 453 to drive the simulation model, Figures 2.16 ∿ 2.30 present plots for each of four different variables:

(1) number of aircraft in the sector,

(i) observed per second,

(ii) sixty-second averages,

(iii) sample autocorrelation function,

(iv) sample partial autocorrelation function;

(2) number of aircraft in the queue (i, ii, iii, iv);

(3) queue transforms (ii, iii, iv);

and (4) channel utilization (i, ii, iii, iv).

Using this output, comparisons can be made between the simulated and empirical data. The procedure for validating the model is discussed in a

subsequent chapter.

2.4 Simulations of the Intercommunication Gap Lengths

Because of the complexity and importance of intercommunication gaps, a special discussion on this subject is necessary for a full understanding of the simulation model and its adequacy. This section provides detailed information on the comparison and verification of the simulations.

An initial data analysis of the intercommunication gap lengths for the N.Y. ARTCC has been carried out and is described in the previous yearly report (Chapter 4, Volume II). The construction of the simulation model in detail, particularly the creation of individual intercommunication gap lengths, is explored in this section.

It has been demonstrated that the intercommunication gap lengths depend upon the number of transactions made per aircraft. It has also been found that the number of transactions per aircraft is approximately distributed as a negative binomial variable with the origin shifted to one (or two, if it is an enroute sector). In the simulation model discussed below, the number of transactions per aircraft serves as an input variable.

Let X_{nj} denote the jth gap length associated with an aircraft which makes n + 1 communication transactions (i.e. having n intercommunication gaps), and $\bar{X}_n = \sum_{j=1}^{n} X_{nj}/n$. It has been shown that $\ell n(\bar{X}_n)$ is distributed as a normal variable with mean $\mu_n = a_o + a_1 n$ and standard deviation $\sigma_n = (\mu_n - c)/2.576$, where a_o, a_1 and c are constants and $a_1 \leq 0$. In the case that a_1 is positive, the statement above remains unchanged except that the standard deviation is equal to $(c - \mu_n)/2.576$. Therefore, the probability density function of $\bar{X}_n$ is

$$f(\bar{X}_n) = (\bar{X}_n \quad \sigma_n\sqrt{2\pi})^{-1} \exp\left[-(\ell n\, X_n - \mu_n)^2/2\sigma_n^2\right].$$

Furthermore, from the inspection of the observed X_{nj}, j = 1, ..., n, a very promising hypothesis is that X_{nj} are distributed as exponential variables with mean $\bar{X}_n$, i.e.

$$g(X_{nj}|\bar{X}_n) = \frac{1}{\bar{X}_n} e^{-X_{nj}/\bar{X}_n}, \quad X_{nj} > 0 .$$

This implies that, given n, the distribution of X_{nj} is

$$h(X_{nj}) = \int_0^\infty f(\bar{X}_n) \cdot g(X_{nj}|\bar{X}_n)\, d\bar{X}_n$$

which is a log-Normally weighted exponential distribution. Furthermore, the distribution of n is

$$r(n) = \binom{k + n - 1}{k - 1} p^k (1 - p)^n, \qquad n = 0, 1, 2, \ldots$$

The marginal distribution of X regardless of n is then

$$\ell(X) = \sum_{n=0}^{n} h(X_{nj}) \cdot r(n).$$

Alternatively, the p.d.f. of X_{nj} can be directly specified based on the assumption that X_{nj} is an exponential variable with $E(X_{nj}) = \beta_o e^{a_1 n}$, where $\beta_o = e^{a_o}$. Then

$$h(X_{nj}) = \frac{1}{\beta_o e^{a_1 n}} e^{-X_{nj}/\beta_o e^{a_1 n}}, \quad X_{nj} > 0.$$

This implies that the sample $\bar{X}_n$ (mean intercommunication gap length per aircraft) follows a gamma distribution with parameters α and λ equal to n and $\beta_o e^{a_1 n}/n$, respectively.

Two simulation schemes can thus be devised based on the discussion above and are presented in Figure 2.31.

In order to examine and compare the adequacy of the formulations described above and to exercise the computer programs, an empirical study using Sector 453, one of the busy controllers in the LT function, has been carried out. Many simulation runs of Scheme 1 using different values of the truncation point of the gap lengths, and different sample sizes (number of aircraft created), were exercised. Making use of the parameter values $k = 2.51$, $p = 0.38$, $a_o = 4.639$ and $a_1 = -0.016$ estimated from the observed data of Sector 453, one typical set of plots of the distribution of gap length for different values of n, the number of gaps per aircraft, is given in Figure 2.32. In this example the gap length truncation point equals 720 seconds; the number of aircraft generated equals 500. The ordinates of these distribution curves are based on the simulated frequencies and are smoothed in the figure. For instance, the curve for n = 5 indicates the distribution of gap lengths for those aircraft which produced five intercommunication gaps. From the inspection of these plots, one finds that

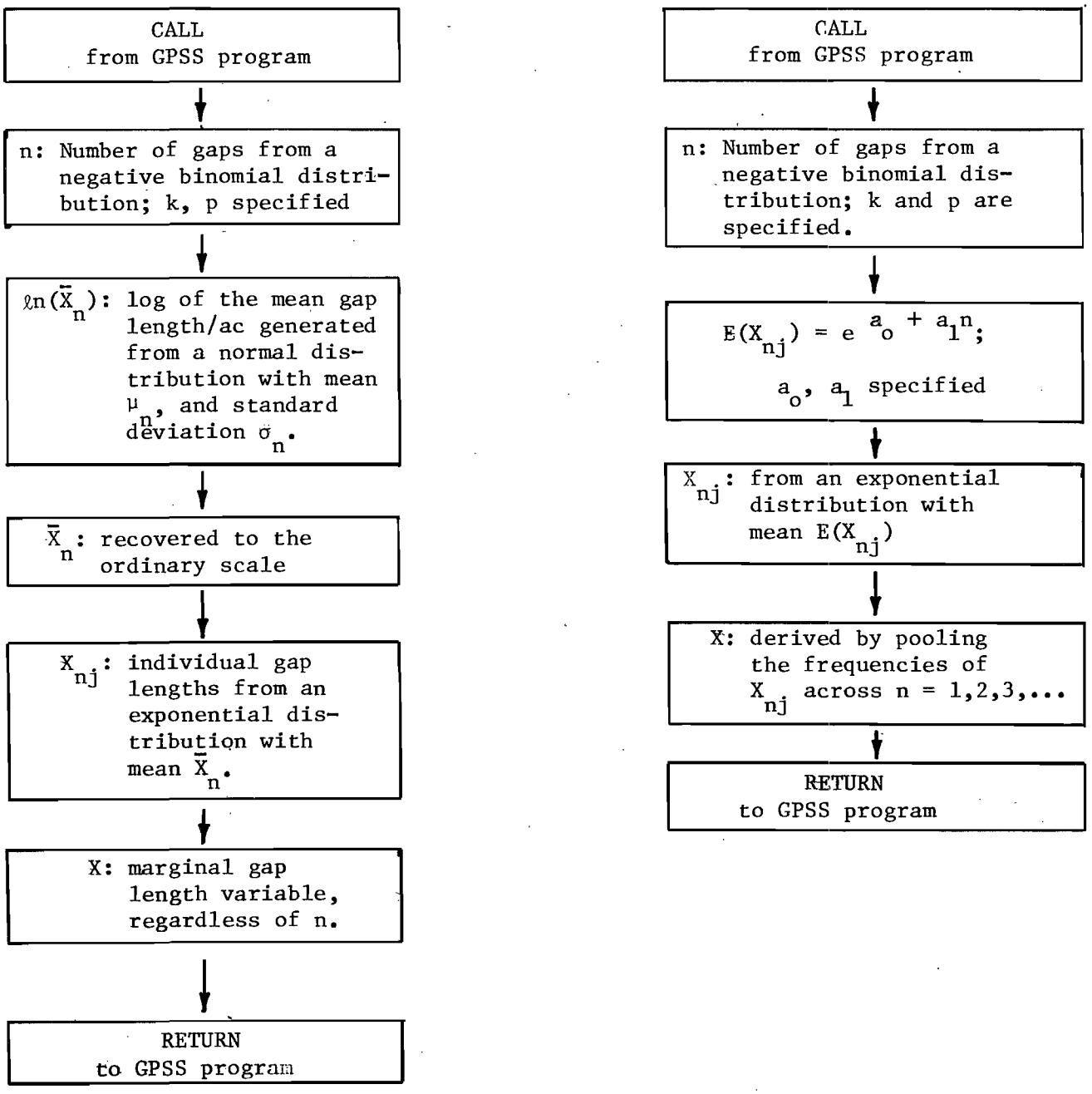

Figure 2.31 Two Different Simulation Schemes for Intercommunication Gap Lengths

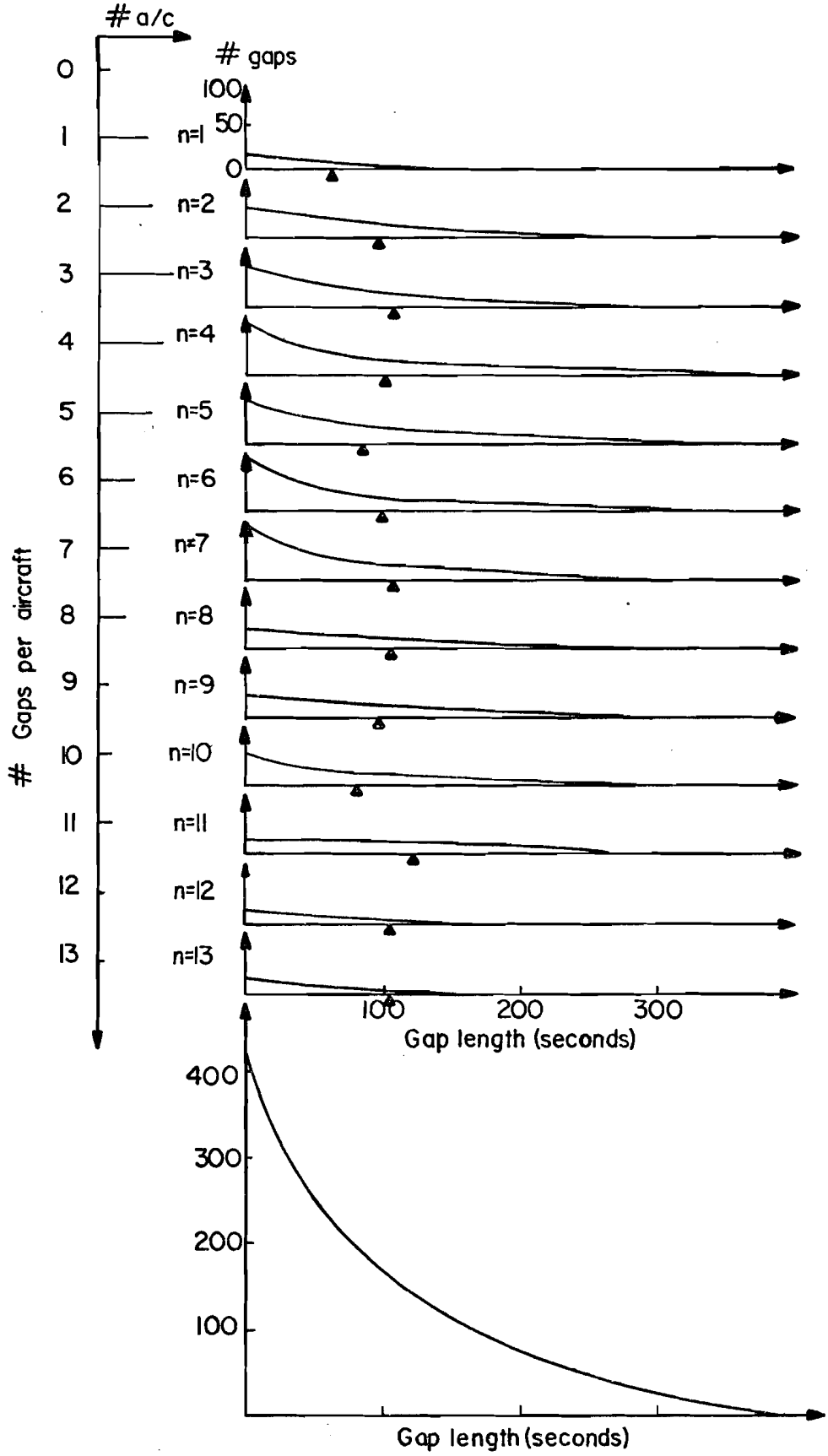

Figure 2.32 Simulated Distributions of Gap Lengths and the Number of Gaps per Aircraft

the average gap length (marked by "Δ") stays at the same level as the number of gaps per aircraft increases. This is attributed to the small magnitude of the slope parameter a_1. When the magnitude of a_1 is moderately large, which is the case for many of the sectors, the average gap length shifts, either upward or downward depending on the sign of a_1, as the number of gaps per aircraft increases. The plot at the bottom of Figure 2.32 is the marginal distribution of gap lengths obtained by adding up the frequencies in the 13 plots above.

In order to explore the appropriateness of the simulation, there are two possible comparisons between the historical and simulated data. One is based on the distribution of average gap length per aircraft, while the other is based on the marginal distribution of gap lengths over all aircraft. Each of the comparisons examines different aspects of the simulation. The first comparison emphasizes the average behavior per aircraft, while the second examines the overall behavior. Still using Sector 453, details of the comparisons are described below.

Using simulation Scheme 1, a visual comparison of the historical versus simulated distributions of average gap lengths per aircraft is given in Figure 2.33 (the truncation point for individual lengths was set equal to 720 seconds in this simulation run). The two distributions are of the same shape. Moreover, the statistics computed from these two sets of data are listed as follows:

$n_1 = 57$ $\quad p_1 = 0.0526$ $\quad \bar{x}_1 = 103.17$ $\quad s_{x_1} = 71.51$

$n_2 = 500$ $\quad p_2 = 0.1020$ $\quad \bar{x}_2 = 113.32$ $\quad s_{x_2} = 83.39$

where subscript "1" indicates "calculated from historical data", subscript "2" indicates "from simulated data", n_i, x_i, and s_{x_i}, $i = 1, 2$, are sample size, mean and standard deviation of mean gap lengths per aircraft respectively, and p_i are the proportions of aircraft which made only one CT (i.e. no intercommunication gaps were observed for the aircraft). In the computation for $\bar{x}_i$ and s_{x_i}, we included only the aircraft which made at least two communication transactions.

Apparently, the distribution of gap lengths consists of two variables of different nature. One is the discrete variable which falls on the point zero indicating no gap being observed. The other is a continuous variable which represents lengths measured from the data. This mixture of discrete with continuous variables makes a formal statistical comparison very difficult, if not impossible. Nevertheless, a comparison of the two sets of statistics listed above indicates that they do not seem to be different.

The results of an experimental run for Scheme 2 are quite similar. The corresponding statistics obtained are $\bar{x}_2 = 121.12$ and $s_{x_2} = 84.72$ which provide evidences for drawing the same conclusion about the adequacy

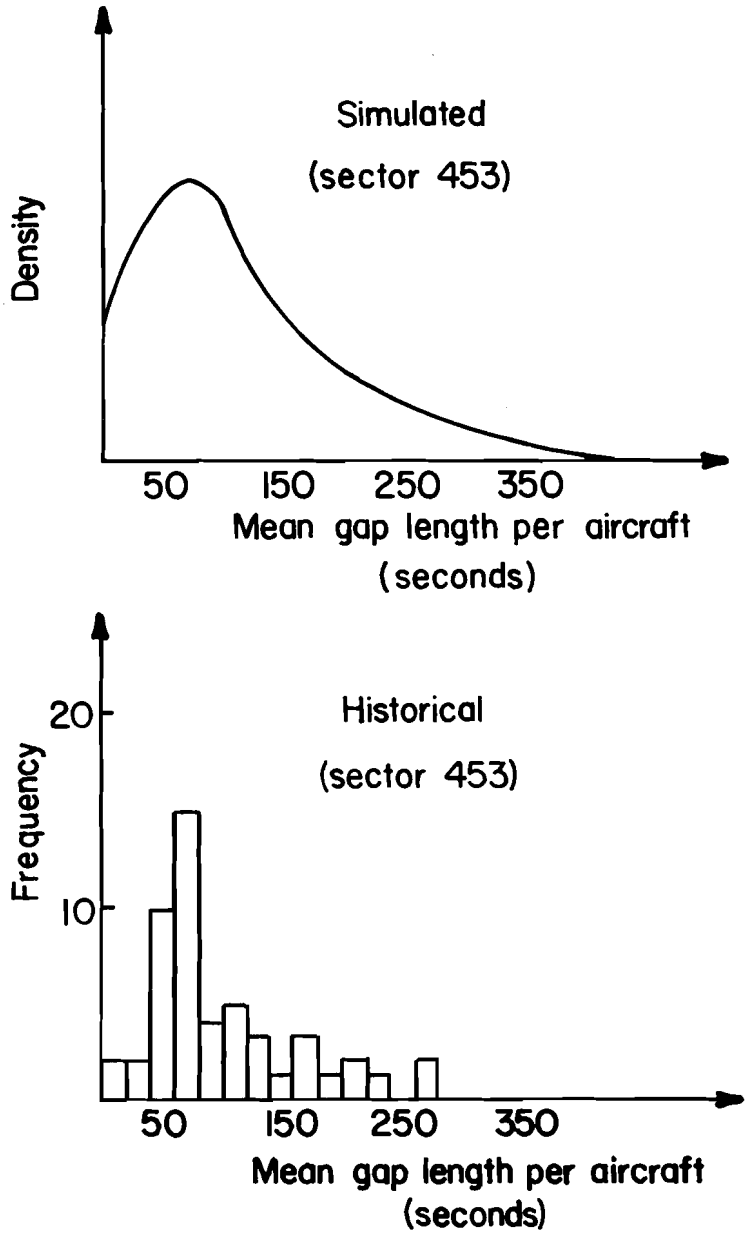

Figure 2.33 Comparison of Historical versus Simulated Mean Gap Length per Aircraft

of the simulation. In the light of the $\bar{x}_2$ calculated, Scheme 1 is more preferable than Scheme 2 for this sector.

Distributions of the sector times directly derived from the intercommunications gap lengths were also examined. For Sector 453, the simulation just described, the use of Scheme 1 produced a set of estimates of the mean and standard deviation almost identical to the historical data. The example using Scheme 2 also produced a pair of values close to that of the historical observations.

Using Scheme 1, the historical and simulated marginal gap length distributions are shown in Figure 2.34. Both have the same exponential-type curve. For the 57 aircraft observed in Sector 453, 250 intercommunication gaps were recorded. On the other hand, 2006 intercommunication gaps were reported for the 500 aircraft generated from the simulation. Detailed data similar to that in the first comparison are listed below:

$$n_1 = 250 \quad p_1 = 0.0526 \quad \bar{x}_1 = 113.54 \quad s_{x_1} = 120.46$$

$$n_2 = 2006 \quad p_2 = 0.1020 \quad \bar{x}_2 = 110.18 \quad s_{x_2} = 118.29.$$

A visual comparison of these statistics indicates that no significant difference can be found between these two sets of data.

Simulations of seven other sectors each selected from different functions were also investigated. Because of the broad structure of Scheme 1 (in fact, Scheme 2 is a special case of Scheme 1) and the favorable results previously obtained from data analyses, Scheme 1 was used in the simulations of these sectors. Statistics similar to those displayed for Sector 453 are summarized in Table 2.3. Most of the evidences confirm the appropriateness of the simulations.

Although the relative advantage of using Scheme 2 over Scheme 1 is still not clear, for the sake of uniformity, we use Scheme 1 in all simulations discussed in the following chapters.

2.5 Summary and Remarks

The structure of the ATC communication simulation model has been described in this chapter. The contents of the GPSS V computer program and the attached subroutines for outputting analyses of responses were illustrated. Output responses and their dynamic interactions, which will be discussed in Chapter 5, were briefly previewed. Detailed formulations of the simulation model for intercommunication gap times and their comparisons were also presented. A sample of the input and output of the simulations is available for review.

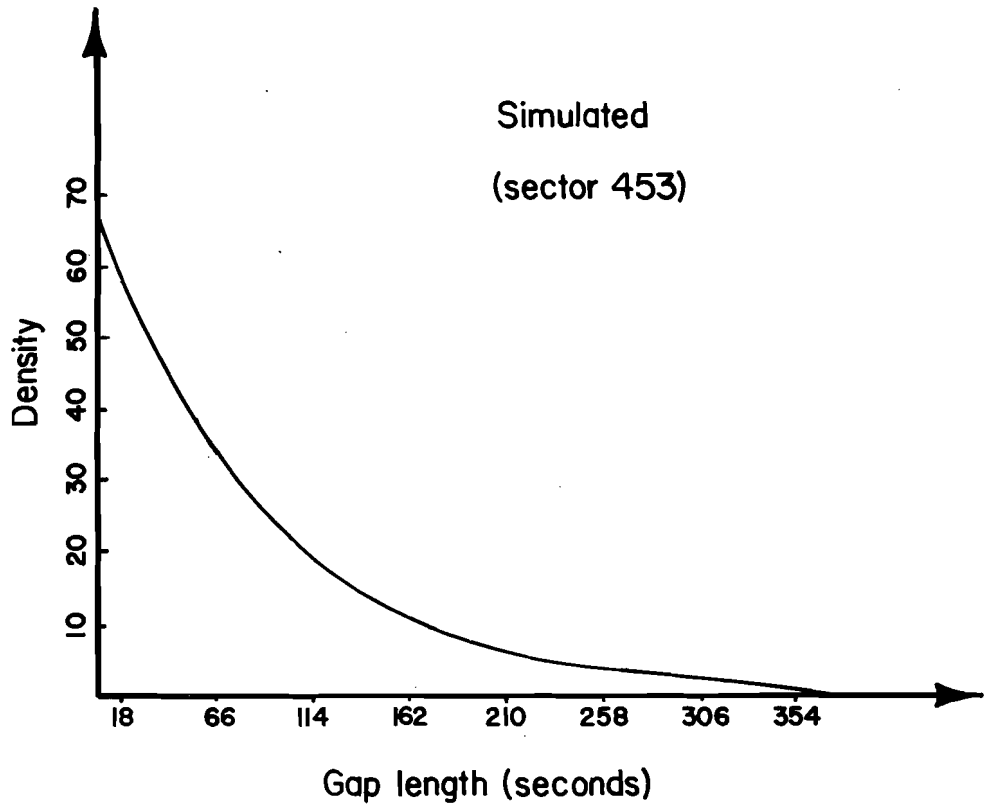

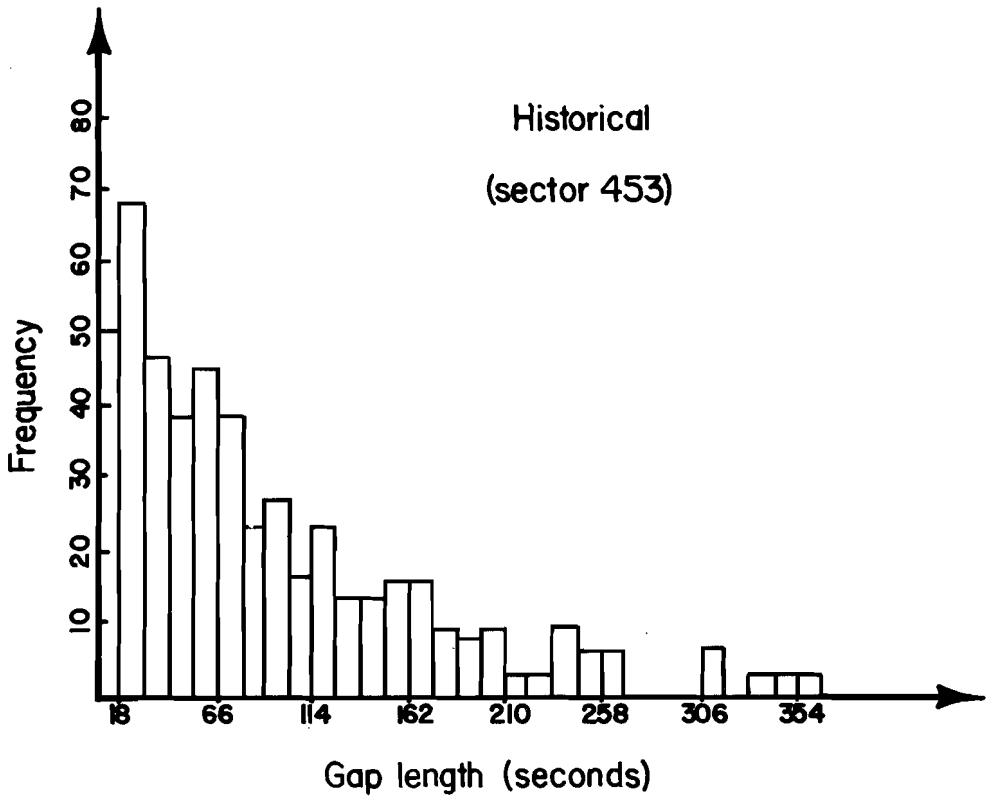

Figure 2.34 Comparison of Historical versus Simulated Gap Lengths

Table 2.3 Comparisons of Historical versus Simulated Gap Length Statistics

Sector ID/data		Percentage of a/c making only one CT (%)	Average gap length per aircraft (A)			Overall gap lengths (B)		
			w	Mean (seconds)	Std. dev. (seconds)	n	Mean (seconds)	Std. dev. (seconds)
453 LT	Historical	5.26	57	103.17	71.51	250	113.54	120.46
	Simulated	10.20	500	113.32	83.39	2006	110.18	118.29
475 HI	Historical	6.45	62	114.39	69.93	263	103.91	98.94
	Simulated	3.60	500	121.33	74.24	2031	107.00	119.38
504 GN	Historical	31.03	87	81.92	74.06	100	86.80	119.72
	Simulated	34.40	500	84.72	89.64	719	95.98	117.12
510 LC	Historical	5.66	53	114.20	88.65	374	104.27	92.13
	Simulated	5.20	500	101.02	78.93	1963	104.56	113.04
524 LG	Historical	6.06	33	144.94	92.95	150	131.28	154.30
	Simulated	6.00	500	133.49	92.35	2086	134.95	139.45
534 DP	Historical	3.50	57	49.09	23.95	203	51.29	45.12
	Simulated	3.60	500	57.66	41.41	1934	58.67	65.44
543 AD	Historical	4.34	23	61.00	47.32	122	62.90	69.77
	Simulated	3.40	500	64.78	44.99	2577	60.10	68.82
553 AR	Historical	6.66	45	78.63	56.50	338	74.59	78.64
	Simulated	0.40	500	87.51	71.31	3632	83.81	100.58

The structure of the simulation model described in this chapter is a natural consequence of the analyses of the communication data. The formulation is not restricted to a specific sector, function, or geographical area. Parameter values employed in the model are different for the different sector functions. Further, sectors in different geographical areas, or those which use different operational facilities (such as the 4096 beacon), can have their characteristics reflected in their master equation parameters. The model structure is offered as applicable to all air/ground communication channels used in an ATC system. Further, the model can be readily adapted to other changes not specifically mentioned thus far. For example, the type of aircraft, the originator of the CT, and the message element comprising a TR can all be modified through simple changes in the program.

Table 2.1 Listing of GPSS Input Statements

```
BLOCK                                                                                STATEMENT
NUMBER  *LOC   OPERATION  A,B,C,D,E,F,G,H,I          COMMENTS                         NUMBER
[A]     ****************************   FUNCTIONS   ************************************   2
         TRCT  FUNCTION   RN1,D14                                                         3
        .125,1/.304,2/.583,3/.737,4/.869,5/.904,6/.946,7/.965,8                           4
        .978,9/.984,10/.990,12/.994,13/.997,14/1,15                                       5
        ****************************   STORAGES    ************************************   6
         SCTR  STORAGE    150                                                             7
        ****************************   MATRICES    ************************************   8
         1     MATRIX     MH,600,1              NAC IN SECTOR                            9
         2     MATRIX     MH,120,1              ARRIVAL TIMES                           10
         3     MATRIX     MH,120,1              CT'S PER AIRCRAFT                       11
         4     MATRIX     MH,400,1              TR'S PER CT                             12
         5     MATRIX     MH,1200,1             TR LENGTHS                              13
         6     MATRIX     MH,400,1              CT LENGTHS                              14
         7     MATRIX     MH,400,1              INTERCOM. GAP LENGTHS                   15
         8     MATRIX     MH,120,1              AC TIME IN SECTOR                       16
         9     MATRIX     MH,120,1              DEPARTURE TIMES                         17
         10    MATRIX     MH,600,1              NAC IN QUEUE                            18
         11    MATRIX     MH,400,1              QUEUEING TIMES                          19
         12    MATRIX     MH,600,1              CHANNEL STATUS                          20
        ****************************   VARIABLES   ************************************  21
         LAMDA FVARIABLE  1.0/(1.7-56.88/XL$AMEAN)                                        22
         ALPHA FVARIABLE  (1.0/XL$PGAM2+2.0)*XL$PGAM2                                     23
        ****************************   SAVEVALUES  ************************************  24
               INITIAL    XL$PNB1,2.51          K FOR CT/AC                             25
               INITIAL    XL$PNB2,0.38          P FOR CT/AC                             26
               INITIAL    XL$PGAP1,4.639        A1 FOR GAP LENGTHS                      27
               INITIAL    XL$PGAP2,-0.016       A2 FOR GAP LENGTHS                      28
               INITIAL    XL$PNBT1,0.0          COMPILING ONLY                          29
               INITIAL    XL$PNBT2,0.0          COMPILING ONLY                          30
               INITIAL    XL$PGAM1,0.0          COMPILING ONLY                          31
               INITIAL    XL$PGAM2,0.0          COMPILING ONLY                          32
               INITIAL    XL$AMEAN,125.48       MEAN INTERARRIVAL TIME                  33
               INITIAL    XH10,453              SECTOR NUMBER                           34
               INITIAL    XF$ONE,73209          RANDOM NUMBER GENERATORS                35
               INITIAL    XF$TWO,15021                                                  36
               INITIAL    XF$THREE,40419                                                37
               INITIAL    XF$FOUR,40219                                                 38
               INITIAL    XF$FIVE,70775                                                 39
               INITIAL    XF$SIX,61369                                                  40
               INITIAL    XF$SEVEN,16213                                                41
               INITIAL    XL$MGAP,0.0           MEAN GAP LENGTH                         42
               INITIAL    XF$XAC,0              # OF CTS PER AC                          43
               INITIAL    XF$TIME,0             CT LENGTHS                              44
               INITIAL    XF$TRL,0              TR LENGTHS                              45
               INITIAL    XF$TGAP,0             INTERCOM. GAPS                          46
               INITIAL    XF$NTR,0              # OF TR'S PER CT                         47
               INITIAL    XF$IAT,0              INTERARRIVAL TIMES                      48
               INITIAL    XF$COUNT,0            SECOND COUNTER FOR MATRIX               49
               INITIAL    XH1,10                MATRIX UNIT COUNTER                     50
               INITIAL    XH2,22                STAT OUTPUT UNIT COUNTER                51
               INITIAL    XH3-XH9,0             MATRIX OUTPUT COUNTERS                  52
               INITIAL    MH1(1-600,1),0        INITIAL MATRICES                        53
               INITIAL    MH2(1-120,1),0                                                54
               INITIAL    MH3(1-120,1),0                                                55
               INITIAL    MH4(1-400,1),0                                                56
```

Table 2.1 Listing of GPSS Input Statements (continued)

```
          INITIAL    MH5(1-1200,1),0
          INITIAL    MH6(1-400,1),0
          INITIAL    MH7(1-400,1),0
          INITIAL    MH8(1-120,1),0
          INITIAL    MH9(1-120,1),0
          INITIAL    MH10(1-600,1),0
          INITIAL    MH11(1-400,1),0
          INITIAL    MH12(1-600,1),0
*****************************   SIMULATION   ***********************************
          SIMULATE
*
* DETERMINE GAMMA PARAMETERS AT BEGINNING OF SIMULATION
          GENERATE   ,,,1,25,0
          SAVEVALUE  PGAM2,V$LAMDA,XL
          SAVEVALUE  PGAM1,V$ALPHA,XL
          TERMINATE
*
* GENERATE POISSON ARRIVALS AT SPECIFIED RATE
          GENERATE   ,,,,15,4PF,1PL
          GATE LR    1
          LOGICS     1
          HELPB      EXPON,AMEAN$XL,IAT$XF,SEVEN$XF,ONE$XF,TWO$XF,FOUR$XF
          ADVANCE    XF$IAT
          LOGICR     1
          MARK                            MARK TIME OF ARRIVAL
*
* SAVE AND TABULATE TIME OF ARRIVAL
          ASSIGN     3,AC1,PF
          SAVEVALUE  3+,1,XH              ARRIVAL COUNTER
          MSAVEVALUE 2,XH3,1,C1,MH        TABULATE ARRIVAL TIME
          ENTER      SCTR                 ENTER THE SECTOR
*
* DETERMINE THE NUMBER OF CT FROM A NEG. BIN. DSN. WITH SHIFTED ORIGIN
          HELPB      SUBNB1,PNB1$XL,PNB2$XL,XAC$XF,ONE$XF,TWO$XF,THREE$XF
          SAVEVALUE  XAC+,1,XF
          MSAVEVALUE 3,XH3,1,XF$XAC,MH    TABULATE CTS PER AIRCRAFT
          ASSIGN     1,XF$XAC,PF
*
* GENERATE MEAN GAP LENGTH FOR ENTERING AIRCRAFT, AS A FUNCTION
*  OF THE NUMBER OF CTS ASSIGNED.
          SAVEVALUE  XAC-,1,XF            NUMBER OF GAPS
          HELPB      GAPM,PGAP1$XL,PGAP2$XL,XAC$XF,MGAP$XL,TWO$XF,THREE$XF
          ASSIGN     1,XL$MGAP,PL
          TRANSFER   ,SCTS                SKIP GAP FOR FIRST CT
*
* ADVANCE INTERCOMMUNICATION GAP TIME, THEN ENTER QUEUE.
*   SEIZE CHANNEL WHEN AVAILABLE.
 SGAP     ADVANCE    XF$TGAP              WAIT TIL GAP COMPLETED
 SCTS     MARK       4PF                  MARK TIME IN QUEUE
          QUEUE      SCTR
          GATE LR    2
          LOGICS     2
 SCTR     SEIZE      CNTRL                SEIZE THE CHANNEL
          DEPART     SCTR
*
* TABULATE TIME IN QUEUE
          SAVEVALUE  9+,1,XH              NUMBER OF QUEUEING TIMES
```

Table 2.1 Listing of GPSS Input Statements (continued)

```
32          MSAVEVALUE 11,XH9,1,MP4PF,MH     TABULATE TIME IN QUEUE
      *
      * GENERATE CT LENGTH
      *    TR'S PER CT FROM EMPIRICAL DISTRIBUTION
      *    TR LENGTHS FROM GAMMA DSN.
33          SAVEVALUE  TIME,0,XF
34          SAVEVALUE  NTR,FN$TRCT,XF        TR'S PER CT
35          SAVEVALUE  4+,1,XH               COUNT OF CT'S
36          MSAVEVALUE 4,XH4,1,XF$NTR,MH     TABULATE TR'S PER CT
37          ASSIGN     2,XF$NTR,PF
38     STRL HELPB      MSSG,PGAM1$XL,PGAM2$XL,NTR$XF,TRL$XF,FIVE$XF,SIX$XF
39          SAVEVALUE  5+,1,XH               COUNT OF TR'S
40          MSAVEVALUE 5,XH5,1,XF$TRL,MH     TABULATE TR LENGTHS
41          SAVEVALUE  TIME+,XF$TRL,XF       ADD TR LENGTH TO CT LENGTH
42          LOOP       2PF,STRL              LOOP FOR MORE TR'S IN CT
43          MSAVEVALUE 6,XH4,1,XF$TIME,MH    TABULATE CT LENGTHS
      *
      * HOLD CHANNEL FOR LENGTH OF CT, THEN FREE CHANNEL.
44          ADVANCE    XF$TIME               WAIT TIL CT COMPLETED
      * IMPOSE MANDATORY GAP OF 1 SECOND BEFORE CHANNEL IS AVAILABLE.
45          SPLIT      1,TEST1
46          RELEASE    CNTRL                 FREE CHANNEL
47          ADVANCE    1                     KEEP CHANNEL CLEAR FOR 1 SECOND
48          LOGICR     2
49          TERMINATE
      *
      * GENERATE INTERCOMMUNICATIONS GAP FROM EXPON. DSN. GIVEN MEAN
      *  GAP LENGTH FOR THE AIRCRAFT.
      * GAPS MUST BE AT LEAST ONE SECOND AND NO MORE THAN 700.
50    TEST1 TEST NE    PF1,K1,SKIP8          NO GAP IF NO CT'S REMAIN
51          SAVEVALUE  MGAP,PL1,XL           RETRIEVE MEAN GAP LENGTH
52    TEST2 HELPB      EXPON,MGAP$XL,TGAP$XF,THREE$XF,TWO$XF,FOUR$XF,FIVE$XF
53          TEST LE    XF$TGAP,700,TEST2     IF OVER 700, TRY AGAIN
54          TEST LE    XF$TGAP,1,SAVE6       IF LESS THAN 1, SET TO 1
55          SAVEVALUE  TGAP,1,XF
56    SAVE6 SAVEVALUE  6+,1,XH               COUNT GAPS
57          MSAVEVALUE 7,XH6,1,XF$TGAP,MH    TABULATE GAP LENGTHS
58          LOOP       1PF,SGAP              LOOP TO MAKE MORE CT'S
      *
      * TABULATE TIME IN SECTOR IF AIRCRAFT ENTERED DURING SAMPLE PERIOD
59    SKIP8 TEST G     PF3,3600,SKIP1
60          SAVEVALUE  7+,1,XH               COUNT OF TIMES IN SECTOR
61          MSAVEVALUE 8,XH7,1,M1,MH         TABULATE TIMES IN SECTOR
      *
      * TABULATE DEPARTURE TIMES
62    SKIP1 SAVEVALUE  8+,1,XH               COUNT OF DEPARTURES
63          MSAVEVALUE 9,XH8,1,C1,MH         TABULATE DEPARTURE TIME
      *
      * LEAVE THE SECTOR
64          LEAVE      SCTR
65          TERMINATE
      ****************************   NAC STATS   ************************************
      *          THIS SECTION OF THE PROGRAM KEEPS TRACK OF THE NUMBER OF
      *     AIRCRAFT IN THE SECTOR IN EACH SECOND AND HAS THE DATA PUNCHED
      *     FOR LATER ANALYSIS.
      *
66          GENERATE   1,,3601,,2,0          SECOND TIMER
```

Table 2.1 Listing of GPSS Input Statements (continued)

```
67          SAVEVALUE  COUNT+,K1,XF          COUNT SECONDS
68          MSAVEVALUE 1,XF$COUNT,1,S1,MH    TABULATE NAC IN SECTOR
69          MSAVEVALUE 10,XF$COUNT,1,Q1,MH   TABULATE NAC IN QUEUE
70          MSAVEVALUE 12,XF$COUNT,1,F1,MH   TABULATE CHANNEL STATUS
71          TERMINATE
72          GENERATE   600,,4200,,1,0        TEN-MINUTE TIMER
73          SAVEVALUE  1+,K1,XH              MATRIX OUTPUT UNIT
74          HELPC      TIME5,MH1(1,1),MH10(1,1),MH12(1,1),XH1,XF$ONE,XF$TWO
75          SAVEVALUE  COUNT,KC,XF           SET SECOND COUNT TO ZERO
76          TERMINATE
77          GENERATE   3600,,7200,,3,0       HOUR TIMER
78          SAVEVALUE  2+,K1,XH              STAT OUTPUT UNIT
79          HELPC      PASS2,XH2,XF$ONE,XF$TWO,XF$THREE,XF$FOUR,XF$FIVE
80          SAVEVALUE  3-9,0,XH              SET COUNTS BACK TO ZERO
81          TERMINATE
82          GENERATE   3600,,3600,1,4,0      INITIAL MATRIX CLEARER
83          SAVEVALUE  3-9,0,XH              SET COUNTS TO ZERO
84          TERMINATE
[D]   ****************************   TIMER   ****************************************
85          GENERATE   3600
86          TERMINATE  1
            START      1,NP
            RESET
[E]         START      2
      ****************************   OUTPUT   ****************************************
            REPORT
            EJECT
      ****** GPSS SIMULATION MODEL FOR ATC VERBAL COMMUNICATIONS SYSTEM *****
      *                        TRANSPORTATION PROGRAM
      *                      DEPT. OF CIVIL ENGINEERING
      *                         PRINCETON UNIVERSITY
      *                              MARCH, 1974
      *
      *
 2    TEXT       INPUT PARAMETERS - SECTOR #XH10,2/XXX#
      *
 5    TEXT       (1) AIRCRAFT INTERARRIVAL TIMES: EXPONENTIAL WITH MEA*
N = #XL1,2/XXXX.XXX# SECONDS
 5    TEXT       (2) TRANSACTIONS PER AIRCRAFT: SHIFTED NEGATIVE BINOM*
IAL WITH K = #XL3,2/XXX.XXX# AND P = #XL4,2/XXX.XXX#
 5    TEXT       (3) TRANSMISSIONS PER TRANSACTION: EMPIRICAL DISTRIBU*
TION
 5    TEXT       (4) TRANSMISSIONS LENGTHS: GAMMA WITH P = #XL2,2/XXX.*
XXXX# AND ALPHA = #XL9,2/XXX.XXXX#
 5    TEXT              (NOTE: GAMMA PARAMETERS DETERMINED FROM EXPECT*
ED ARRIVAL RATE)
 5    TEXT       (5) INTERCOMMUNICATION GAP LENGTHS ARE A FUNCTION OF *
TRANSACTIONS PER AIRCRAFT
*
*
*     SIMULATION RESPONSE - 2 HOUR ANALYSIS
*
*   (1) SECTOR AIRCRAFT LOADING
 10   TEXT       NUMBER OF AIRCRAFT IDENTIFIED IN SECTOR = #S1,5/XXXX#
 10   TEXT       AVERAGE NUMBER OF AIRCRAFT PER SECOND = #S1,3/XXX.XXX*
#
 10   TEXT       MAXIMUM NUMBER OF AIRCRAFT PER SECOND = #S1,8/XXX#
```

Table 2.1 Listing of GPSS Input Statements (continued)

```
*
*     (2) COMMUNICATIONS CHANNEL LOADING
 10     TEXT        AVERAGE CHANNEL UTILIZATION = #F1,2/X.XXX#
 10     TEXT        TOTAL NUMBER OF TRANSACTIONS = #F1,3/XXXX#
 10     TEXT        AVERAGE LENGTH OF TRANSACTIONS = #F1,4/XXX.XXX# SECON*
DS
*
*     (3) CHANNEL QUEUEING EFFECTS
 10     TEXT        AVERAGE TIME IN QUEUE = #Q1,7/XXXX.XXX# SECONDS
 10     TEXT        AVERAGE TIME EXCLUDING ZERO ENTRIES = #Q1,8/XXXX.XXX#*
 SECONDS
 10     TEXT        TOTAL ENTRIES INTO QUEUE = #Q1,4/XXXX#
 10     TEXT        NUMBER OF ZERO ENTRIES (NON-WAITING) = #Q1,5/1LXXXX#
 10     TEXT        PERCENT OF ZERO ENTRIES = #Q1,6/XXX.X#
 10     TEXT        AVERAGE NUMBER OF AIRCRAFT IN QUEUE = #Q1,3/XXX.XXX#
 10     TEXT        MAXIMUM NUMBER OF AIRCRAFT IN QUEUE = #Q1,2/XXX#
        EJECT
****************************   END   ****************************************
        END
        END
```

GPSS SIMULATION OUTPUT - DISTRIBUTION OF AIRCRAFT INTERARRIVAL TIMES

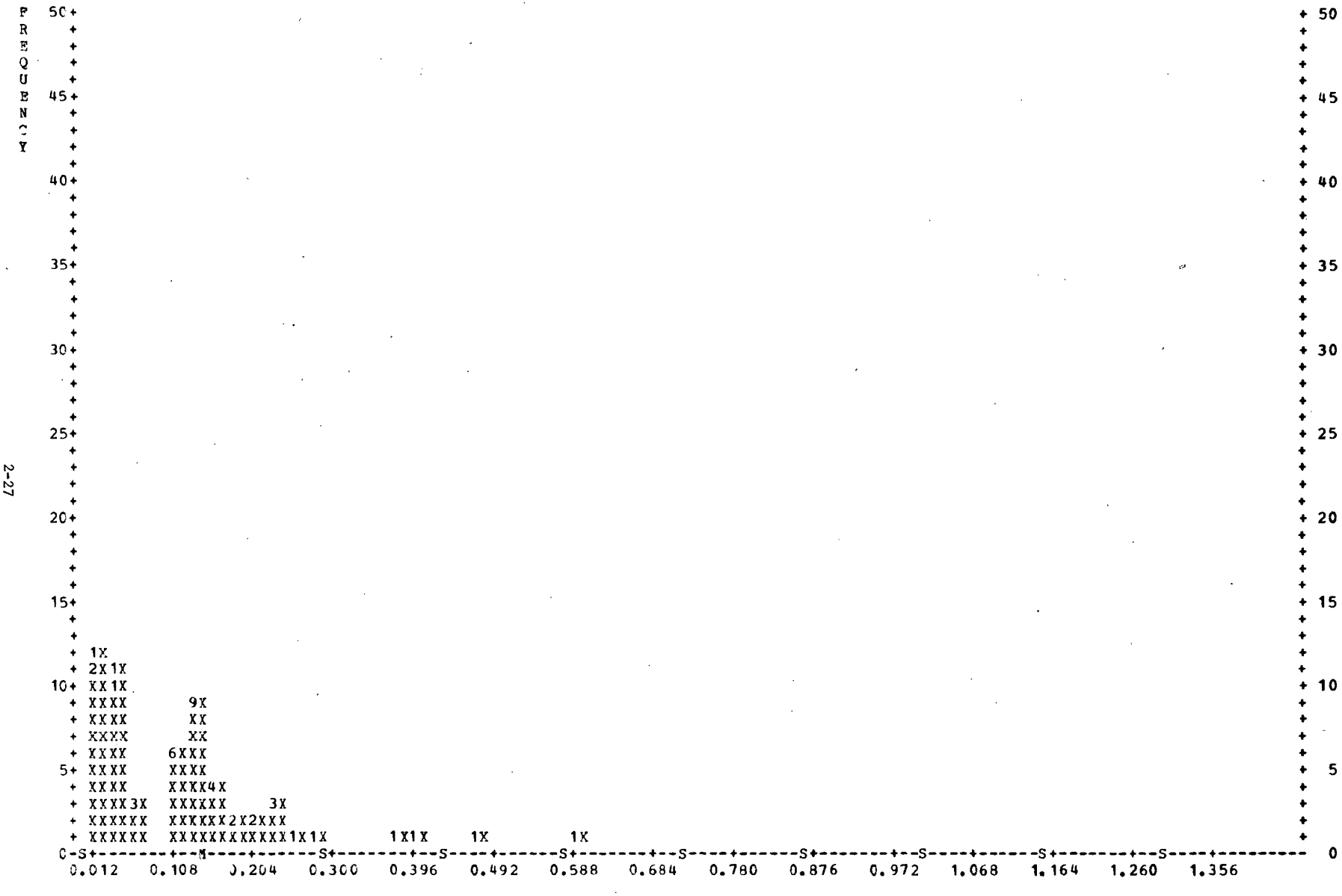

NUMBER OF CLASSES= 50 DATA POINTS ON GRAPH= 58 DATA POINTS OFF GRAPH= 0

MEAN	VARIANCE	ST. DEV.	SKEWNESS	KURTOSIS	ST. SKEW.	ST. KURT.
121.0690	14313.2148	119.6378	1.8436	3.9099	5.7320	6.0782

Figure 2.3 Histogram of Aircraft Interarrival Times from GPSS V Simulation

GPSS SIMULATION OUTPUT - DISTRIBUTION OF TRANSACTIONS PER AIRCRAFT

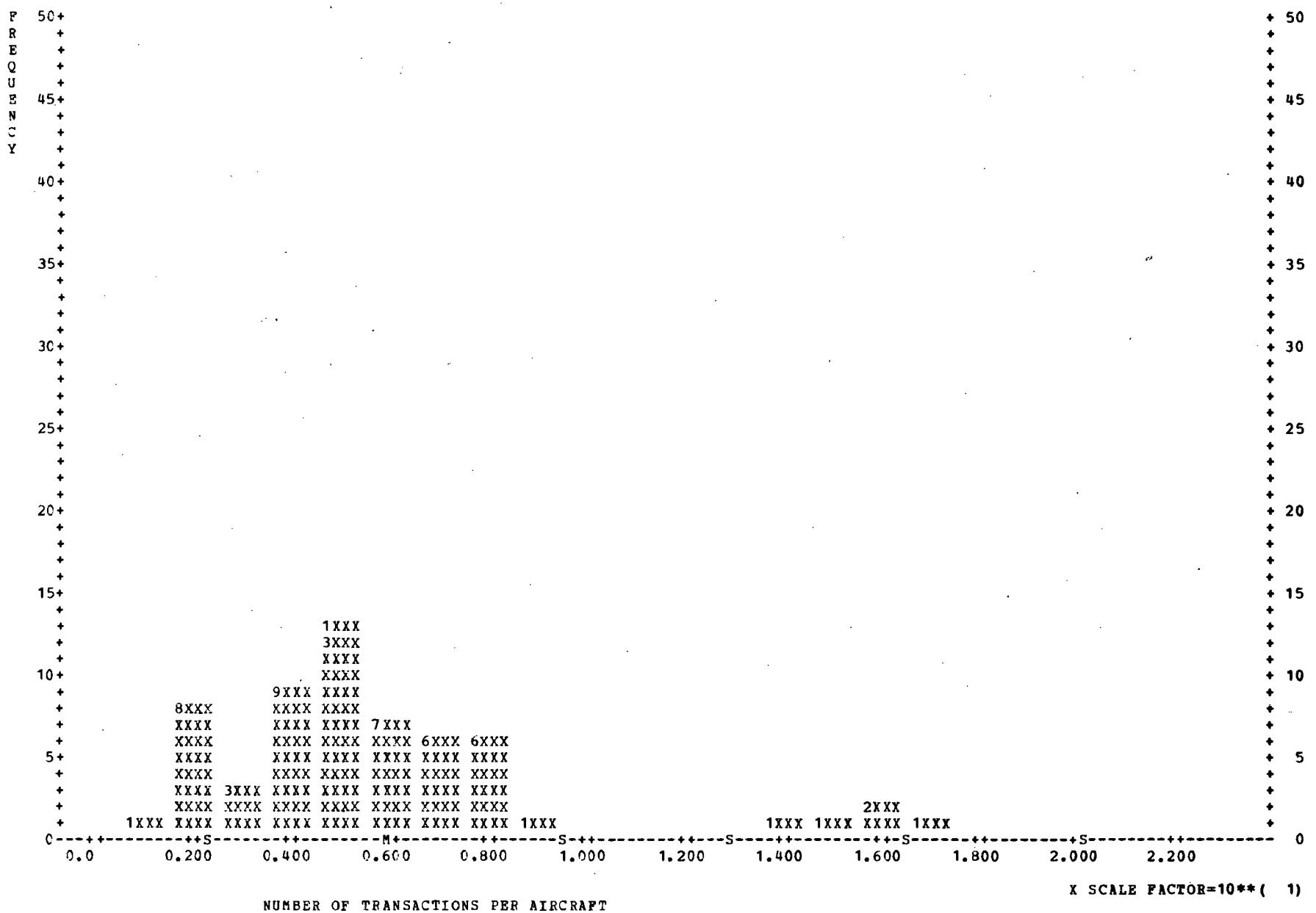

NUMBER OF TRANSACTIONS PER AIRCRAFT

NUMBER OF CLASSES= 24 DATA POINTS ON GRAPH= 59 DATA POINTS OFF GRAPH= 0

MEAN	VARIANCE	ST. DEV.	SKEWNESS	KURTOSIS	ST. SKEW.	ST. KURT.
5.8644	12.6364	3.5548	1.6059	2.5713	5.0358	4.0315

Figure 2.4 Histogram of the Number of Transactions per Aircraft from GPSS V Simulation

GPSS SIMULATION OUTPUT - DISTRIBUTION OF TRANSMISSIONS PER TRANSACTION

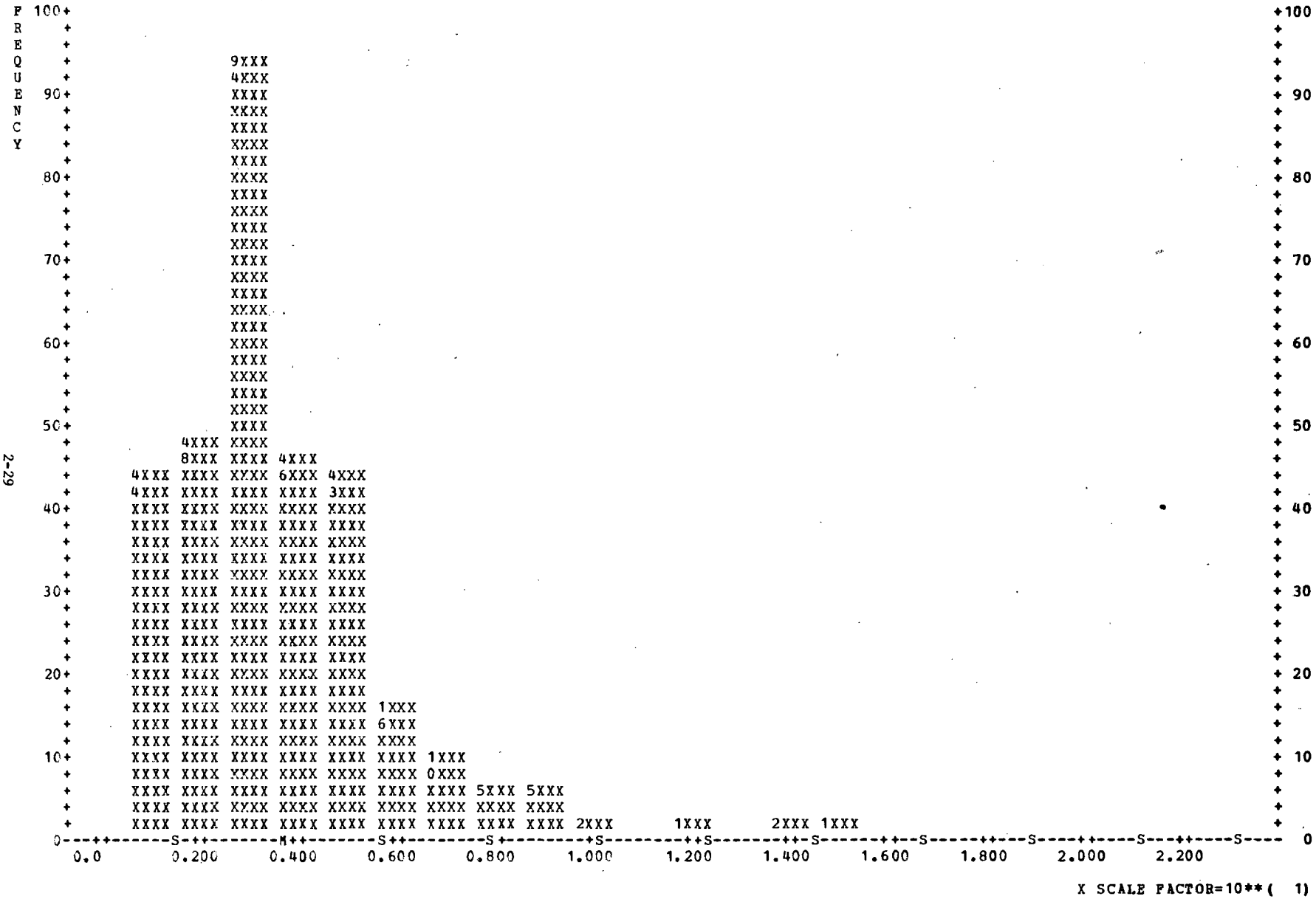

NUMBER OF TRANSMISSIONS PER TRANSACTION

NUMBER OF CLASSES= 24 DATA POINTS ON GRAPH= 317 DATA POINTS OFF GRAPH= 0

MEAN	VARIANCE	ST. DEV.	SKEWNESS	KURTOSIS	ST. SKEW.	ST. KURT.
3.6183	4.7303	2.1749	1.7635	5.3274	12.8185	19.3616

Figure 2.5 Histogram of the Number of Transmissions per Transaction from GPSS V Simulation

GPSS SIMULATION OUTPUT - DISTRIBUTION OF TRANSMISSION LENGTHS

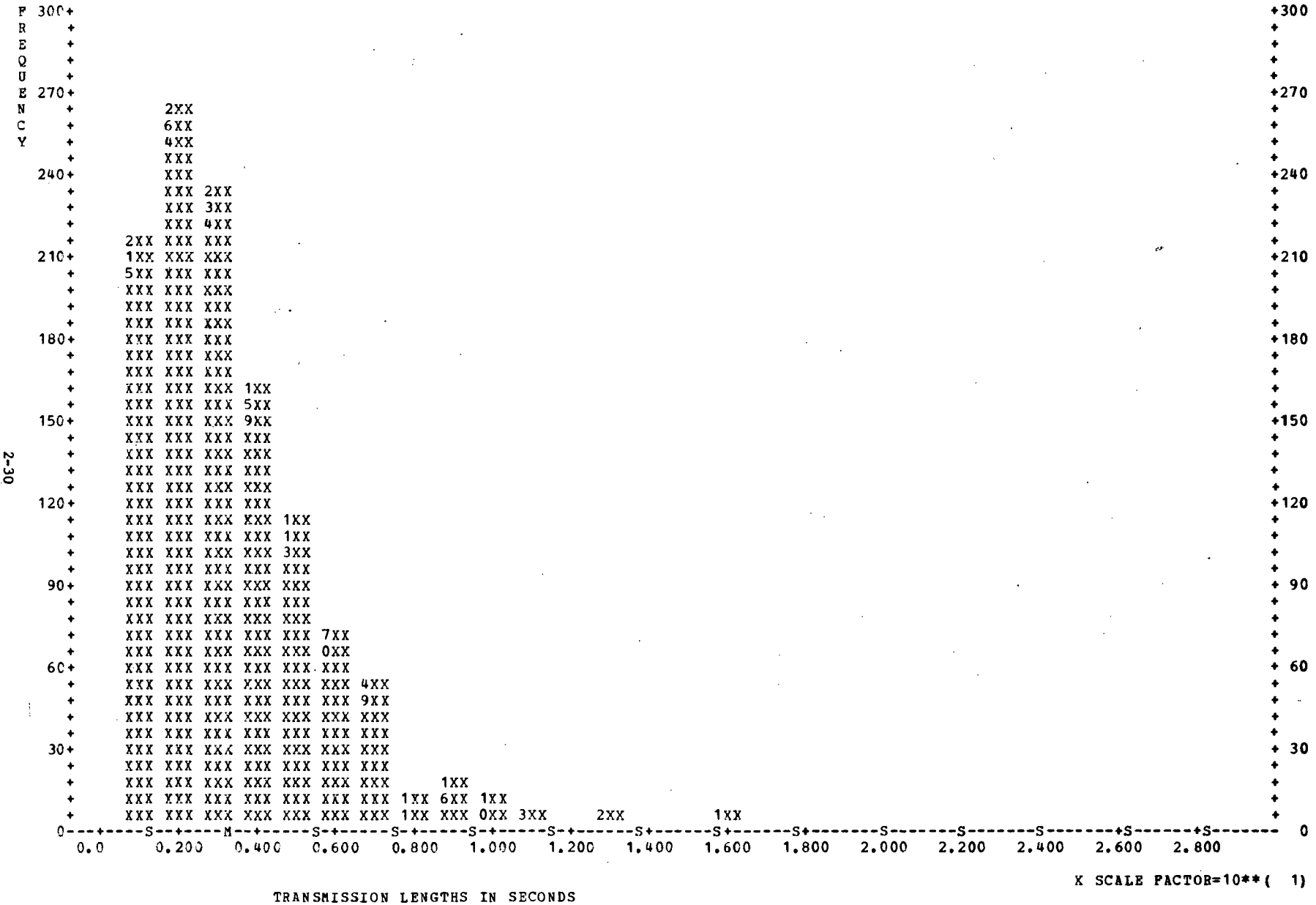

TRANSMISSION LENGTHS IN SECONDS

NUMBER OF CLASSES= 30 DATA POINTS ON GRAPH= 1147 DATA POINTS OFF GRAPH= 0

MEAN	VARIANCE	ST. DEV.	SKEWNESS	KURTOSIS	ST. SKEW.	ST. KURT.
3.3269	4.3002	2.0737	1.2946	2.4730	17.8993	17.0963

Figure 2.6 Histogram of Transmission Lengths from GPSS V Simulation

GPSS SIMULATION OUTPUT - DISTRIBUTION OF TRANSACTION LENGTHS

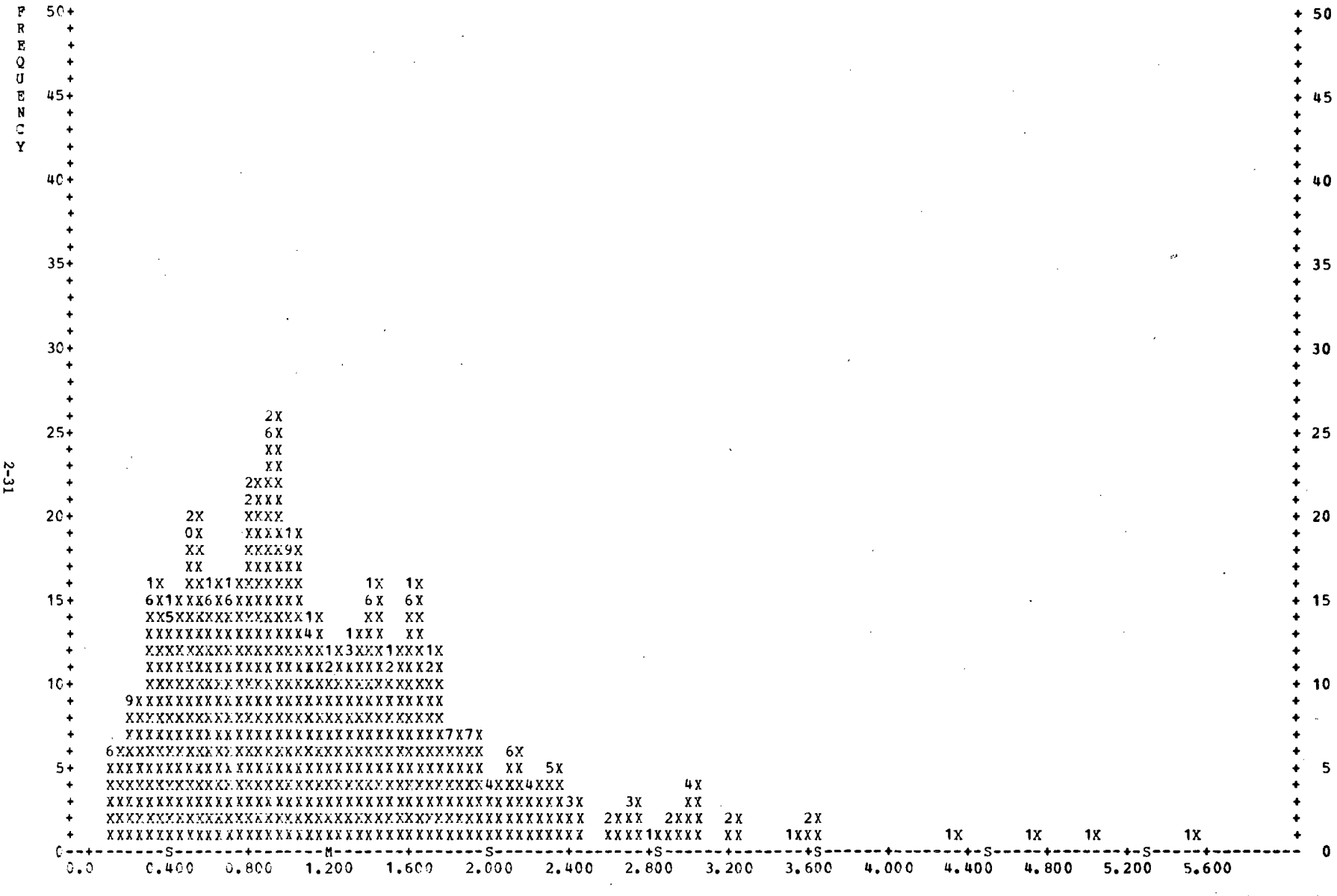

TRANSACTION LENGTHS IN SECONDS

NUMBER OF CLASSES= 60 DATA POINTS ON GRAPH= 317 DATA POINTS OFF GRAPH= 0

MEAN	VARIANCE	ST. DEV.	SKEWNESS	KURTOSIS	ST. SKEW.	ST. KURT.
12.0379	67.0412	8.1879	1.6835	4.5782	12.2364	16.6388

Figure 2.7 Histogram of Transaction Lengths from GPSS V Simulation

GPSS SIMULATION OUTPUT - DISTRIBUTION OF INTERCOMMUNICATION GAP LENGTHS

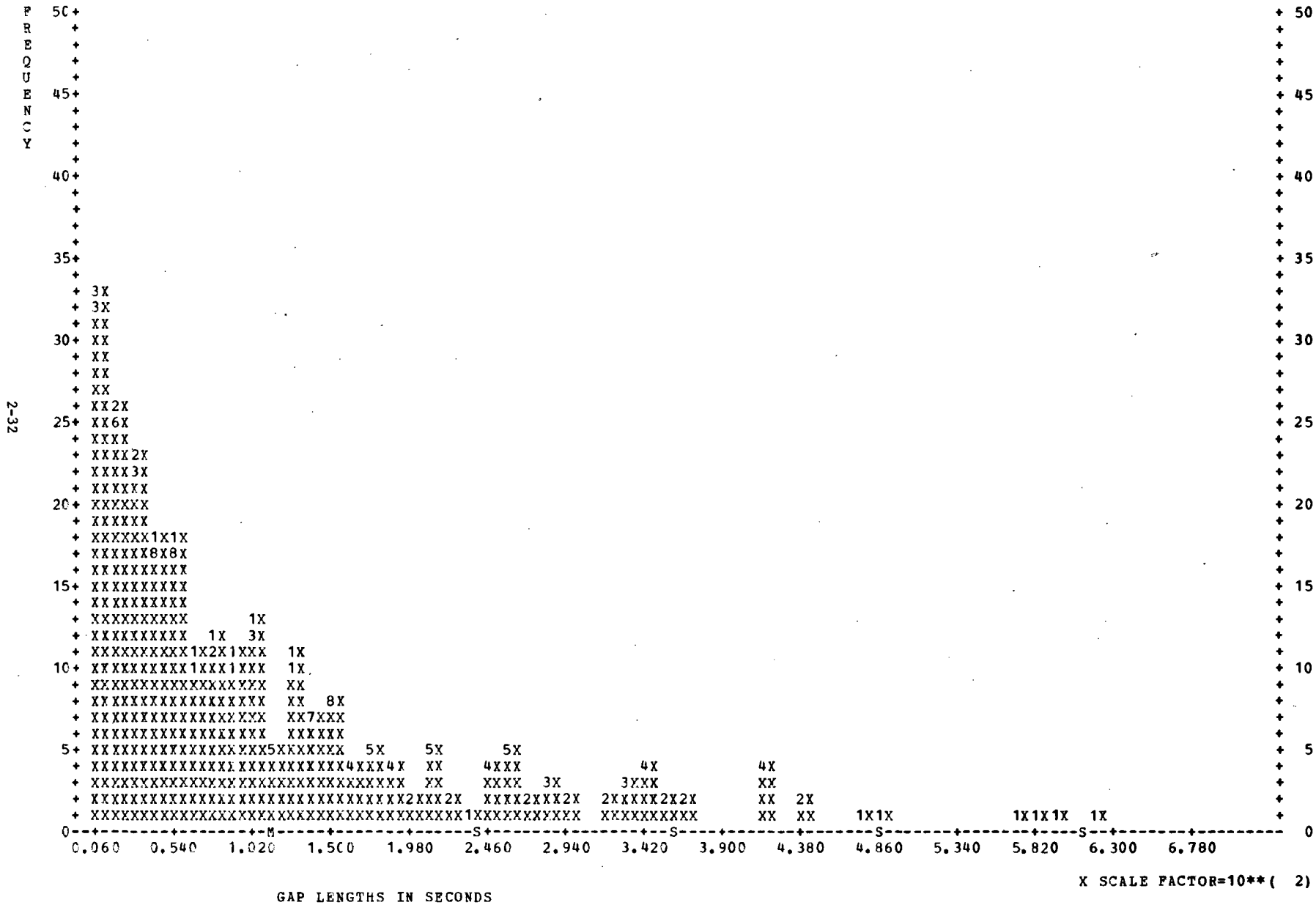

NUMBER OF CLASSES= 60 DATA POINTS ON GRAPH= 260 DATA POINTS OFF GRAPH= 0

MEAN	VARIANCE	ST. DEV.	SKEWNESS	KURTOSIS	ST. SKEW.	ST. KURT.
115.1962	15266.5000	123.5577	1.6701	2.6951	10.9942	8.8707

Figure 2.8 Histogram of Intercommunication Gap Lengths from GPSS V Simulation

GPSS SIMULATION OUTPUT - DISTRIBUTION OF AIRCRAFT TIME IN SECTOR

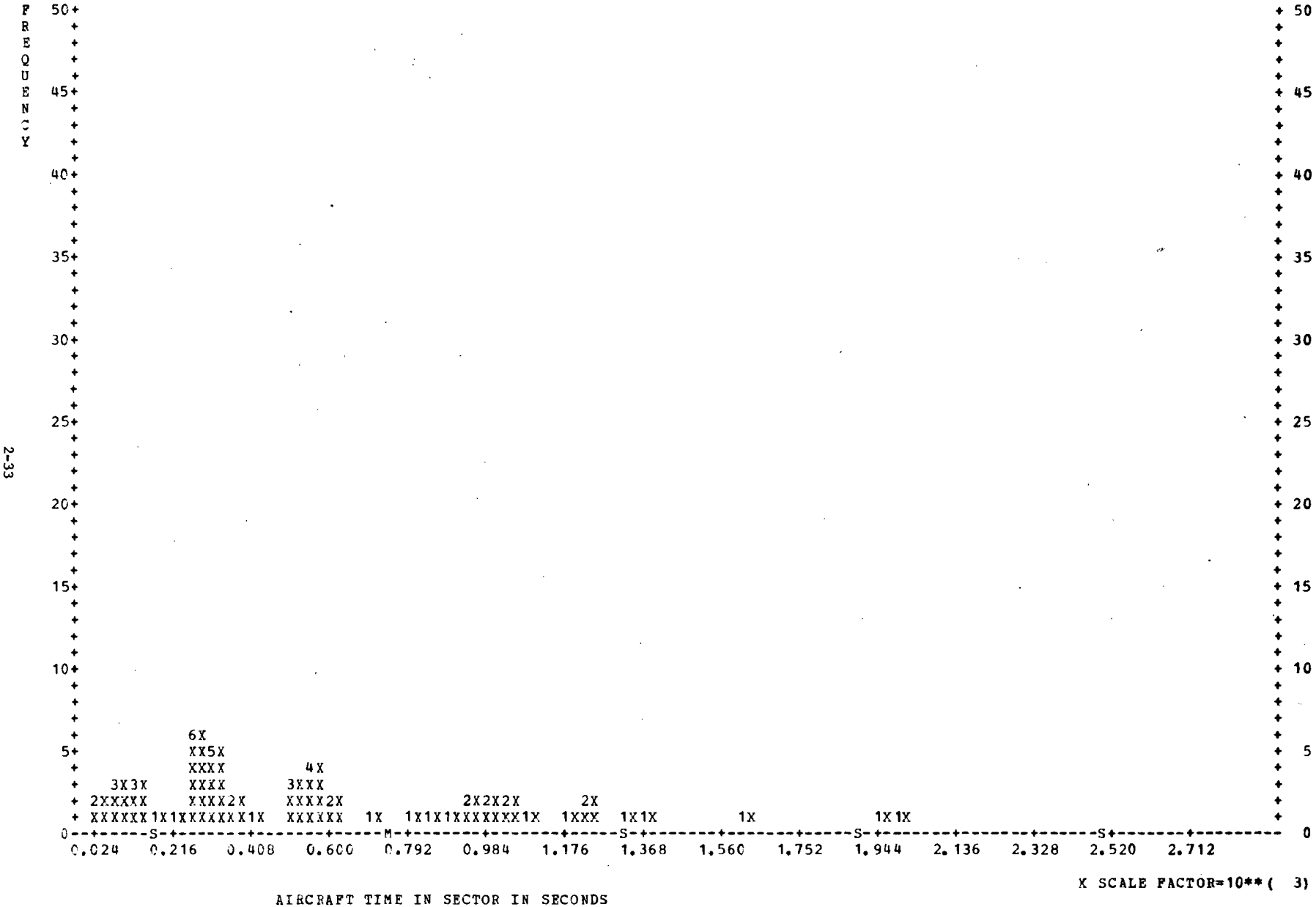

AIRCRAFT TIME IN SECTOR IN SECONDS

NUMBER OF CLASSES= 50 DATA POINTS ON GRAPH= 52 DATA POINTS OFF GRAPH= 0

MEAN	VARIANCE	ST. DEV.	SKEWNESS	KURTOSIS	ST. SKEW.	ST. KURT.
620.3076	235694.0625	485.4834	0.9911	0.4159	2.9176	0.6121

Figure 2.9 Histogram of Aircraft Times in Sector from GPSS V Simulation

GPSS SIMULATION OUTPUT - DISTRIBUTION OF AIRCRAFT INTERDEPARTURE TIMES

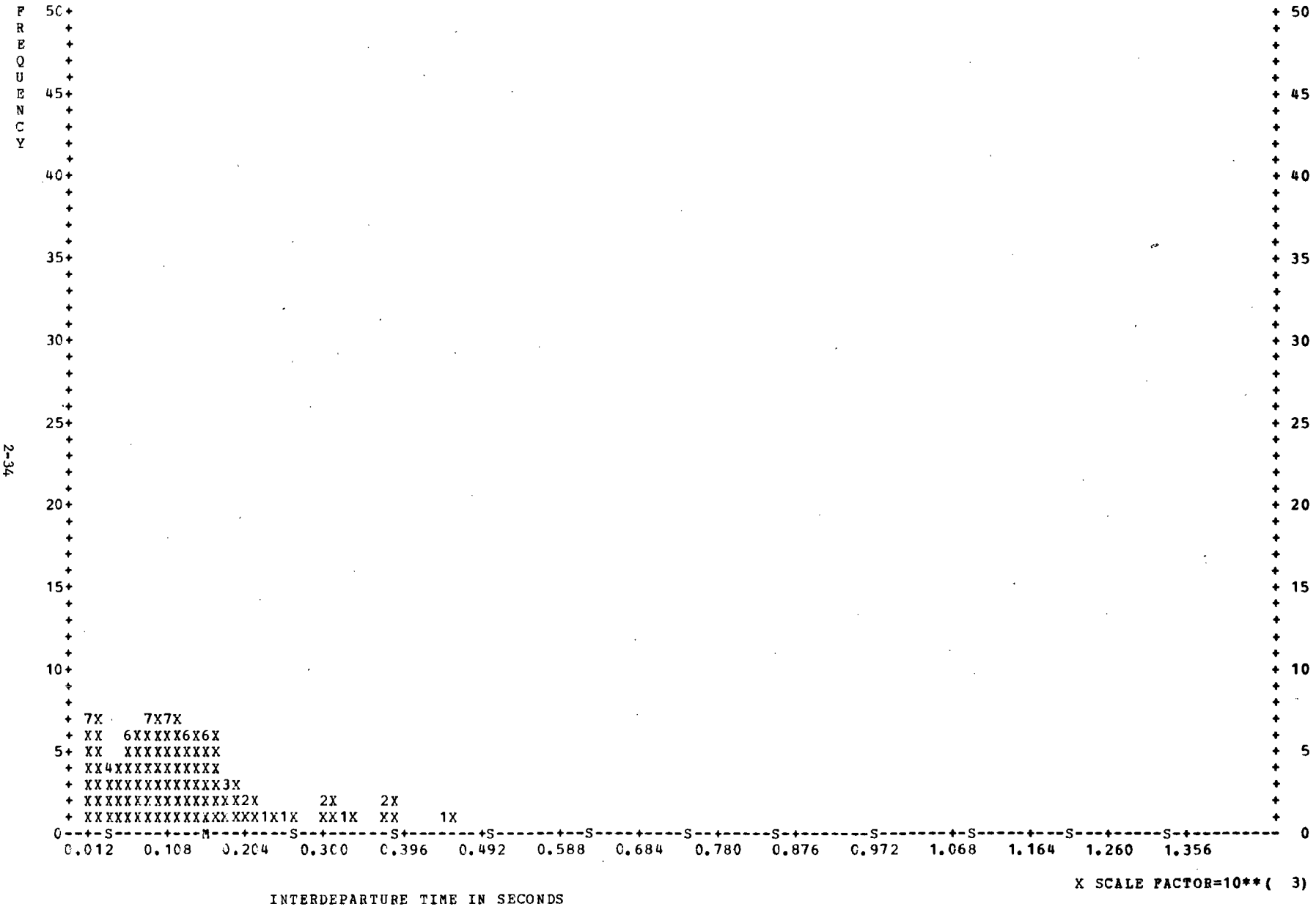

INTERDEPARTURE TIME IN SECONDS

NUMBER OF CLASSES= 50 DATA POINTS ON GRAPH= 56 DATA POINTS OFF GRAPH= 0

MEAN	VARIANCE	ST. DEV.	SKEWNESS	KURTOSIS	ST. SKEW.	ST. KURT.
127.0536	9629.6172	98.1306	1.2119	1.2482	3.7025	1.9066

Figure 2.10 Histogram of Aircraft Interdeparture Times from GPSS V Simulation

GPSS SIMULATION OUTPUT - DISTRIBUTION OF QUEUEING TIMES

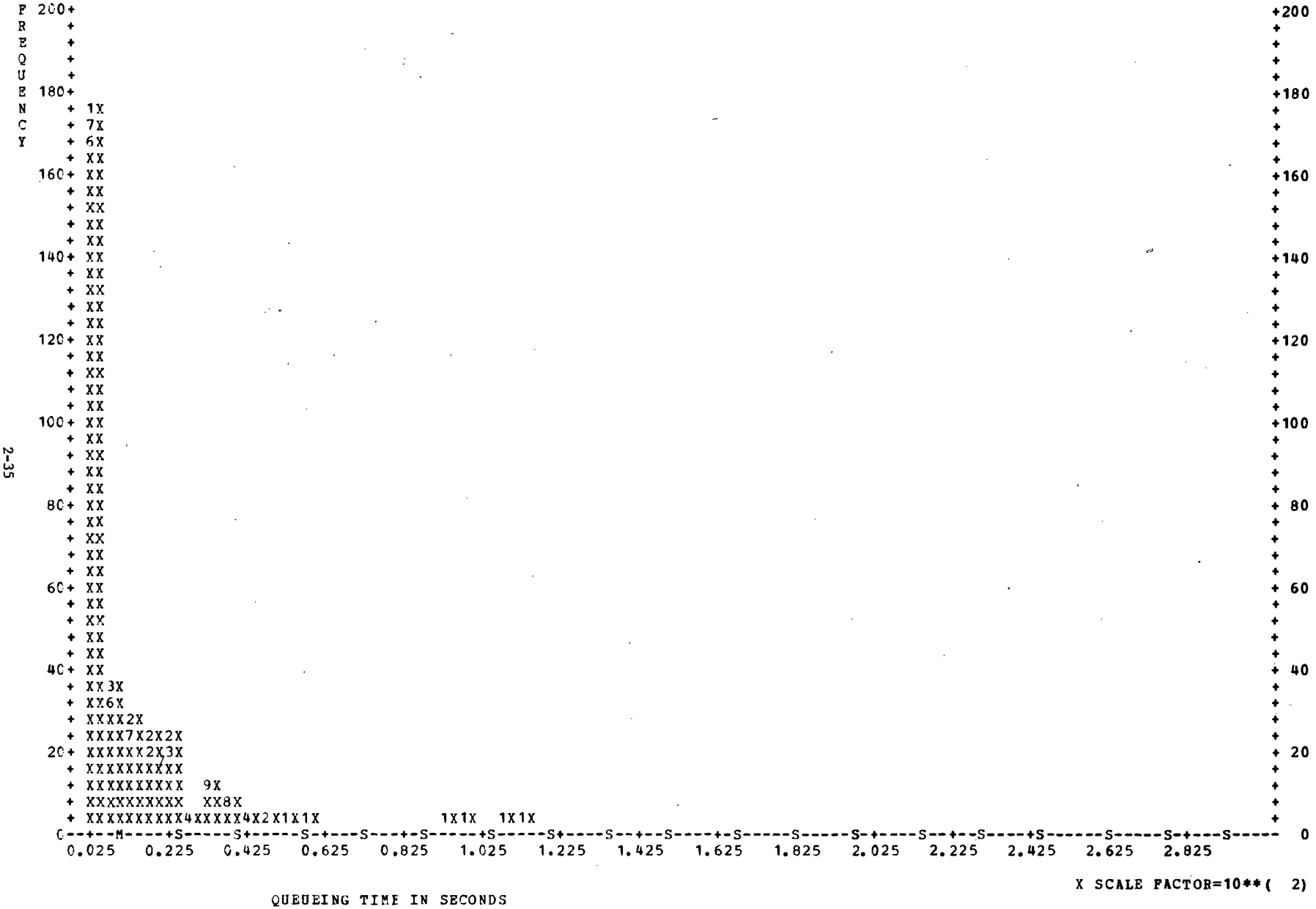

NUMBER OF CLASSES= 60 DATA POINTS ON GRAPH= 317 DATA POINTS OFF GRAPH= 0

MEAN	VARIANCE	ST. DEV.	SKEWNESS	KURTOSIS	ST. SKEW.	ST. KURT.
9.4038	248.3010	15.7576	3.2390	14.7600	23.5431	53.6426

Figure 2.11 Histogram of Channel Queuing Times from GPSS V Simulation

GPSS SIMULATION OUTPUT - DISTRIBUTION OF NUMBER OF AIRCRAFT IN SECTOR

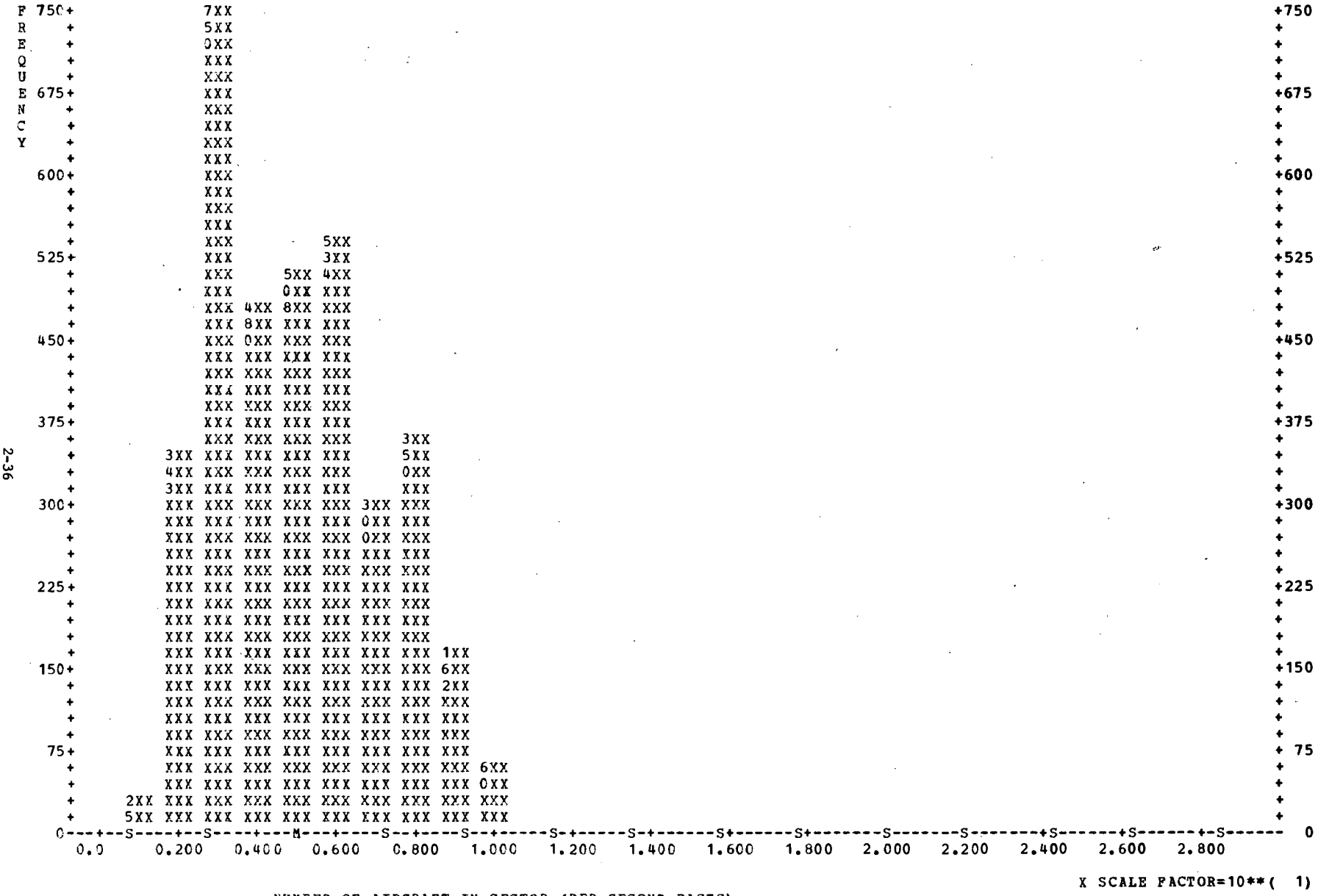

NUMBER OF AIRCRAFT IN SECTOR (PER-SECOND BASIS)

NUMBER OF CLASSES= 30 DATA POINTS ON GRAPH= 7200 DATA POINTS OFF GRAPH= 0

THE CELL COUNTS HAVE BEEN SCALED BY A FACTOR OF 0.48828

MEAN	VARIANCE	ST. DEV.	SKEWNESS	KURTOSIS	ST. SKEW.	ST. KURT.
5.0064	4.5438	2.1316	0.3707	-0.8011	12.8423	-13.8762

Figure 2.12 Histogram of the Number of Aircraft in the Sector per Second from GPSS V Simulation

GPSS SIMULATION OUTPUT - DISTRIBUTION OF NUMBER OF AIRCRAFT IN QUEUE

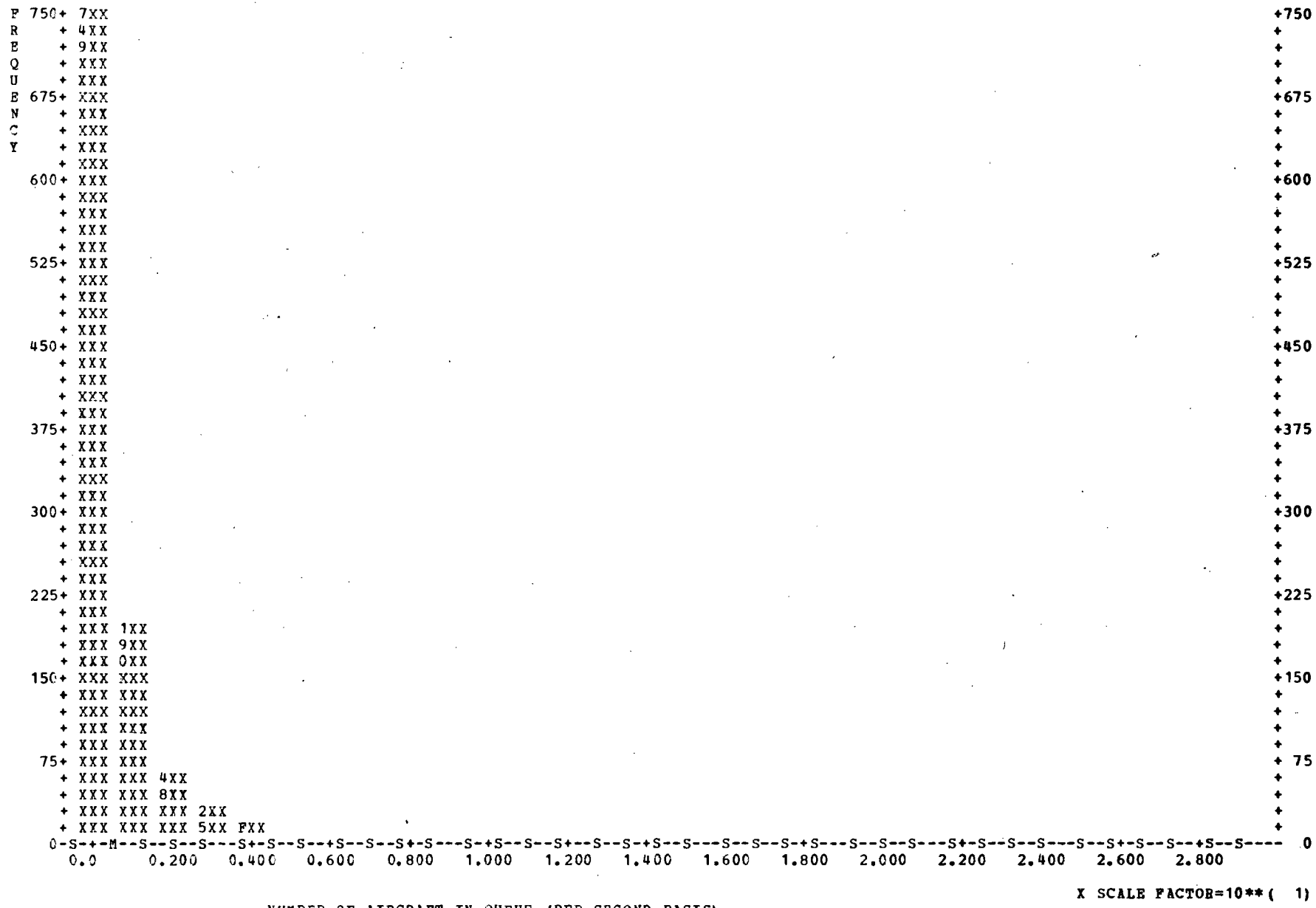

NUMBER OF AIRCRAFT IN QUEUE (PER-SECOND BASIS)

NUMBER OF CLASSES= 30 DATA POINTS ON GRAPH= 7200 DATA POINTS OFF GRAPH= 0

THE CELL COUNTS HAVE BEEN SCALED BY A FACTOR OF 0.14305

MEAN	VARIANCE	ST. DEV.	SKEWNESS	KURTOSIS	ST. SKEW.	ST. KURT.
0.4136	0.6662	0.8162	2.3941	5.9682	82.9333	103.3718

Figure 2.13 Histogram of the Number of Aircraft in the Queue per Second from GPSS V Simulation

GPSS SIMULATION OUTPUT - DISTRIBUTION OF THE DURATION OF NON-ZERO QUEUEING

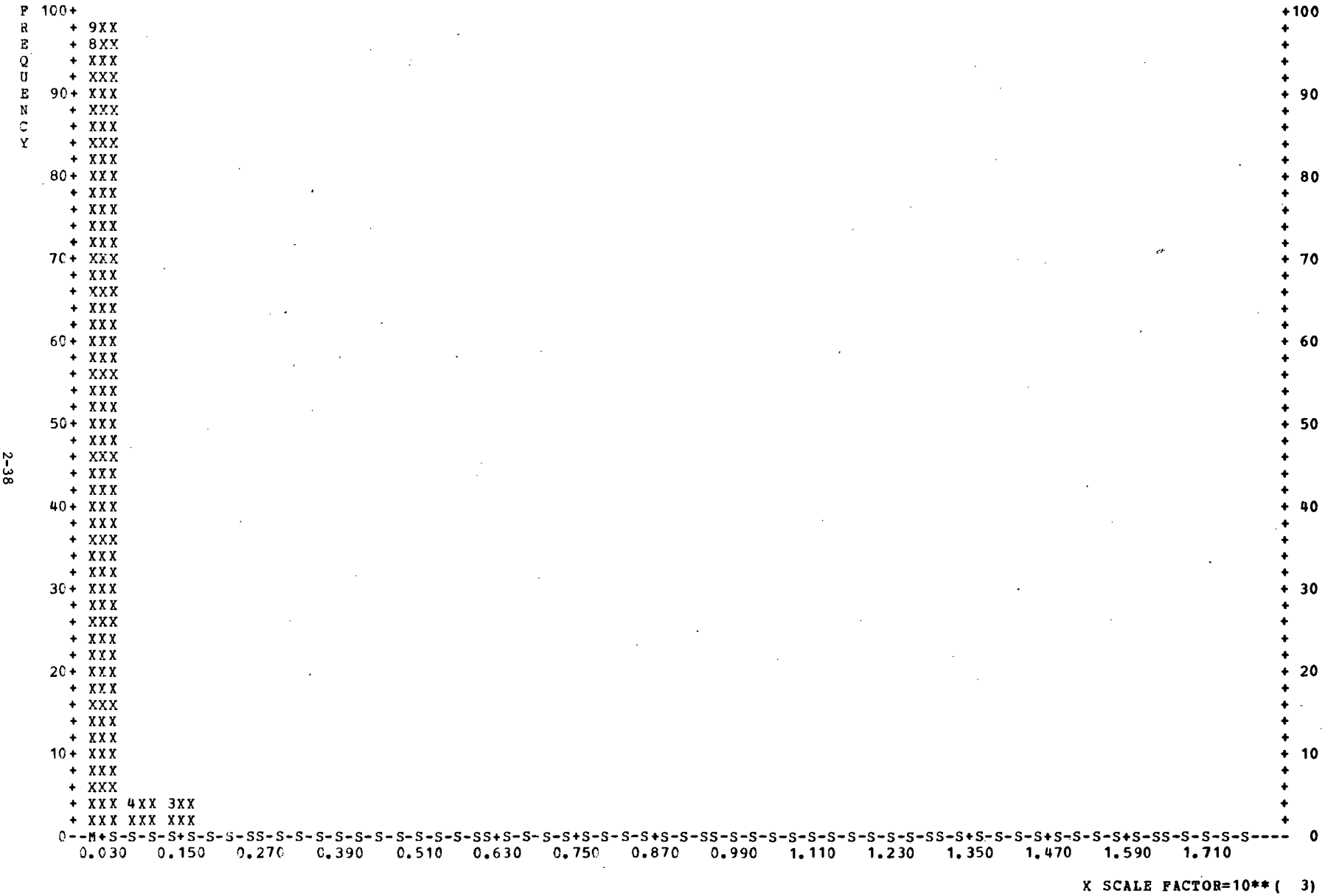

DURATION OF NON-ZERO QUEUE IN SECONDS

NUMBER OF CLASSES= 30 DATA POINTS ON GRAPH= 105 DATA POINTS OFF GRAPH= 0

MEAN	VARIANCE	ST. DEV.	SKEWNESS	KURTOSIS	ST. SKEW.	ST. KURT.
18.5905	825.5420	28.7323	3.5878	14.4498	15.0088	30.2238

Figure 2.14 Histogram of the Durations of Non-Zero Queuing from GPSS V Simulation

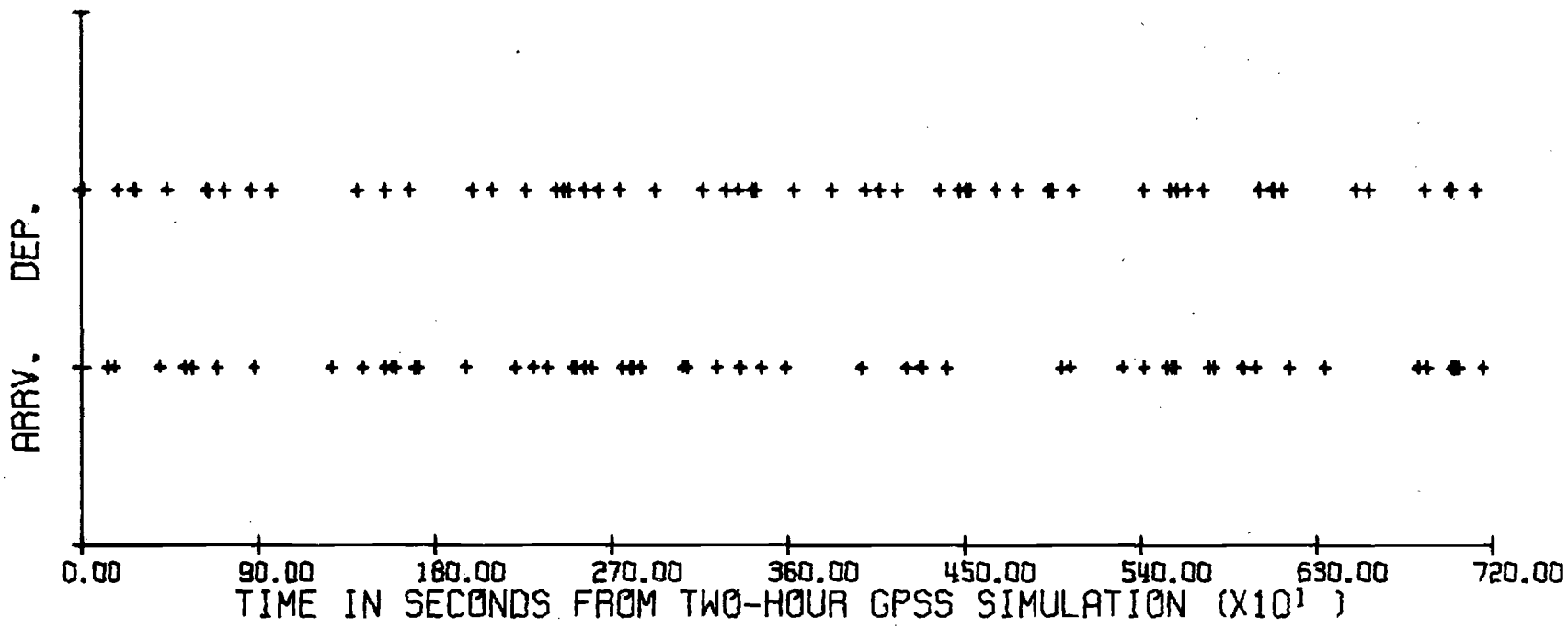

Figure 2.15 Plot of Arrivals and Departures from GPSS V Simulation

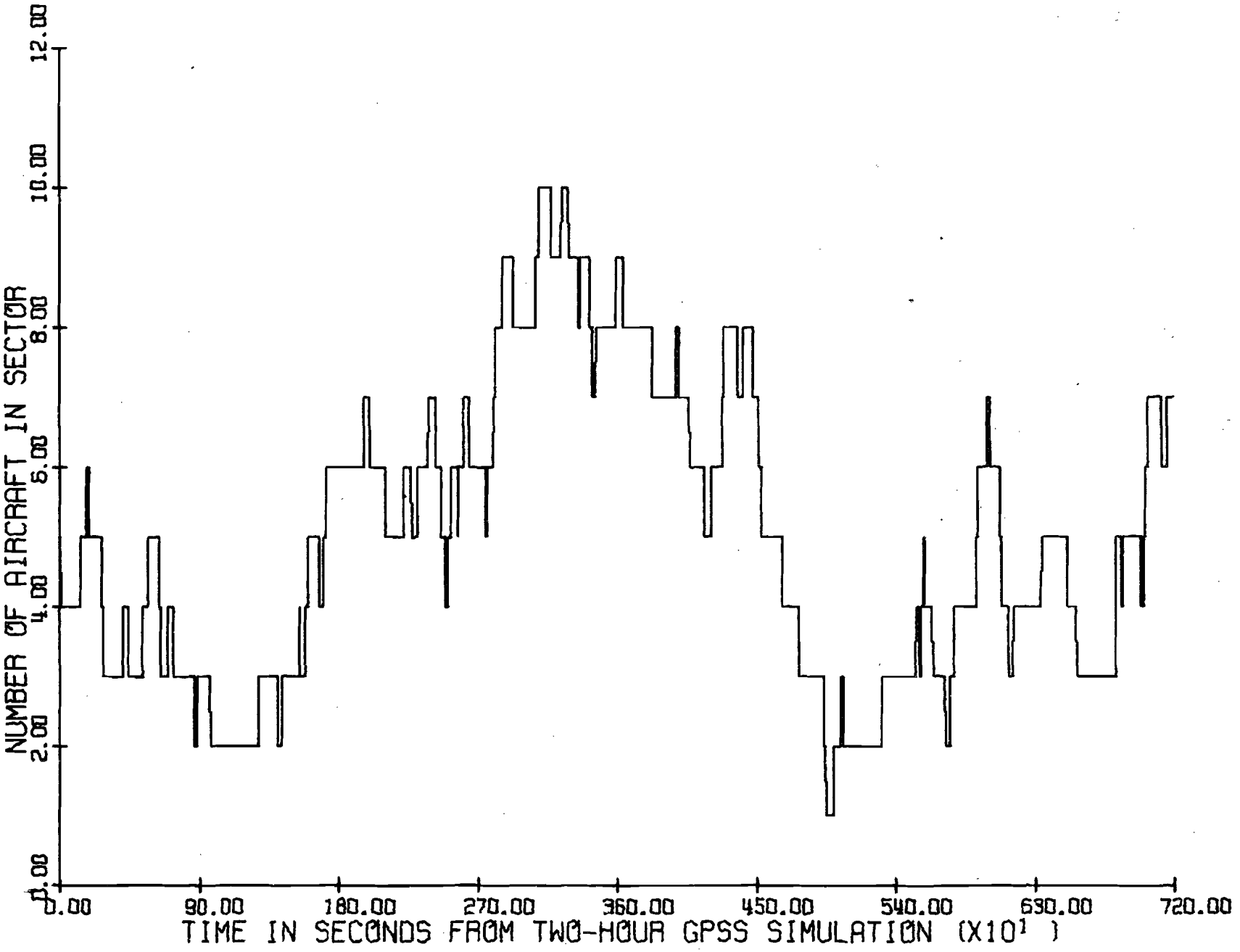

Figure 2.16 Plot of the Number of Aircraft in the Sector from GPSS V Simulation

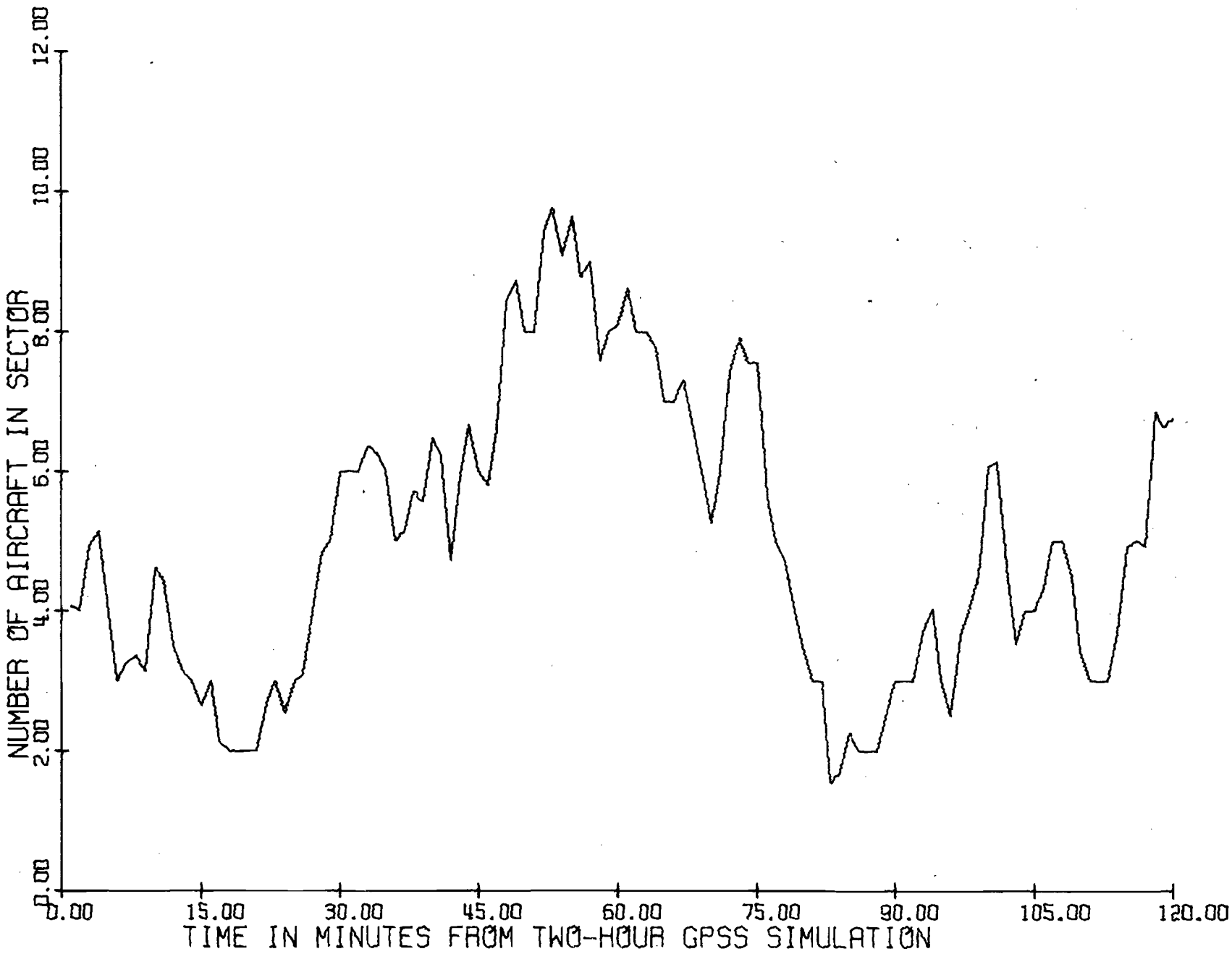

Figure 2.17 Plot of Sixty-Second Average Aircraft Loadings from GPSS V Simulation

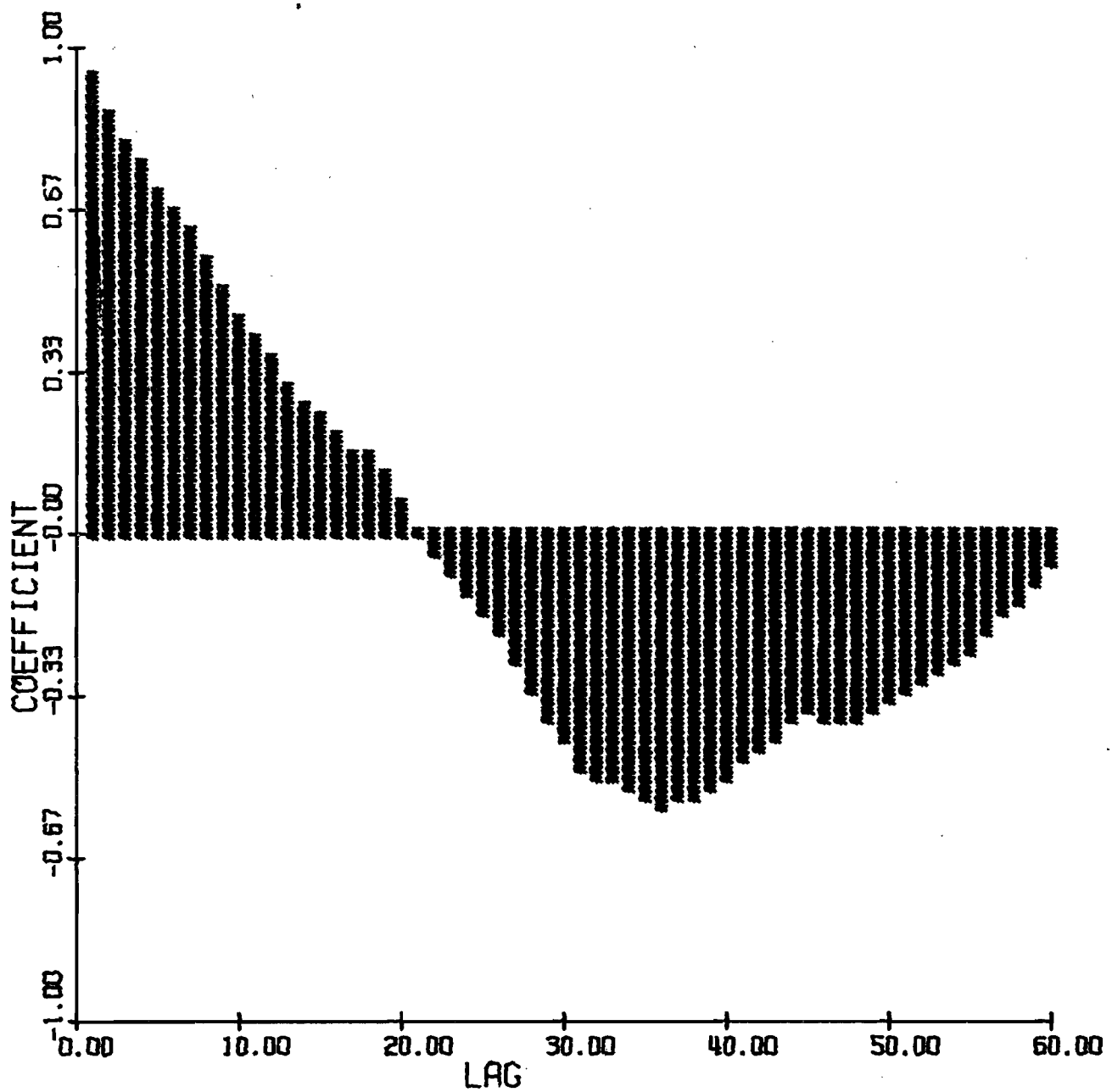

Figure 2.18 Sample Autocorrelation Function for the Aircraft Loading Series from GPSS V Simulation

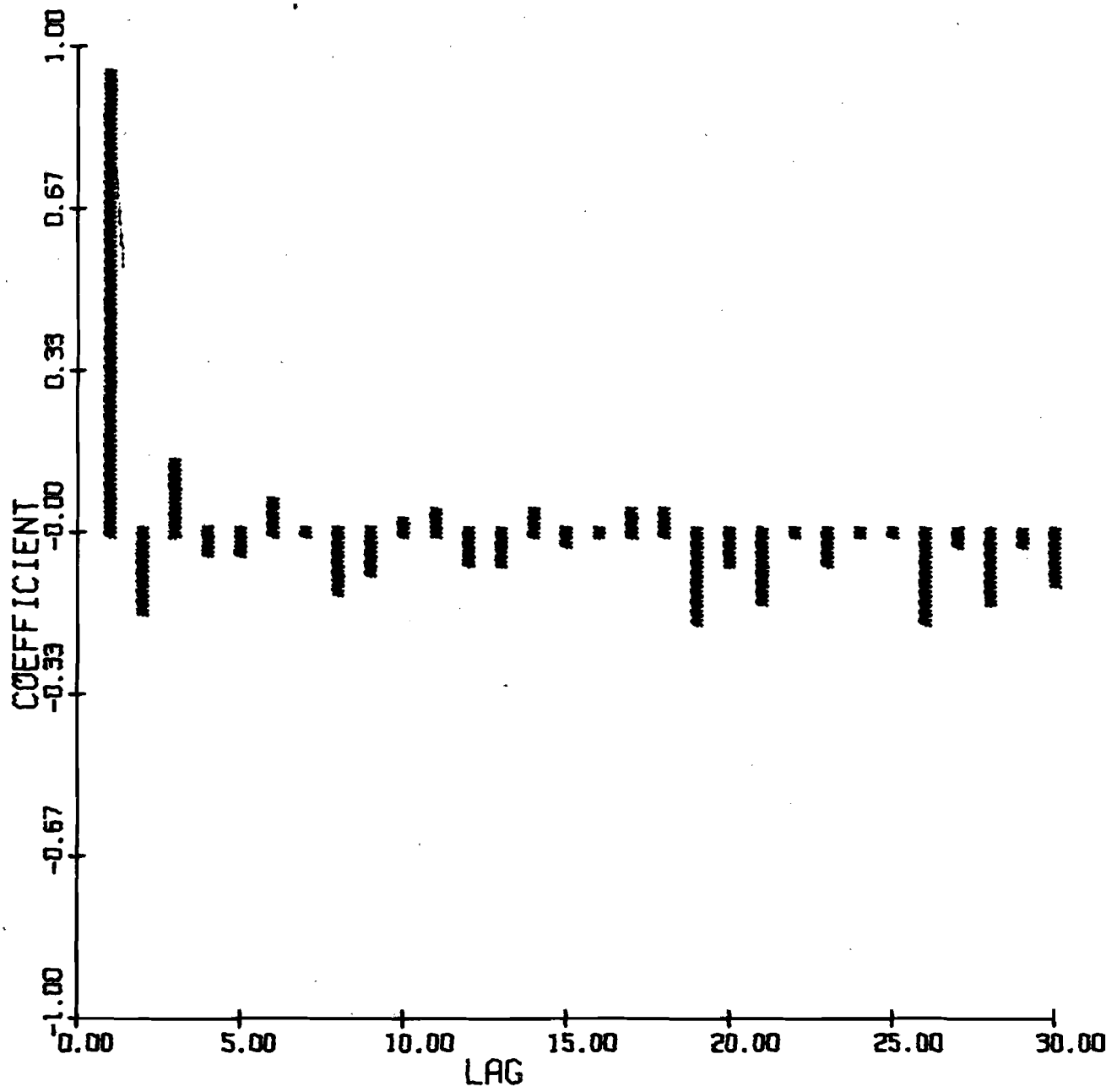

Figure 2.19 Sample Partial Autocorrelation Function for the Aircraft Loading Series from GPSS V Simulation

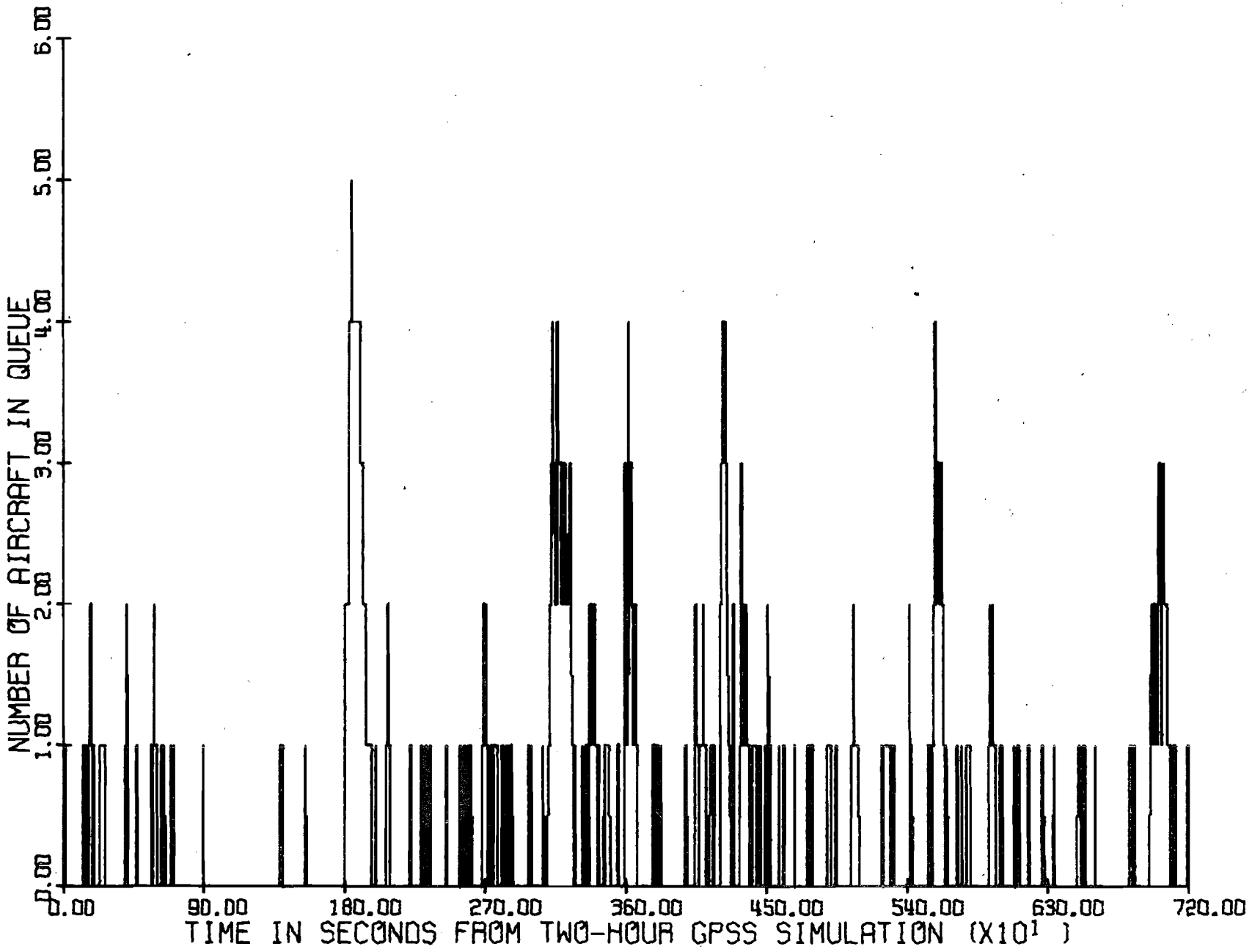

Figure 2.20 Plot of the Number of Aircraft in the Queue from GPSS V Simulation

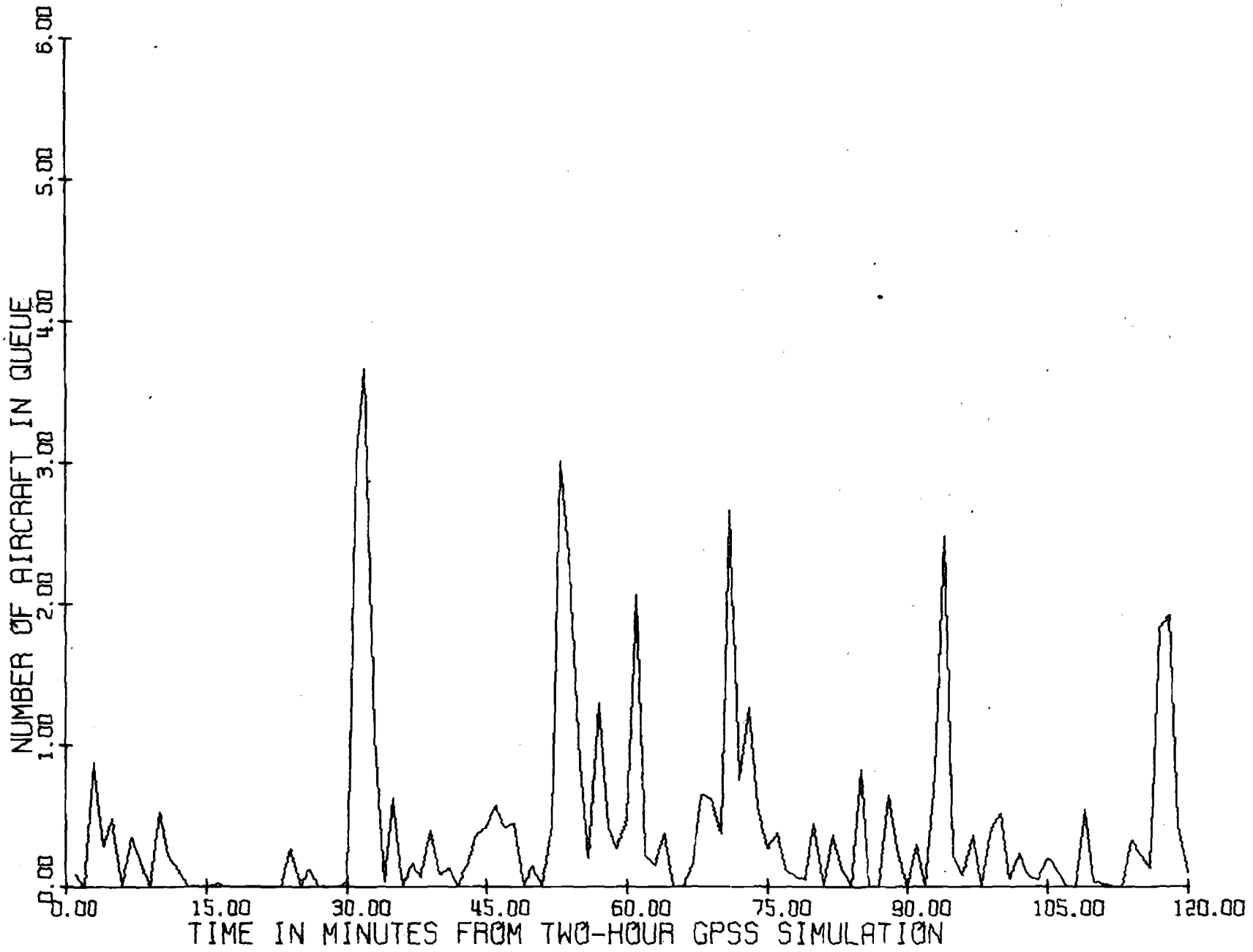

Figure 2.21 Plot of Sixty-Second Average Queue Lengths from GPSS V Simulation

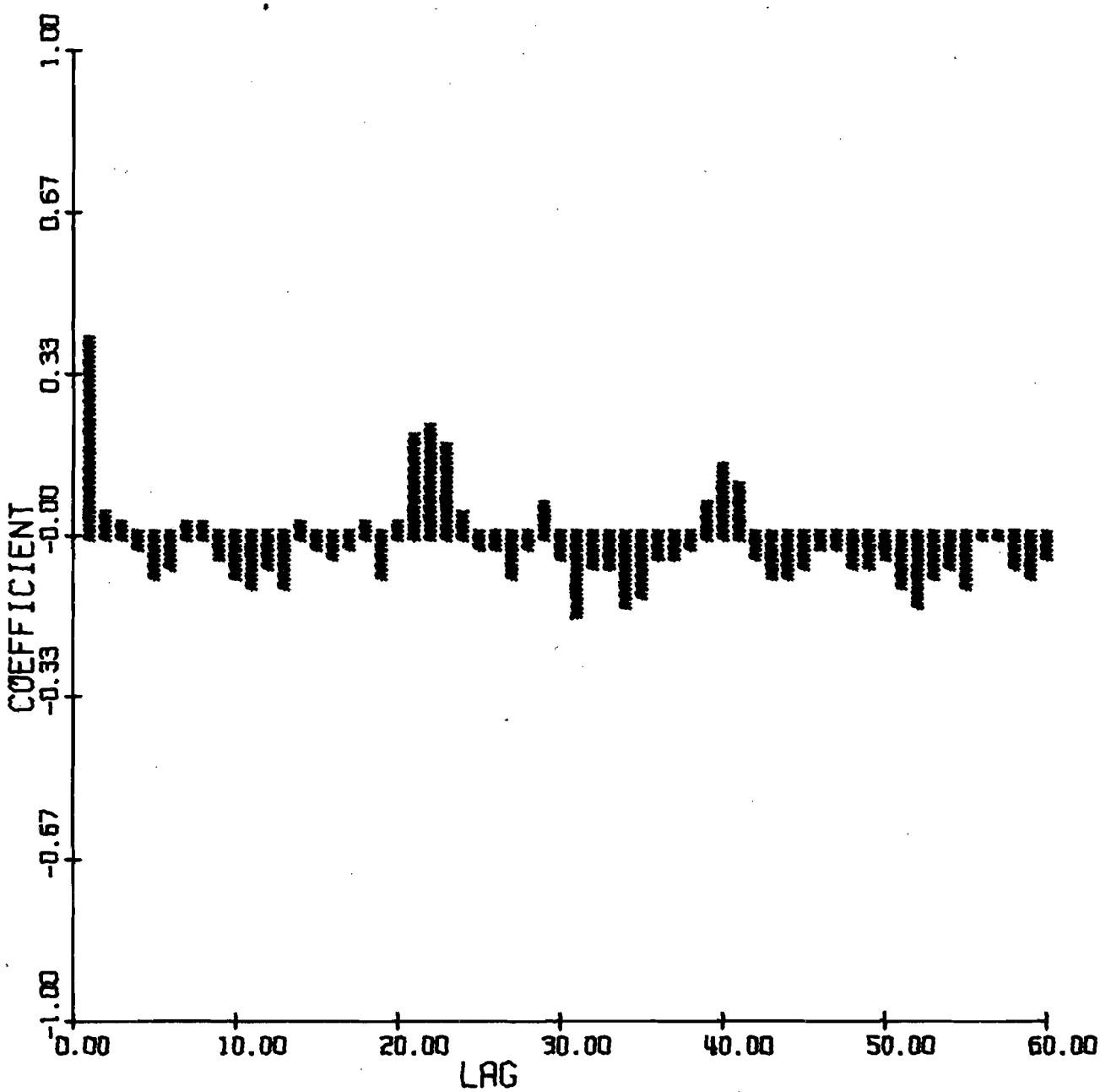

Figure 2.22 Sample Autocorrelation Function for the Queue Length Series from GPSS V Simulation

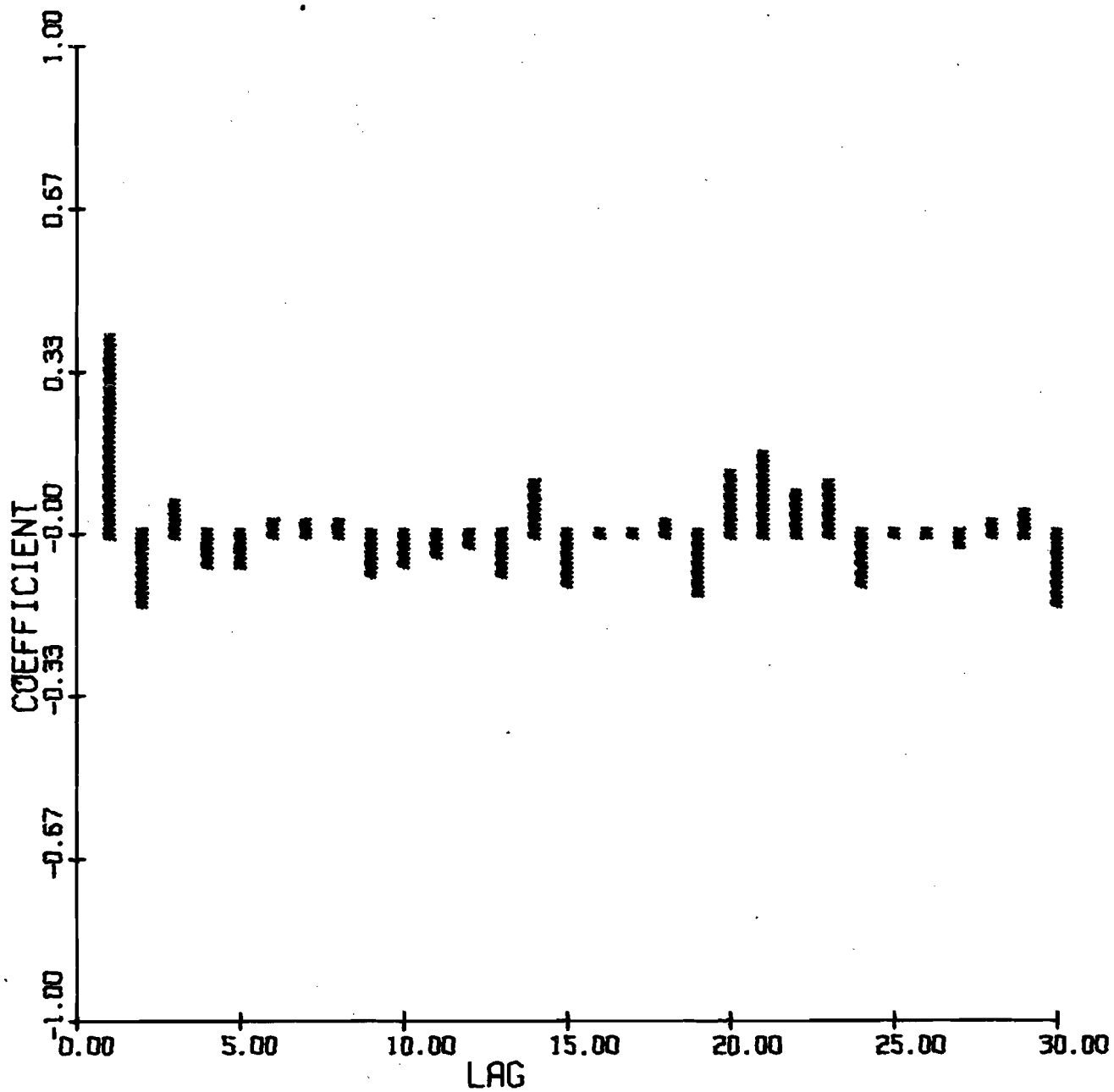

Figure 2.23 Sample Partial Autocorrelation Function for the Queue Length Series from GPSS V Simulation

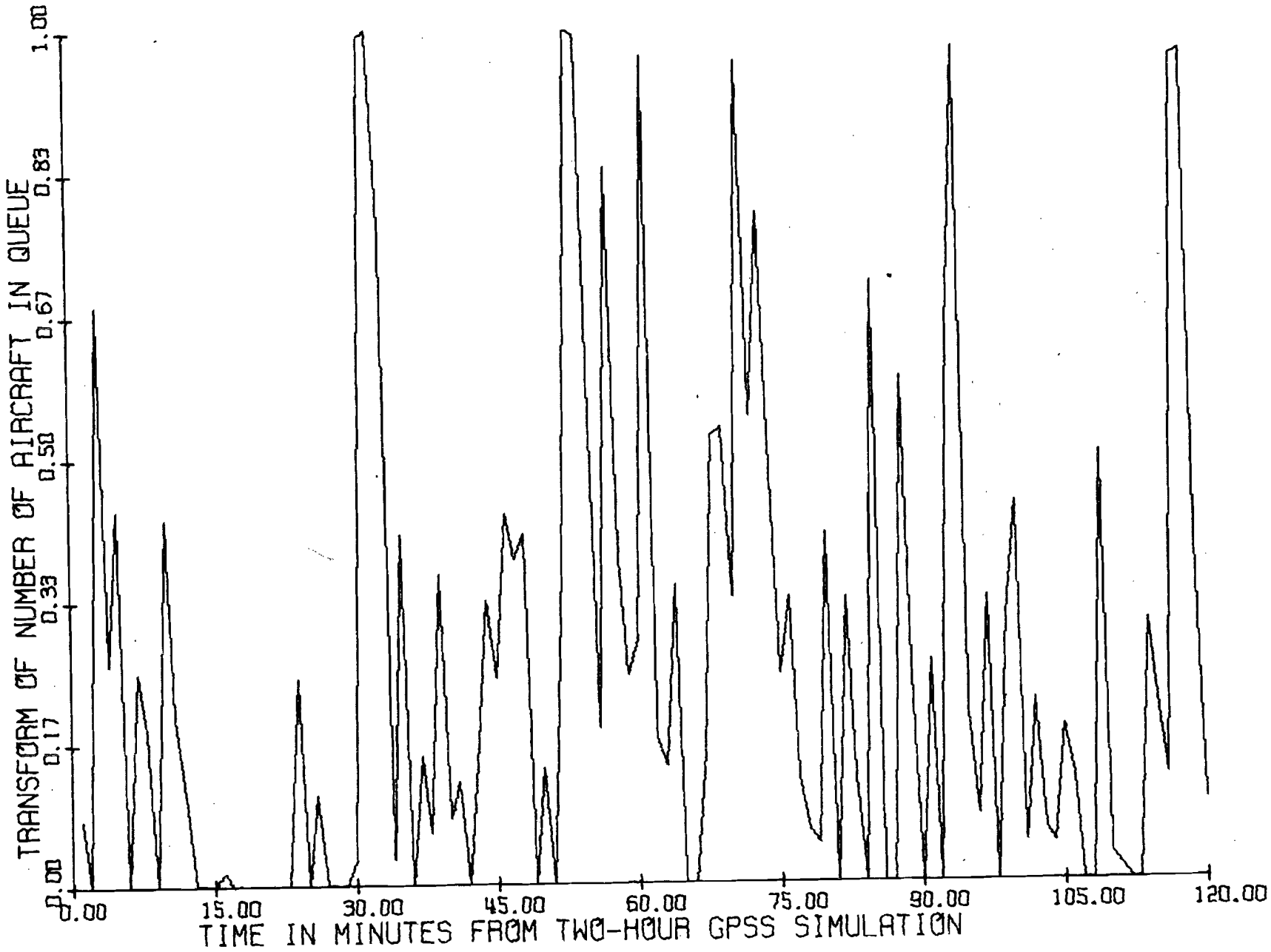

Figure 2.24 Plot of Sixty-Second Average Queue Transforms from GPSS V Simulation

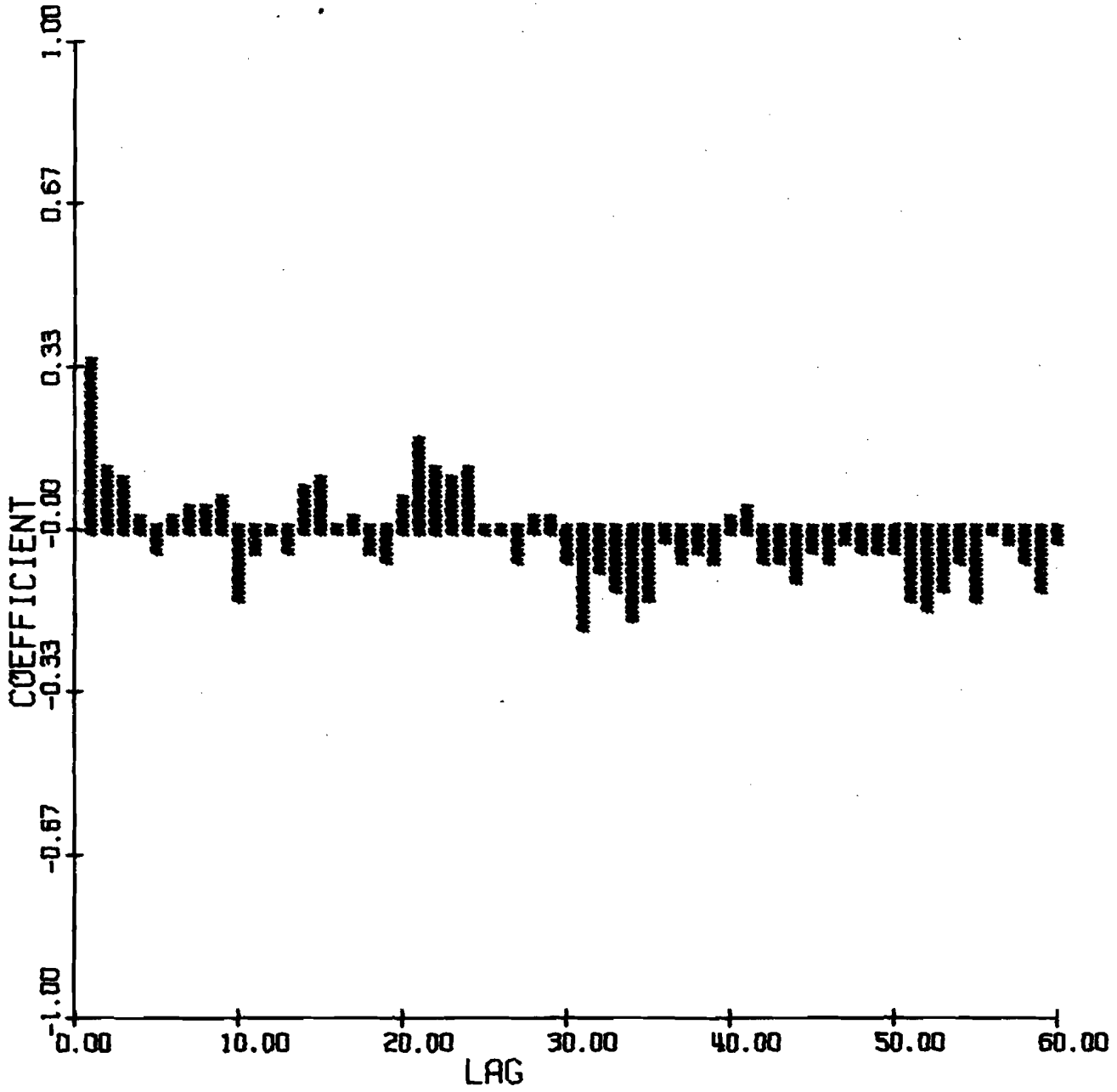

Figure 2.25 Sample Autocorrelation Function for the Queue Transform Series from GPSS V Simulation

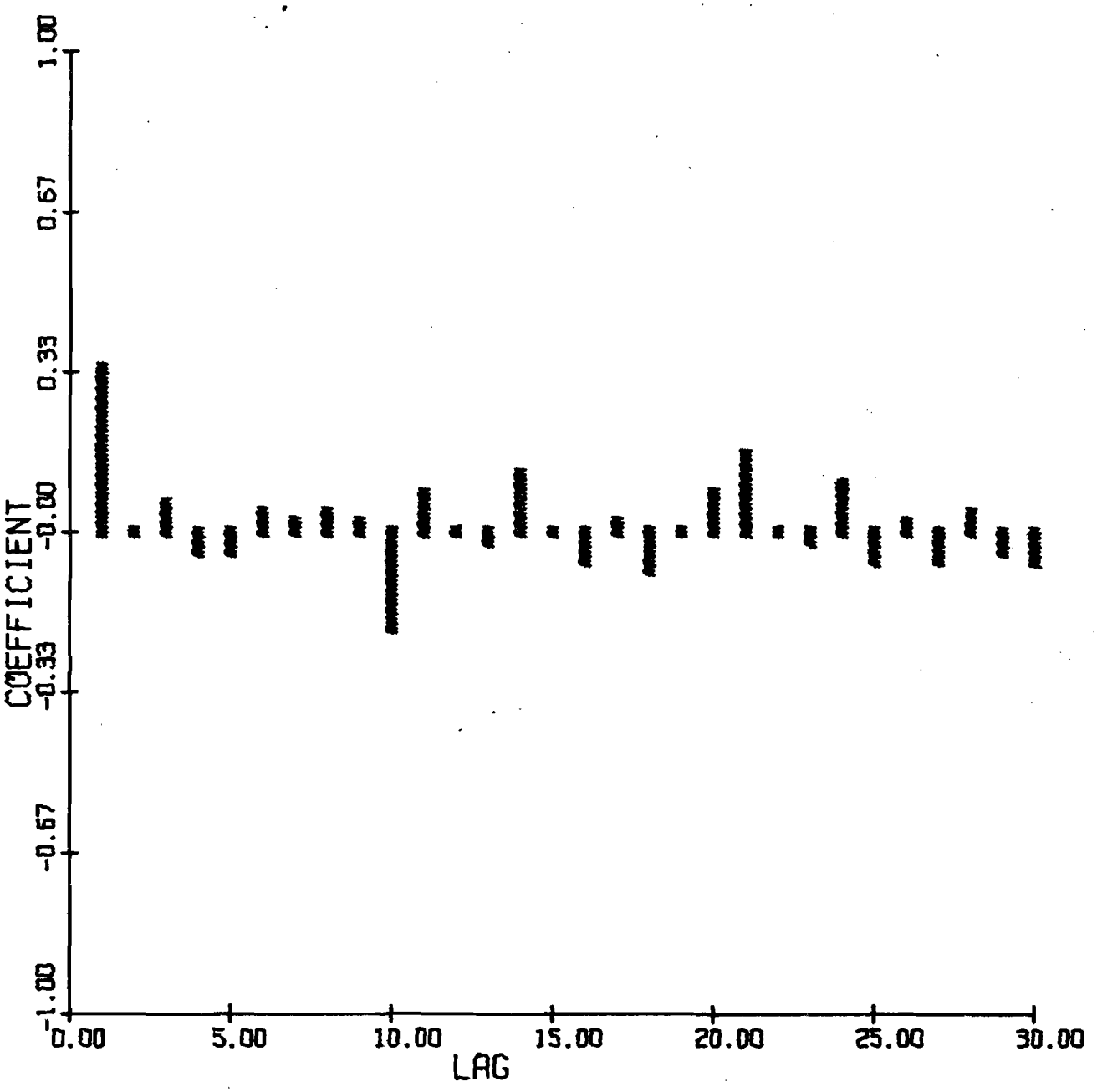

Figure 2.26 Sample Partial Autocorrelation Function for the Queue Transform Series from GPSS V Simulation

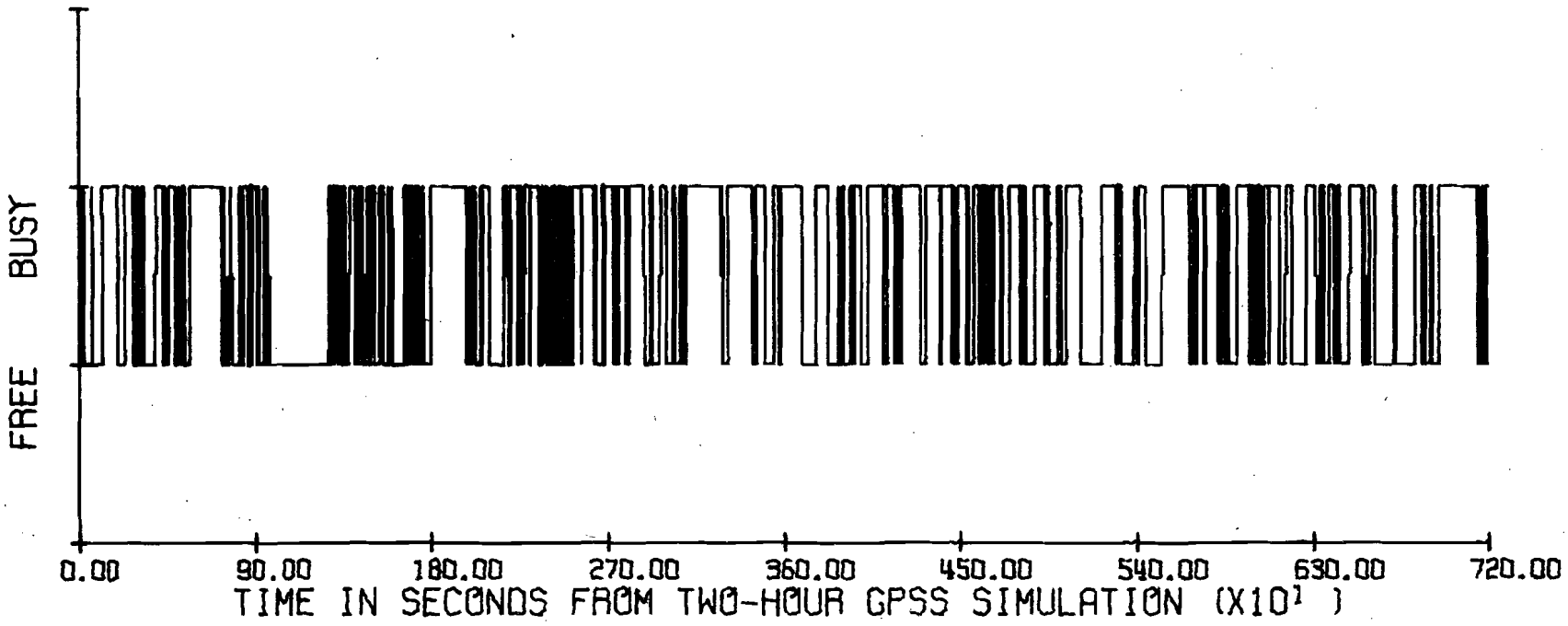

Figure 2.27 Plot of the Channel Status per Second from GPSS V Simulation

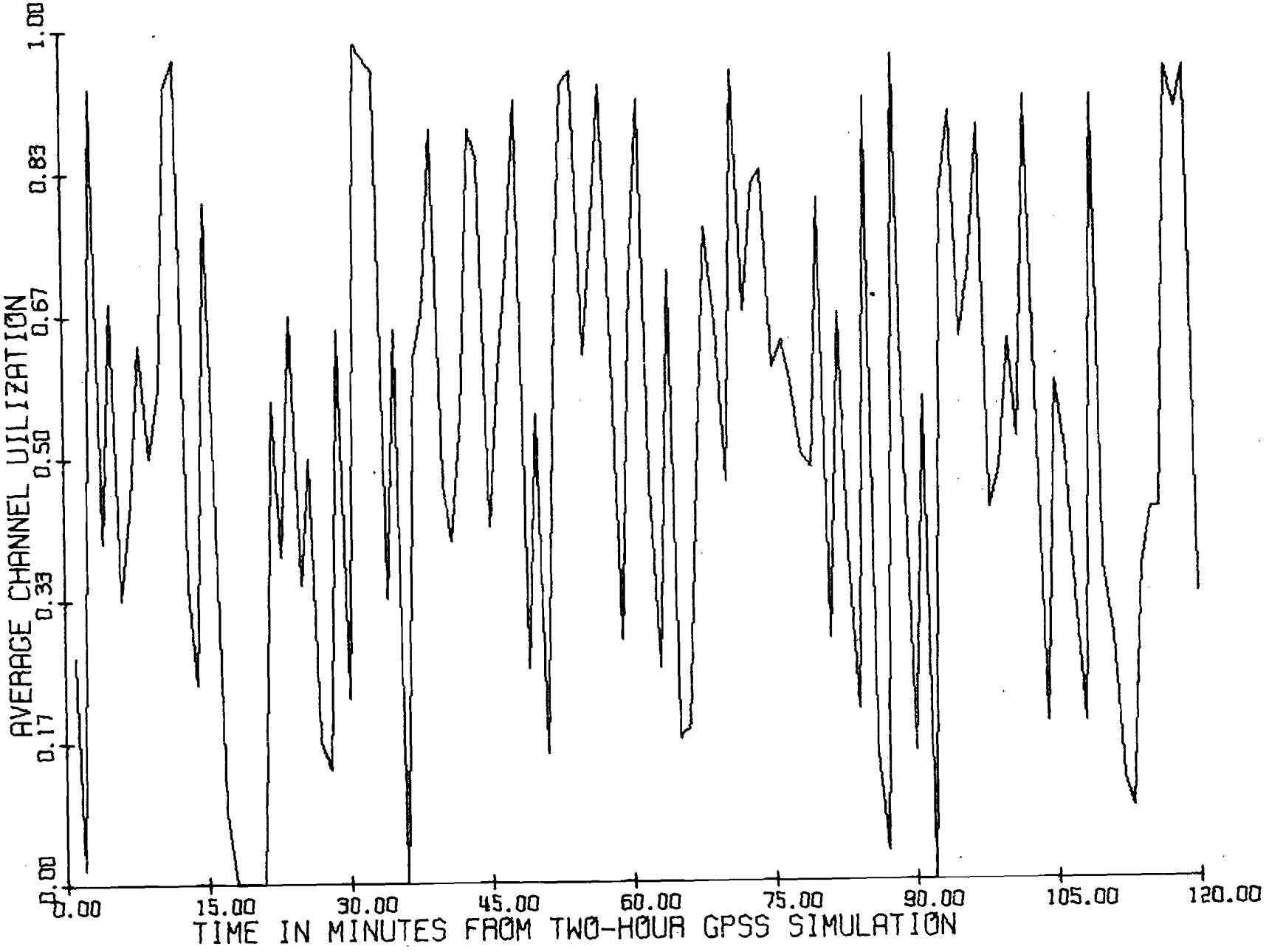

Figure 2.28 Plot of Sixty-Second Average Channel Utilizations from GPSS V Simulation

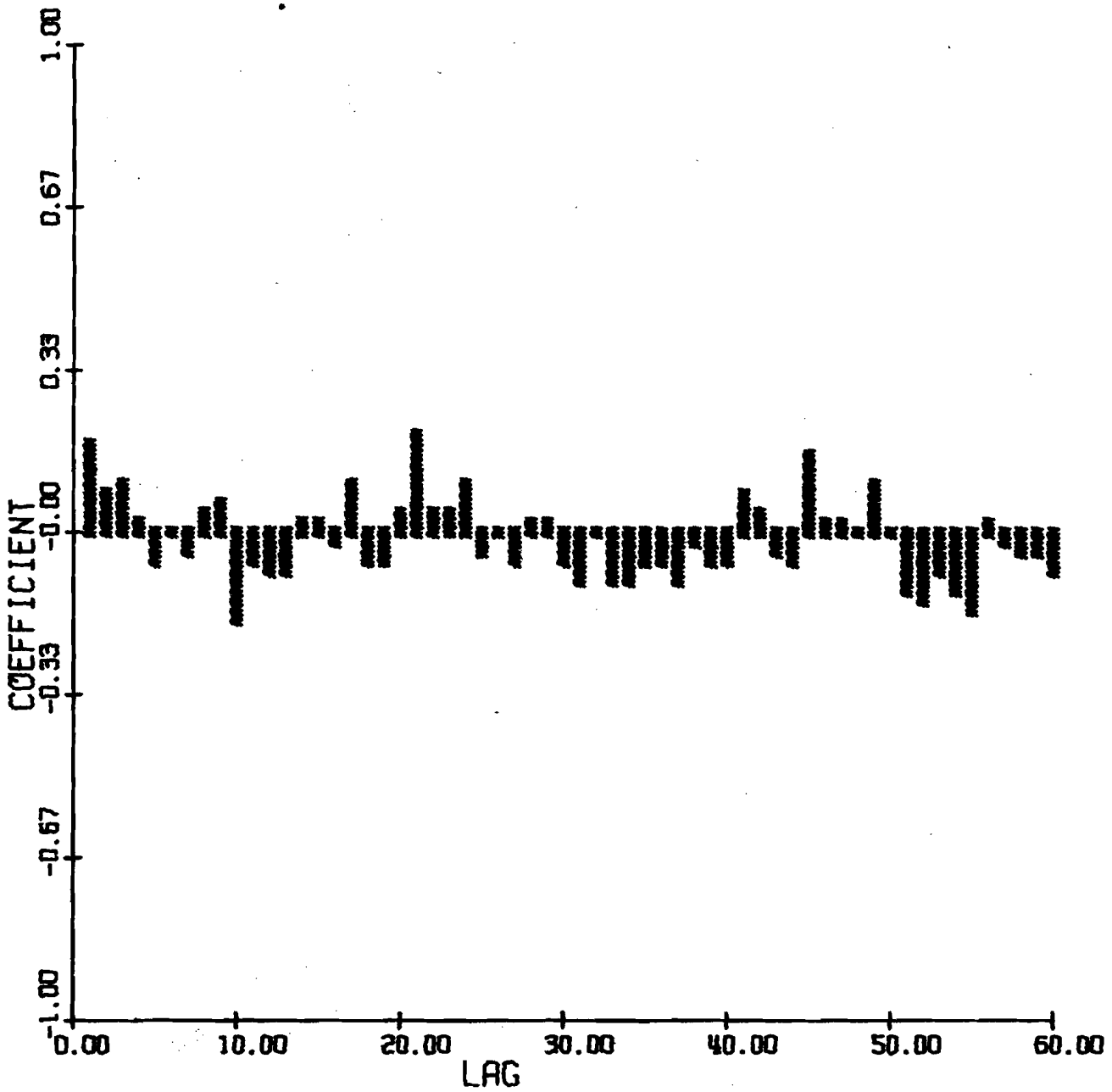

Figure 2.29 Sample Autocorrelation Function for the Channel Utilization Series from GPSS V Simulation

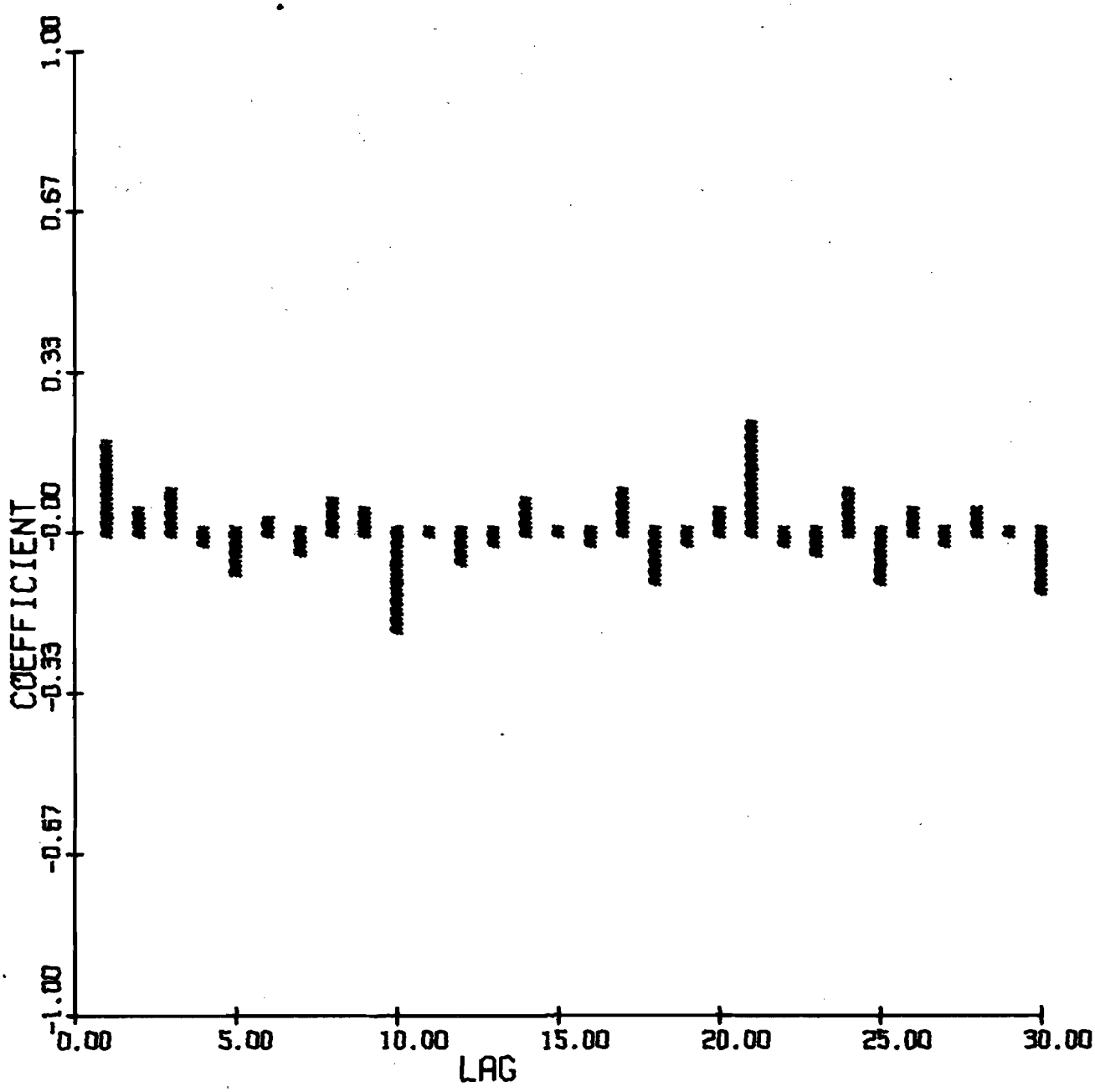

Figure 2.30 Sample Partial Autocorrelation Function for the Channel Utilization Series from GPSS V Simulation

CHAPTER 3

VALIDATION OF THE SIMULATION MODEL

3.1 Introduction

Historically, the construction of the present simulation model began with early attempts to simulate various sector responses using preliminary GPSS V programs. The present model was built upon these early efforts in an iterative fashion: observed discrepancies between simulated and observed data were used to correct and modify the initial models. Many defects in programming, data usage and parameter estimation were thus discovered and remedied. In addition, the observed discrepancies supplied insights about the real system which in turn often led to important modifications in the formulation of the simulation model.

The model was constructed in two stages. The observed data for individual sectors was first simulated, and then validated. The model was then adapted to perform general simulations of sector functions and the resulting responses again validated.

Philosophical and methodological discussions about the validation of computer simulations are available in many academic journals. As some authors suggested, the validation of a simulation model is equivalent to establishment of a theory in science. The formulation of the theory is usually based upon one's comprehension of an observed phenomenon and tested using appropriately collected data. Similarly, the construction of a simulation model must be based upon one's understanding of a system and validated by comparing simulated data against the historical record.

The problems of comparing simulated versus observed data can be awkward. For example, the data generated from many computer simulations are usually not serially independent in time. Often, this lack of independence is due to the interaction of many variables and to the time lag of their effects in a dynamic system. One unfortunate consequence is that the usual statistical testing techniques for examining "goodness of fit" are not very meaningful. Nevertheless, time dependent means, standard deviations, and other statistics employed to describe the simulated and observed time dependent data for ATC communications systems must be adequately compared. These issues have motivated the use of new statistical testing procedures for the comparison of time dependent observations.

To illustrate the difficulty of the problem, consider the two time series co-plotted in Figure 3.1. The question is raised as to whether both time series are, in fact, realizations of the same dynamic system. They are in this case since the two series are simply the two halves of the same time series, both halves recorded under the same conditions. To the eye the two series are different. However, the basic structures of both series are

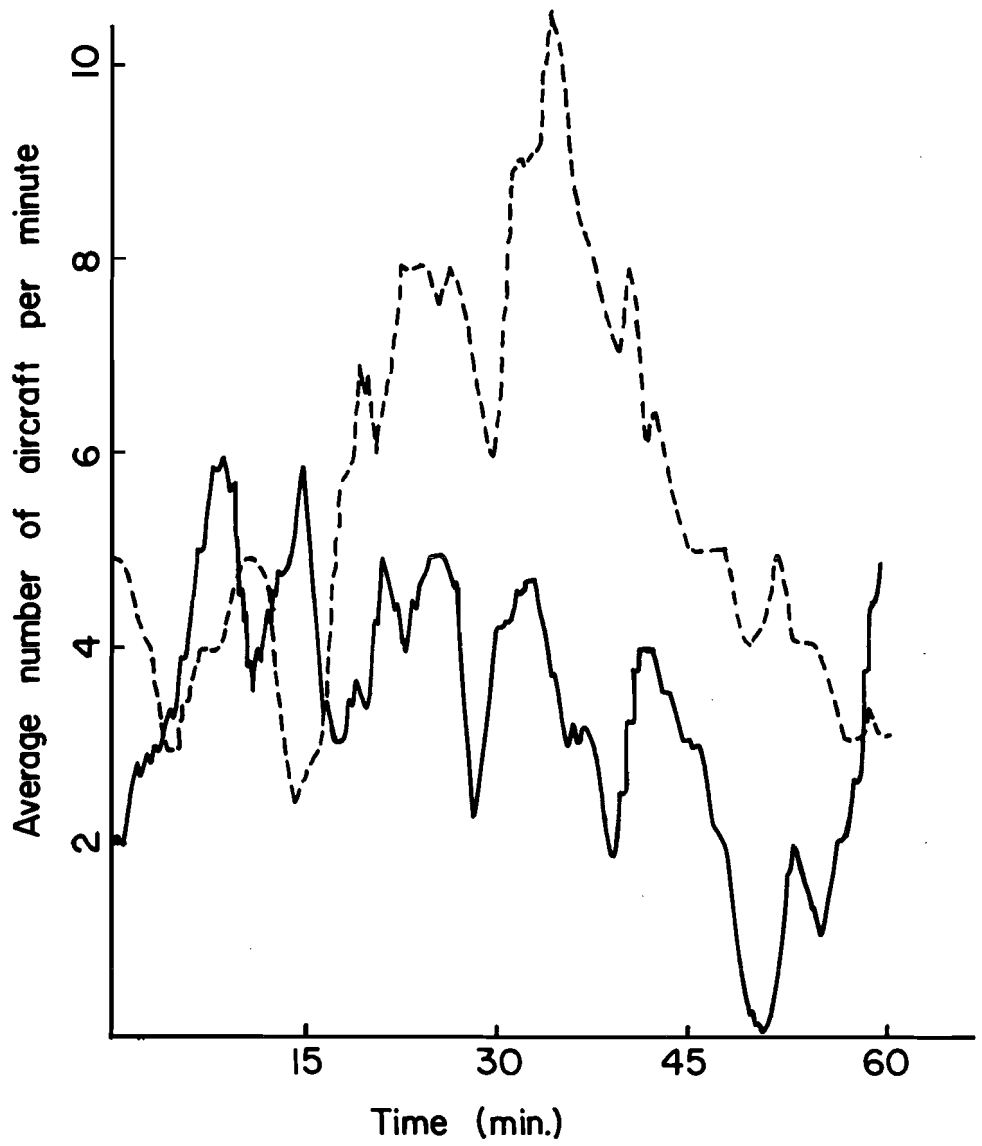

Figure 3.1 Two Time Series Recorded from the Same Real System

identical and what the eye beholds is the result of the manner in which random unstructured noise affects a dynamic system. No two realizations of the time series from the same system are going to be identical. The trick comes in determining when two observed series are so different as to suggest their basic structures are different.

As has been demonstrated in Chapter 7, Volume II, the time series modelling techniques suggested by Box and Jenkins are very useful in the analyses of the kinds of dynamic responses observed in ATC communication channels. In Section 3.2 we derive a test statistic $G(\psi, \gamma)$ distributed as a χ^2 variable and useful for comparing two time series with respect to their estimated parameters and variances. In Section 3.3 another test statistic distributed as Student's t is also derived to test the difference in means of two autoregressive time series. Readers not interested in the details of these derivations should feel free to skip these sections.

The final sections of this chapter describe the construction of the simulation model for ATC communications for two different situations. The first is the simulation of individual sectors for which the initiating parameter values are estimated from the historical data provided by each sector, (except for the parameters α and λ for transmission lengths which were determined by the two master equations described in Section 1.5). Validations of the individual sector simulations are discussed in Section 3.4 and illustrated in detail for Sector 453. Similar tests performed on seven other typical sectors, each selected from different sector functions, are summarized in tables. The second, and more important situation, is the general simulation for the individual sector functions. All parameters used in these simulations are obtained from master equations or master tables. Validation of the general simulation for sector functions is discussed using the HI sector function as an example.

3.2 A Testing Scheme for Autoregressive Parameters and Error Variance

Assume that we have an autoregressive time series model of order p

$$y_t = \phi_1 y_{t-1} + \phi_2 y_{t-2} + \phi_3 y_{t-3} + \dots + \phi_p y_{t-p} + a_t \qquad (3.1)$$

where $E(y_t) = 0$ for all equally spaced time points t, ϕ_i, i = 1, 2, ..., p satisfy the stationarity condition that all the roots of the corresponding characteristic equation fall outside the unit circle, and the a's are independent, identically distributed normal variables with mean zero and variance σ^2. Consider a pair of mutually independent time series each containing n observations. Suppose that one series is generated by the model (3.1) with parameters $\underset{\sim}{\phi}^{(1)} = (\phi_1^{(1)}, \phi_2^{(1)}, \dots, \phi_p^{(1)})'$ and σ_1^2 while the other is generated by (3.1) with parameters $\underset{\sim}{\phi}^{(2)} = (\phi_1^{(2)}, \phi_2^{(2)}, \dots, \phi_p^{(2)})'$

and σ_2^2. In both series $p < n$. In other words, the last $n - p$ observations of the first series can be written as

$$y_{p+1}^{(1)} = \phi_1^{(1)} y_p^{(1)} + \phi_2^{(1)} y_{p-1}^{(1)} + \ldots + \phi_p^{(1)} y_1^{(1)} + a_{p+1}^{(1)},$$

$$y_{p+2}^{(1)} = \phi_1^{(1)} y_{p+1}^{(1)} + \phi_2^{(1)} y_p^{(1)} + \ldots + \phi_p^{(1)} y_2^{(1)} + a_{p+2}^{(1)}$$

$$\cdots\cdots\cdots\cdots\cdots\cdots\cdots\cdots\cdots\cdots\cdots\cdots$$

$$y_n^{(1)} = \phi_1^{(1)} y_{n-1}^{(1)} + \phi_2^{(1)} y_{n-2}^{(1)} + \ldots + \phi_p^{(1)} y_{n-p}^{(1)} + a_n^{(1)}$$

or in matrix notation,

$$\underset{(n-p)\times 1}{\underset{\sim}{y}^{(1)}} = \underset{(n-p)\times p}{X^{(1)}} \; \underset{p\times 1}{\underset{\sim}{\phi}^{(1)}} + \underset{(n-p)\times 1}{\underset{\sim}{a}^{(1)}}$$

where $\underset{\sim}{a}^{(1)} \sim N_{n-p}(\underset{\sim}{0}, I_{n-p}\sigma_1^2)$, in which "$\sim N_{n-p}$" denotes "is distributed as a multivariate normal variable with $n - p$ dimensions", and I_{n-p} denotes an identity matrix of order $n - p$. Similarly, the corresponding observations of the second series can be expressed as

$$\underset{\sim}{y}^{(2)} = X^{(2)} \underset{\sim}{\phi}^{(2)} + \underset{\sim}{a}^{(2)}$$

where $\underset{\sim}{a}^{(2)} \sim N_{n-p}(\underset{\sim}{0}, I_{n-p}\sigma_2^2)$.

For the first series we assume

(i) the first p observations are assumed fixed and serve as the initial condition of the rest of series,

(ii) $\underset{\sim}{\phi}^{(1)}$ and σ_1^2 are independent <u>a priori</u>,

and using a Bayesian approach we further assume

(iii) the prior density of $(\underset{\sim}{\phi}^{(1)}, \sigma_1^2)$ is proportional to $1/\sigma_1^2$,

and that the likelihood function of $(\underset{\sim}{\phi}^{(1)}, \sigma_1^2)$ is given by

(iv) $$\ell(\underset{\sim}{\phi}^{(1)}, \sigma_1^2 | \underset{\sim}{y}^{(1)}) \propto (\sigma_1^2)^{\frac{-(n-p)}{2}} \exp\left\{-(1/2\sigma_1^2)(\underset{\sim}{y}^{(1)} - X^{(1)}\underset{\sim}{\phi}^{(1)})' (\underset{\sim}{y}^{(1)} - X^{(1)}\underset{\sim}{\phi}^{(1)})\right\}.$$

The likelihood function can be combined with the prior to secure the posterior density

$$P(\underset{\sim}{\phi}^{(1)}, \sigma_1^2 | \underset{\sim}{y}^{(1)}) \propto (\sigma_1^2)^{-(\frac{n-p}{2}+1)} \exp\left\{-\frac{1}{2\sigma_1^2}(\underset{\sim}{y}^{(1)} - X^{(1)}\underset{\sim}{\phi}^{(1)})' (\underset{\sim}{y}^{(1)} - X^{(1)}\underset{\sim}{\phi}^{(1)})\right\}.$$

Using a well-known factorization of the exponent, we obtain

$$P(\underset{\sim}{\phi}^{(1)}, \sigma_1^2|\underset{\sim}{y}^{(1)}) \propto (\sigma_1^2)^{-(\frac{n-p}{2}+1)} \exp\left\{-\frac{1}{2\sigma_1^2}\left[S_1(\hat{\underset{\sim}{\phi}}^{(1)}) + (\underset{\sim}{\phi}^{(1)} - \hat{\underset{\sim}{\phi}}^{(1)})' X^{(1)'} X^{(1)} (\underset{\sim}{\phi}^{(1)} - \hat{\underset{\sim}{\phi}}^{(1)})\right]\right\} \tag{3.2}$$

where $\hat{\underset{\sim}{\phi}}^{(1)} = (X^{(1)'}X^{(1)})^{-1}X^{(1)'}\underset{\sim}{y}^{(1)}$ (i.e., the least squares estimate (LSE) of $\underset{\sim}{\phi}^{(1)}$), and

$$S_1(\hat{\underset{\sim}{\phi}}^{(1)}) = (\underset{\sim}{y}^{(1)} - X^{(1)}\hat{\underset{\sim}{\phi}}^{(1)})'(\underset{\sim}{y}^{(1)} - X^{(1)}\hat{\underset{\sim}{\phi}}^{(1)}). \tag{3.3}$$

Integrating out $\underset{\sim}{\phi}^{(1)}$ from (3.2), we have

$$p(\sigma_1^2|\underset{\sim}{y}^{(1)}) \propto (\sigma_1^2)^{-(\frac{n-2p}{2}+1)} \exp\left\{-S_1(\hat{\underset{\sim}{\phi}}^{(1)})/2\sigma_1^2\right\}. \tag{3.4}$$

Employing the same process and similar assumptions, one may derive the posterior density function of the parameters $\underset{\sim}{\phi}^{(2)}$ and σ_2^2, which are

$$P(\underset{\sim}{\phi}_2^{(2)}, \sigma_2^2|\underset{\sim}{y}^{(2)}) \propto (\sigma_2^2)^{-(\frac{n-p}{2}+1)} \exp\left\{-\frac{1}{2\sigma_2^2}\left[S_2(\hat{\underset{\sim}{\phi}}^{(2)}) + (\underset{\sim}{\phi}^{(2)} - \hat{\underset{\sim}{\phi}}^{(2)})' X^{(2)'} X^{(2)} (\underset{\sim}{\phi}^{(2)} - \hat{\underset{\sim}{\phi}}^{(2)})\right]\right\} \tag{3.5}$$

and

$$P(\sigma_2^2|\underset{\sim}{y}^{(2)}) \propto (\sigma_2^2)^{-(\frac{n-2p}{2}+1)} \exp\left\{-S_2(\hat{\underset{\sim}{\phi}}^{(2)})/2\sigma_2^2\right\} \tag{3.6}$$

where

$$\hat{\underset{\sim}{\phi}}^{(2)} = (X^{(2)'}X^{(2)})^{-1}X^{(2)'}\underset{\sim}{y}^{(2)}$$

and

$$S_2(\hat{\underset{\sim}{\phi}}^{(2)}) = (\underset{\sim}{y}^{(2)} - X^{(2)}\hat{\underset{\sim}{\phi}}^{(2)})'(\underset{\sim}{y}^{(2)} - X^{(2)}\hat{\underset{\sim}{\phi}}^{(2)}). \tag{3.7}$$

We further assume that $(\phi^{(1)}, \sigma_1^2)$ and $(\phi^{(2)}, \sigma_2^2)$ are independent <u>a priori</u>. Then the joint posterior density function of $(\underset{\sim}{\phi}^{(1)}, \underset{\sim}{\phi}^{(2)}, \sigma_1^2, \sigma_2^2)$ is

$$p(\underset{\sim}{\phi}^{(1)}, \underset{\sim}{\phi}^{(2)}, \sigma_1^2, \sigma_2^2|\underset{\sim}{y}^{(1)}, \underset{\sim}{y}^{(2)}) = p(\underset{\sim}{\phi}^{(1)}, \sigma_1^2|\underset{\sim}{y}^{(1)})\ p(\underset{\sim}{\phi}^{(2)}, \sigma_2^2|\underset{\sim}{y}^{(2)})$$

where $p(\underset{\sim}{\phi}^{(1)}, \sigma_1^2|\underset{\sim}{y}^{(1)})$ and $p(\underset{\sim}{\phi}^{(2)}, \sigma_2^2|\underset{\sim}{y}^{(2)})$ are given in (3.2) and (3.5). Define $\underset{\sim}{\psi} = \underset{\sim}{\phi}_1 - \underset{\sim}{\phi}_2$, $\gamma = \sigma_2^2/\sigma_1^2$, and $\nu = n - 2p$.

Clearly, $\underset{\sim}{\phi}^{(1)} | \sigma_1^2 \sim N_p\left(\hat{\underset{\sim}{\phi}}^{(1)}, \sigma_1^2 (X^{(1)'} X^{(1)})^{-1}\right)$

$$\underset{\sim}{\phi}^{(2)} | \sigma_2^2 \sim N_p\left(\hat{\underset{\sim}{\phi}}^{(2)}, \sigma_2^2 (X^{(2)'} X^{(2)})^{-1}\right),$$

and hence, $\underset{\sim}{\psi} | \sigma_1^2, \sigma_2^2 \sim N\left(\hat{\underset{\sim}{\psi}}, \sigma_1^2 (X^{(1)'} X^{(1)})^{-1} + \sigma_2^2 (X^{(2)'} X^{(2)})^{-1}\right)$ (3.8)

where $\hat{\underset{\sim}{\psi}} = \hat{\underset{\sim}{\phi}}^{(1)} - \hat{\underset{\sim}{\phi}}^{(2)}$. Again from (3.4) and (3.6)

$$\frac{S_1(\hat{\underset{\sim}{\phi}}^{(1)})}{\sigma_1^2} \Big| \underset{\sim}{y}^{(1)} \sim \chi_\nu^2$$

and

$$\frac{S_2(\hat{\underset{\sim}{\phi}}^{(2)})}{\sigma_2^2} \Big| \underset{\sim}{y}^{(2)} \sim \chi_\nu^2$$

where χ_ν^2 is a random variable having a chi-square distribution with ν degrees of freedom. Since σ_1^2 and σ_2^2 are conditionally independent,

$$\frac{S_1(\hat{\underset{\sim}{\phi}}^{(1)})}{\sigma_1^2} \Big/ \frac{S_2(\hat{\underset{\sim}{\phi}}^{(2)})}{\sigma_2^2} \Big| \underset{\sim}{y}^{(1)}, \underset{\sim}{y}^{(2)} \sim F_{\nu,\nu}$$

i.e. $$\gamma \frac{S_1(\hat{\underset{\sim}{\phi}}^{(1)})}{S_2(\hat{\underset{\sim}{\phi}}^{(2)})} \Big| \underset{\sim}{y}^{(1)}, \underset{\sim}{y}^{(2)} \sim F_{\nu,\nu} \qquad (3.9)$$

where $F_{\nu,\nu}$ is Snedecor's F with ν and ν degrees of freedom. Since

$$P(\sigma_1^2, \sigma_2^2 | \underset{\sim}{y}^{(1)}, \underset{\sim}{y}^{(2)}) = P(\sigma_1^2 | \underset{\sim}{y}^{(1)}) P(\sigma_2^2 | \underset{\sim}{y}^{(2)})$$

$$\propto (\sigma_1^2)^{-(\frac{\nu}{2}+1)} (\sigma_2^2)^{-(\frac{\nu}{2}+1)} \exp\left\{-\frac{1}{2}\left[\frac{S_1(\hat{\underset{\sim}{\phi}}^{(1)})}{\sigma_1^2} + \frac{S_2(\hat{\underset{\sim}{\phi}}^{(2)})}{\sigma_2^2}\right]\right\}$$

by making a transformation of the variables we obtain

$$P(\sigma_1^2, \gamma | \underset{\sim}{y}^{(1)}, \underset{\sim}{y}^{(2)}) \propto (\sigma_1^2)^{-(\nu+1)} \gamma^{-(\frac{\nu}{2}+1)} \exp\left\{-\frac{1}{2\sigma_1^2}\left[S_1(\hat{\underset{\sim}{\phi}}^{(1)}) + \frac{1}{\gamma} S_2(\hat{\underset{\sim}{\phi}}^{(2)})\right]\right\}.$$

Thus

$$P(\sigma_1^2 | \gamma, \underset{\sim}{y}^{(1)}, \underset{\sim}{y}^{(2)}) \propto (\sigma_1^2)^{-(\nu+1)} \exp\left\{-\frac{1}{2\sigma_1^2}\left[S_1(\hat{\underset{\sim}{\phi}}^{(1)}) + \frac{1}{\gamma} S_2(\hat{\underset{\sim}{\phi}}^{(2)})\right]\right\}$$

or

$$P(\sigma_1^2 | \gamma, \underset{\sim}{y}^{(1)}, \underset{\sim}{y}^{(2)}) = \frac{\left[S_1(\hat{\underset{\sim}{\phi}}^{(1)}) + \frac{1}{\gamma} S_2(\hat{\underset{\sim}{\phi}}^{(2)})\right]^{\nu}}{\Gamma(\nu)\, 2^{\nu}} (\sigma_1^2)^{-(\nu+1)}$$

$$\exp\left\{-\frac{1}{2\sigma_1^2}\left[S_1(\hat{\underset{\sim}{\phi}}^{(1)}) + \frac{1}{\gamma} S_2(\hat{\underset{\sim}{\phi}}^{(2)})\right]\right\}.$$

From (3.8)

$$p(\underset{\sim}{\psi} | \sigma_1^2, \gamma, \underset{\sim}{y}^{(1)}, \underset{\sim}{y}^{(2)}) = \frac{\left|(X^{(1)'}X^{(1)})^{-1} + \gamma(X^{(2)'}X^{(2)})^{-1}\right|^{-\frac{1}{2}}}{(2\pi)^{p/2}(\sigma_1^2)^{p/2}}$$

$$\exp\left\{-\frac{1}{2\sigma_1^2}(\underset{\sim}{\psi} - \hat{\underset{\sim}{\psi}})'\left[(X^{(1)'}X^{(1)})^{-1} + \gamma(X^{(2)'}X^{(2)})^{-1}\right]^{-1}(\underset{\sim}{\psi} - \hat{\underset{\sim}{\psi}})\right\}.$$

Combine the last two formulas to obtain

$$p(\underset{\sim}{\psi} | \gamma, \underset{\sim}{y}^{(1)}, \underset{\sim}{y}^{(2)}) = \int_0^{\infty} p(\underset{\sim}{\psi} | \sigma_1^2, \gamma, \underset{\sim}{y}^{(1)}, \underset{\sim}{y}^{(2)})\, P(\sigma_1^2 | \gamma, \underset{\sim}{y}^{(1)}, \underset{\sim}{y}^{(2)})\, d\sigma_1^2$$

$$= \frac{\Gamma(\nu + \frac{p}{2})\left|(X^{(1)'}X^{(1)})^{-1} + \gamma(X^{(2)'}X^{(2)})^{-1}\right|^{-1/2}}{(2\nu\pi)^{p/2}[s(\gamma)]^{p}\Gamma(\nu)}$$

$$\left\{1 + \frac{(\underset{\sim}{\psi} - \hat{\underset{\sim}{\psi}})'\left[(X^{(1)'}X^{(1)})^{-1} + \gamma(X^{(2)'}X^{(2)})^{-1}\right]^{-1}(\underset{\sim}{\psi} - \hat{\underset{\sim}{\psi}})}{s^2(\gamma)2\nu}\right\}^{-(\nu+\frac{p}{2})} \qquad (3.10)$$

where $s^2(\gamma) = \frac{1}{2\nu}\left[S_1(\hat{\underset{\sim}{\phi}}^{(1)}) + \frac{1}{\gamma} S_2(\hat{\underset{\sim}{\phi}}^{(2)})\right]$.

From (3.9)

$$P(\gamma|\underset{\sim}{y}^{(1)}, \underset{\sim}{y}^{(2)}) = \frac{\left[S_1(\hat{\underset{\sim}{\phi}}^{(1)})/S_2(\hat{\underset{\sim}{\phi}}^{(2)})\right]^{\nu/2}}{B(\nu/2, \nu/2)} \gamma^{(\frac{\nu}{2} - 1)}\left[1 + \frac{S_1(\hat{\underset{\sim}{\phi}}^{(1)})}{S_2(\hat{\underset{\sim}{\phi}}^{(2)})}\right]^{-\nu}. \tag{3.11}$$

Since

$$P(\underset{\sim}{\psi},\gamma|\underset{\sim}{y}^{(1)}, \underset{\sim}{y}^{(2)}) = P(\underset{\sim}{\psi}|\gamma, \underset{\sim}{y}^{(1)}, \underset{\sim}{y}^{(2)})P(\gamma|\underset{\sim}{y}^{(1)}, \underset{\sim}{y}^{(2)}),$$

employing (3.10) and (3.11), we have

$$P(\underset{\sim}{\psi},\gamma|\underset{\sim}{y}^{(1)}, \underset{\sim}{y}^{(2)}) \quad \frac{\left|(X^{(1)'}X^{(1)})^{-1} + \gamma(X^{(2)'}X^{(2)})^{-1}\right|^{-\frac{1}{2}}}{(s(\gamma))^p}$$

$$\left\{1 + \frac{(\underset{\sim}{\psi} - \hat{\underset{\sim}{\psi}})'\left[(X^{(1)'}X^{(1)})^{-1} + \gamma(X^{(2)'}X^{(2)})^{-1}\right]^{-1}(\underset{\sim}{\psi} - \hat{\underset{\sim}{\psi}})}{s^2(\gamma)2\nu}\right\}^{(\nu+\frac{p}{2})}$$

$$\cdot\ \gamma^{\frac{\nu}{2}-1}\left(1 + \frac{S_1(\hat{\underset{\sim}{\phi}}^{(1)})}{S_2(\hat{\underset{\sim}{\phi}}^{(2)})}\gamma\right)^{-\nu} \tag{3.12}$$

where $\gamma > 0$ and $-\infty < \psi_i < \infty$, $i = 1, 2, \ldots, p$. Equation (3.12) is the key distribution, as to be demonstrated below, in a multiple-stage testing scheme.

It is obvious that for every $\gamma > 0$ the mode of the posterior density function of $(\underset{\sim}{\psi}|\gamma)$ is $\hat{\underset{\sim}{\psi}}$. In order to find the global mode over all $(\underset{\sim}{\psi}, \gamma)$, one may use a searching routine to locate the maximum point of the density function

$$P(\hat{\underset{\sim}{\psi}},\gamma|\underset{\sim}{y}^{(1)}, \underset{\sim}{y}^{(2)}) = \frac{\left|(X^{(1)'}X^{(1)})^{-1} + \gamma(X^{(2)'}X^{(2)})^{-1}\right|^{-\frac{1}{2}}}{(s(\gamma))^p} \gamma^{\frac{\nu}{2}-1}$$

$$\cdot\left[1 + \frac{S_1(\hat{\underset{\sim}{\phi}}^{(1)})}{S_2(\hat{\underset{\sim}{\phi}}^{(2)})}\gamma\right]^{-\nu} \tag{3.13}$$

with the aid of a computer. The $\hat{\gamma}$ thus obtained is usually very close to the ratio $S_2(\hat{\underset{\sim}{\phi}}^{(2)})/S_1(\hat{\underset{\sim}{\phi}}^{(1)})$ when n is moderately large. Therefore, it is

advisable to use $S_2(\hat{\underset{\sim}{\phi}}^{(2)})/S_1(\hat{\underset{\sim}{\phi}}^{(1)})$ as the starting point of the searching procedure.

It is well known that under some regularity conditions the logarithm of the likelihood ratio is asymptotically distributed as one half of a χ^2 variable. When the non-informative reference prior is used, the logarithm of the ratio of two posterior density functions follows the same result. The satisfaction of the regularity conditions in our case by the joint posterior density of $(\underset{\sim}{\psi}, \gamma)$ can be shown. The resulting theorem produces the following test statistic

$$G(\underset{\sim}{\psi}, \gamma) = \log \left\{ \frac{P(\hat{\underset{\sim}{\psi}}, \hat{\gamma} | \hat{\underset{\sim}{y}}^{(1)}, \hat{\underset{\sim}{y}}^{(2)})}{P(\underset{\sim}{\psi}, \gamma | \underset{\sim}{y}^{(1)}, \underset{\sim}{y}^{(2)})} \right\} \overset{\cdot}{\sim} \frac{1}{2} \chi^2_{p+1} . \tag{3.14}$$

The accuracy of this χ^2 limiting approximation for the posterior ratio seems in our experience to be fairly satisfactory when n, the length of the series, is no less than 40. Using the upper 100α percentage point of the χ^2 variable with p + 1 d.f., an approximate $(1 - \alpha)100\%$ HPD region of $(\underset{\sim}{\psi}, \gamma)$ can be found.

Let us now turn to the problem of making simultaneous inferences about $\underset{\sim}{\psi}$ and γ. Assume p = 1, i.e., the first-order autoregressive model. There are four situations of interest: (i) $\psi = 0$, $\gamma = 1$, (ii) $\psi \neq 0$, $\gamma = 1$ (iii) $\psi = 0$, $\gamma \neq 1$, and (iv) $\psi \neq 0$, $\gamma \neq 1$. Typical HPD contours corresponding to these four cases are presented in Figure 3.2. For case (i) the contour surrounds the point $(\psi, \gamma) = (0, 1)$. For case (ii) the contour lies on the line $\gamma = 1$ at either side of the vertical axis. For case (iii) the contour falls on the vertical axis, γ, without surrounding the point (0, 1) or touching the line $\gamma = 1$. When the contour does not touch either the line $\psi = 0$ or $\gamma = 1$, it is case (iv). One inference procedure, which involves two stages, for distinguishing these four cases is reported below. <u>Stage 1</u>: Check to see if the point $(\psi, \gamma) = (0, 1)$ is inside the contour. If the answer is "yes", we decide that the situation is case (i). Otherwise, go ahead to the second stage. <u>Stage 2:</u> See if either the line $\gamma = 1$ or $\psi = 0$ goes through the contour. If the line $\gamma = 1$ does, but $\psi = 0$ does not, we have case (ii). When the situation is turned around we have case (iii). However, when both do go through the contour but the point (0, 1) is not inside the contour, we have a contradiction between stage 1 and stage 2. A subjective choice based on the purpose of the study and hence the criterion of making inference seems required. Nevertheless, when the number of observations is moderately large, this dilemma will rarely occur. Obviously, when neither $\gamma = 1$ or $\psi = 0$ touches the contour, it can be decided as case (iv).

The procedure stated above is a variant of the technique due to Scheffé which is usually called the χ^2 or F projection method in simultaneous inference literature. A method similar to, but older than, Scheffé's was suggested by Fisher. Called the least significant difference test, it has a relative advantage of shrinking the area which may cause the con-

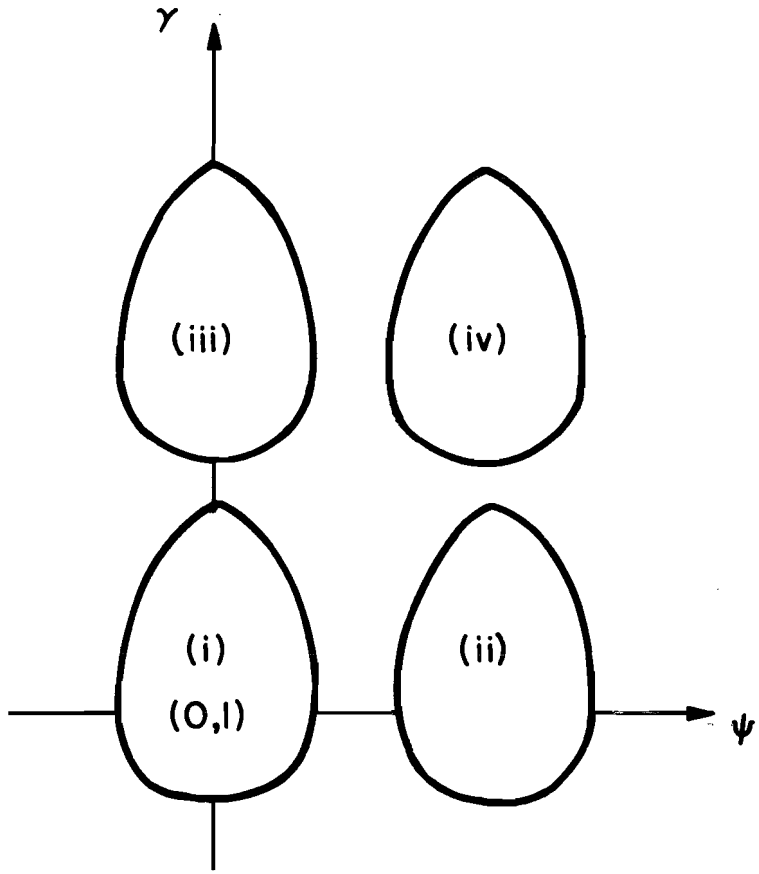

Figure 3.2 HPD Contours of $(\underset{\sim}{\psi},\gamma)$ for p=1 under Four Cases

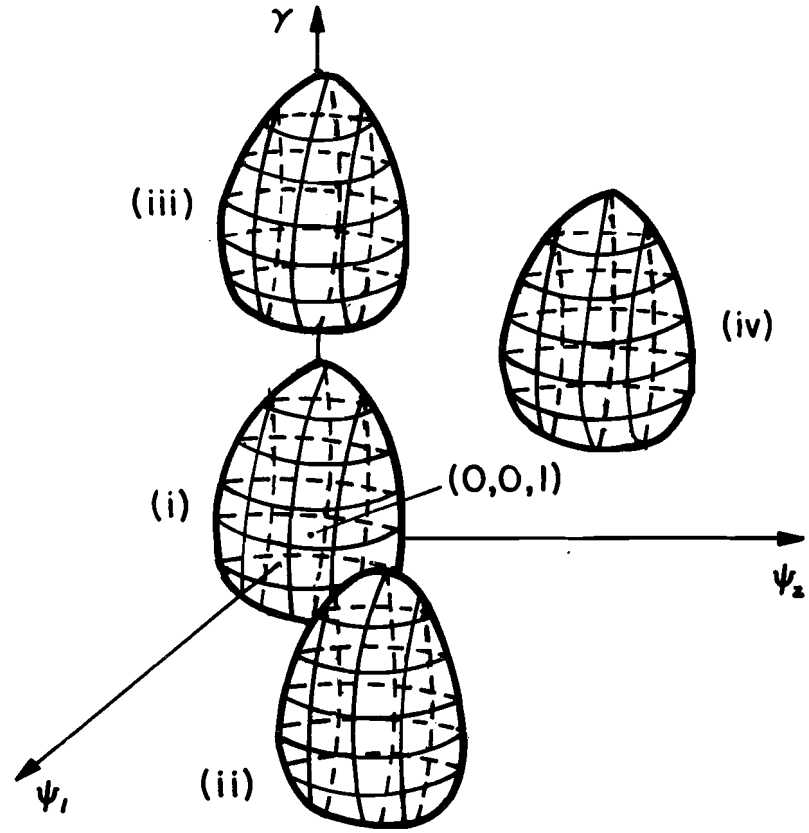

Figure 3.3 HPD Contours of $(\underset{\sim}{\psi},\gamma)$ for p=2 under Four Cases

tradiction mentioned above. However, for the sake of convenience, we prefer using the former in the discrimination procedure.

The generalization of the procedure to higher order models can be similarly presented as follows. Due to the high correlation which usually exists among elements of $\underset{\sim}{\psi}$ a posteriori, we treat them together as a unit in the process.

Stage 1: Substitute $(\underset{\sim}{0}, 1)$ into the formula (3.14) and compare the resulting figure with one half of the upper 100α percentage point of a χ^2 variable with $p + 1$ d.f. If it is smaller than the critical point we determine that $\underset{\sim}{\psi} = 0$ and $\gamma = 1$. Otherwise, go to the second stage.

Stage 2: Sbustitute $(\hat{\underset{\sim}{\psi}}, 1)$ into the same formula and repeat the same comparison. Since the model of $p(\underset{\sim}{\psi}|\gamma, \underset{\sim}{y}^{(1)}, \underset{\sim}{y}^{(2)})$ always locates at $\hat{\underset{\sim}{\psi}}$, it is sufficient to check the point $(\hat{\underset{\sim}{\psi}}, 1)$ to decide if the hyperplane $\gamma = 1$ touches the $(p + 1)$-dimensional contour. If $(\hat{\underset{\sim}{\psi}}, 1)$ does lie inside the contour, we determine that $\underset{\sim}{\psi} \neq 0$ and $\gamma = 1$. Otherwise, go on to examine the line $\underset{\sim}{\psi} = \underset{\sim}{0}$ in the neighborhood of $\hat{\gamma}$ to see if there is any value of which $G(\underset{\sim}{0}, \gamma)$ gives a value lower than the critical point. If there is, it is case (iii), $\underset{\sim}{\psi} = \underset{\sim}{0}$ and $\gamma \neq 1$. Otherwise, it is (iv). Of course, a contradiction may theoretically occur here, but it will rarely happen in practice if n is moderate. A graphical presentation of typical three-dimensional HPD contours for these four cases is also shown in Figure 3.3. When it is case (i), the contour surrounds the point $(\psi_1, \psi_2, \gamma) = (0, 0, 1)$. For other cases the point (0, 0, 1) will be outside of the contours. If the case is (ii), the plane $\gamma = 0$ cuts across the contour. For case (iii), the vertical axis γ goes through the contour. When the situation does not belong to any one of these three, it is case (iv).

3.3 Comparison of the Means of Two Autoregressive Time Series

In the testing scheme described in Section 3.2, partially because of the attempt to avoid the extreme complexity and partially because of the justification from some practical applications, the mean value of the series y_t is assumed equal to zero. In case the average levels of the two series to be compared are both equal to the same non-zero value, the y_t series may represent the deviations of the observations from a constant mean and thus comparison of these two y_t series is equivalent to the comparison performed on the original observations. But from our experience with ATC communication simulations, in addition to the potential difference in the autoregressive parameters and error variance between historical and simulated data, the mean levels of the time series often appear to be different. In order to examine this difference in means, we derive a test statistic in this section by assuming the autoregressive parameter values to be known. Consider a sequence of observations, z_t, $t = 1, 2, \ldots, n$ which follow an autoregressive time series model of order ρ with mean μ, i.e.,

$$z_t - \mu = \phi_1(z_{t-1} - \mu) + \phi_2(z_{t-2} - \mu) + \ldots + \phi_p(z_{t-p} - \mu) + a_t,$$
$$t = p + 1, \ldots, n \qquad (3.15)$$

where $a_t \sim N(0, \sigma^2)$. By shifting all terms of μ in equation (3.15) to the right side and z's to the left, we obtain

$$u_t = z_t - \phi_1 z_{t-1} \ldots - \phi_p z_{t-p} = (1 - \phi_1 \ldots - \phi_p)\mu + a_t . \qquad (3.16)$$

Dividing both sides of (3.16) by $(1 - \phi_1 \ldots - \phi_p)$, i.e.

$$w_t = \frac{u_t}{1 - \phi_1 \ldots - \phi_p} = \mu + \frac{a_t}{(1 - \phi_1 - \ldots - \phi_p)} = \mu + b_t \qquad (3.17)$$

where $b_t \sim N(0, \sigma^2/(1 - \phi_1 \ldots -\phi_p)^2)$, we find that the transformed variable w_t is a white noise series with mean μ and variance equal to $\sigma^2/(1 - \phi_1 \ldots - \phi_p)^2$.

Assume that now we have two series $\{z_1^{(1)}, z_2^{(1)}, \ldots, z_n^{(1)}\}$ and $\{z_1^{(2)}, z_2^{(2)}, \ldots, z_n^{(2)}\}$. The two series can be transformed into $\{w_{p+1}^{(1)}, \ldots w_n^{(1)}\}$ and $\{w_{p+1}^{(2)}, \ldots, w_n^{(2)}\}$, following the procedure specified by (3.16) and (3.17), which have mean and error terms μ_1, $b_t^{(1)}$ and μ_2, $b_t^{(2)}$ respectively. Again adopting the Bayesian approach, the test statistic for $(\mu_2 - \mu_1)$ is

$$t = \frac{\bar{w}_2 - \bar{w}_1}{\alpha\sqrt{(s_1^2 + s_2^2)/n}}$$

where $\bar{w}_2 = \sum_{i=p+1}^{n} w_i^{(2)}/(n - p)$

$$\bar{w}_1 = \sum_{i=p+1}^{n} w_i^{(1)}/(n - p)$$

$$\alpha^2 = \frac{(\beta - 2)}{\beta} f_1$$

$$\beta = 4 + \frac{f_1^2}{f_2}$$

$$f_1 = \left(\frac{\nu_2}{\nu_2 - 2}\right)\cos^2\phi + \left(\frac{\nu_1}{\nu_1 - 2}\right)\sin^2\phi,$$

$$f_2 = \frac{\nu_2^2}{(\nu_2 - 2)^2(\nu_2 - 4)}\cos^4\phi + \frac{\nu_1^2}{(\nu_1 - 2)^2(\nu_1 - 4)}\sin^4\phi,$$

$$\cos^2\phi = \frac{s_2^2}{(s_1 + s_2)}, \quad \sin^2\phi = 1 - \cos^2\phi$$

$$s_1^2 = \sum_{i=p+1}^{n} (w_i^{(1)} - \bar{w}_1)^2/(n - p - 1),$$

$$s_2^2 = \sum_{i=p+1}^{n} (w_i^{(2)} - \bar{w}_2)^2/(n - p - 1) \qquad (3.18)$$

and $\nu_1 = \nu_2 = n - p - 1$.

The value of t calculated from these two series should be compared with a Student t distribution with β degrees of freedom. For instance, assume that t computed from the set of data is 1.67 and β obtained is 17.9. From the table of the t distribution, the 5% significance points (2.5% on each tail) are -2.101 and 2.101 for 18 degrees of freedom. Since 1.67 falls in the range (-2.101, 2.101), the t calculated indicates that $(\mu_2 - \mu_1)$ is not different from zero at 5% level.

In practice, the value of $\underset{\sim}{\phi}^{(1)}$ and $\underset{\sim}{\phi}^{(2)}$ are usually unknown. However, their estimates $\hat{\underset{\sim}{\phi}}^{(1)}$ and $\hat{\underset{\sim}{\phi}}^{(2)}$, obtained from the first stage of the test described in Section 3.2, can be used to replace the $\underset{\sim}{\phi}$ in Equation (3.17) for the derivation of $\underset{\sim}{w}^{(1)}$ and $\underset{\sim}{w}^{(2)}$.

3.4 Validation of Sector Simulations

As described in Chapter 2, the initiation of an individual sector simulation proceeds as follows:

(i) the traffic density ρ (expected number of arrivals per hour) is set equal to the observed value for the individual sector;

(ii) the parameter values of p and k for the distribution of the number of CT's per aircraft are directly estimated from the sector data;

(iii) the historical sector histogram is used for the TR/CT distribution;

(iv) the parameter values of α and λ in the distribution of transmission lengths are obtained from the pair of master equations described in Section 1.5 using the assigned traffic density;

(v) the a_o and a_1 parameters for generating intercommunication gap lengths are estimated from the individual sector data.

Altogether seven parameter values are required to establish the driving variables for each sector simulation. As noted in Chapter 2 and illustrated in Figures 2.3 through 2.20, histograms descriptive of the driving variables are provided by the simulation. These data are primarily used to monitor the simulation.

Of much greater importance to the validation of the simulation model are the two responses aircraft loading n_t and channel utilization C_t. Both these responses are generated as time series. The essential validation step consists of testing the hypothesis that the structure of the simulated time series, and the structure of the observed time series, for both responses, are identical.

To supply an example, the observed and simulated time series plots of aircraft loading for Sector 453, one of the busiest enroute sectors, are displayed in Figures 3.4 and 3.5. Although the two aircraft loading series are not identical, the pattern of fluctuations do look similar. Following the suggestions of Box and Jenkins, the sample autocorrelation functions of both series were calculated. These are presented in Figures 3.6 and 3.7. Again, the estimated autocorrelation functions appear very much alike and both are consistent with a second order autoregressive, an AR(2), model. The AR(2) model was thus fitted to both series, and the two sets of parameters were estimated. The parameter estimates are listed in the first row of Table 3.1. A test of the hypothesis that both time series have the same structure, using the statistic $G(\underset{\sim}{0}, 1)$, was then performed. The value of $G(\underset{\sim}{0}, 1)$ calculated, 0.7771, was far below its 1% critical point, 5.6. The test of the hypothesis that there is a zero difference in the mean level of both aircraft loading series gave an observed value of t equal to 0.6330. Once again the simulated and observed means were not statistically significantly different. It was therefore concluded that the simulation of aircraft loading for this sector was satisfactory. Similar tests on the channel utilization series were carried out. The results for Sector 453 are listed in Table 3.2. Again the structure of the simulated series is indistinguishable from that of the observed series.

Seven other sectors, each selected from different sector functions, were also simulated and tested. Sectors were selected which had high traffic density and for which the negative binomial distribution appropriately represented the distribution of CT/aircraft. Individual sectors from the CD, AP, and RA sector functions were omitted due to their small number of observations and to consequent difficulty in modelling. The LE sectors were also omitted from this initial study because of their great similarity to LT and HI sectors. The test statistics calculated for these sectors are listed in Tables 3.1 and 3.2. The hypothesis that the observed and simulated time series have the same structure is found acceptable in every case.

At this stage of the investigation considerable confidence had been generated in the simulation model. Although there are occasional individual sectors for which validation is not possible, this failure is generally

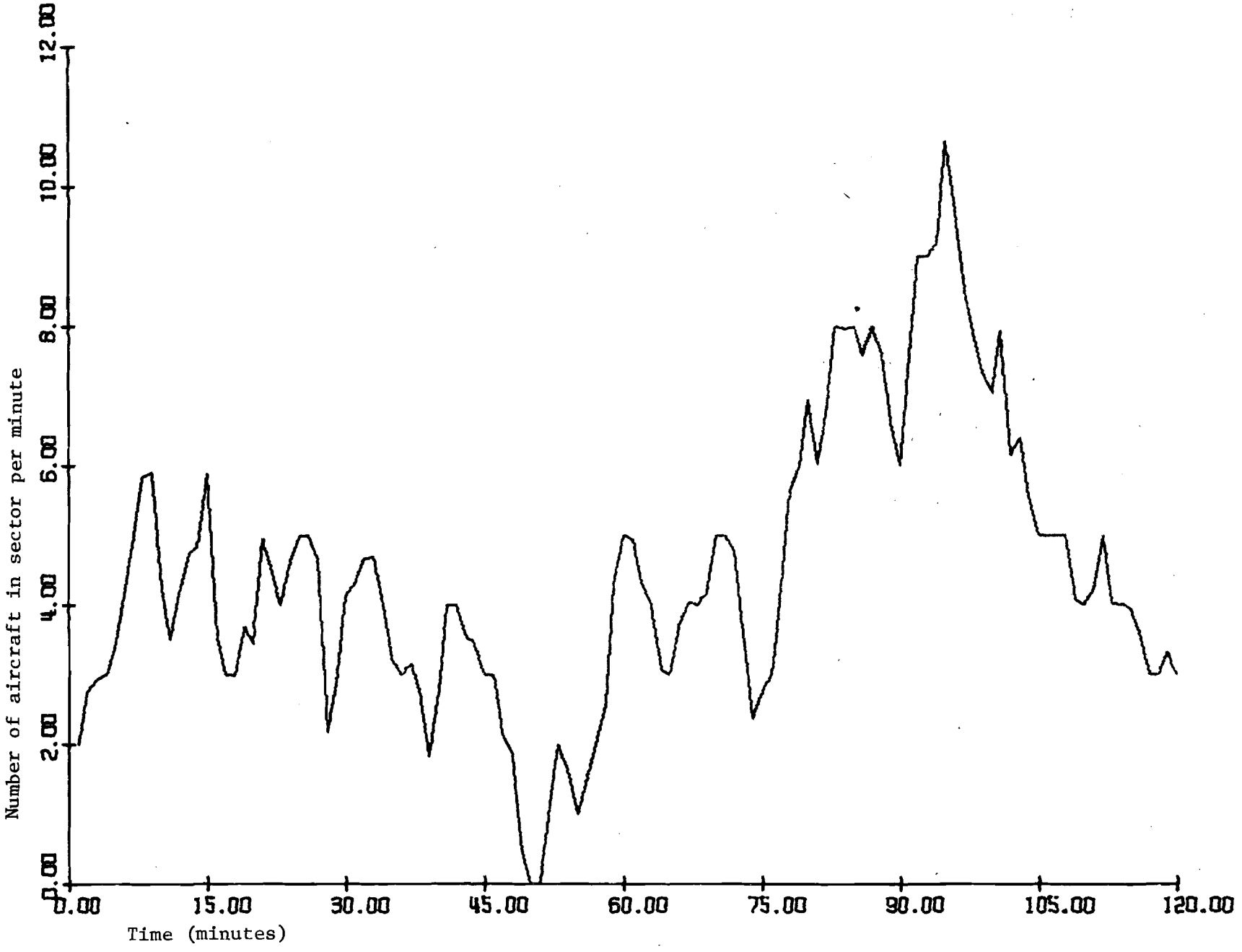

Figure 3.4 Historical Time Series of Aircraft Loading in Sector 453 LT

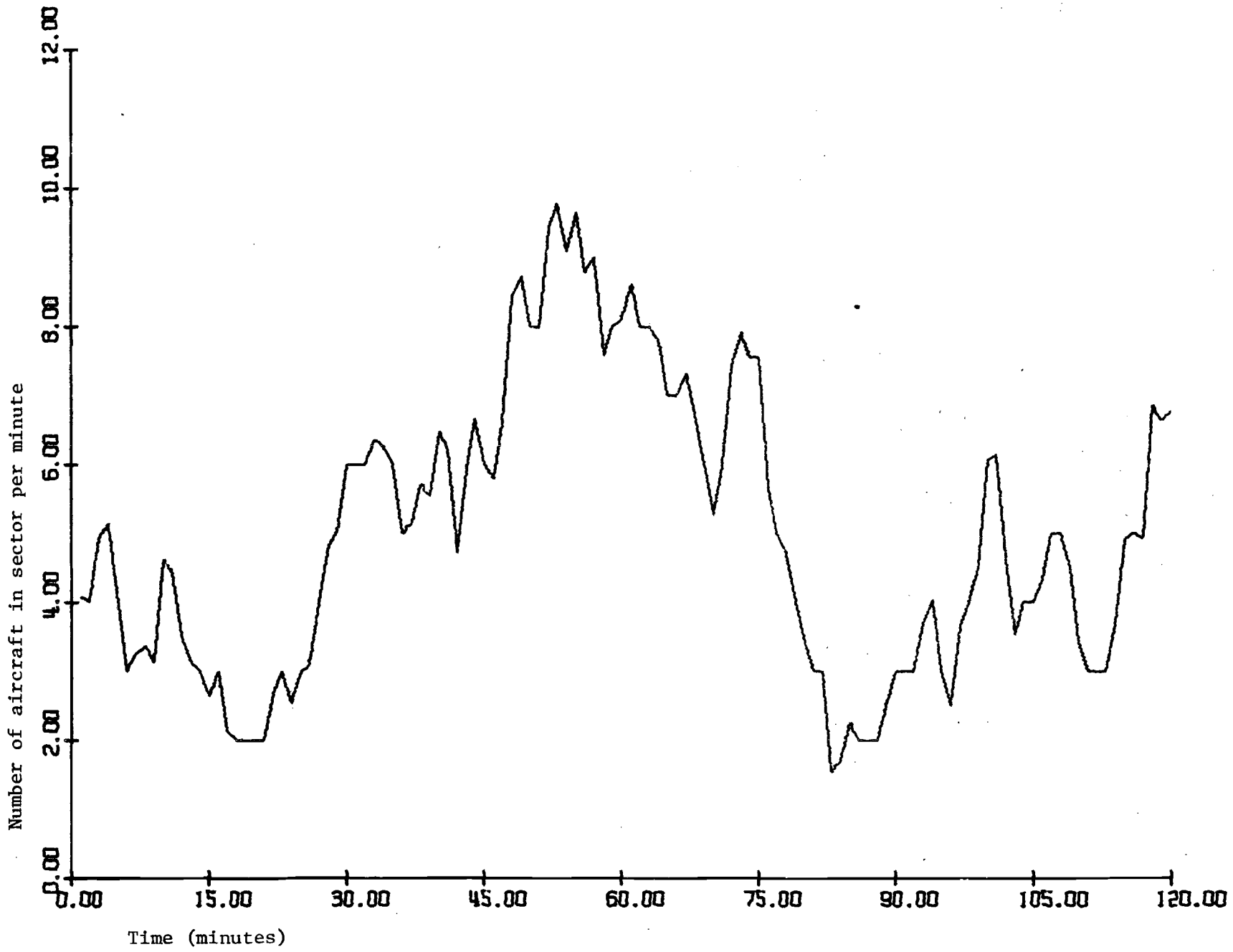

Figure 3.5 Simulated Time Series of Aircraft Loading in Sector 453 LT at 100% of Historical Traffic Density

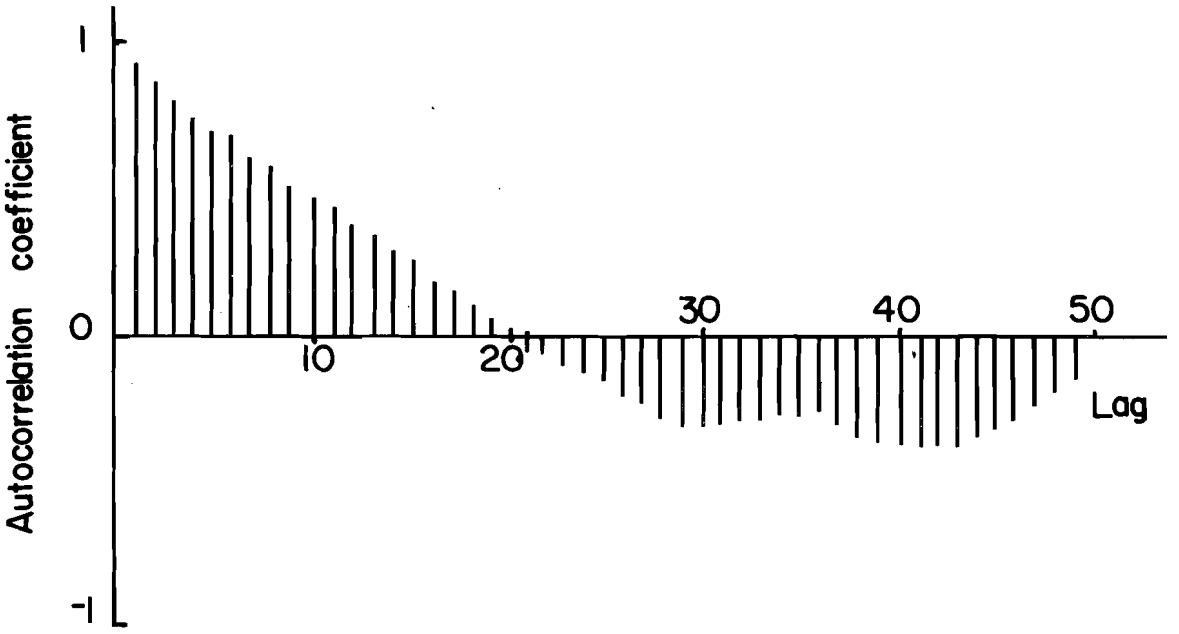

Figure 3.6 Autocorrelation Function of Historical Aircraft Loading Series (Sector 453)

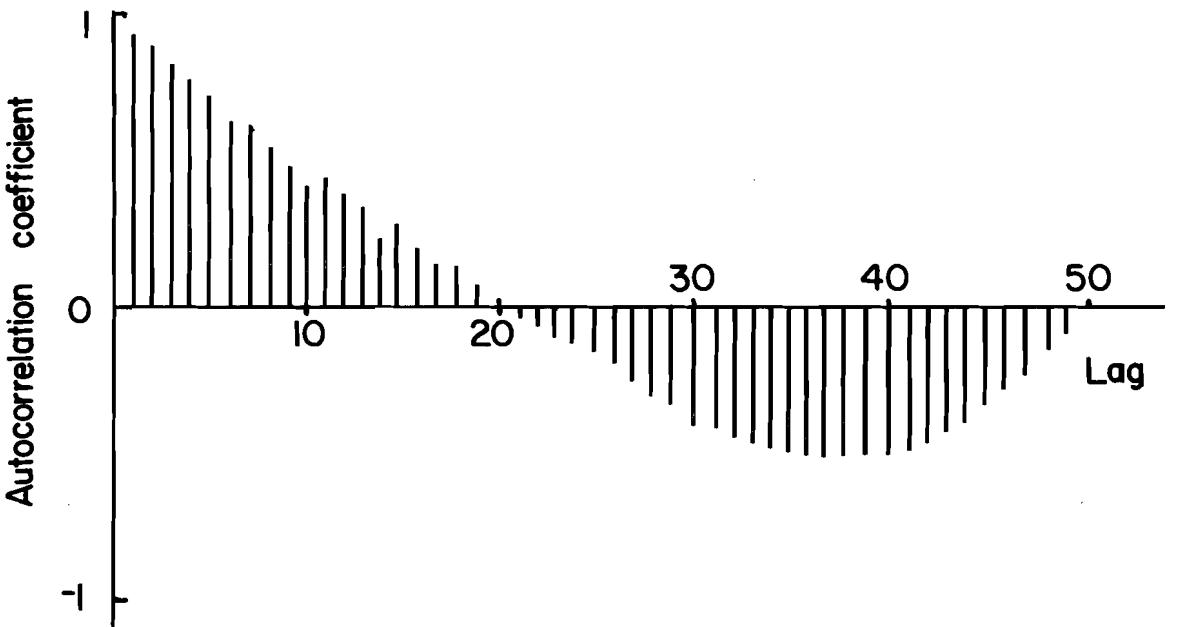

Figure 3.7 Autocorrelation Function of Simulated Aircraft Loading Series (Sector 453)

Table 3.1 Comparison of Historical versus Simulated Aircraft Loading Series

Sector I.D.			$\hat{\mu}$	$\hat{\phi}_1$	$\hat{\phi}_2$	$\hat{\sigma}^2$	t^a	$G(\underset{\sim}{0},1)^b$
453	LT	Historical	4.4669	1.1131	-0.2015	0.5783	0.6330	0.7771
		Simulated	5.0064	1.1000	-0.1666	0.4893		
475	HI	Historical	4.5895	1.2874	-0.4048	0.5559	1.6062	0.5464
		Simulated	5.6786	1.2401	-0.4054	0.6304		
504	GN	Historical	2.4093	0.9155	-0.0698	0.5269	0.7298	0.9302
		Simulated	2.7012	1.0349	-0.1481	0.6612		
510	LC	Historical	6.1327	0.9737	-0.1314	0.5182	-0.1344	4.0359
		Simulated	5.9831	1.1148	-0.1969	0.8538		
524	LG	Historical	2.9246	1.2741	-0.3681	4.4062	0.3360	1.7248
		Simulated	3.7668	1.2692	-0.3151	0.5467		
534	DP	Historical	1.8651	0.9404	-0.2310	0.3617	1.5560	4.4130
		Simulated	2.5098	1.1876	-0.3596	0.5491		
543	AD	Historical	1.3675	1.2273	-0.3855	0.2209	1.6554	3.9694
		Simulated	2.4656	1.2436	-0.3127	0.3459		
553	AR	Historical	4.0454	1.0482	-0.0891	0.3960	0.6963	0.4224
		Simulated	4.2994	1.0971	-0.1549	0.3634		

a $t_{.005}(200) = 2.6$

b $\frac{1}{2}\chi^2_{0.01}(3) = 5.6$

Table 3.2 Comparison of Historical versus Simulated

Channel Utilization Series

Sector I.D.			$\hat{\mu}$	$\hat{\phi}_1$	$\hat{\phi}_2$	$\hat{\sigma}^2$	t^a	$G(\underset{\sim}{0},1)^b$
453	LT	Historical	0.4935	0.1303	0.2064	0.0501	0.9674	3.1163
		Simulated	0.5300	0.1622	0.0414	0.0777		
475	HI	Historical	0.5693	0.3502	0.1485	0.0482	-0.2376	2.2130
		Simulated	0.5631	0.3924	0.0030	0.0698		
504	GN	Historical	0.5136	0.5094	0.0667	0.0729	-0.2119	1.4480
		Simulated	0.4740	0.4099	-0.0301	0.0906		
510	LC	Historical	0.5589	0.2194	0.0407	0.0462	-1.6534	2.3554
		Simulated	0.4693	0.3279	0.1867	0.0634		
524	LG	Historical	0.3081	0.2989	0.2286	0.0511	0.2232	0.7029
		Simulated	0.3360	0.4168	0.1928	0.0609		
534	DP	Historical	0.4340	0.2513	0.2124	0.0433	0.5629	4.4186
		Simulated	0.4683	0.4489	0.0972	0.0722		
543	AD	Historical	0.5467	0.3171	0.1153	0.0826	-1.1203	3.4167
		Simulated	0.4563	0.5798	0.1368	0.0739		
553	AR	Historical	0.5567	0.3268	0.1879	0.0565	0.7865	0.1368
		Simulated	0.5931	0.3301	0.1852	0.0648		

a $t_{.005}(200) = 2.6$

b $\frac{1}{2}\chi^2_{0.01}(3) = 5.6$

attributable to the paucity of data for these sectors, unusually large numbers of maverick observations which make the distribution assumptions untenable, or, as in the case of the GN (ground control) sectors, the pronounced lack of independence of the arrivals of incoming aircraft. But the vast majority of the individual sectors (the enroute, the local control, the local and ground control, plus the IFR Room departure, arrival, and arrival-departure control sectors) can be successfully simulated.

3.5 The Validation of Sector Function Simulations

The objective of the simulation modeling was not, however, the duplication of the time histories of particular sectors. Each sector would, of course, have its own idiosyncrasies reflected, in part, by the sector's seven parameter values. Of greater interest was the use of the model as a general simulation for sector functions. Using the structure of the individual sector model, the general simulation of a sector function proceeded by:

(i) specifying the sector function;
(ii) specifying ρ, the traffic density to be studied;
(iii) determining the six remaining simulation parameters from master tables and master equations compiled for each sector function.

More specifically, parameters p and k were decided by Table 1.2 and the supplementary table, Table 1.3, a_0 and a_1 determined by the simultaneous use of Table 1.4 and Equation (1.3) and finally α and λ determined by solving Equation (1.6).

In order to validate the results provided by the general simulation of a sector function, a traffic density was chosen equal to the observed traffic density of a specific representative sector. The two time series responses derived from the general simulation were then tested against the historical data for that sector.

As an example, the general simulation model was exercised for the HI sector function. The traffic density employed was that of Sector 475, that is, $\rho = 33.1$ aircraft arrivals per hour. The values $p = 0.76$ and $k = 12.13$ were read from Table 1.2 (for HI sectors one has the option to choose either Table 1.2 or Table 1.3, since both non-shifted and shifted negative binomial distributions fit the data satisfactorily). The value $a_0 = 5.1841$ is found from column 1 of Table 1.4 and $a_1 = 0.1133$ determined from Equation (1.3). Finally, since the expected number of aircraft arrivals in the two hour period $x = 33.1 \times 2 = 66.2$ we find, using Equation (1.6), that $\alpha = 2.6995$ and $\lambda = 1.1768$. Comparisons of the simulated system against the historical data responses of Sector 475 are listed in Table 3.3.

Table 3.3 Comparisons of Historical versus Simulated Data

(General HI Simulation)

Aircraft Loading Series	$\hat{\mu}$	$\hat{\phi}_1$	$\hat{\phi}_2$	$\hat{\sigma}^2$	t^a	$G(\underset{\sim}{0},1)^b$
Sector 475 Data	4.5895	1.2874	-0.4048	0.5559	0.749	1.0887
General HI Simulation	5.0154	1.1647	-0.3319	0.6849		
Channel Utilization Series						
Sector 475 Data	0.5693	0.3502	0.1485	0.0482	-0.8195	0.9569
General HI Simulation	0.5256	0.4932	0.1022	0.0593		

a $t_{.005}(200) = 2.6$

b $\frac{1}{2}\chi^2_{0.01}(3) = 5.6$

Comparing the test statistics t and $G(\underset{\sim}{0}, 1)$ in Table 3.3 with equivalent entries in Table 3.1 and 3.2 for Sector 475, one finds that the general simulation works as well as the individual sector simulation.

3.6 Summary and Remarks

After several iterations, the framework for a simulation model appropriate to ATC communications has been constructed. This model may be used to simulate an individual sector given the seven parameter values unique to that sector. Further, the model may be used to characterize a sector function through the use of parameters generated from master tables and equations descriptive of the functions. Both types of simulations have been validated through the use of special statistical testing procedures. There are occasional sectors that have not proved amenable to the simulation model, but they are few in number and possess unique characteristics. As a consequence, the present simulation model would appear to be a valuable tool for further study and experimentation with ATC communications. The following figures are published to provide the reader with further insights into the aircraft loading and channel utilization generated from the sector simulations. Figures are given for both the historical and simulated responses for those sectors included in Table 3.1 and 3.2.

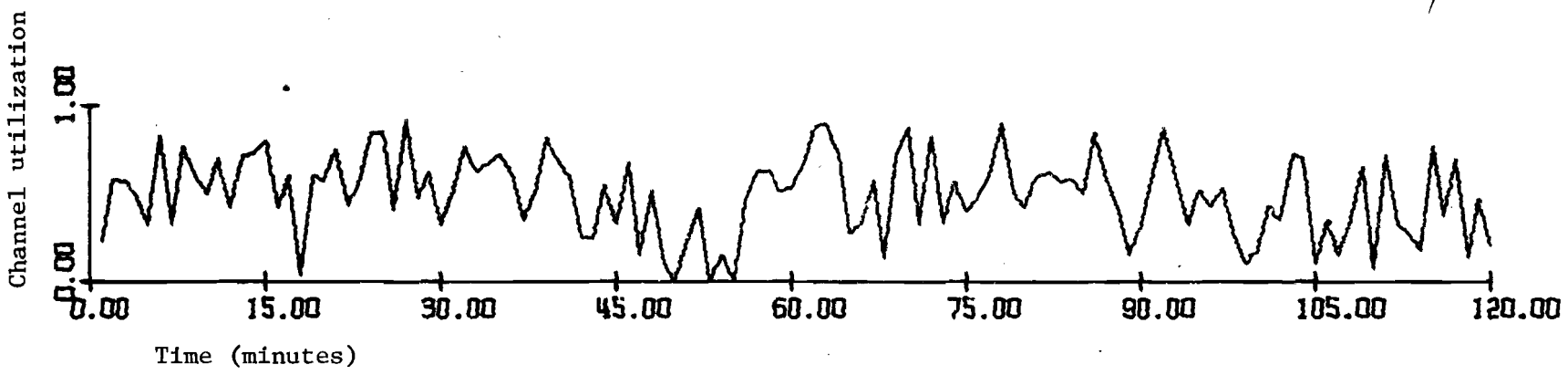

Figure 3.8 Historical Time Series of Channel Utilization in Sector 453 LT

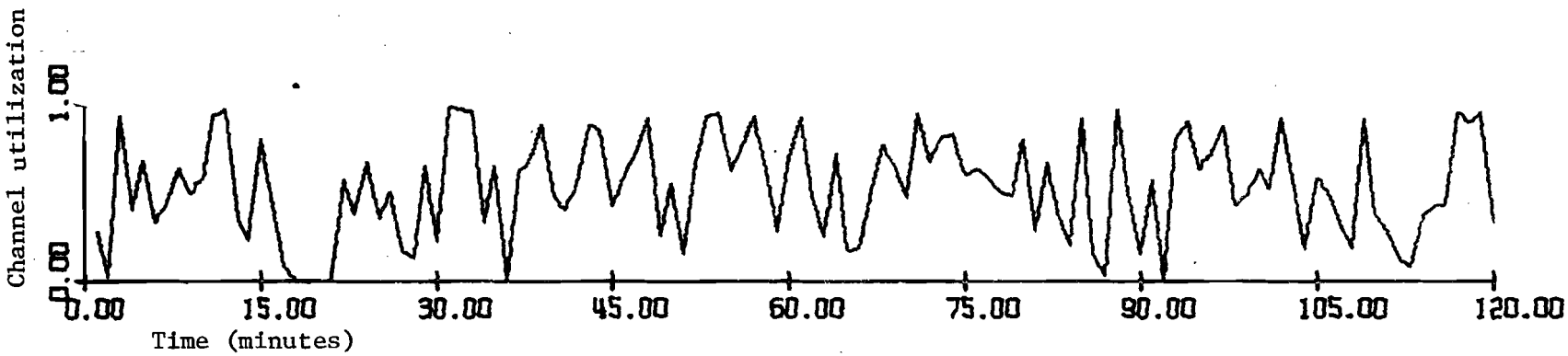

Figure 3.9 Simulated Time Series of Channel Utilization in Sector 453 LT at 100% of Historical Traffic Density

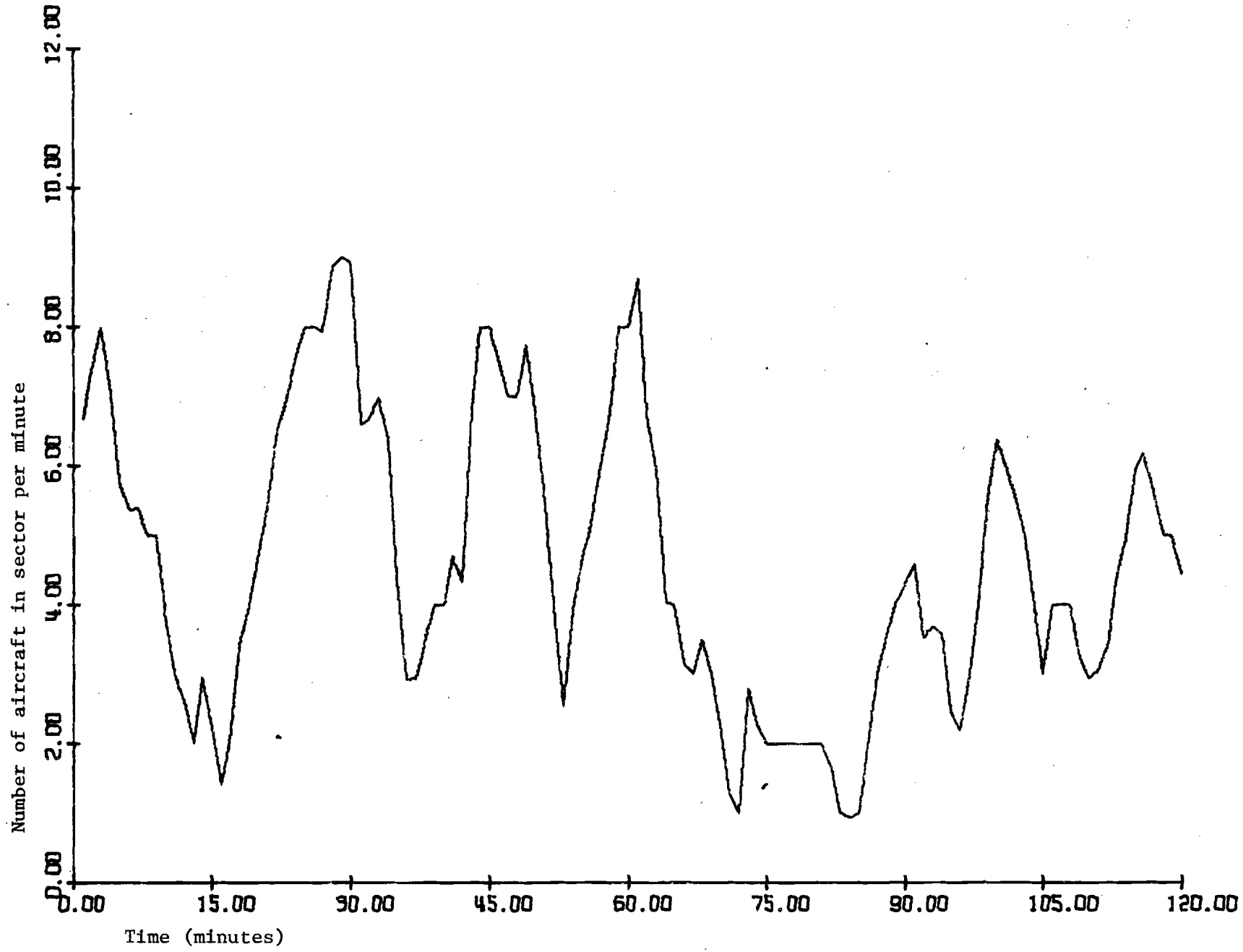

Figure 3.10 Historical Time Series of Aircraft Loading in Sector 475 HI

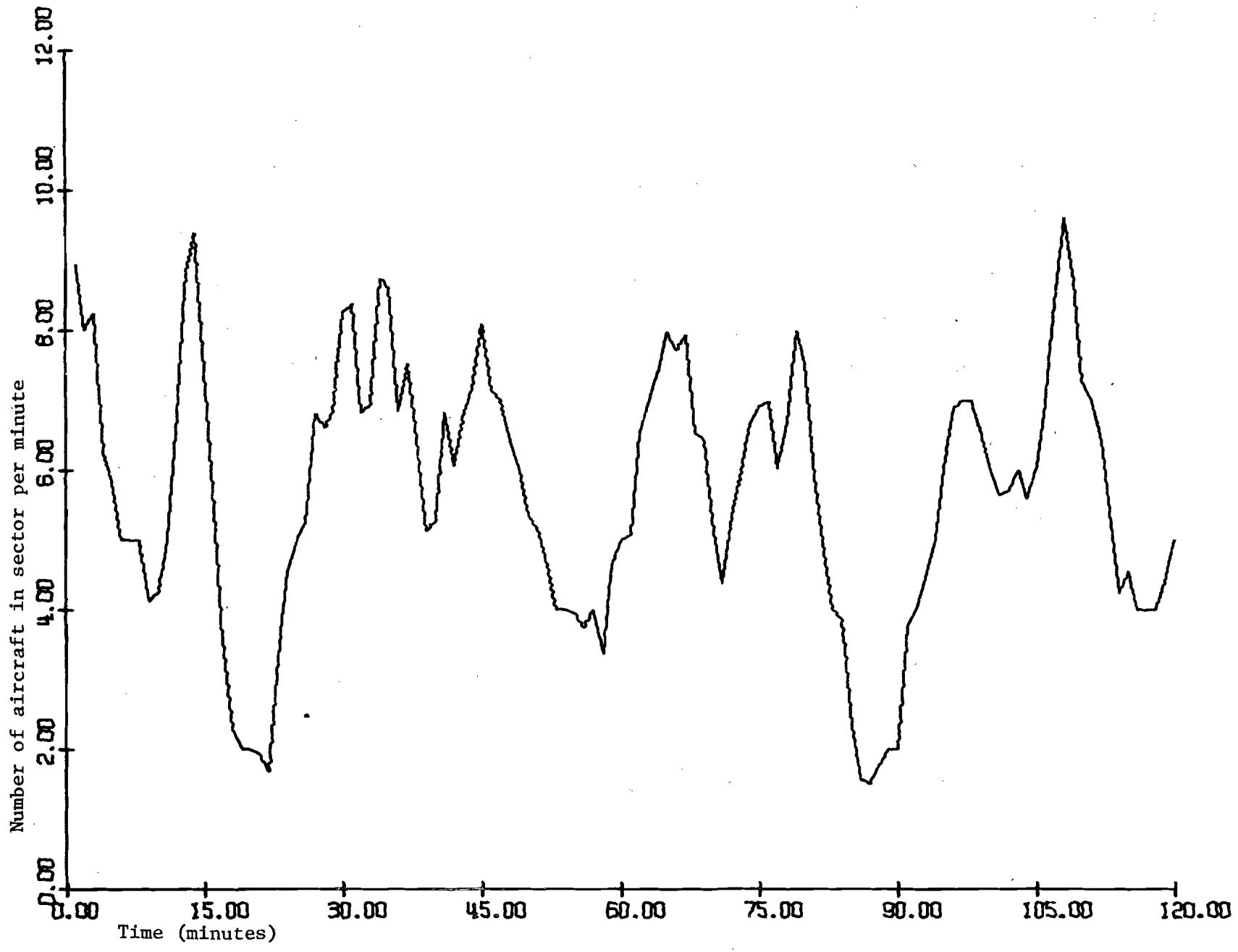

Figure 3.11 Simulated Time Series of Aircraft Loading in Sector 475 HI at 100% of Historical Traffic Density

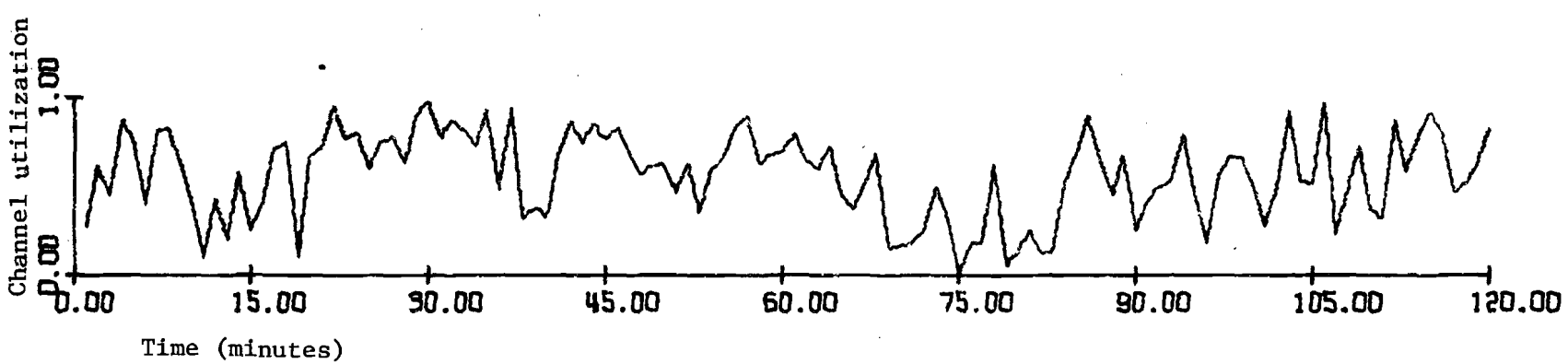

Figure 3.12 Historical Time Series of Channel Utilization in Sector 475 HI

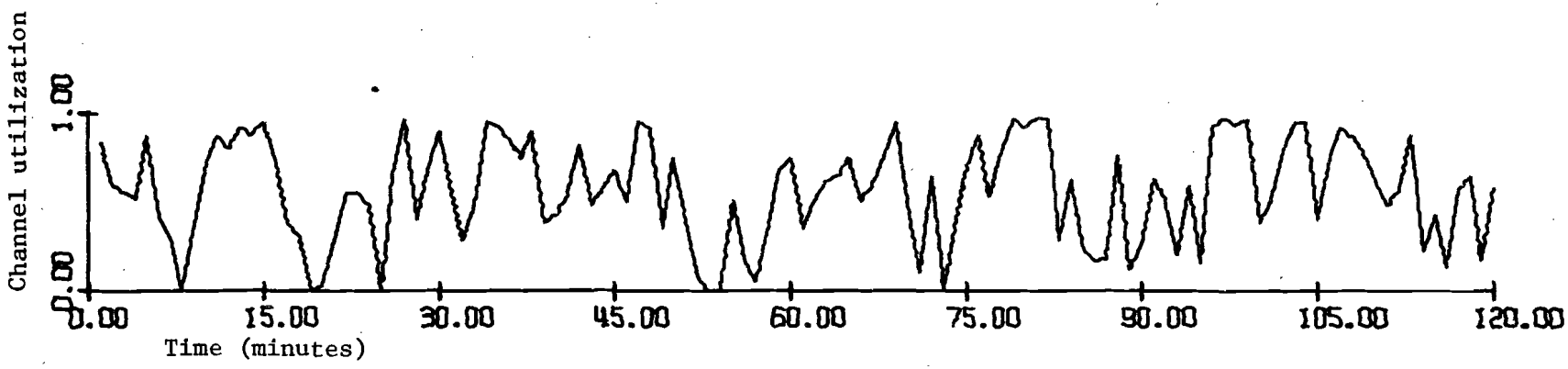

Figure 3.13 Simulated Time Series of Channel Utilization in Sector 475 HI at 100% of Historical Traffic Density

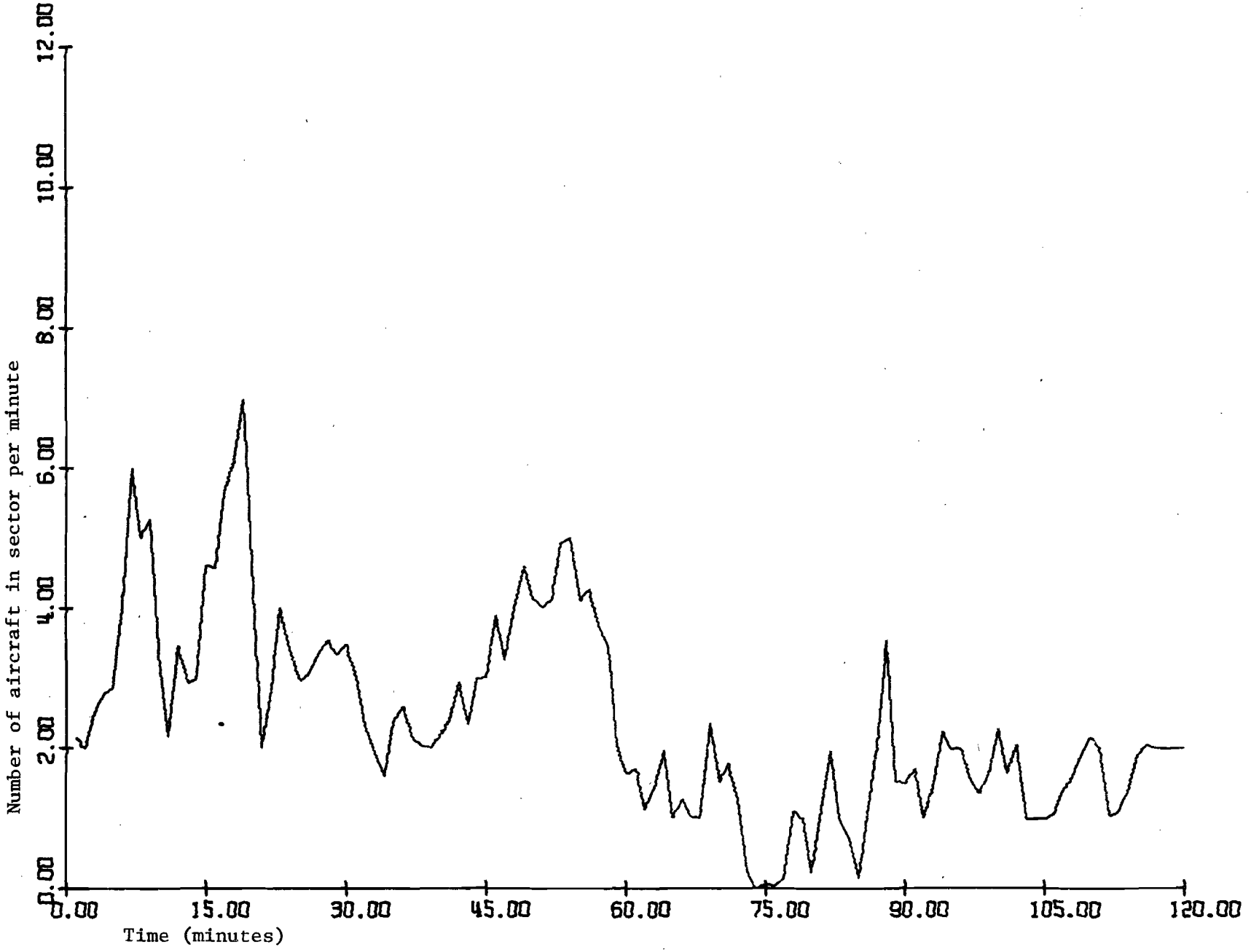

Figure 3.14 Historical Time Series of Aircraft Loading in Sector 504 GN

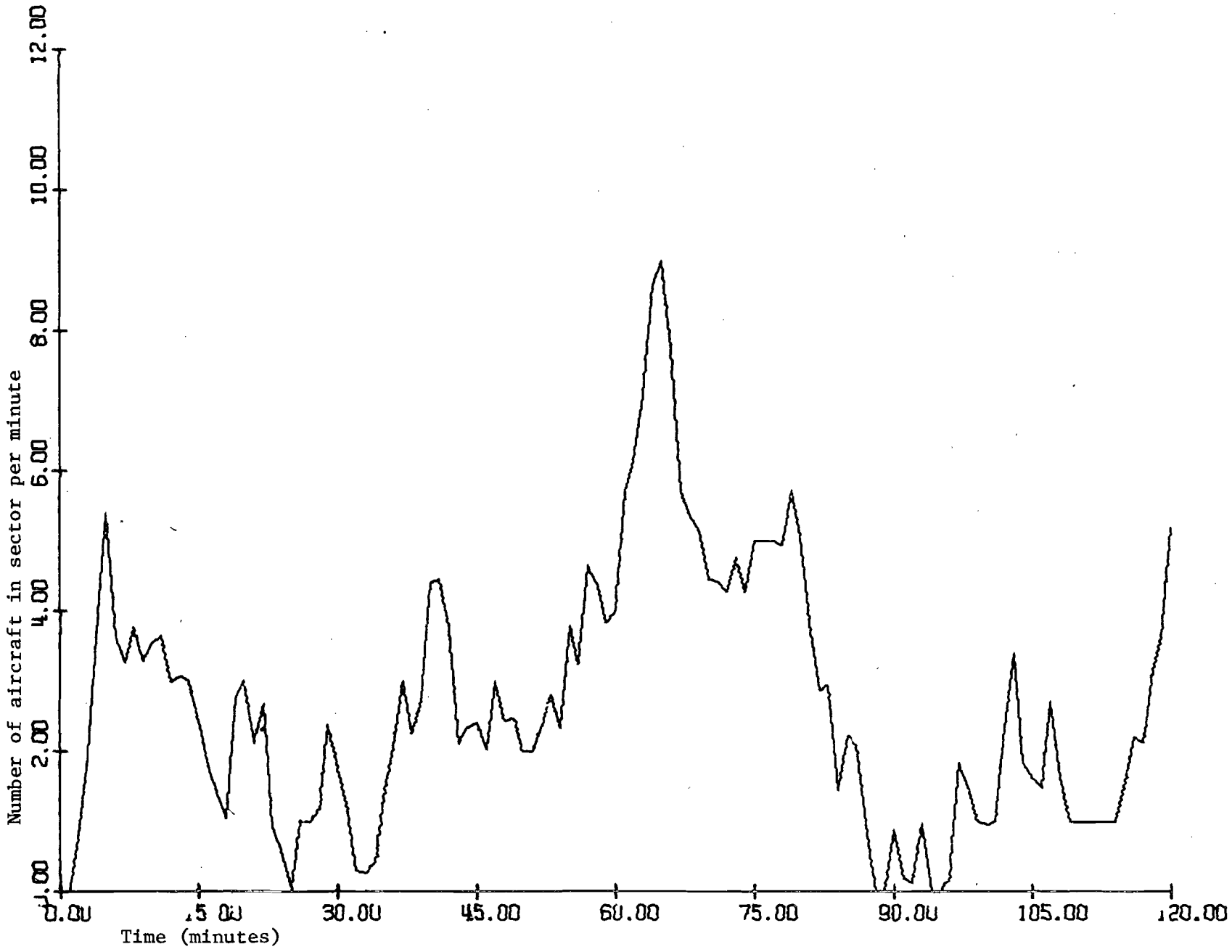

Figure 3.15 Simulated Time Series of Aircraft Loading in Sector 504 GN at 100% of Historical Traffic Density

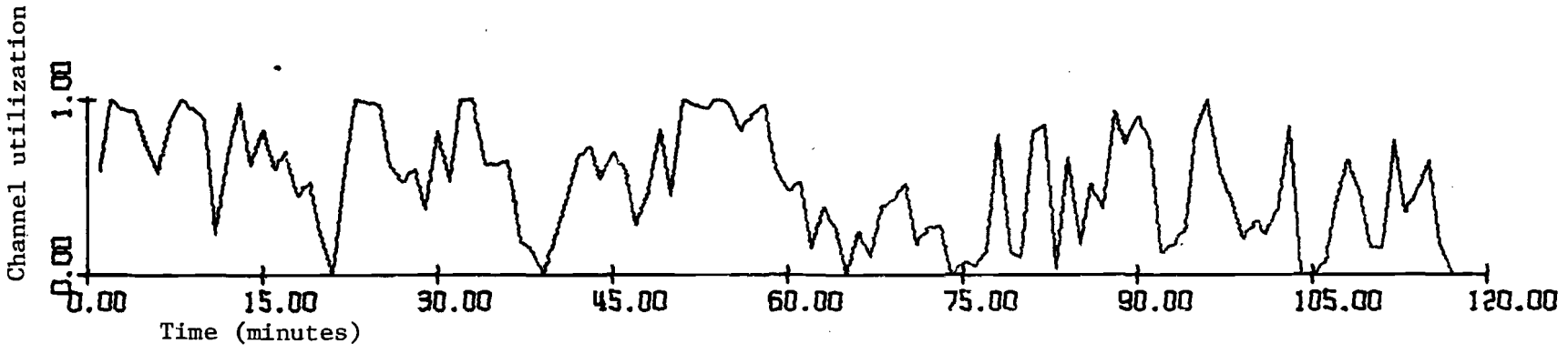

Figure 3.16 Historical Time Series of Channel Utilization in Sector 504 GN

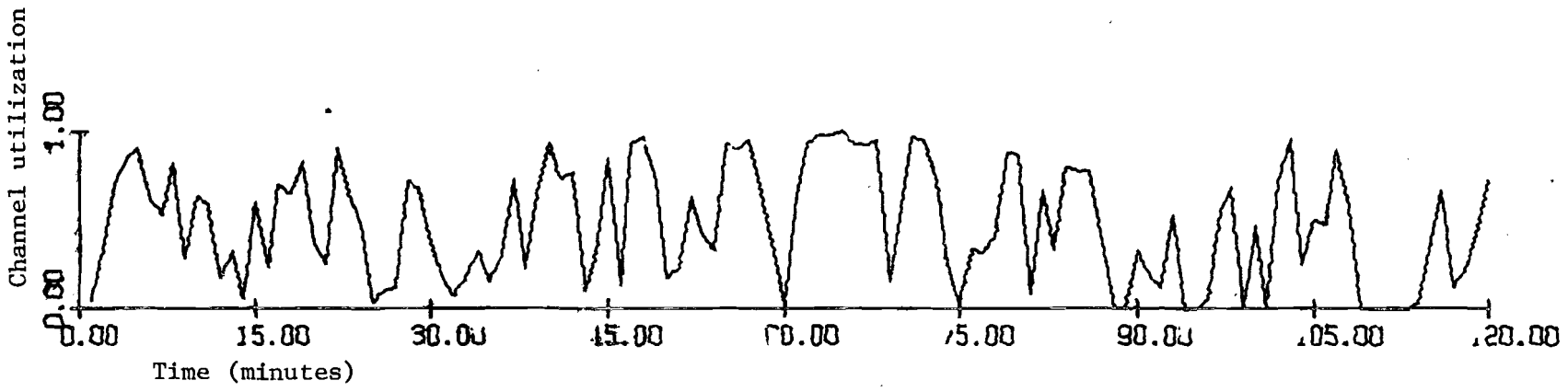

Figure 3.17 Simulated Time Series of Channel Utilization in Sector 504 GN at 100% of Historical Traffic Density

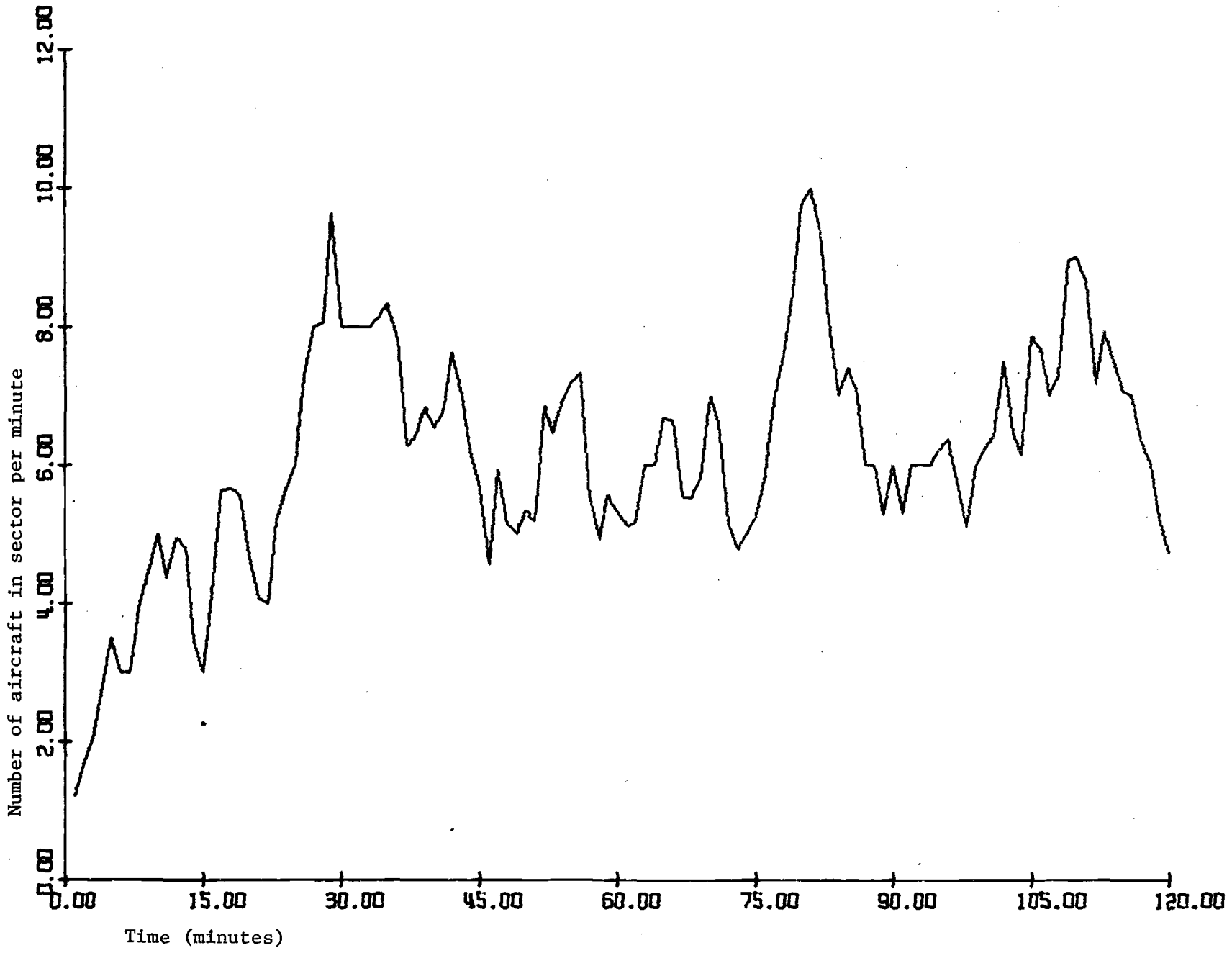

Figure 3.18 Historical Time Series of Aircraft Loading in Sector 510 LC

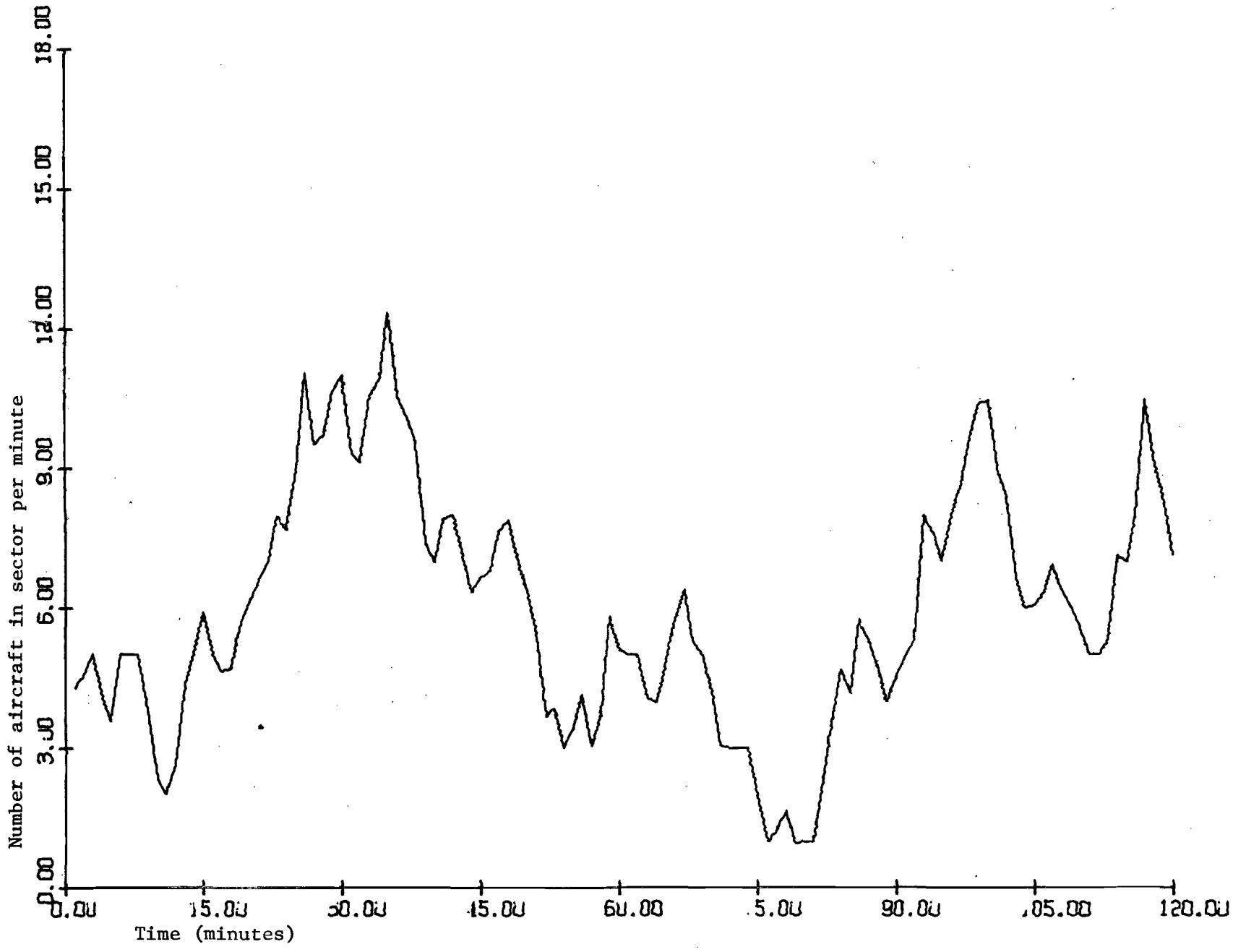

Figure 3.19 Simulated Time Series of Aircraft Loading in Sector 510 LC at 100% of Historical Traffic Density

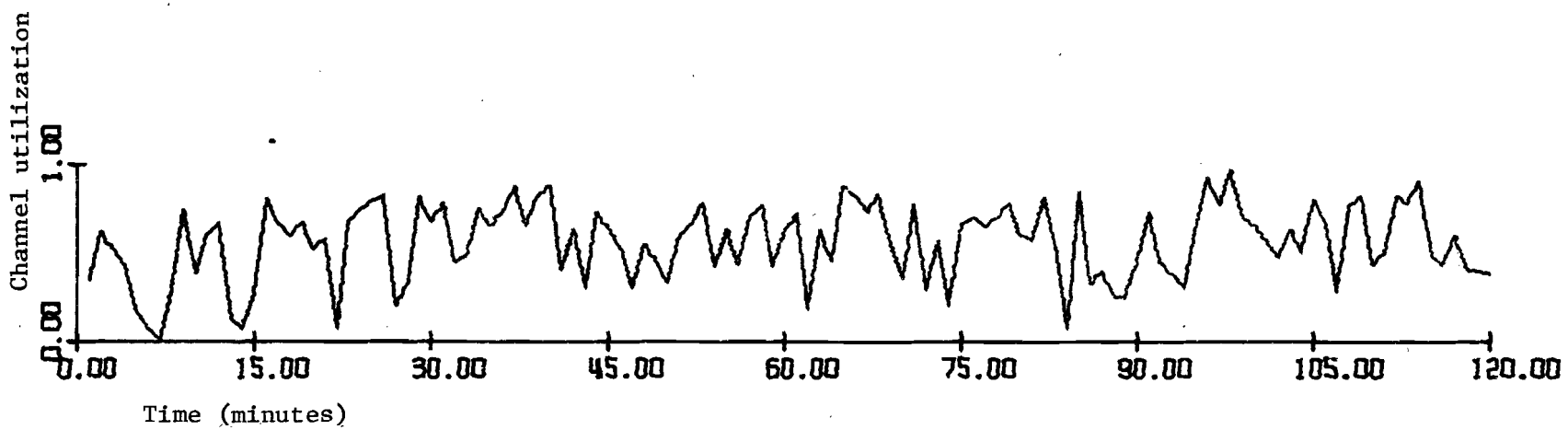

Figure 3.20 Historical Time Series of Channel Utilization in Sector 510 LC

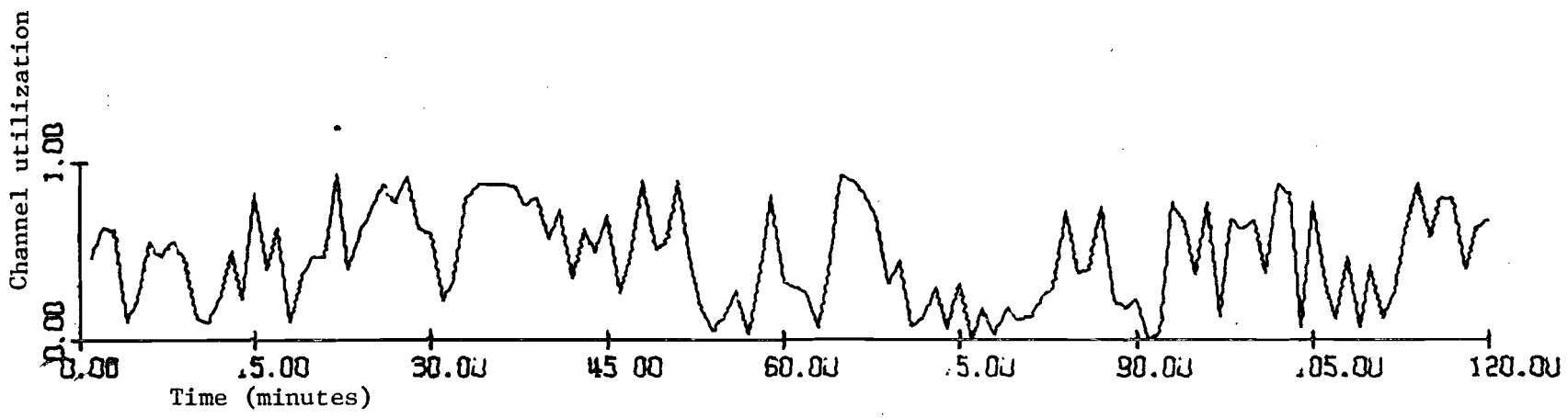

Figure 3.21 Simulated Time Series of Channel Utilization in Sector 510 LC at 100% of Historical Traffic Density

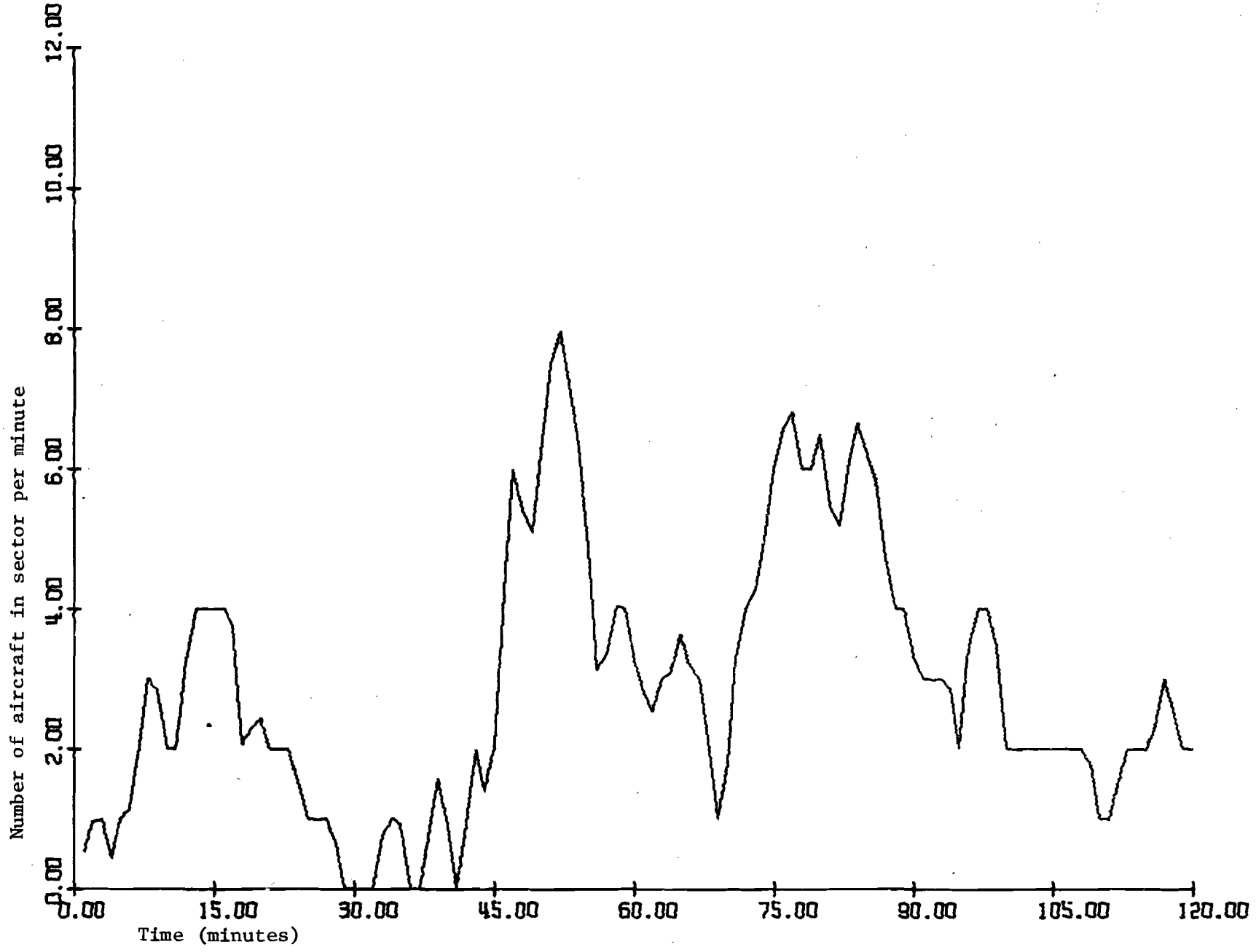

Figure 3.22 Historical Time Series of Aircraft Loading in Sector 524 LG

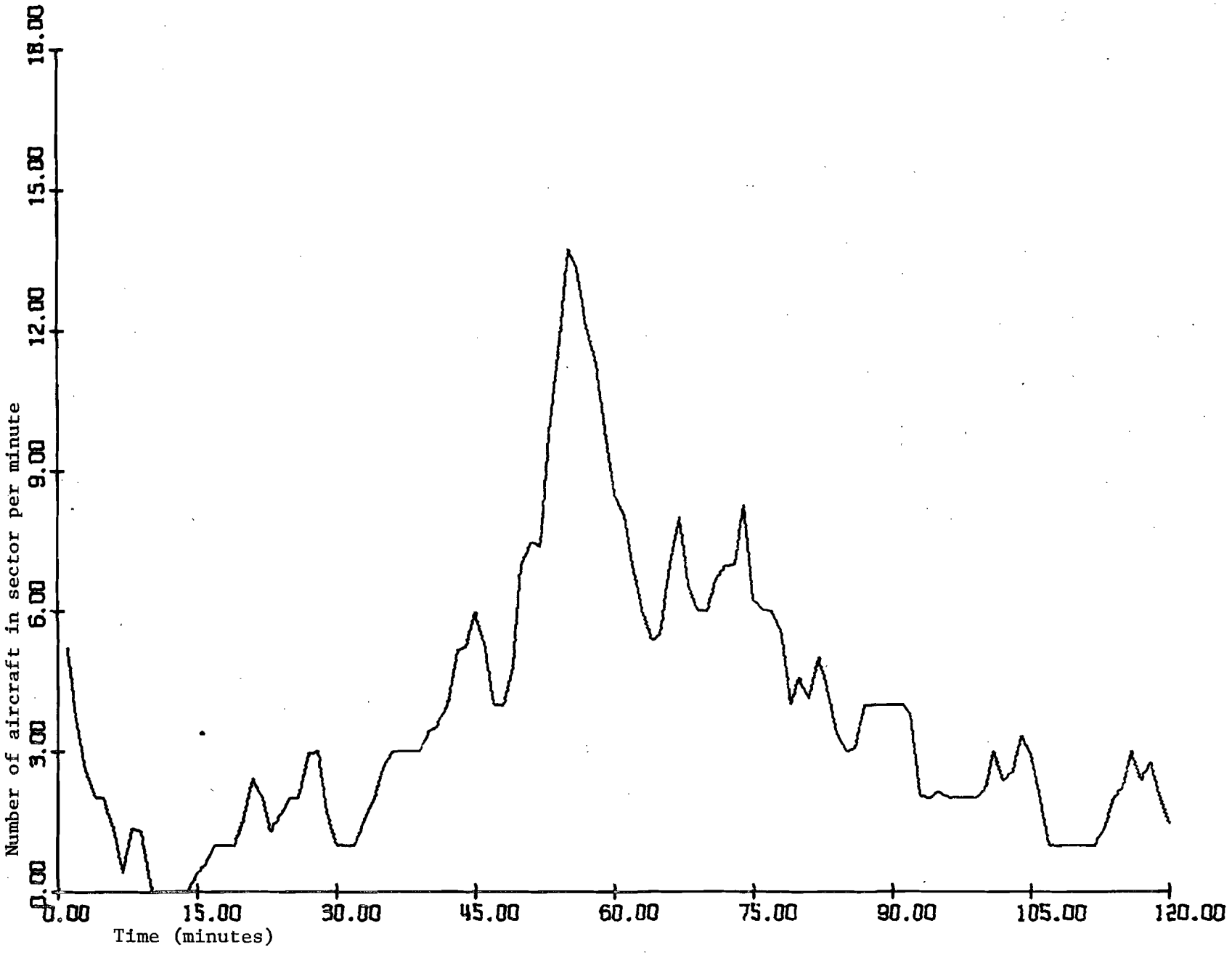

Figure 3.23 Simulated Time Series of Aircraft Loading in Sector 524 LG at 100% of Historical Traffic Density

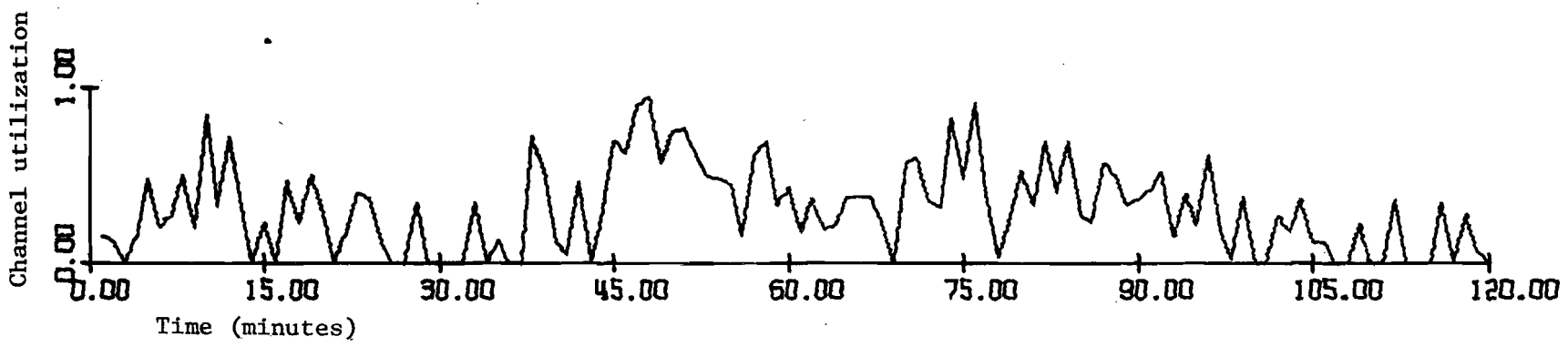

Figure 3.24 Historical Time Series of Channel Utilization in Sector 524 LG

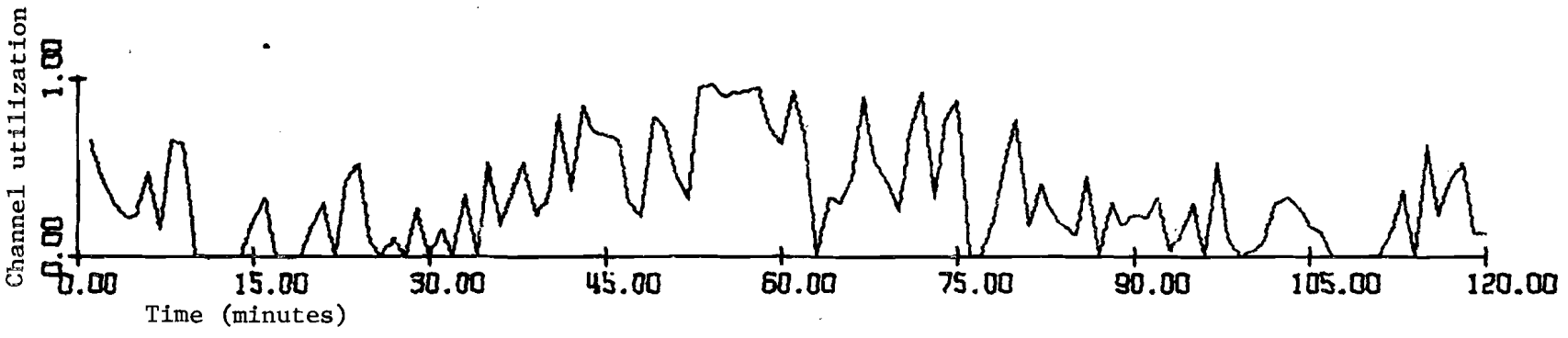

Figure 3.25 Simulated Time Series of Channel Utilization in Sector 524 LG at 100% of Historical Traffic Density

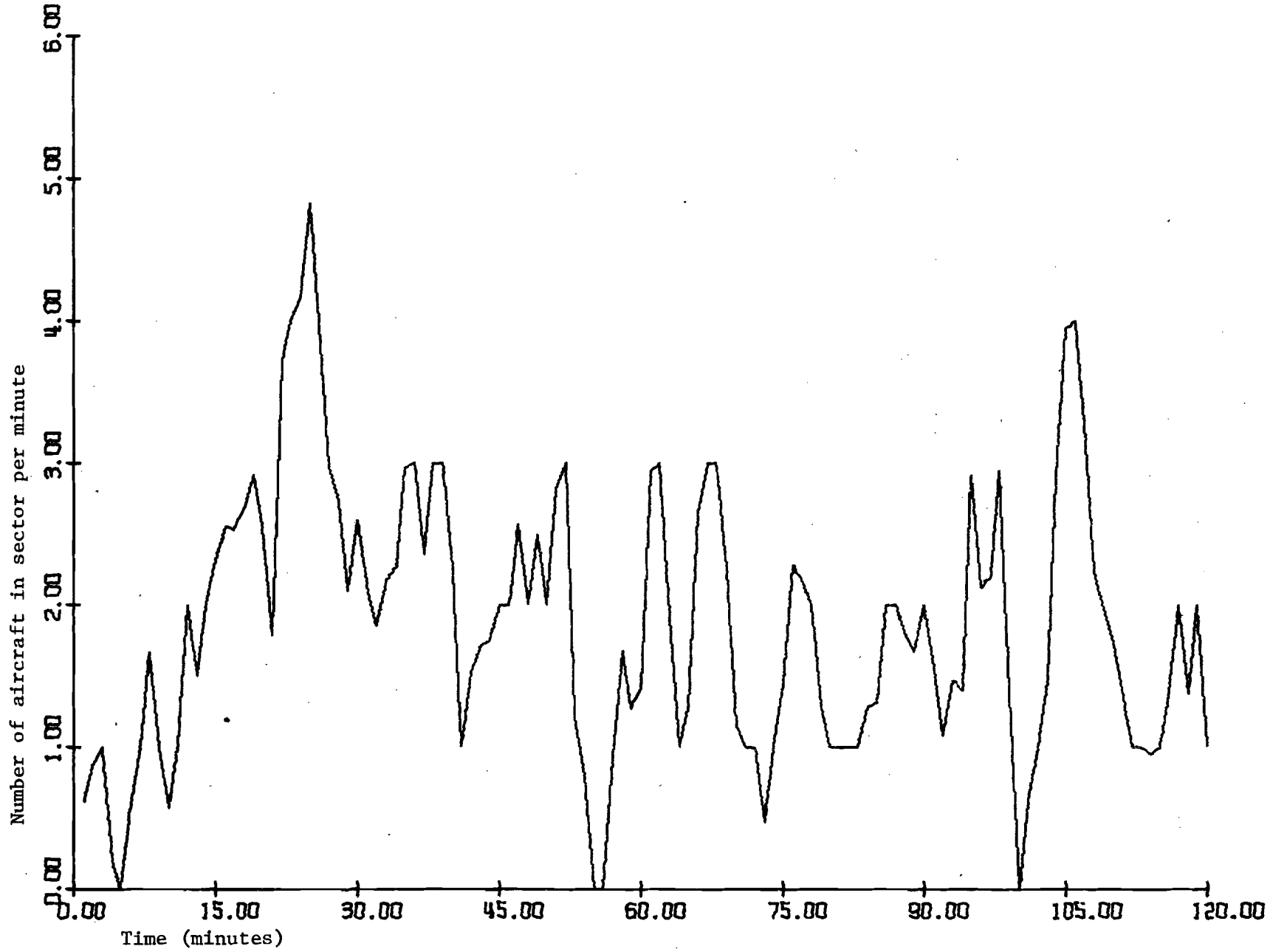

Figure 3.26 Historical Time Series of Aircraft Loading in Sector 534 DP

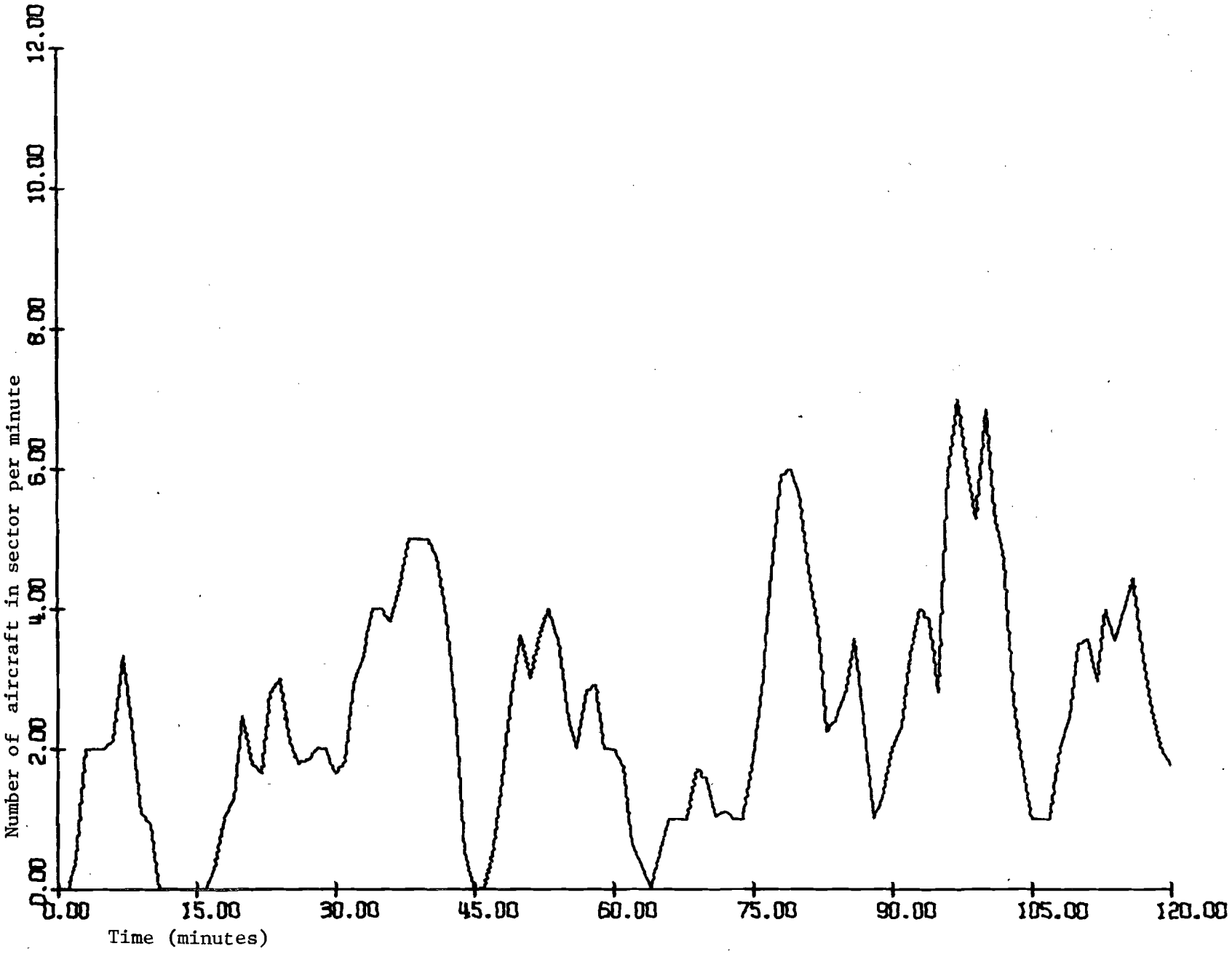

Figure 3.27 Simulated Time Series of Aircraft Loading in Sector 534 DP at 100% of Historical Traffic Density

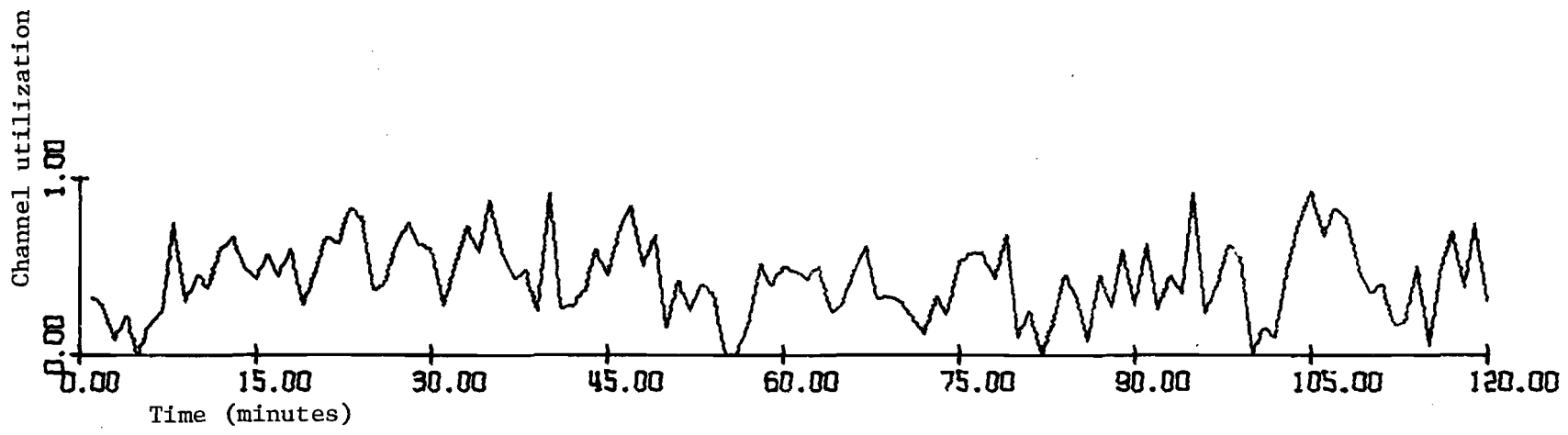

Figure 3.28 Historical Time Series of Channel Utilization in Sector 534 DP

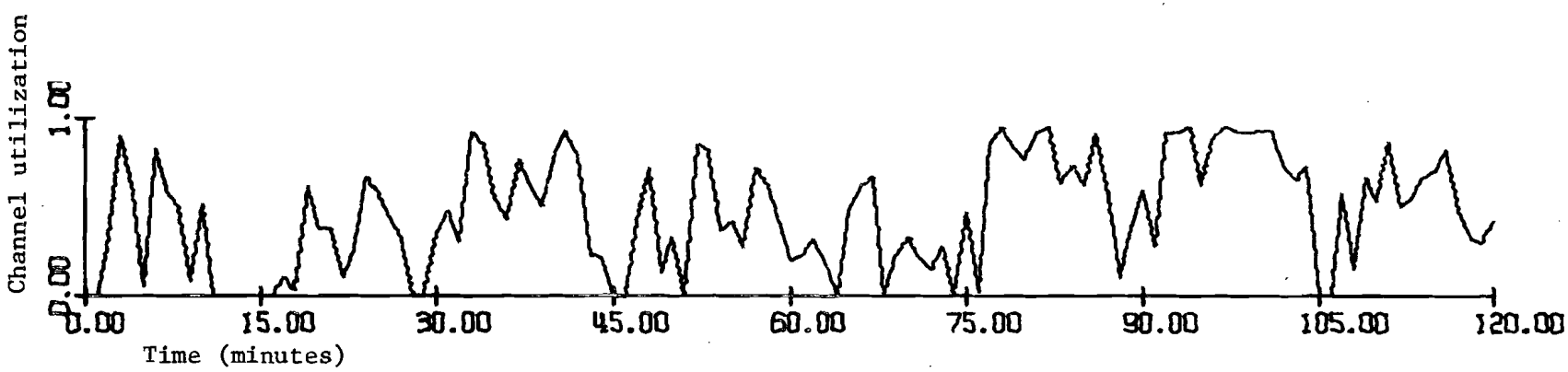

Figure 3.29 Simulated Time Series of Channel Utilization in Sector 534 DP at 100% of Historical Traffic Density

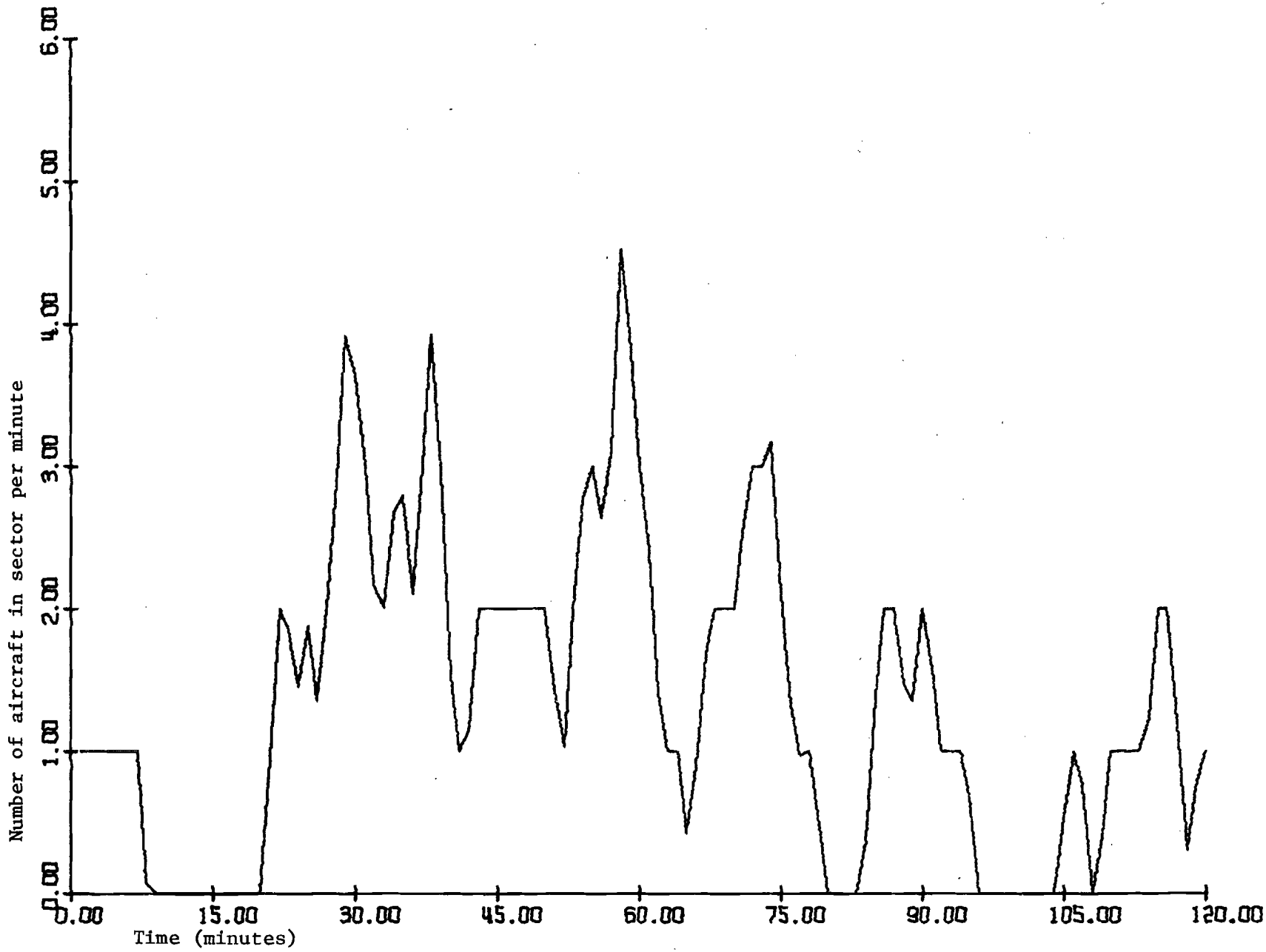

Figure 3.30 Historical Time Series of Aircraft Loading in Sector 543 AD

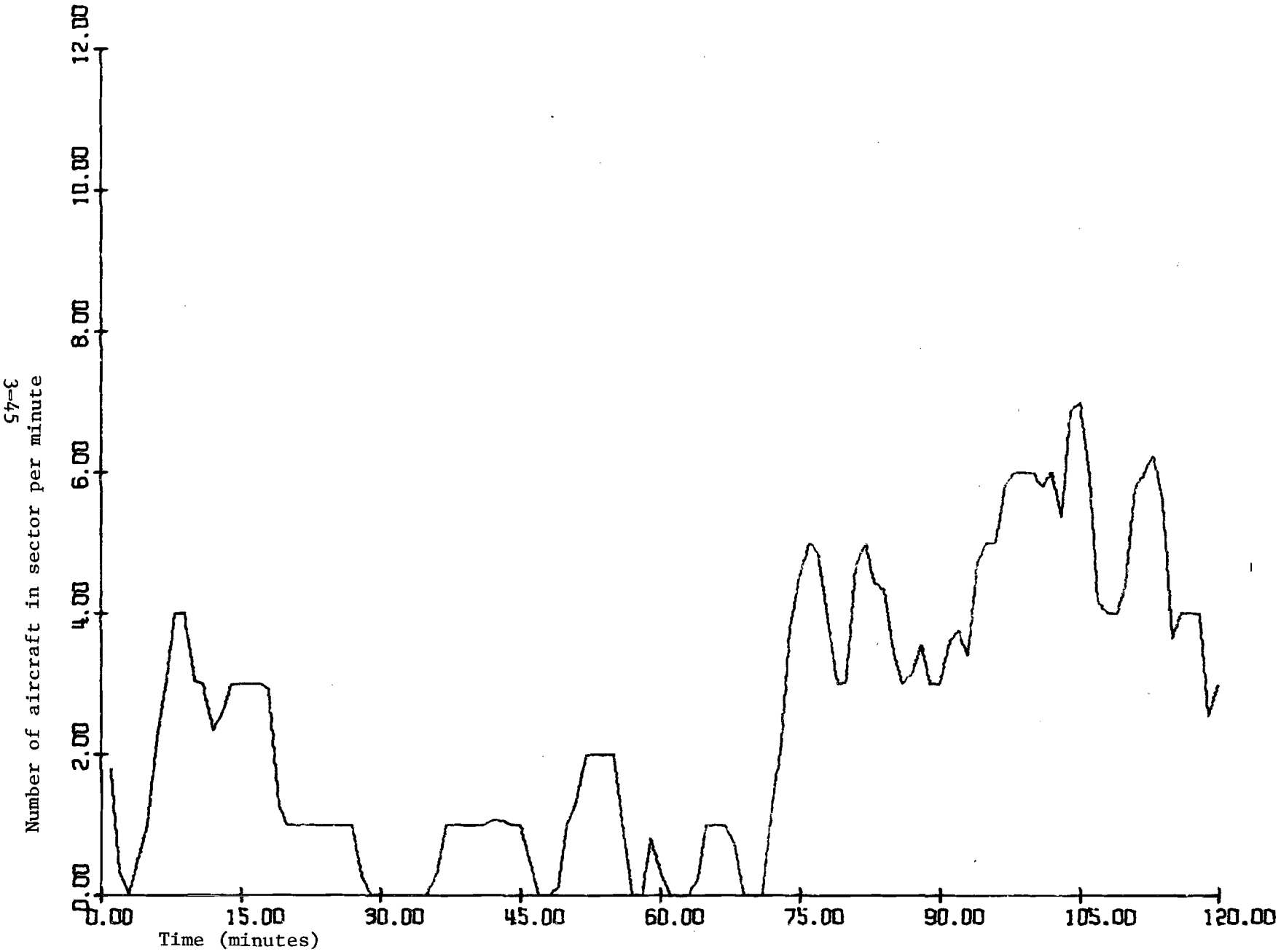

Figure 3.31 Simulated Time Series of Aircraft Loading in Sector 543 AD at 100% of Historical Traffic Density

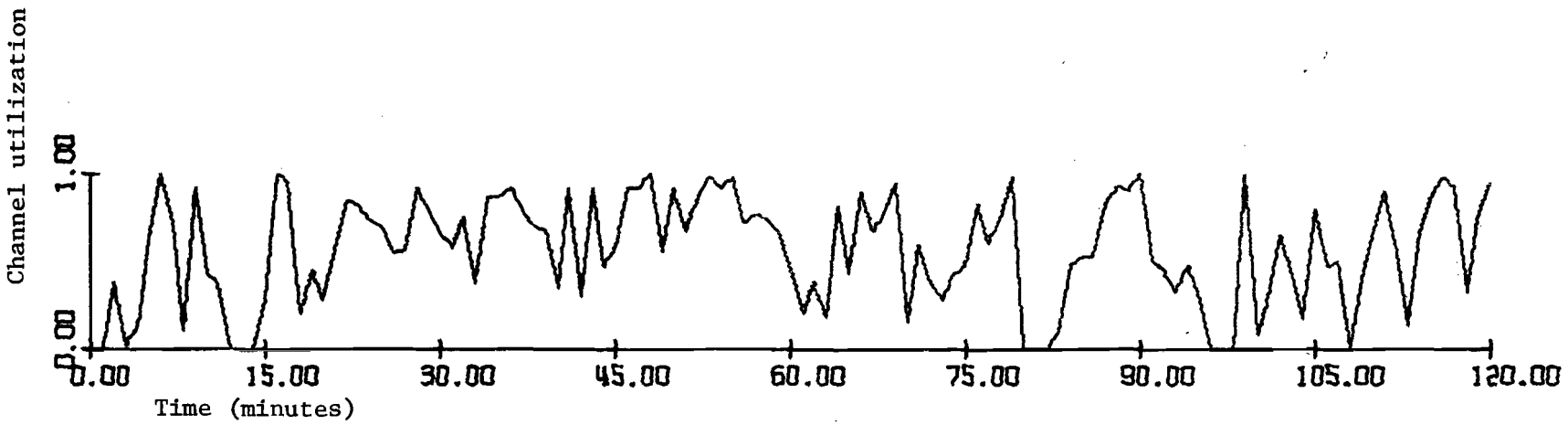

Figure 3.32 Historical Time Series of Channel Utilization in Sector 543 AD

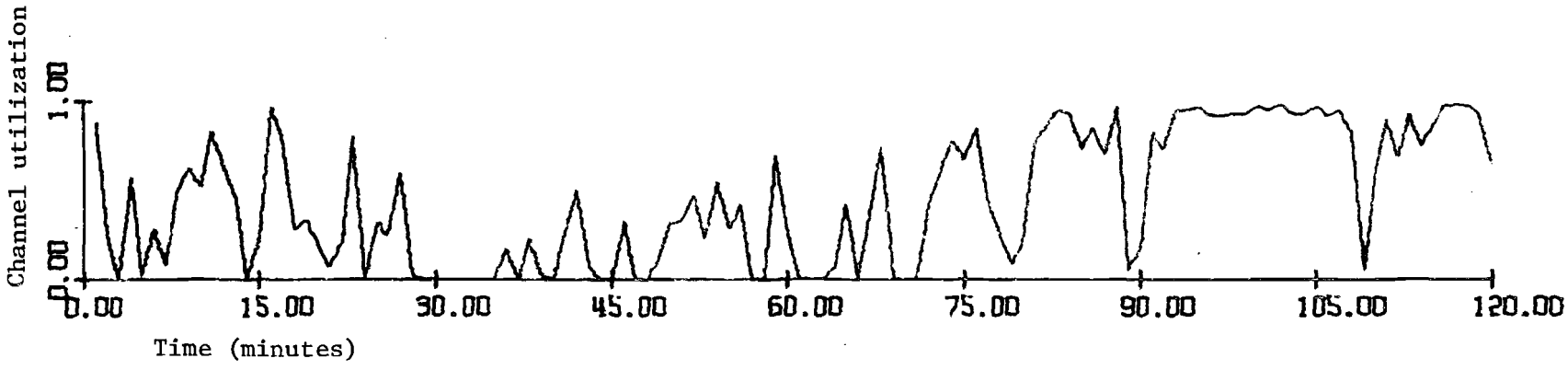

Figure 3.33 Simulated Time Series of Channel Utilization in Sector 543 AD at 100% of Historical Traffic Density

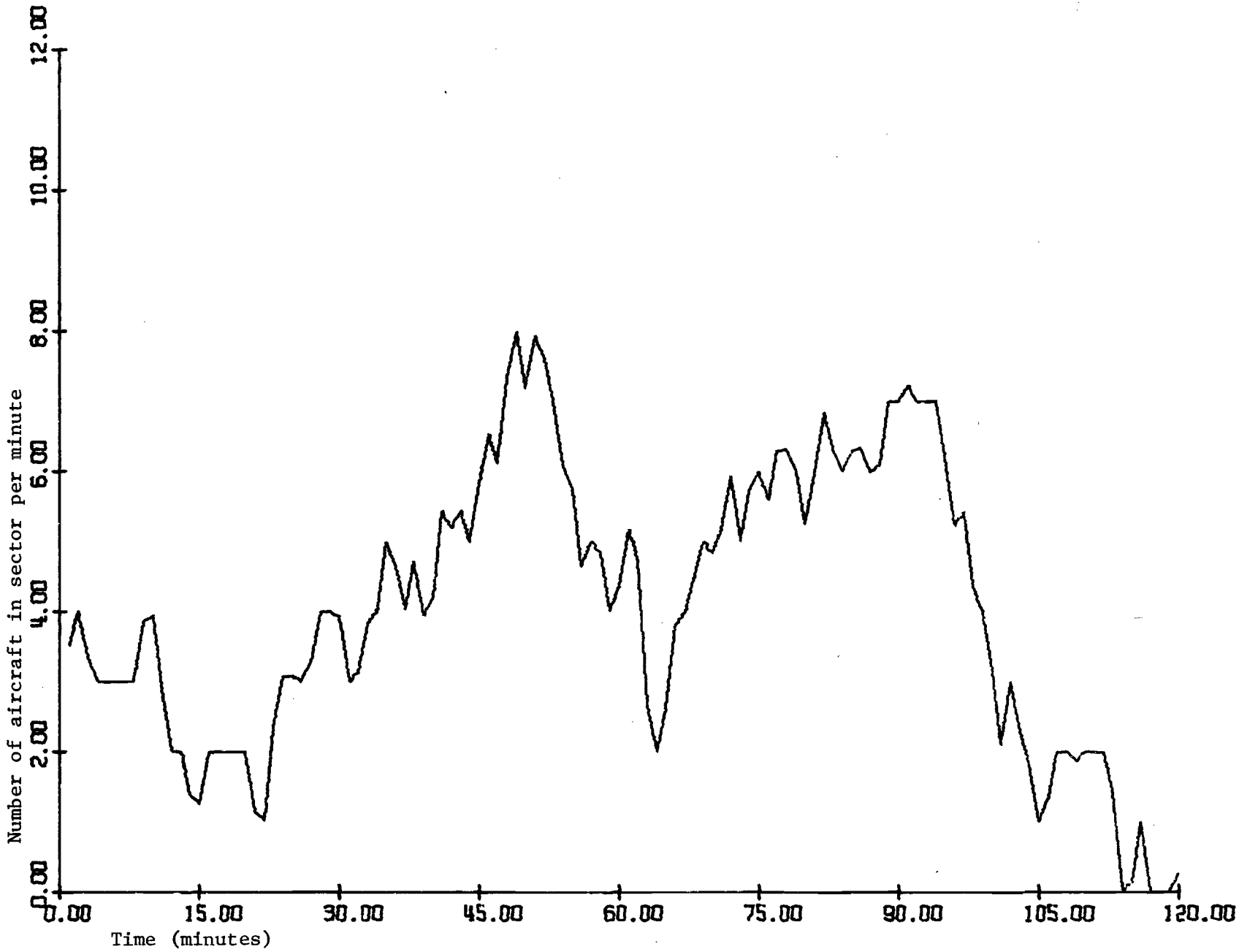

Figure 3.34 Historical Time Series of Aircraft Loading in Sector 553 AR

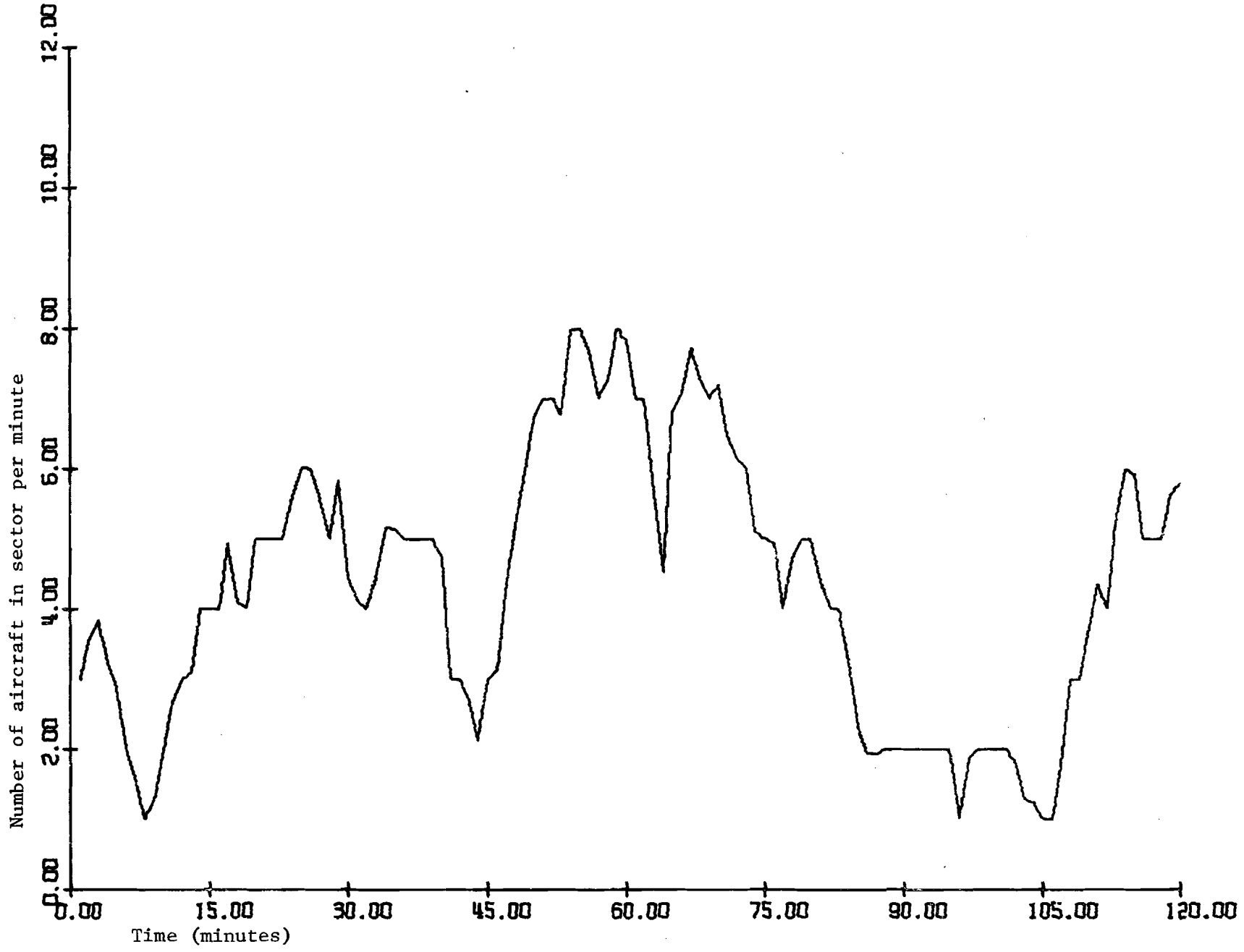

Figure 3.35 Simulated Time Series of Aircraft Loading in Sector 553 AR at 100% of Historical Traffic Density

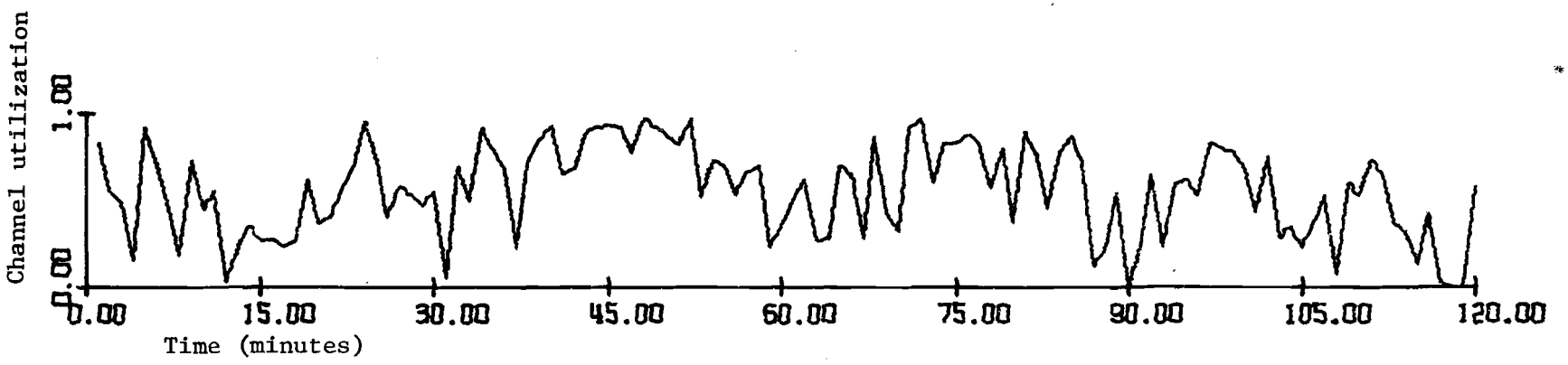

Figure 3.36 Historical Time Series of Channel Utilization in Sector 553 AR

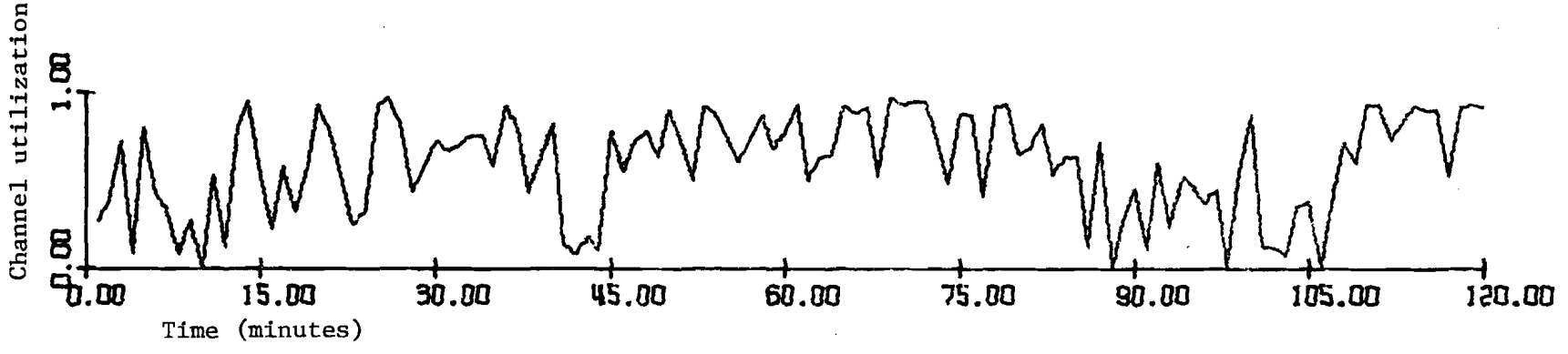

Figure 3.37 Simulated Time Series of Channel Utilization in Sector 553 AR at 100% of Historical Traffic Density

CHAPTER 4

APPLICATIONS OF THE SIMULATION MODEL

4.1 Introduction

A simulation model for the ATC communications performance system has been proposed and validated in the two previous chapters. Valuable insights about ATC communication performance have been gained and confidence with the simulation model system built up. Our objective now is to illustrate how the simulation model may be put to practical use.

There are two immediate ways a simulation model may serve the practitioner:

(i) experiments can be performed using the simulation model as a surrogate for the actual system; and

(ii) system responses unavailable in the real world can be simulated and studied.

For example, using the ATC simulation models, all of the input variables can be varied, individually or more interestingly in combination in order to unfold their interactions. Data on the number of aircraft waiting to communicate can be generated and studied. The effects of deleting message elements, or modifying the time requirements of certain transmissions, can be estimated by appropriate changes in the message dictionaries. The consequences of various trauma, such as the sudden failure of certain instruments, or system components, can be estimated. The interactions between various external and internal variables, such as management protocols and the estimated costs of alternative communications facilities, can also be explored.

The ATC simulation model is offered as a means for increasing understanding. Of course, the output of the model is in every case an estimate or better still, a "guestimate" of what might happen in the real world should certain changes be made. If the model ever provided esimates that were seriously contrary to the intuition of a subject matter expert, the fault would almost certainly lie with the model. Such occasions, when they occur, invariably lead to a closer examination of the model's assumptions and structure, and ultimately to improvements in the model. The authors of this report sincerely hope the present ATC simulation model will be exercised, and look forward to its continual evolution as a useful instrument.

4.2 An Experiment in Changing Traffic Density

As an example of how the ATC model may be employed, consider the problem of determining the communication capacity of a single sector as a function of incoming traffic density. To begin, the traffic density is varied simply by changing the parameter ρ of the Poisson process for generating arriving aircraft in the simulation model. The communication 'capacity' of a sector is a multi-variable response which can be monitored by studying the aircraft loading n_t, the channel utilization C_t, and the queuing Q_t. Because no historical record of the communications queues exists, the simulation of Q_t becomes one of the most interesting yields from this exercise. Special research on the dynamic relationship existing between Q_t, C_t and n_t is discussed in Chapter 5.

Sector 475, representive of the enroute functions, is selected for our illustration. Both the individual sector and general sector function simulations employing Sector 475 have been shown to work equally well. For ease of explanation, we chose the individual sector simulation model described earlier in Section 3.4(a).

The experiment with Sector 475 began using the seven parameter values:

$$\rho = 33.1,\ p = 0.699,\ k = 9.439$$
$$a_o = 4.896,\ a_1 = -0.045,\ \alpha = 2.900,\ \lambda = 1.053.$$

We note here that the incoming traffic density is $\rho = 33$ aircraft arrivals per hour. The simulation is run for one hour before any data is recorded. The remaining two-hour time series simulation of the three responses, aircraft loading, channel utilization and queue lengths are presented in Figures 4.1, 4.2 and 4.3.

In viewing the plot of the channel utilization C_t, it should be remembered that a gap of at least one second always separates consecutive communication transactions. Further the values of C_t plotted are the proportions of time the communications channel is being used, each minute. Given that most communications transactions last only a few seconds, the corresponding computed value of C_t will seldom exceed 0.80.

The incoming traffic density was now increased to 125%, that is, an incoming traffic density of $\rho = 1.25(33) = 41$ aircraft arrivals per hour was imposed on the system. All the other system parameters, except the parameters α and λ which were determined by the master equation (Equation (1.6)), remained unchanged. Keeping the pseudo-random numbers identical to the previous run wherever possible, the simulation of the three responses was repeated. The resulting time series are shown in Figures 4.4, 4.5 and 4.6. Close comparisons of the plots for ρ and 1.25ρ indicate that the levels of all the three series have increased only slightly with the higher density.

The traffic density was then raised to 50 aircrafts per hour, that is, to 150% of the historical level of $\rho = 33$ per hour. This time all the three response series show tremendous increases in level, along with clear changes in pattern. These time series are displayed in Figures 4.7, 4.8 and 4.9. (Note the change of the vertical axes plotting scales from the previous figures.) The aircraft loading climbs up to 20; channel utilization reaches and stays at its ceiling; and the queue length touches a record of 16. Obviously, the sector is in serious trouble at this level of traffic density. A visual appreciation of what is happening can be obtained by merely matching the time series for $\rho = 33$, 41 and 50 for each of the three responses.

One conclusion from these experiments is that the maximum acceptable aircraft arrival density for Sector 475 is somewhere between 41 and 50 aircraft per hour. Further values of ρ could of course be chosen in an effort to find the "optimum" density. However, a more thorough investigation of the response time series is required.

It seems natural that, at first, the only change in the communication capacity of a sector caused by a small increase in ρ, the incoming traffic density, would be to increase modestly aircraft loading and channel utilization. However, the sector communications system is dynamic and as ρ increases, the consequences of small additional increments in ρ have a cascading effect. The system responses go "critical", proceeding rapidly and dramatically to ever higher levels of loading, to almost complete channel utilization, and to excessive queues. We now turn to how the onslaught of this explosive character of the responses can be characterized.

4.3 Stochastic Stationarity and the Operational Stability of a Communication Sector

One attractive statistical formulation for expressing what we have described above is that the operational stability of a communication sector system can be characterized in part by the stochastic stationarity of the derived responses.

To explain, the usual operations within the capacity of a controller seem closely related to the concept of stationarity defined in the literature of stochastic processes. Thus a sector performing under usual operating conditions, though a dynamic system subject to random variations, remains in a controlled state. The major system responses, although varying time series, are "stationary", that is, their intrinsic structure is fixed. For example, high or burdensome levels of n_t or C_t are truly transient and of short duration. Further, there is nothing in the usual excitation of the system to compel a change in this intrinsic structure. Through long experience, the workloads that comprise a sector function seem to have been tuned to this level of performance.

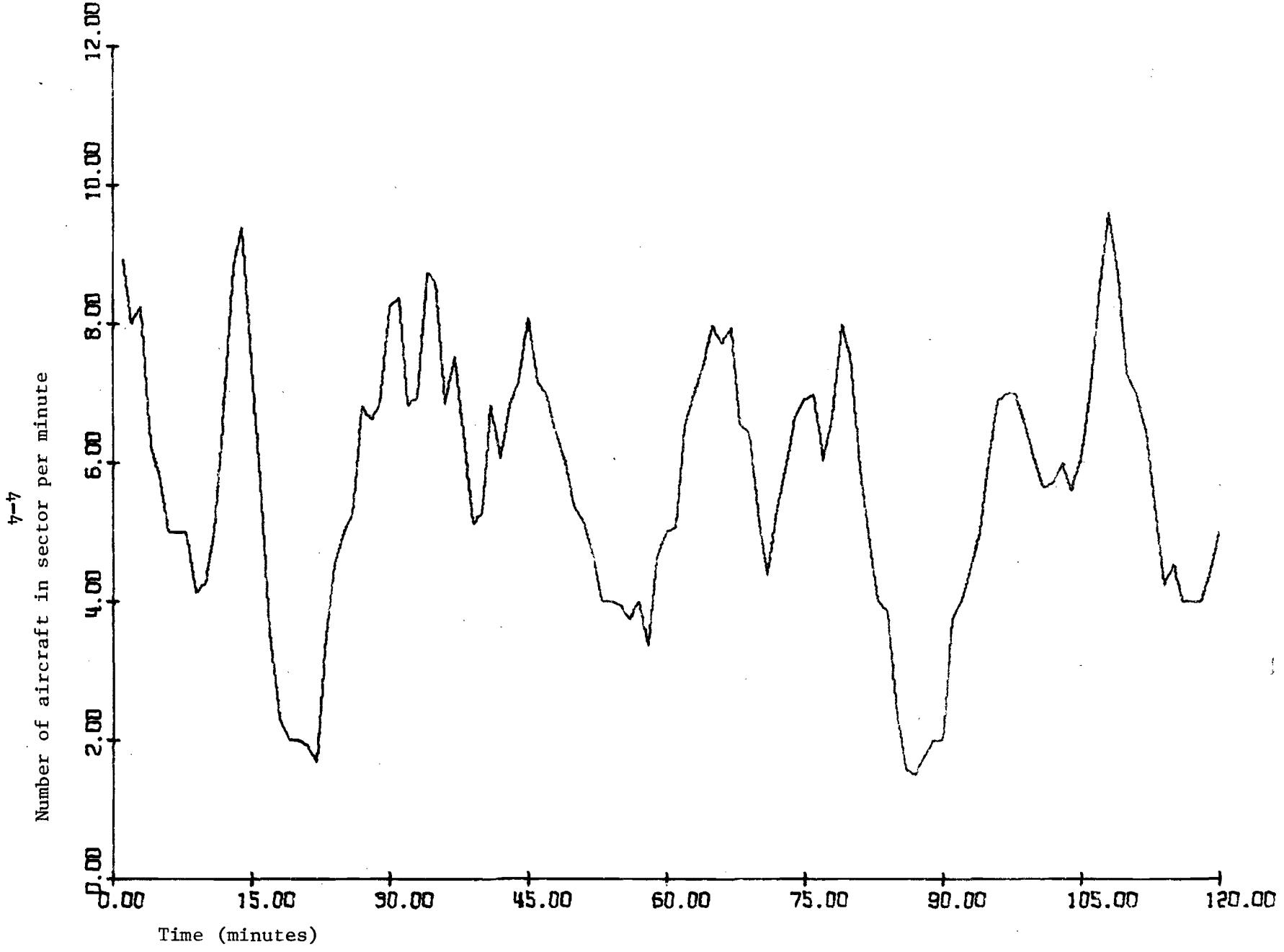

Figure 4.1 Simulated Time Series of Aircraft Loading in Sector 475 HI at 100% of Historical Traffic Density

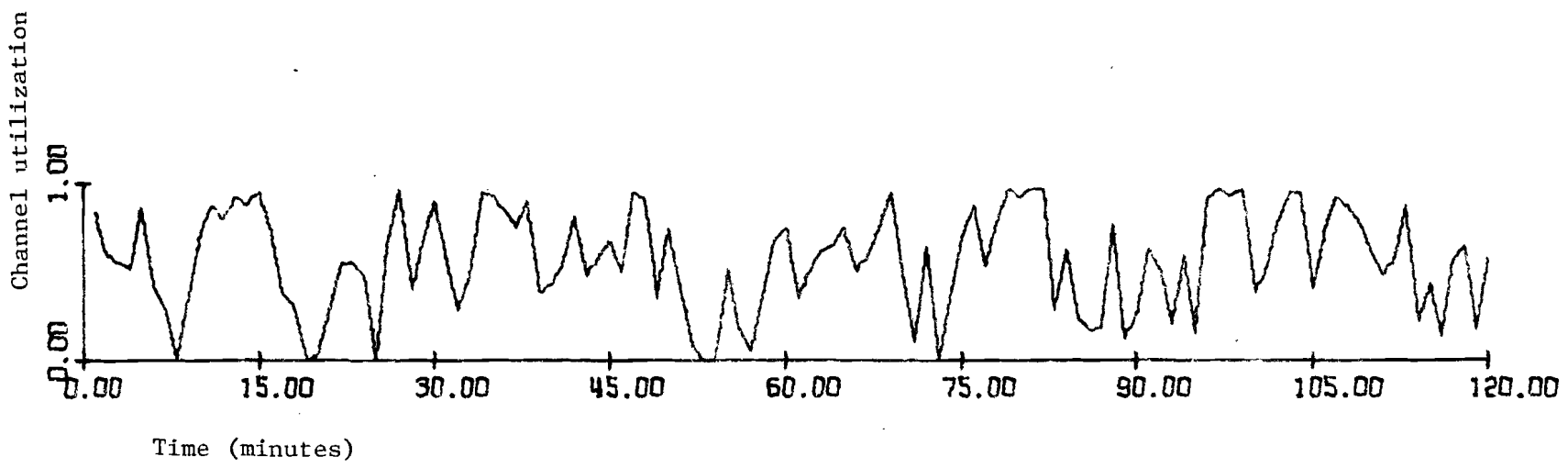

Figure 4.2 Simulated Time Series of Channel Utilization in Sector 475 HI at 100% of Historical Traffic Density

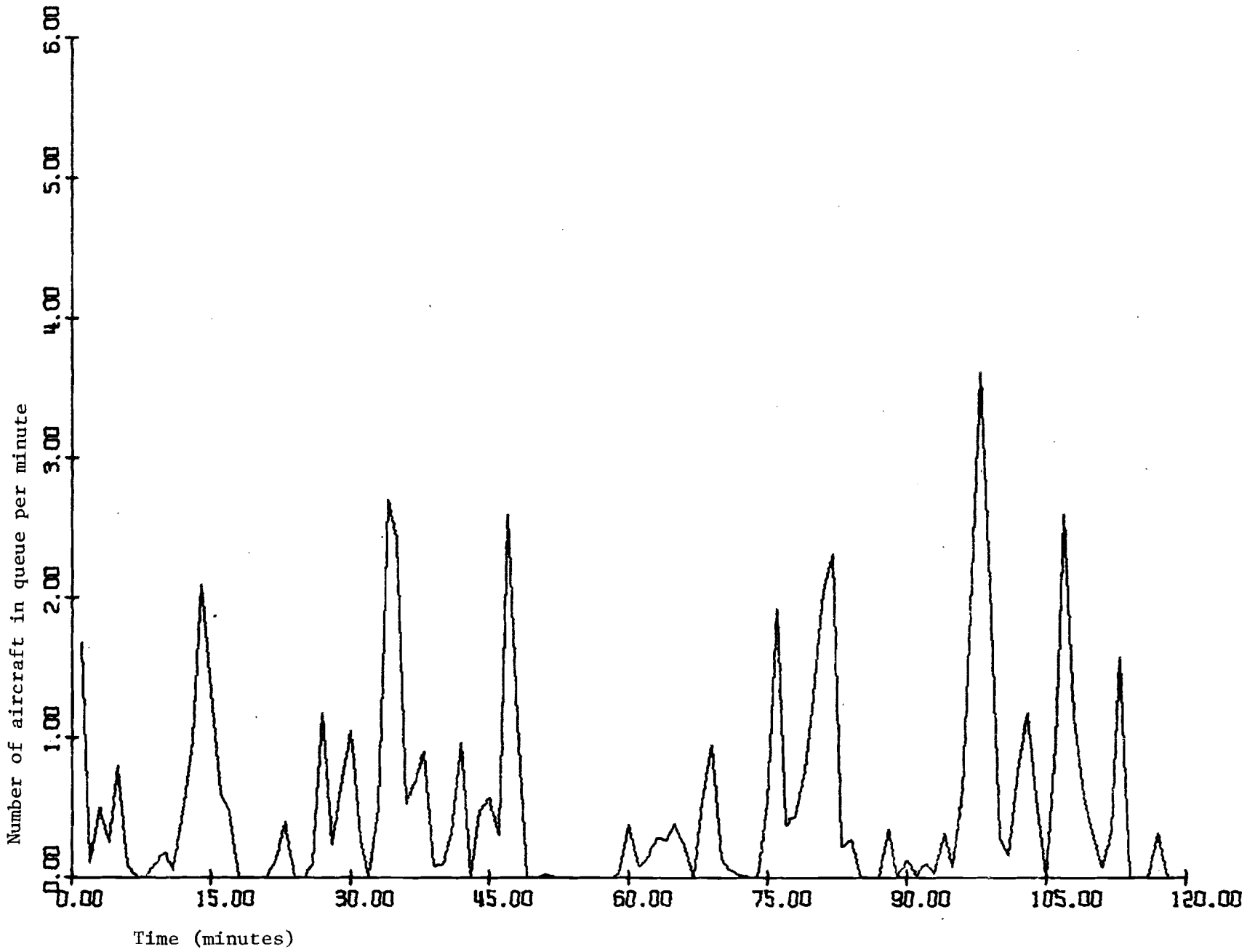

Figure 4.3 Simulated Time Series of Queue Length in Sector 475 HI at 100% of Historical Traffic Density

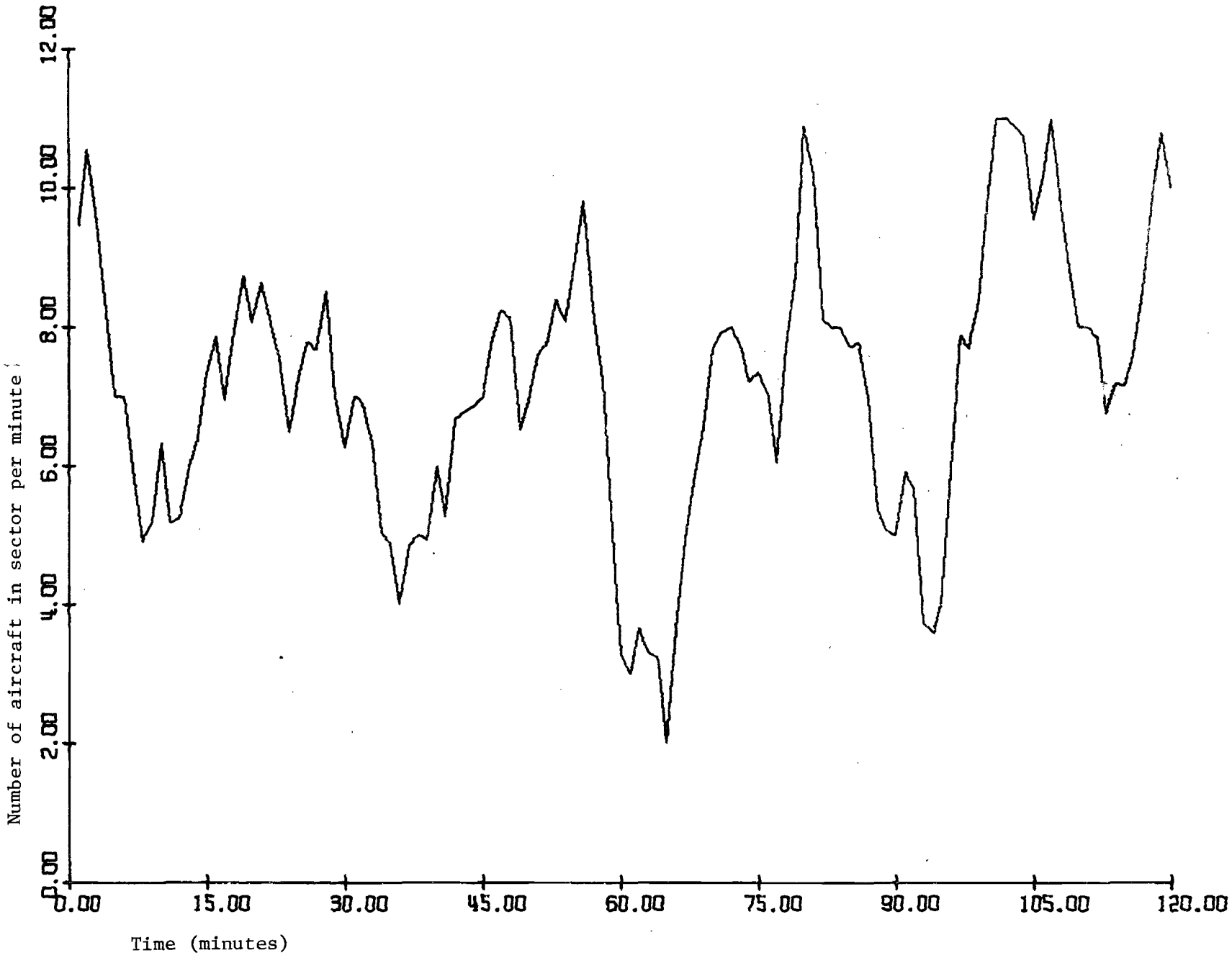

Figure 4.4 Simulated Time Series of Aircraft Loading in Sector 475 HI at 125% of Historical Traffic Density

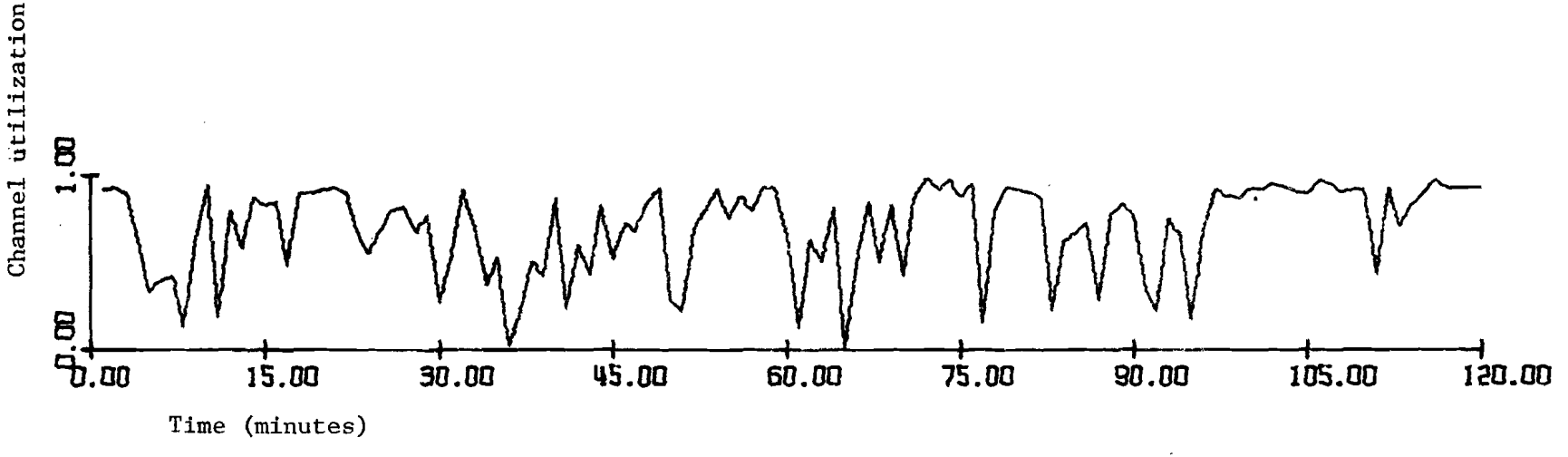

Figure 4.5 Simulated Time Series of Channel Utilization in Sector 475 HI at 125% of Historical Traffic Density

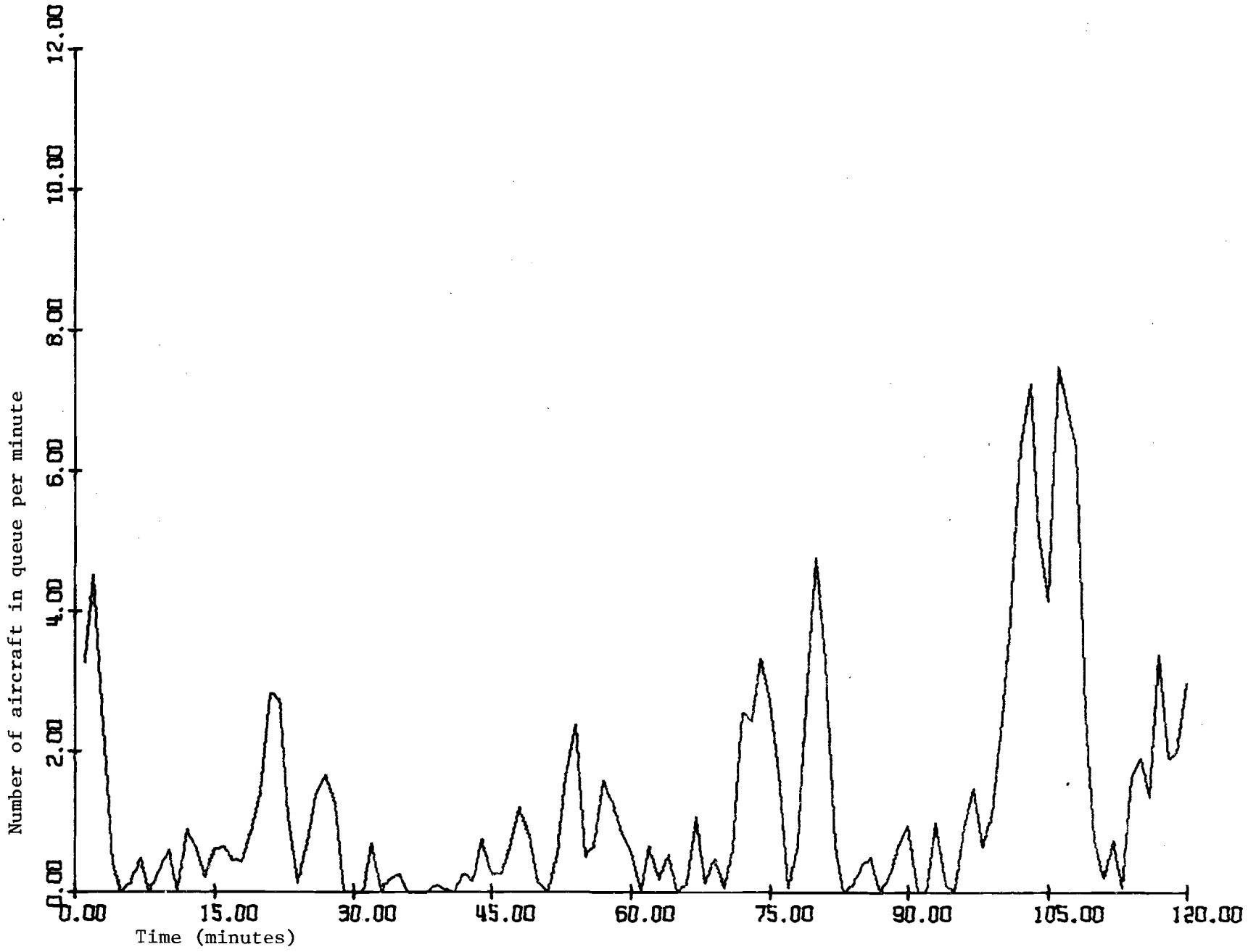

Figure 4.6 Simulated Time Series of Queue Length in Sector 475 HI at 125% of Historical Traffic Density

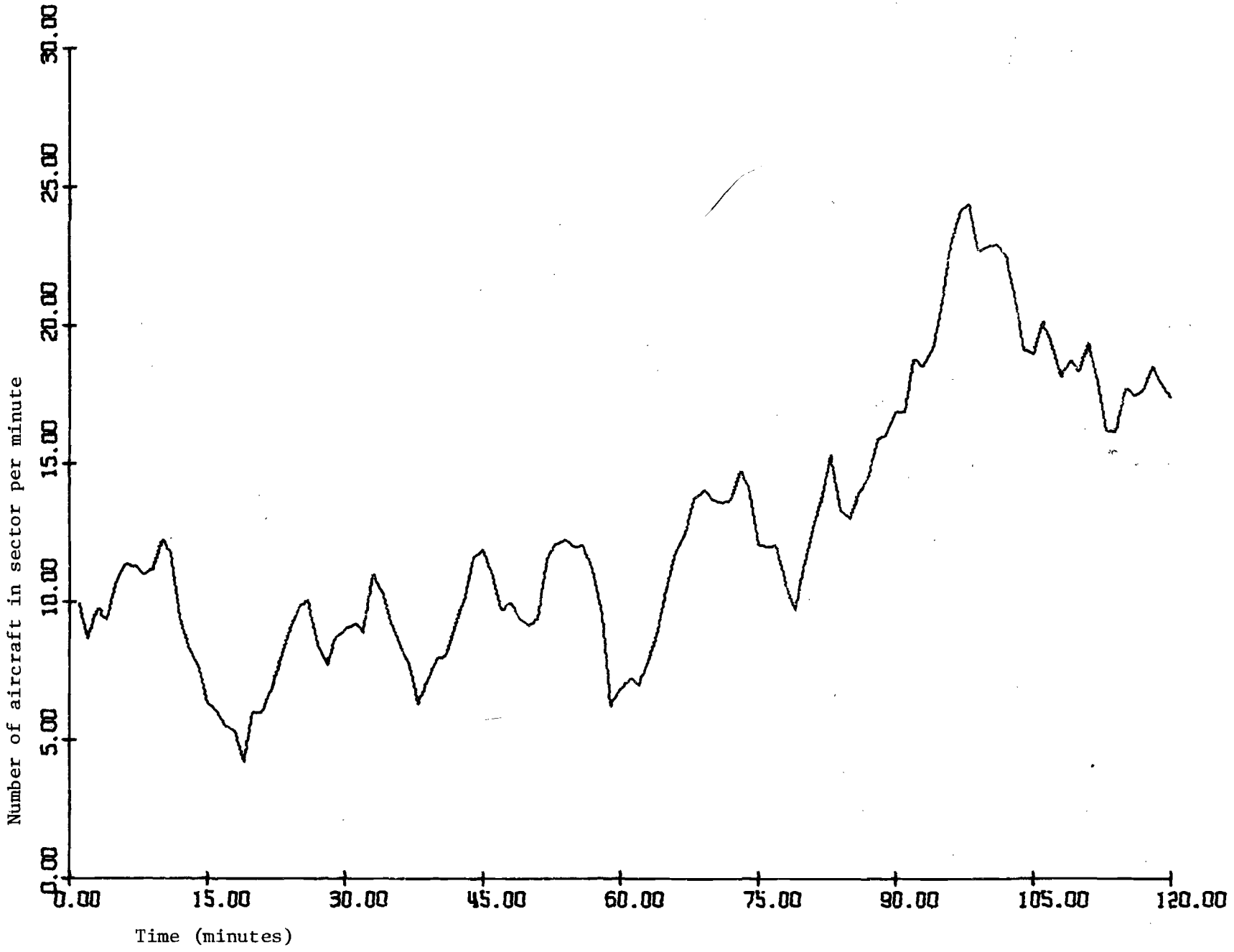

Figure 4.7 Simulated Time Series of Aircraft Loading in Sector 475 HI at 150% of Historical Traffic Density

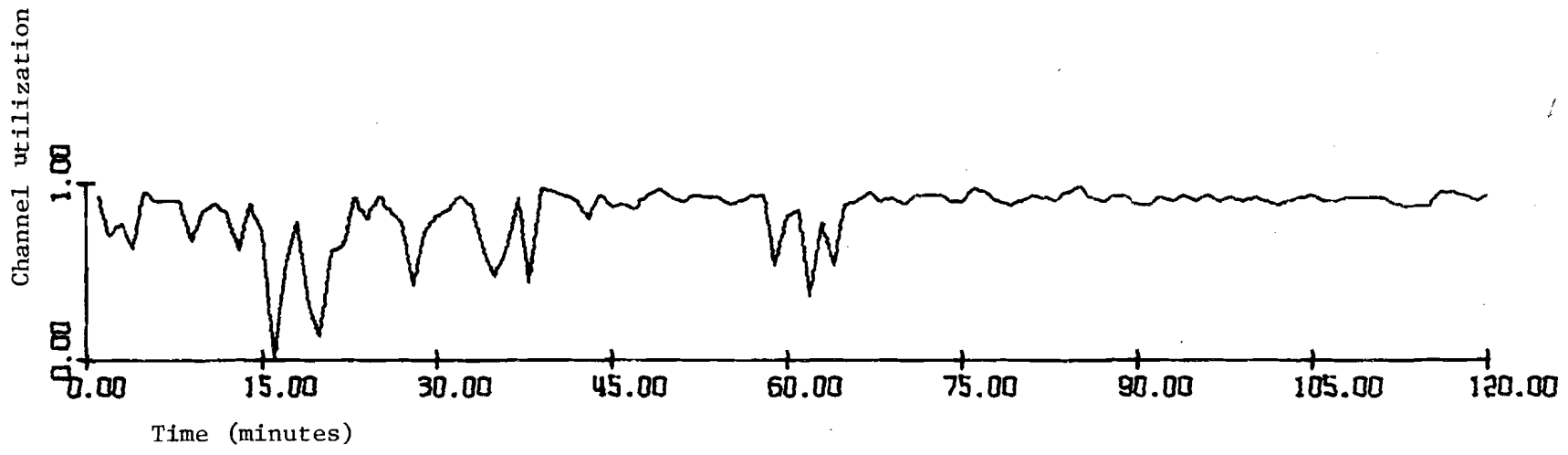

Figure 4.8 Simulated Time Series of Channel Utilization in Sector 475 HI at 150% of Historical Traffic Density

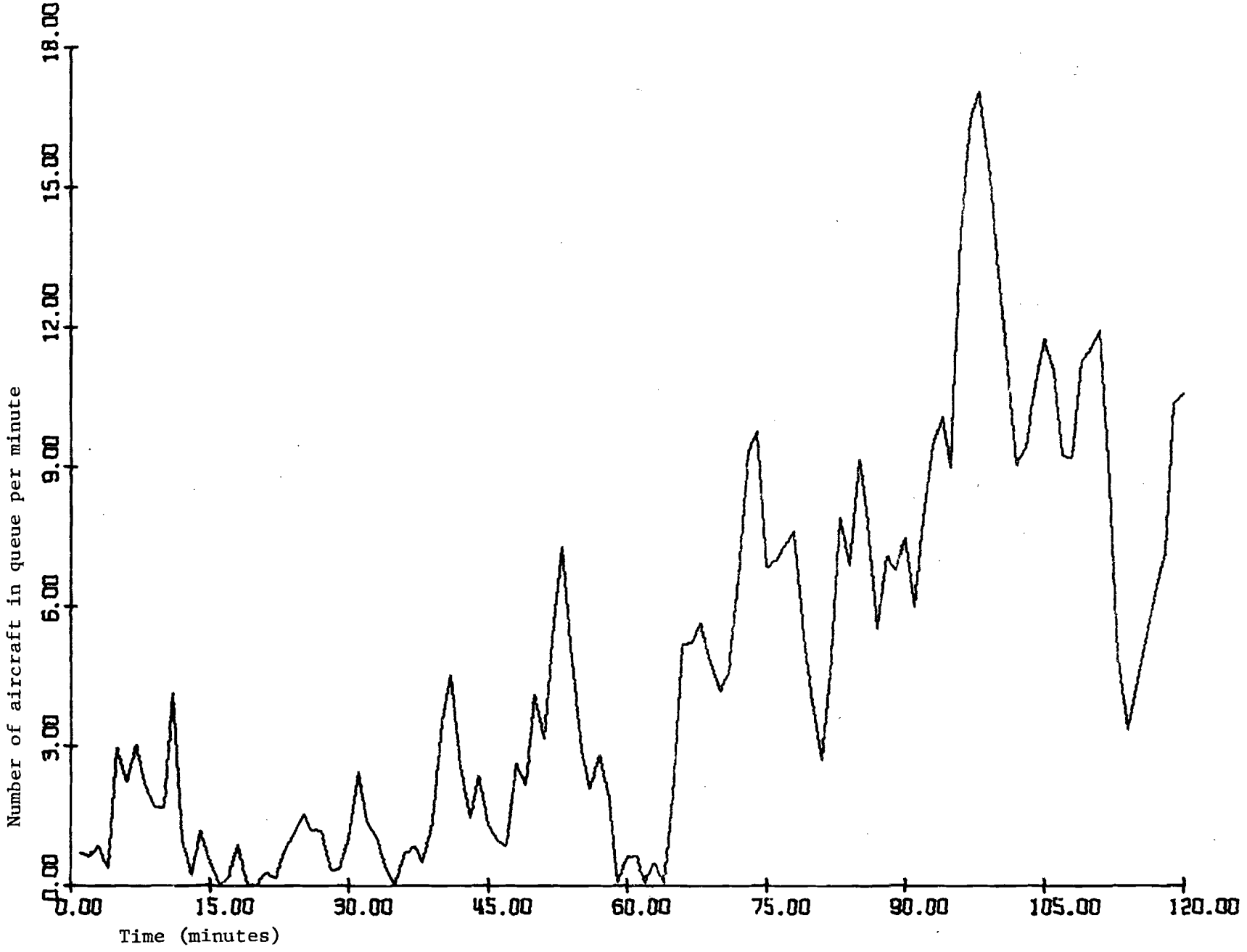

Figure 4.9 Simulated Time Series of Queue Length in Sector 475 HI at 150% of Historical Traffic Density

However, when the excitation of the system grows beyond its usual levels, the response time series undergo drastic shifts accompanied by explosive trends. The intrinsic structure of these reponse time series becomes non-stationary. There is obviously a considerable interest in determining the safe upper bounds of excitation.

Of the three time series responses produced by the simulation, though they are highly correlated, the one most suitable for the statistical study of departures from stationarity is the aircraft loading series, n_t. (Some further study presented in Chapter 5 will justify this choice). From results of many previous investigations, an autoregressive model of order two has been shown to adequately describe the time series of n_t, the sixty-second averages of the aircraft loading variable. To explore the stationarity of a time series, two statistical instruments are now derived. The application of these statistical tools for the Sector 475 example is discussed following completion of each derivation.

4.4 The Highest Posterior Density (HPD) Contours of the Autoregressive Parameters

Let $y_t = Y_t - \hat{\mu}$ where Y_t is an observation at time $t = 0, 1, 2, \ldots,$ and $\hat{\mu}$ is the estimated mean level of the series. Then the general equation for an autoregressive model of order two is given by

$$y_t = \phi_1 y_{t-1} + \phi_2 y_{t-2} + a_t,$$

where ϕ_1 and ϕ_2 are parameters and a_t is NID(0, σ^2). For an AR(2) model to be stationary, it can be shown that the parameters ϕ_1 and ϕ_1 must satisfy the following constraints:

$$\phi_1 + \phi_2 \leq 1,$$
$$-\phi_1 + \phi_2 \leq 1,$$
$$\phi_2 \geq -1.$$

In practice, ϕ_1 and ϕ_2 must be estimated from the data y_t. These estimates, in turn, can be bounded by a $(1 - \alpha)\%$ confidence region. The construction of the associated Highest Posterior Density (HPD) region for the parameters ϕ_1 and ϕ_2 is described in the next paragraph.

Assuming that n observations of an AR(2) series are available, the last (n - 2) observations can be described as follows:

$$y_3 = \phi_1 y_2 + \phi_2 y_1 + a_3,$$

$$y_4 = \phi_1 y_3 + \phi_2 y_2 + a_4,$$

$$\cdots\cdots\cdots\cdots$$

$$y_n = \phi_1 y_{n-1} + \phi_2 y_{n-2} + a_n. \tag{4.1}$$

Written in matrix notations, Equation (4.1) becomes

$$\underset{\sim}{y} = X\underset{\sim}{\phi} + \underset{\sim}{a} \tag{4.2}$$

where $\underset{\sim}{y}$ is the $(n - 2) \times 1$ vector of observations, X is the $(n - 2) \times 2$ matrix of derivatives, $\underset{\sim}{\phi}$ is the (2×1) vector of coefficients and $\underset{\sim}{a}$ is the $(n - 2) \times 1$ vector of independent Gaussian errors. Let $\hat{\underset{\sim}{\phi}} = (X'X)^{-1}X'\underset{\sim}{y}$ be the least squares estimator of $\underset{\sim}{\phi}$ (equivalently, in this case, a generalized maximum likelihood estimator), and let $S(\underset{\sim}{\phi}) = (\underset{\sim}{y} - X\underset{\sim}{\phi})'(\underset{\sim}{y} - X\underset{\sim}{\phi})$, a quadratic function of $\underset{\sim}{\phi}$ used to determine the level of the posterior density function and hence the contours for the HPD regions. It can be easily shown that, given a non-informative prior density function for the parameters $\underset{\sim}{\phi}$, the equation

$$S(\underset{\sim}{\phi}) \leq S(\hat{\underset{\sim}{\phi}}) \{1 + [2F_\alpha(2, n - 2)]/(n - 2)\} \tag{4.3}$$

can be used to determine the $100(1 - \alpha)\%$ HPD region. All values of $\underset{\sim}{\phi}$ which satisfy (4.3) are in the HPD region desired.

The 95% and 99% HPD contours constructed from the historical data and from the simulated data with $\rho = 33$, 41 and 50 expected aircraft arrivals per hour are displayed in Figures 4.10 ∿ 4.13 for Sector 475. The contours reveal a clear movement of the HPD mass, toward the stationarity boundary $\phi_1 + \phi_2 = 1$. The HPD mass crosses this boundary at $\rho = 50$, the highest traffic density. Thus we could conclude that at $\rho = 50$ the AR(2) series could, with probability greater than 0.01, become non-stationary. This behavior motivated the construction of a test for the stationarity of the series.

4.5 A Test Statistic for Stationarity

Given Equation (4.3) to be true, the values of the parameters can be shown to be distributed as a bivariate t variable. Thus the values of their linear combination $\xi = \phi_1 + \phi_2$ is distributed as a univariate t variable, i.e.

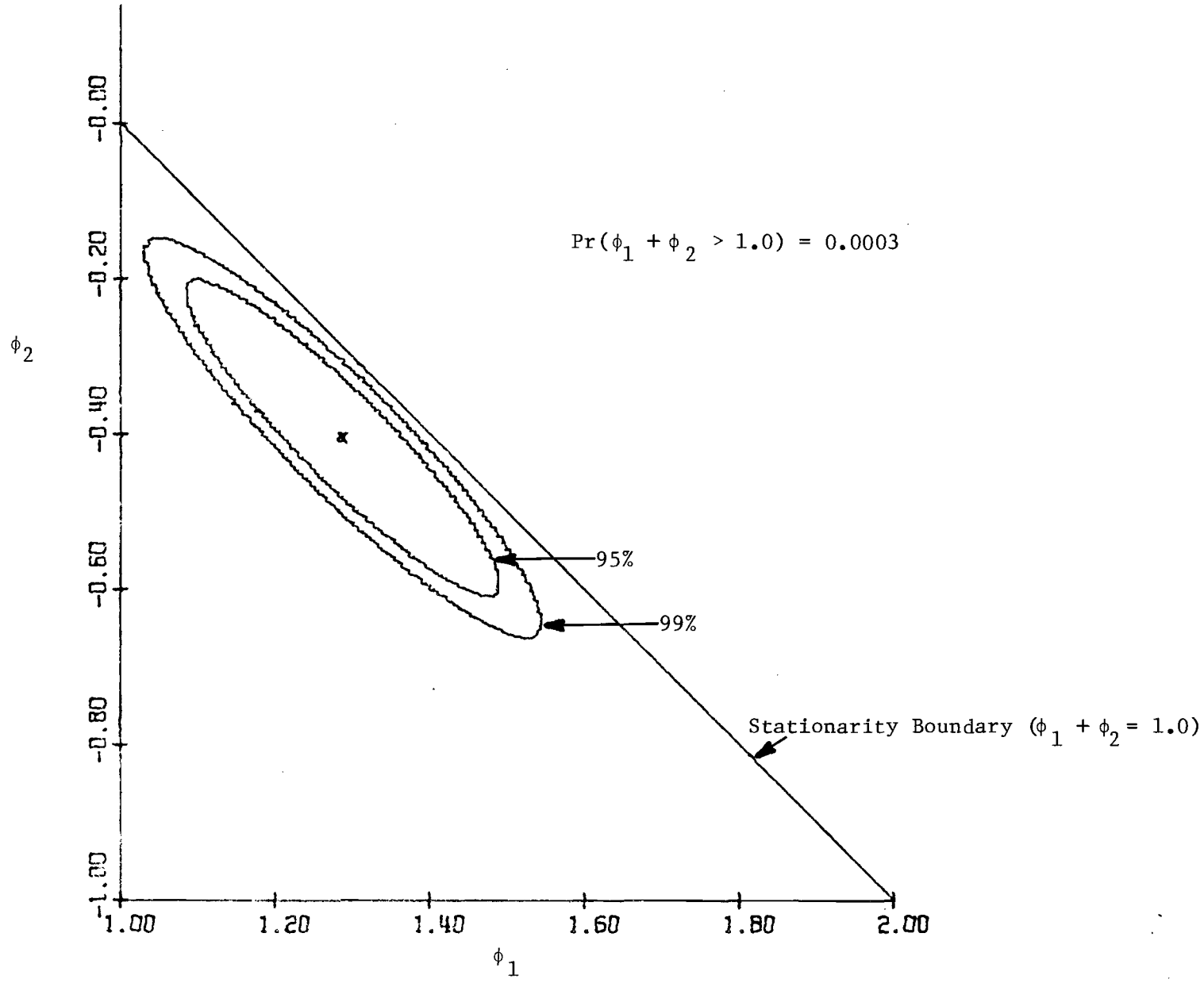

Figure 4.10 Confidence Regions of (ϕ_1, ϕ_2) Based on Historical Aircraft Loading Time Series for Sector 475

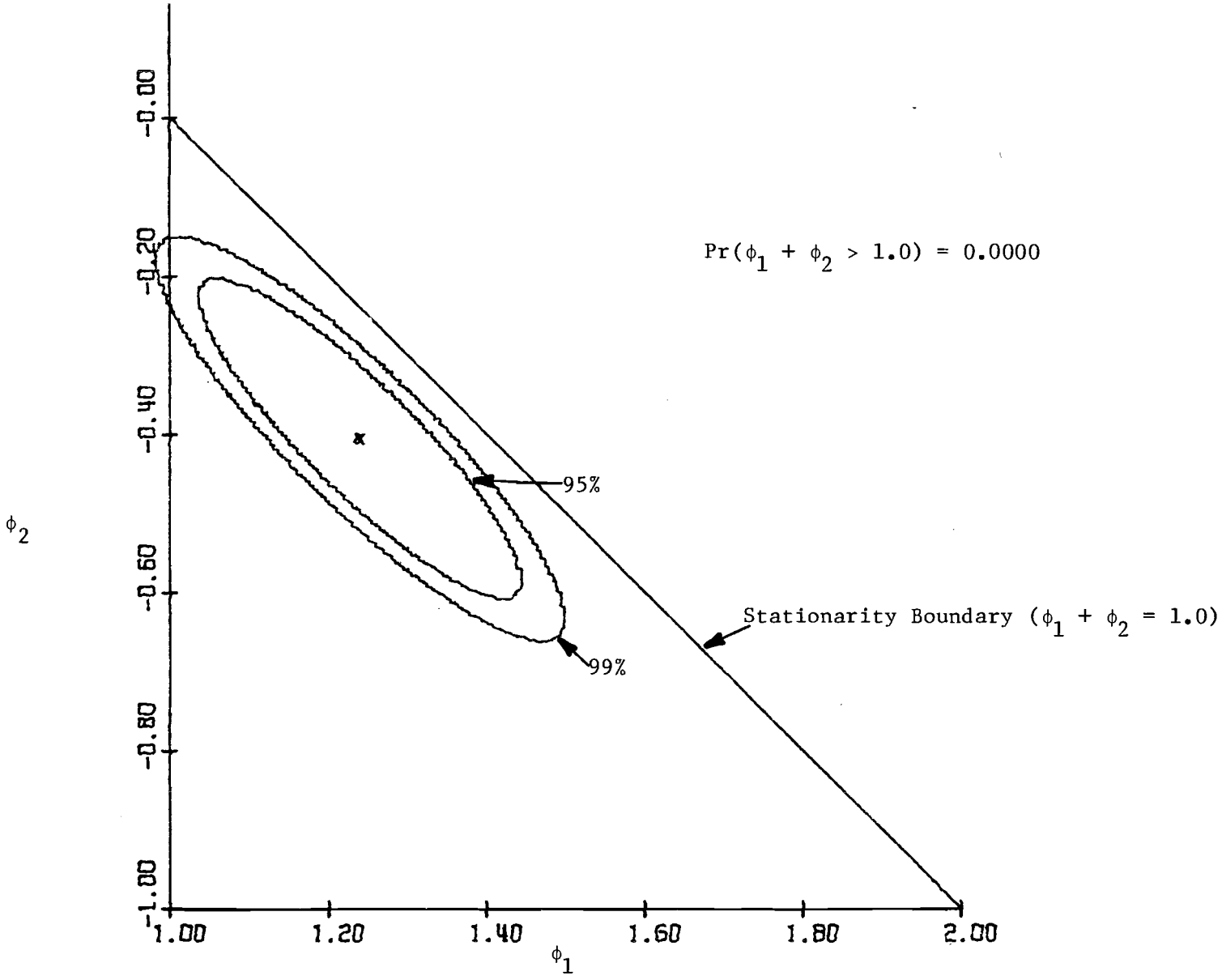

Figure 4.11 Confidence Regions of (ϕ_1, ϕ_2) Based on Simulated Aircraft Loading Time Series for Sector 475 at 100% of Historical Traffic Density

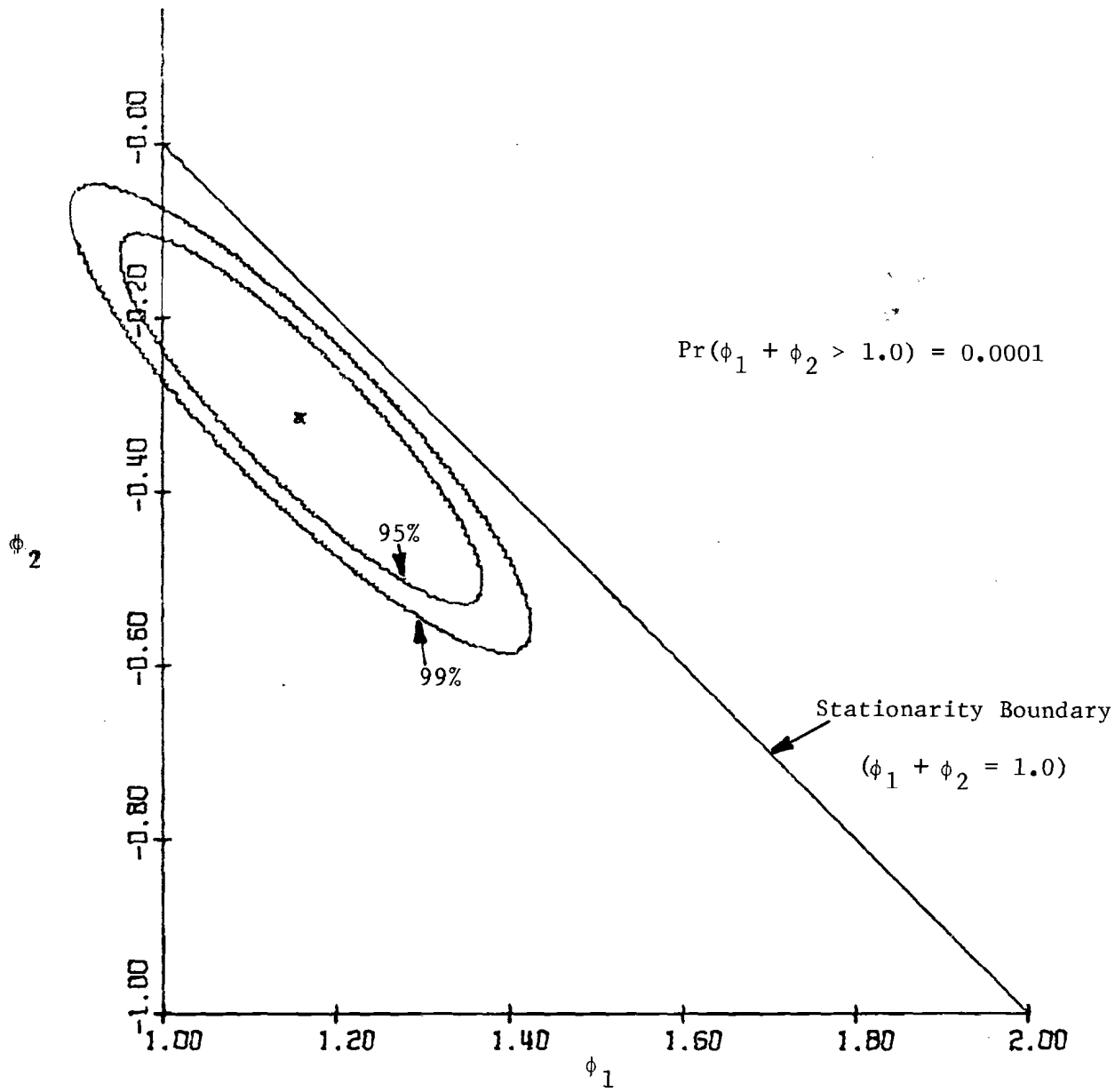

Figure 4.12 Confidence Regions of (ϕ_1, ϕ_2) Based on Simulated Aircraft Loading Time Series at 125% of Historical Traffic Density (Sector 475)

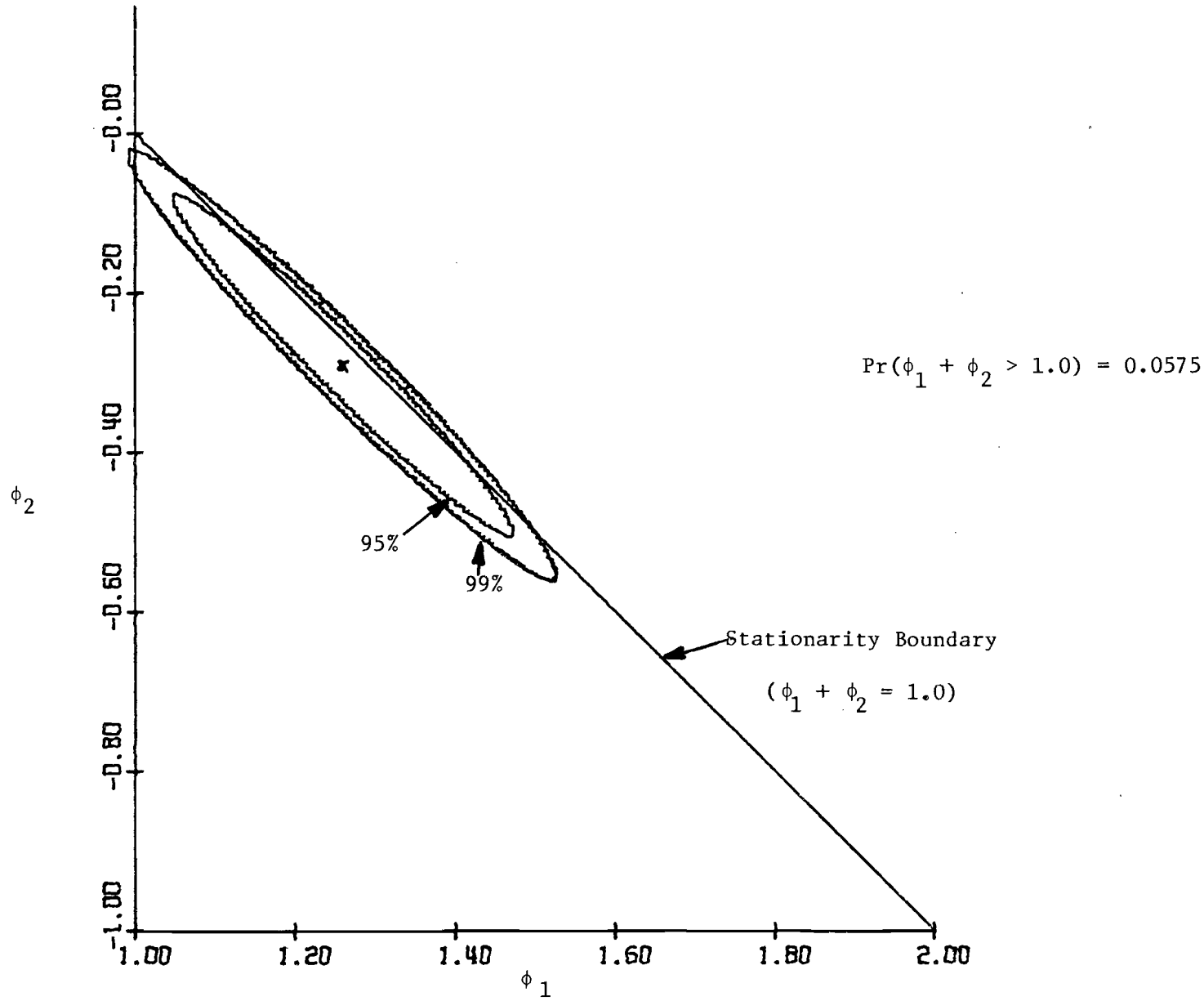

Figure 4.13 Confidence Regions of (ϕ_1, ϕ_2) Based on Simulated Aircraft Loading Time Series at 150% of Historical Traffic Density (Sector 475)

$$p(\xi|\underset{\sim}{y}) = \frac{1}{B(\frac{1}{2}, \frac{\nu}{2})\sqrt{\nu}\, s_*} \; 1 + \left[\frac{(\xi - \hat{\xi})^2}{s_*^2\, \nu}\right]^{-\frac{\nu+1}{2}}$$

where $\nu = n - 2$, $\xi = \phi_1 + \phi_2$, $s_* = s^2 \begin{pmatrix} 1 & 1 \end{pmatrix} (X'X)^{-1} \begin{pmatrix} 1 \\ 1 \end{pmatrix}$ and $s^2 = S(\hat{\underset{\sim}{\phi}})/(n-2)$.

Values of $p(\xi \geq 1|\underset{\sim}{y})$, the probability that ξ exceeds the boundary $\phi_1 + \phi_2 = 1$, have been calculated for the four series whose contours are displayed in Figures 4.10 ∿ 4.13. These individual probabilities are given at the right-hand upper corner of each of the corresponding contour plots. Note that the boundary $\phi_1 + \phi_2 = 1$ (i.e. $\xi = 1$) falls inside the 95% HPD region of ξ at the highest traffic density experimented with, (since $p(\xi \geq 1|\underset{\sim}{y}) = 0.0575 > 0.025$). A conventional statistical inference derived from this evidence is, therefore, that the time series of the aircraft loading variable at the highest traffic density may no longer be stationary.

4.6 Studies of the Simulated Queuing

Up to this point the simulation experiment with varying traffic densities has studied the time series responses, particularly for the aircraft loading n_t. We now investigate the simulated results from another perspective using the average responses over the two-hour period. Particular emphasis is placed on the average queuing time and average queue length since both these quantities are currently unavailable in real world data.

To obtain more information for the queuing study, one extra simulation was run at a traffic density 50% of the value recorded in the data file. Thus the traffic density equals 33 × .5 = 16.5 aircraft arrivals expected per hour. Results from this extra run and the other three runs at 100%, 125% and 150% of the observed density previously reported are listed in Table 4.1. In the table, the column labeled n is the number of simulated observations recorded for each event. For instance, for the queuing time seen at 50%, there were n = 188 different occasions where an aircraft was recorded entering the communications queue (some aircraft may enter the queue on more than one occasion). In Table 4.1, the x and s_x are the estimated mean and standard deviation computed from these observations. The column labeled $\hat{\gamma}_1$ is the measure of skewness given by $\hat{\mu}_3/\hat{\mu}_2^{1.5}$ where $\hat{\mu}_2$ and $\hat{\mu}_3$ are the sample second and third central moments, respectively. These sample statistics are listed for the purpose of providing an appreciation of the nature of the distribution curve of the data.

Table 4.1 Results of Simulations for Sector 475 at Four Different Traffic Densities

Response	Traffic Density ρ (100%=33 arrivals/hour) %	n	x	s_x	$\hat{\gamma}_1$
Queuing Times	50	188	3.8617	7.6445	3.0566
	100	300	10.4278	14.9162	1.9094
	125	445	20.5258	25.2667	1.8494
	150	577	56.8180	48.7602	8.4708
Queue Length (number of aircraft per second)	50	7200	0.1008	0.3329	3.4632
	100	7200	0.5100	0.8829	1.8220
	125	7200	1.2276	1.7887	1.9074
	150	7200	4.7086	4.2514	0.8074
Aircraft Loading (number of aircraft per second)	50	7200	2.8739	1.6813	0.3499
	100	7200	5.6325	1.9100	-0.2449
	125	7200	7.1269	1.9990	-0.1401
	150	7200	12.6635	4.8429	0.5898
Channel Utilization (per minute)	50	120	0.3299	0.2929	0.6128
	100	120	0.5631	0.2884	-0.3198
	125	120	0.6976	0.2595	-0.9793
	150	120	0.8353	0.1703	-2.5759

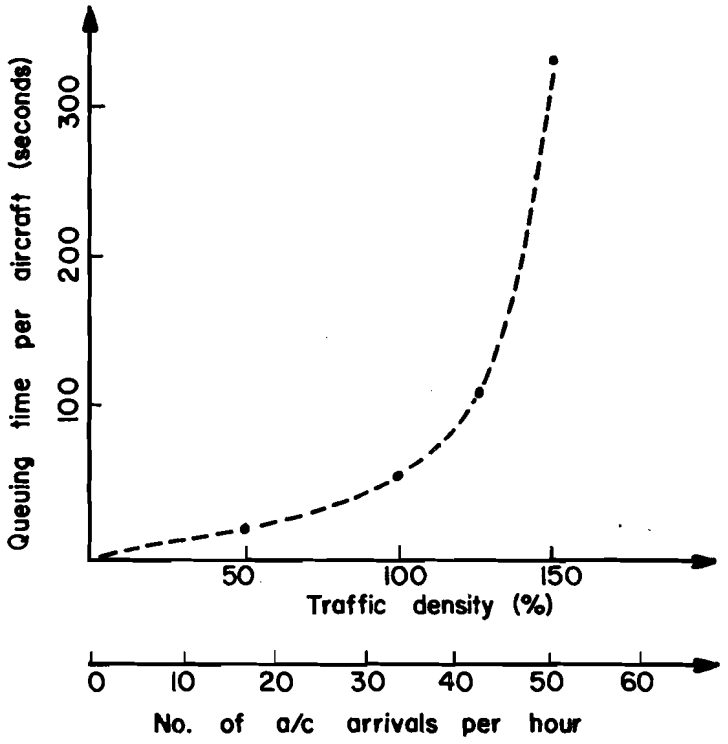

Figure 4.14 Average Queuing Time per Aircraft versus Traffic Density

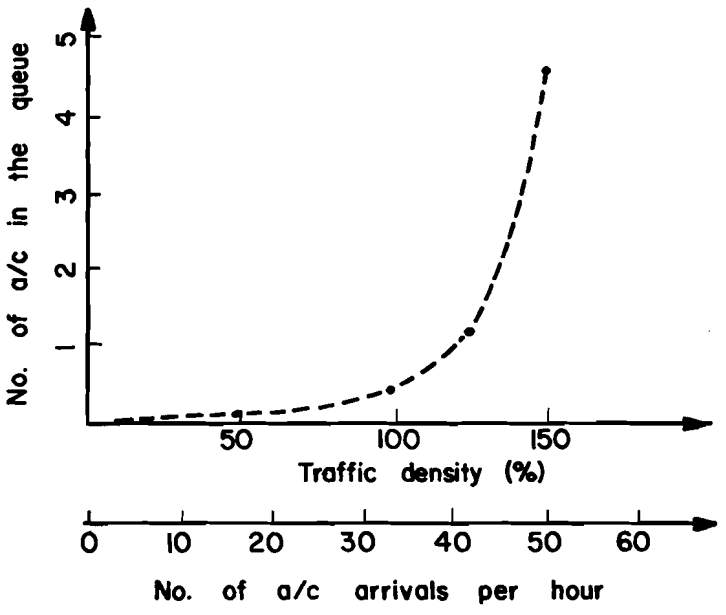

Figure 4.15 Average Queue Length versus Traffic Density

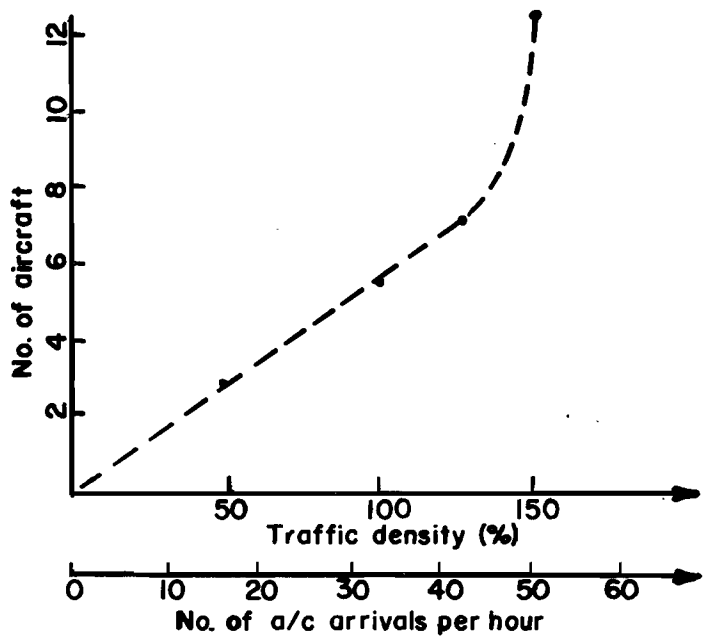

Figure 4.16 Average Aircraft Loading versus Traffic Density

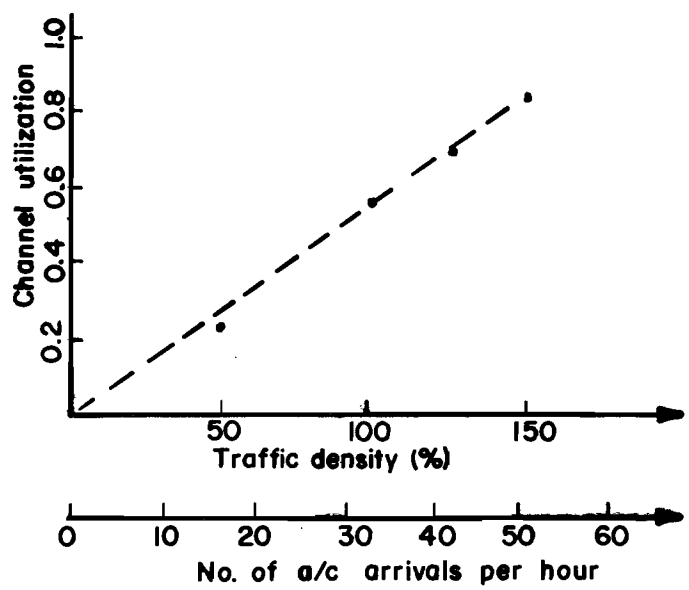

Figure 4.17 Average Channel Utilization versus Traffic Density

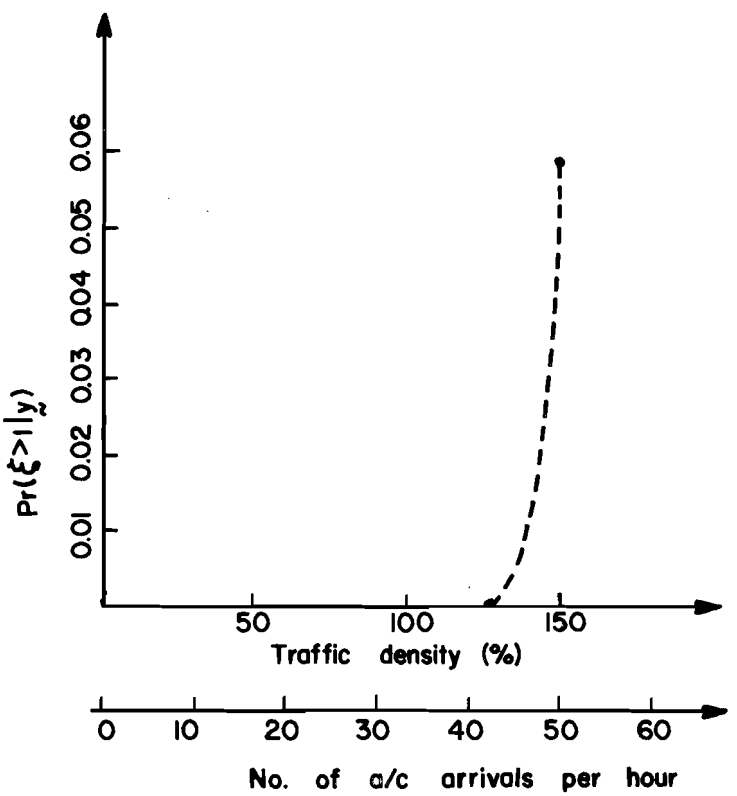

Figure 4.18 $Pr(\xi>1|\underset{\sim}{y})$ versus Traffic Density

The average of the queuing time per CT, computed at the various traffic densities, is listed in Table 4.2. These various average measures are plotted in Figures 4.14 ∿ 4.18. Figure 4.18 is the plot of the measure Prob $(\xi > 1 \mid \underset{\sim}{y})$ where $\xi = \phi_1 + \phi_2$, discussed in Section 4.3, against the traffic density.

Table 4.2 Average Queuing Time per Aircraft

Traffic Density (%)	Ave. Queuing Time/CT (seconds)
50	22.0000
100	56.8789
125	110.7100
150	331.1514

Many interesting phenomena can be observed from the table and plots.

(i) Both the average queuing time per CT and the average queue length increase exponentially with linear increases in traffic density.

(ii) The average aircraft loading forms a linear function with the traffic density when the latter is less than 125%. But the line suddenly turns upward exponentially starting somewhere between 125% and 150%.

(iii) The average channel utilization increases proportionally to the traffic density even at the highest traffic density considered. Obviously, since the maximum channel utilization is theoretically equal to unity, a further increase in traffic density cannot increase CT proportionally.

(iv) The value of Prob $(\xi > 1 \mid \underset{\sim}{y})$ takes off from zero somewhere between 125% and 150% traffic density.

The sudden turning of the curve for aircraft loading can be explained by the exponential increase of the average queue length. The extra amounts of aircraft loading come from the aircraft waiting in the communication queue. The straight line for channel utilization appears to be linear but must asymptote to the horizontal for further increases in traffic density. Most strikingly, the value of Prob$(\xi > 1 \mid \underset{\sim}{y})$ seems to be an alarm, setting off warning signals that the system responses may have become non-stationary.

4.7 Summary and Remarks

The ATC simulation model has been used as part of an experimental program to investigate the consequences of increasing incoming traffic density. One important output of the simulation model consists of time series plots of aircraft loading, channel utilization and communications queuing. One of the responses, communications queuing, is not available in the real world and can only be monitored through a simulation procedure. The time series plots have intrinsic value since they provide a ready visual appreciation of how the system responds to different excitations. In addition to these graphical results, statistical techniques for judging the response time series have been derived and illustrated. These techniques detect the onset of operational instability through tests for stochastic non-stationarity. Finally, the average behavior of the responses over the two-hour period were also investigated, and graphs were provided displaying how the responses, on the average, varied as a consequence of changing incoming traffic density.

The experimental program used in exercising the ATC simulation was a very simple one and should serve as an illustration of the usefulness of the simulation model.

CHAPTER 5

FURTHER RELATED STUDIES

5.1 Introduction

The availability of the simulation model has stimulated much additional thinking about the nature of the system responses. Of particular concern is the idea that the three time series responses n_t, C_t and Q_t are dynamically coupled. The study to determine the presence, and nature, of this coupling is explored in the following section.

A further kind of coupling also exists between adjacent sectors. The present model is appropriate to a single sector function, but it has not yet been adapted to a sequence of sector functions. A preliminary investigation into the nature of a network of sectors has been completed and is discussed in Section 5.3.

In handling the data on intercommunication gaps, the feeling arose that the initial gap, that is, the gap between the first and second CT's, differed from the remaining gaps. A special study of the sequential structure of the intercommunication gaps is presented in Section 5.4. An investigation into the use of classical queueing theory in handling the special problem of aircraft communications queueing is discussed in Section 5.5. The last section of this chapter describes additional efforts to characterize the distribution of the number of TR's per CT. A completely new distribution function, the Sichel distribution, is found to provide an improvement over the present truncated negative binomial distribution. Attempts to use the log Normal and gamma distribution as approximations are also described.

5.2 Analysis of the Response Coupling

In Chapter 4 the three time series responses of aircraft loading n_t, channel utilization C_t and communication queueing Q_t were individually generated and studied. However, a study of the dynamic interactions between these responses is required if we are to fully understand the communication capacity of a sector. Our present purpose then is to investigate the nature of the dynamic coupling between n_t, C_t and Q_t. This is accomplished through the techniques of transfer function modelling. We begin by a brief description of a transfer function.

Consider an input variable x_t and a response or output variable y_t, $t = 0, 1, 2 \ldots$, where both variables are discrete time series. At time t let the influence of x_t on y_t be given by $y_t = \nu_0 x_t$, where ν_0 is a parameter to be estimated from the data. Suppose now that the previous setting of the

input variable x_{t-1} has a legacy and can also influence the value of the present response y_t. The expression for y_t now becomes $y_t = \nu_0 x_t + \nu_1 x_{t-1}$. In fact, one can imagine a situation in which the setting of x some p periods back in historical time can still influence y_t, that is, a response system with a long memory. In general then

$$y_t = \nu_0 x_t + \nu_1 x_{t-1} + \nu_2 x_{t-2} + \ldots + \nu_p x_{t-p}. \tag{5.1}$$

The parameters $\nu_0, \nu_1, \ldots, \nu_p$ determine how each historical value of x is weighted to produce the response observed at time t. In more mathematical terms, the parameters define an impulse response function which together with the values of $x_t, x_{t-1} \ldots$, give the linear transfer function.

The mathematical model for y_t can be made more realistic by adding a term N_t, a shock or element of noise which also occurs at time t. Usually one assumes the successive values of N_t to behave as independent events from a Normal distribution, but in what follows we choose the less restrictive assumption that the shocks can be characterized by a parametric time series. Thus, the stochastic response variable y_t can be described as a weighted sum of the input variable x_t corrupted by a super-imposed noise process, that is

$$y_t = \nu_0 x_t + \nu_1 x_{t-1} + \ldots + \nu_p x_{t-p} + N_t. \tag{5.2}$$

To explore the interrelationship between two time series the impulse response function must be estimated.

The identification of the series n_t, C_t and Q_t as autoregressive second order models required the estimation of the autocorrelation function for each series. To determine the transfer function, the cross-correlation function must be determined for each pair of series. When the input variable has been "pre-whitened", the estimated cross-correlation function provides the estimated transfer function. The computational details of pre-whitening and determining the cross-correlation function were performed at Princeton using the BOXJEN program.

Before applying the time series techniques described above, a transformation on the queue length series seemed necessary. From visual inspection of the time series plot, as well as the histogram produced by the GPSS V program, it was obvious that the queue lengths were not Normally distributed, but rather followed an exponential distribution. We therefore decided to make a negative exponential transformation on the raw data of queue lengths recorded on a per second basis. Each value of queue length denoted by Q_t, is transformed into q_t using the formula:

$$q_t = \int_0^{Q_t} \frac{1}{\mu_Q} e^{-\frac{x}{\mu_Q}} dx = 1 - e^{-\frac{Q_t}{\mu_Q}}, \tag{5.3}$$

where μ_Q is the mean of Q_t estimated from the generated data. Three series of 60-second averages, after the transformation on the data from Sector 475, at three different traffic density simulations, are shown in Figures 5.1 ∿ 5.3. The reader may wish to compare these normalized series against the series without transformation displayed earlier in Figures 4.3, 4.6 and 4.9. The difference between the normalized and original simulated series of Q_t are also displayed in Figures 5.4 and 5.5 for Sector 453, Figures 5.6 and 5.7 for Sector 524 and Figures 5.8 and 5.9 for Sector 553. Similar figures for the other simulated sectors are available.

The analyses then proceed for the triple-series, n_t, C_t and q_t, each constructed on a 60-second average basis using data from Sector 475. The following three pairwise combinations were chosen: (C_t, n_t), (q_t, n_t) and (q_t, C_t), where the first argument within the parentheses is the output series, and the second argument is the input series. The estimated parameters comprising the transfer function for the couplet (C_t, n_t) based upon the historical data are displayed in column 1 of Table 5.1. The simulated data is displayed in column 2. Using the data simulated from the experiments described in Chapter 4 created by varying the input density ρ, the simulated transfer functions for 125% and 150% of ρ are given in columns 3 and 4 respectively.

When the estimated transfer function coefficients determined from the historical and simulated data for 100%ρ are compared, a pattern emerges for the first eight estimates. Further, rough estimates of the standard errors of these coefficients are given by $r/\sqrt{n}$ where n = 120 pairs of observations and r is the ratio of the standard deviation of y_t to the standard error of x_t, both y_t and x_t based on the pre-whitened data. The estimated standard errors are obtained and listed at the bottom of Table 5.1. Approximate statistical significance can be claimed by all estimates falling outside the range ($-2r/\sqrt{n}$, $2r/\sqrt{n}$). Using this criteria the first of the transfer function coefficients for the pair (C_t, n_t) is statistically significantly different from zero for both sets of data. In contemplating the combined roles of n_t and C_t, it seems intuitively obvious that the two responses should be highly correlated and that a viable transfer function should exist between the two time series. The statistical significance observed for $\hat{\nu}_0$ on both historical and simulated data is consistent with this reasoning. Further, the pattern of the coefficients, though not statistically significant, further confirms the hypothesis that a transfer function does exist.

A similar set of circumstances was found to exist for the (q_t, n_t) couplet. The estimated transfer function parameters for the (q_t, n_t) series are displayed in Table 5.2.

Strong statistical evidence exists for a response function for (q_t, C_t) as evidenced by the estimated transfer function parameters displayed in Table 5.3. Under usual operating conditions (100% ρ) both $\hat{\nu}_0 = 0.744$ and $\hat{\nu}_1 = 0.192$ are greater than twice their standard error and to a rough approximation we may write $\hat{q}_t = 0.744\ C_t + 0.192\ C_{t-1}$. As the incoming traffic density increases to 125% we find once more that the first two estimated transfer function parameters are statistically significant, i.e. $\hat{\nu}_0 = 0.753$ and $\hat{\nu}_1 = 0.254$. Further, the $\hat{\nu}_0$ and $\hat{\nu}_1$ when compared across 100% and 125% are

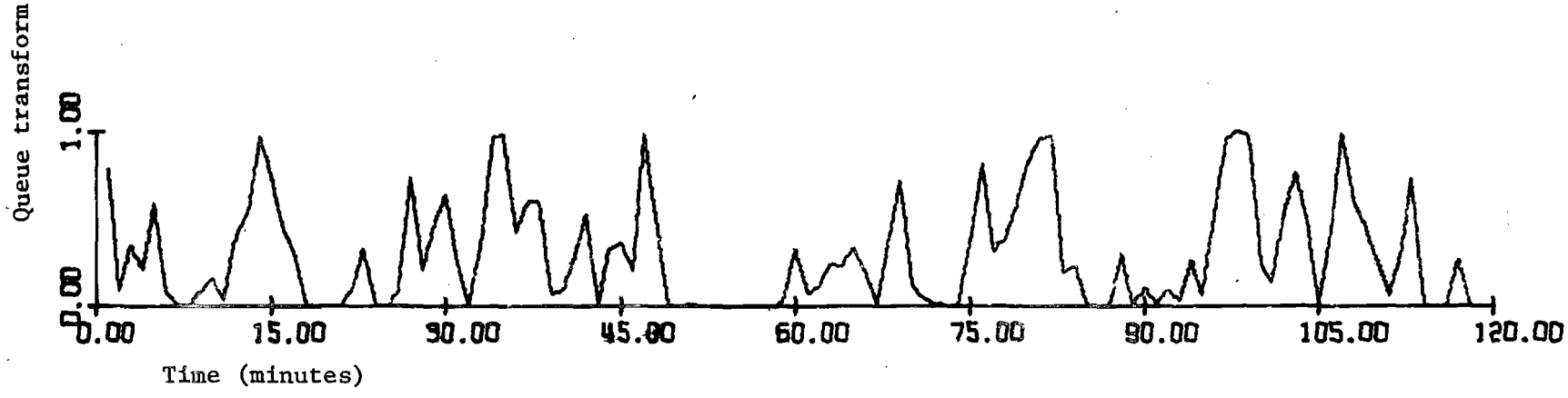

Figure 5.1 Simulated Time Series of Queue Transforms in Sector 475 HI at 100% of Historical Traffic Density

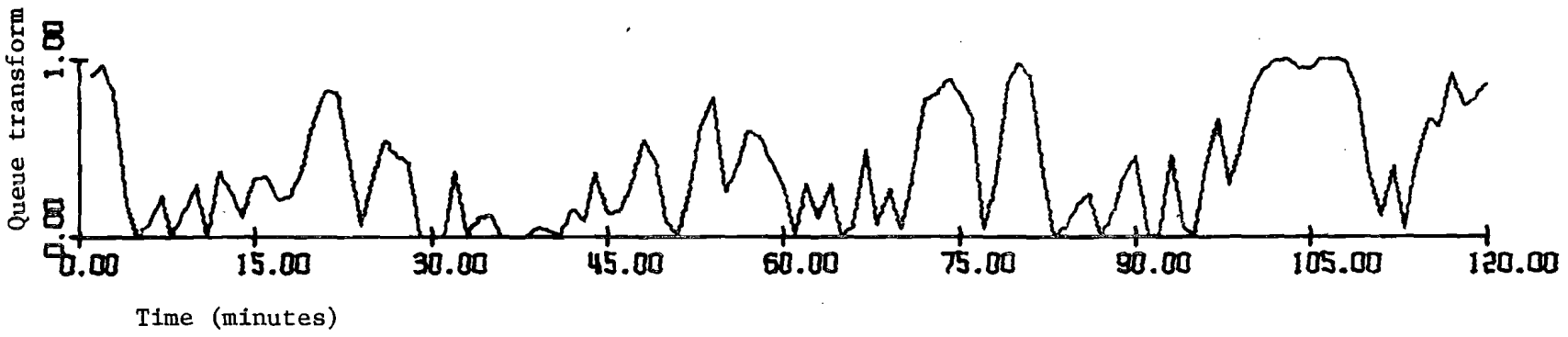

Figure 5.2 Simulated Time Series of Queue Transforms in Sector 475 HI at 125% of Historical Traffic Density

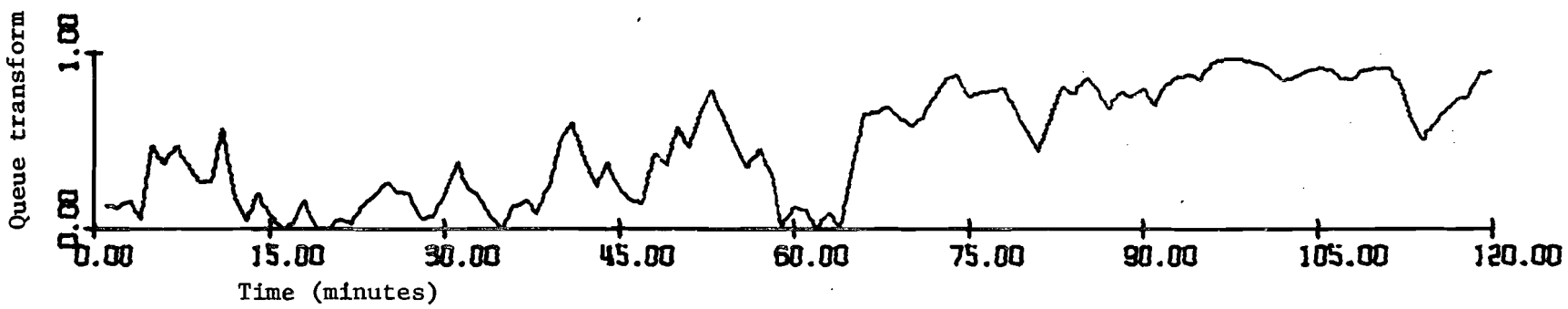

Figure 5.3 Simulated Time Series of Queue Transforms in Sector 475 HI at 150% of Historical Traffic Density

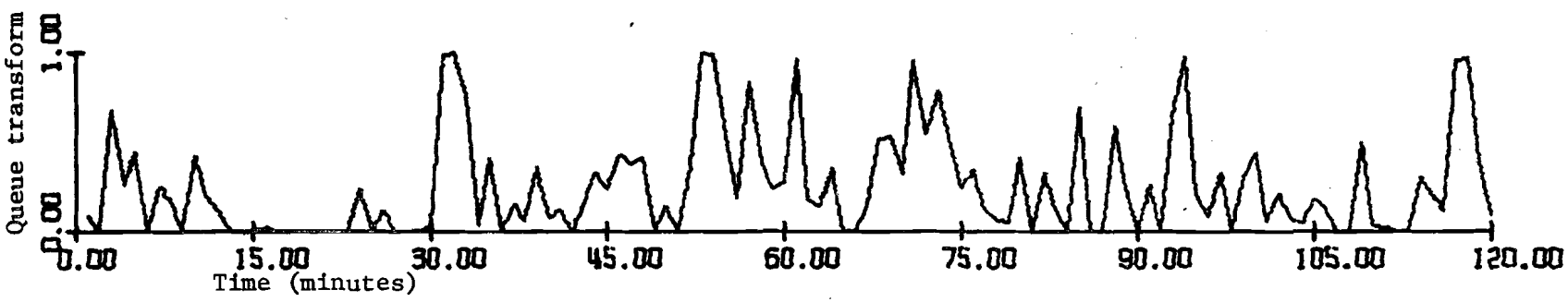

Figure 5.4 Simulated Time Series of Queue Transforms in Sector 453 LT at 100% of Historical Traffic Density

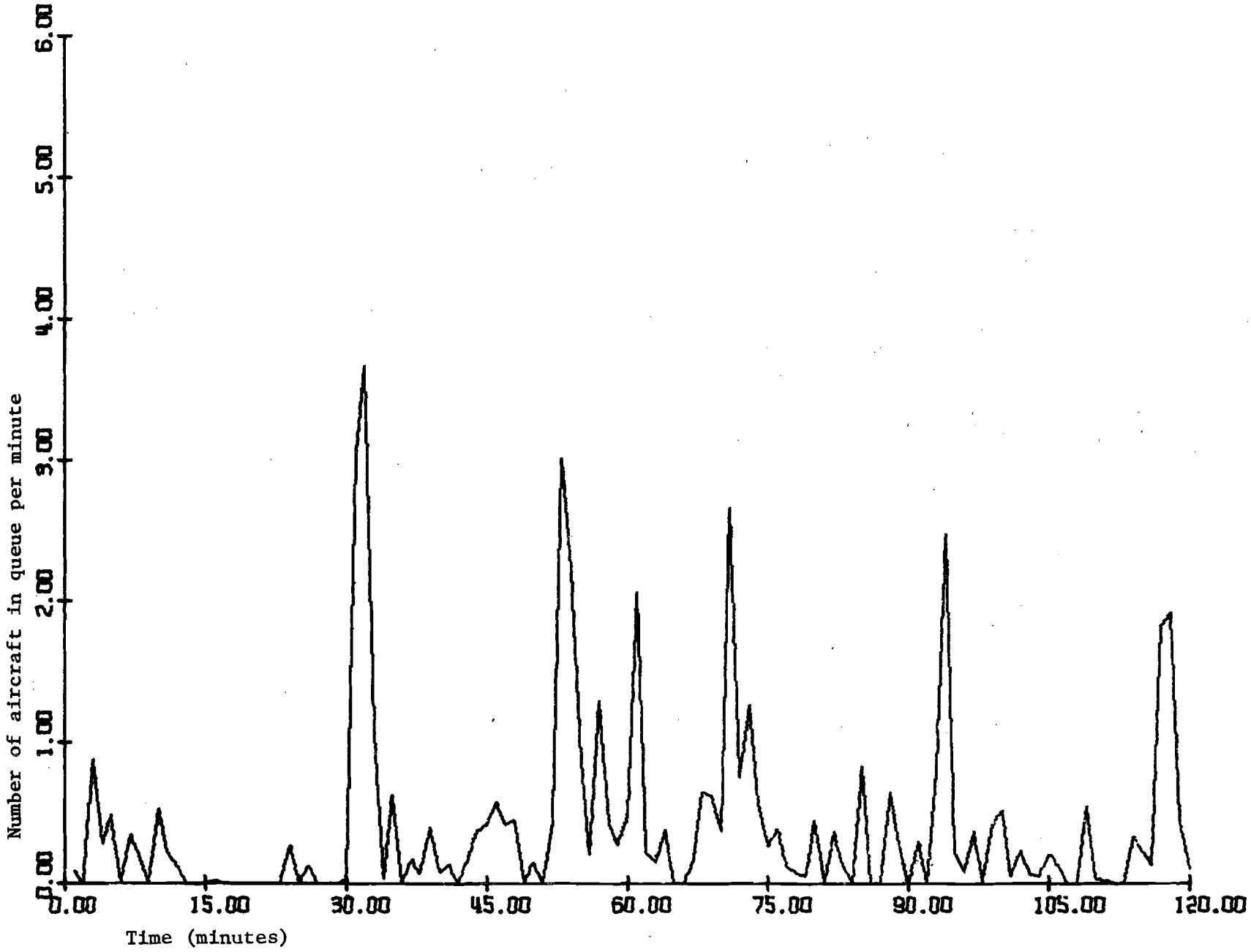

Figure 5.5 Simulated Time Series of Queue Length in Sector 453 LT at 100% of Historical Traffic Density

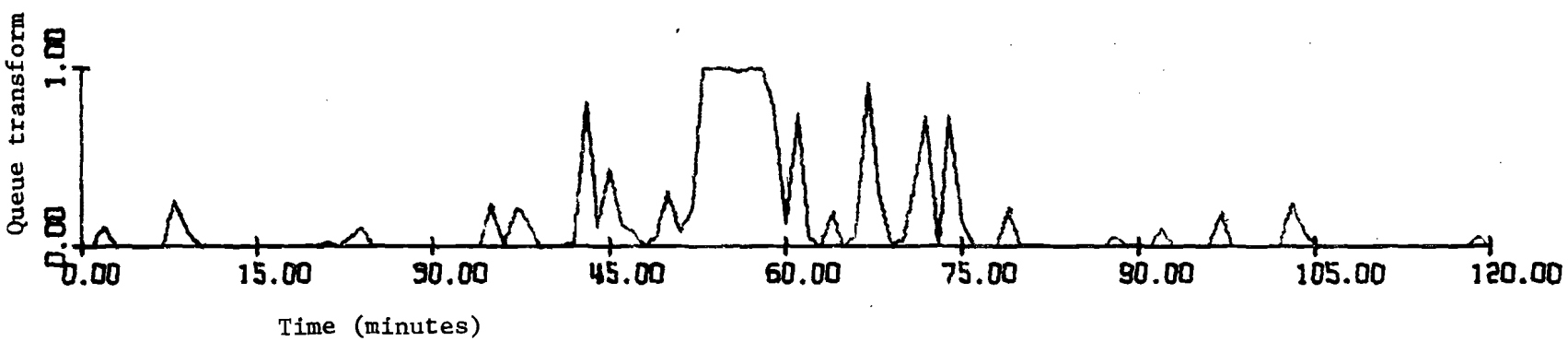

Figure 5.6 Simulated Time Series of Queue Transforms in Sector 524 LG at 100% of Historical Traffic Density

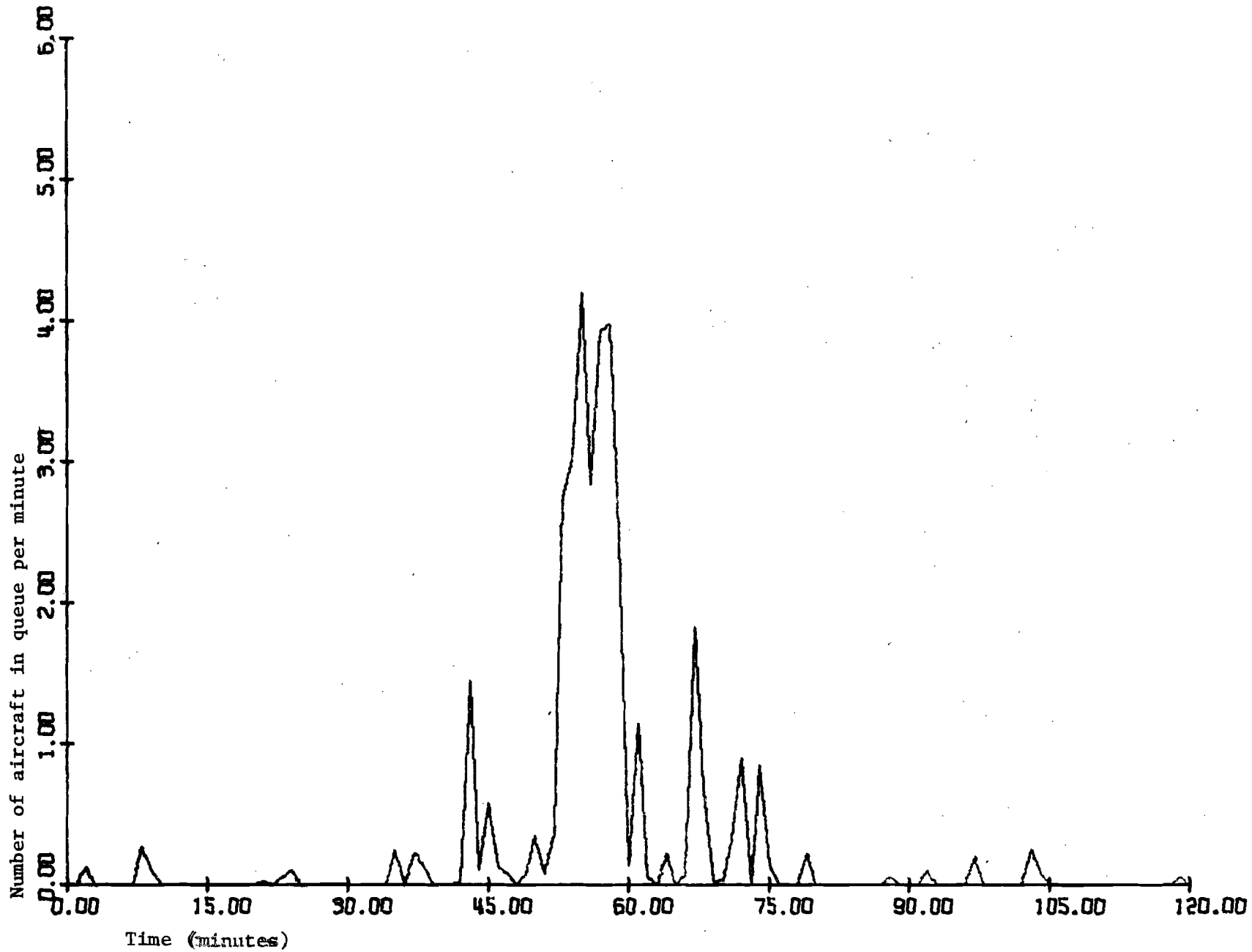

Figure 5.7 Simulated Time Series of Queue Length in Sector 524 LG at 100% of Historical Traffic Density

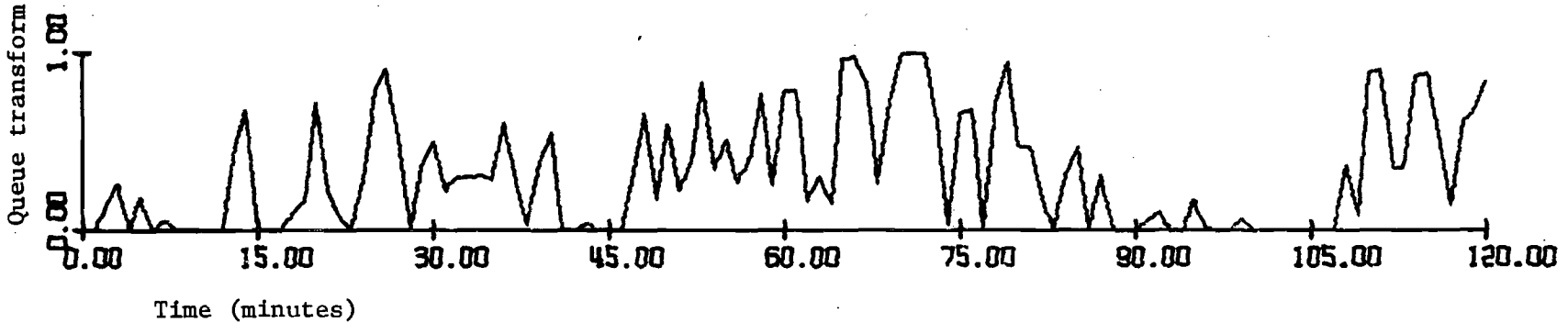

Figure 5.8 Simulated Time Series of Queue Transforms in Sector 553 AR at 100% of Historical Traffic Density

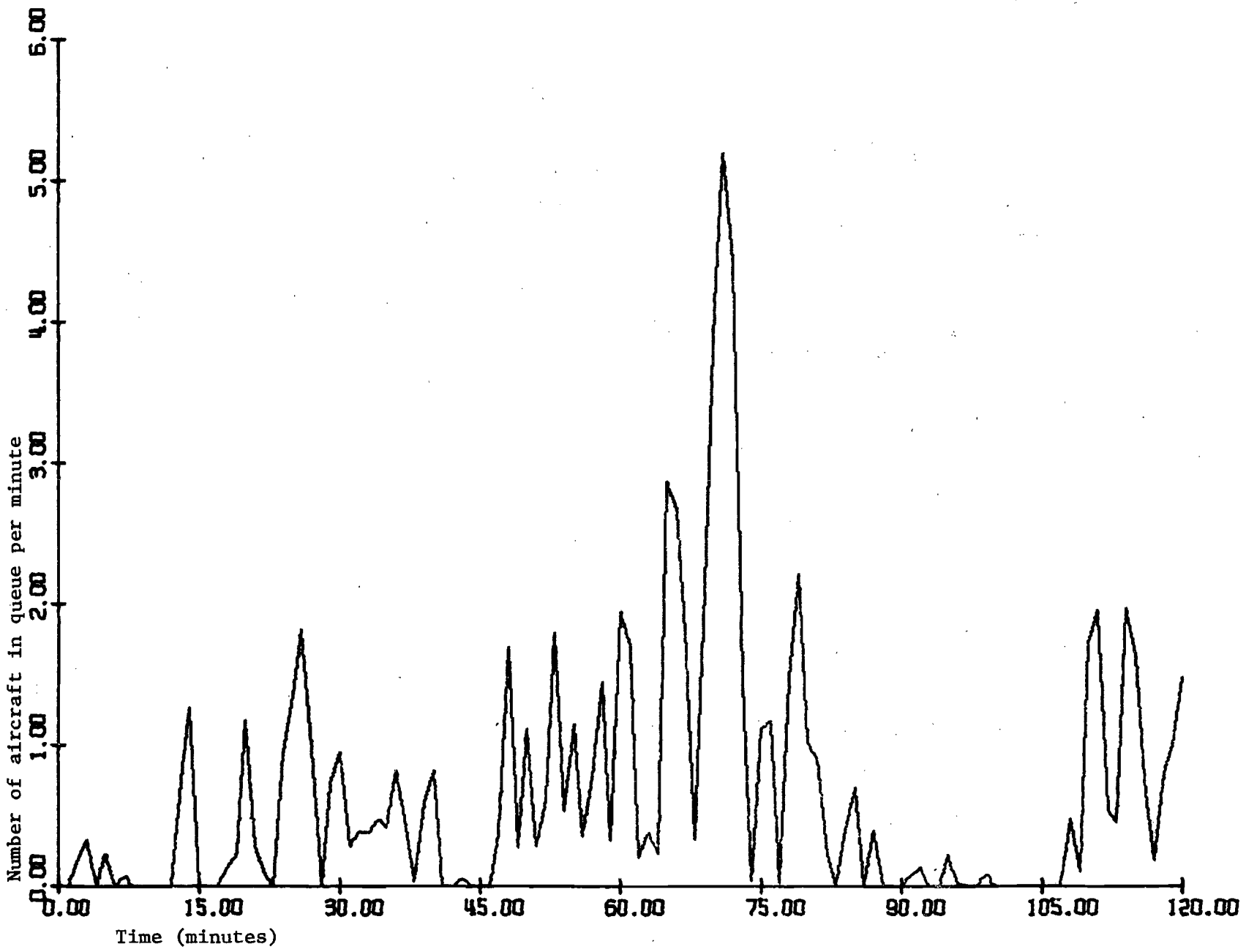

Figure 5.9 Simulated Time Series of Queue Length in Sector 553 AR at 100% of Historical Traffic Density

Table 5.1 Estimates of the Transfer Function Parameters Comprising the Impulse Response Function of (C_t, n_t)

Estimated Transfer Function Parameters	Historical Data (C_t, n_t)	Simulated Data 100%	Simulated Data 125%	Simulated Data 150%
$\hat{\nu}_0$	0.083*	0.118*	0.126*	0.049*
$\hat{\nu}_1$	-0.042	-0.030	-0.008	-0.004
$\hat{\nu}_2$	-0.027	-0.006	0.024	-0.021
$\hat{\nu}_3$	0.066	0.068	-0.019	0.018
$\hat{\nu}_4$	-0.052	-0.043	-0.007	0.004
$\hat{\nu}_5$	0.060	-0.003	-0.002	-0.006
$\hat{\nu}_6$	-0.034	-0.030	0.041	-0.019
$\hat{\nu}_7$	0.021	0.033	-0.029	0.016
$\hat{\nu}_8$	-0.015	-0.025	-0.008	0.003
$\hat{\nu}_9$	0.042	-0.043	-0.006	-0.004
$\hat{\nu}_{10}$	-0.066	0.078	0.008	-0.031
$\hat{\nu}_{11}$	0.000	-0.090*	-0.037	0.019
$\hat{\nu}_{12}$	0.025	0.012	0.037	0.001
$\hat{\nu}_{13}$	0.055	0.042	-0.015	0.000
Approximate Standard Error	0.0377	0.0402	0.0365	0.0180

*Significantly different from zero at 0.05 level

Table 5.2 Estimates of the Transfer Function Parameters Comprising the Impulse Response Function of (q_t, n_t)

Estimated Transfer Function Parameters	Historical Data (Q_t not available)	Simulated Data 100% ρ	Simulated Data 125% ρ	Simulated Data 150% ρ
$\hat{\nu}_0$	-	0.145*	0.086*	0.055*
$\hat{\nu}_1$	-	-0.012	0.046	0.004
$\hat{\nu}_2$	-	0.008	-0.003	0.005
$\hat{\nu}_3$	-	0.008	-0.001	-0.015
$\hat{\nu}_4$	-	0.044	-0.015	0.002
$\hat{\nu}_5$	-	-0.081*	0.021	0.013
$\hat{\nu}_6$	-	0.026	0.046	-0.007
$\hat{\nu}_7$	-	0.048	-0.027	-0.013
$\hat{\nu}_8$	-	-0.062	-0.031	0.014
$\hat{\nu}_9$	-	-0.027	0.005	0.001
$\hat{\nu}_{10}$	-	0.043	0.002	-0.006
$\hat{\nu}_{11}$	-	-0.026	-0.004	0.013
$\hat{\nu}_{12}$	-	-0.036	-0.009	-0.014
$\hat{\nu}_{13}$	-	0.010	-0.015	0.003
Approximate Standard Error		0.0369	0.0263	0.0120

*Significantly different from zero at 0.05 level

Table 5.3 Estimates of the Transfer Function Parameters Comprising the Impulse Response Function of (q_t, C_t)

Estimated Transfer Function Parameters	Historical Data (Q_t not available)	Simulated Data 100% ρ	Simulated Data 125% ρ	Simulated Data 150% ρ
$\hat{\nu}_0$	-	0.744*	0.753*	0.621*
$\hat{\nu}_1$	-	0.192*	0.254*	0.343*
$\hat{\nu}_2$	-	-0.028	0.062	0.201
$\hat{\nu}_3$	-	0.062	0.147	0.231*
$\hat{\nu}_4$	-	0.125	0.139	0.214
$\hat{\nu}_5$	-	-0.003	0.193	0.149
$\hat{\nu}_6$	-	-0.014	0.054	0.141
$\hat{\nu}_7$	-	-0.089	0.088	0.143
$\hat{\nu}_8$	-	-0.127	0.058	0.239*
$\hat{\nu}_9$	-	-0.109	-0.006	0.233*
$\hat{\nu}_{10}$	-	-0.015	-0.044	0.124
$\hat{\nu}_{11}$	-	-0.034	-0.093	0.148
$\hat{\nu}_{12}$	-	-0.044	-0.032	0.119
$\hat{\nu}_{13}$	-	-0.059	-0.112	0.210
Approximate Standard Error		0.0932	0.0978	0.1108

*Significantly different from zero at 0.05 level.

not significantly different, an event which suggests that increasing ρ to 125% has no effect on the association between Q_t and C_t. However, for 150%ρ a dramatic change occurs in the transfer function estimates. Not only has the association between Q_t and C_t changed, but channel utilization as much as five time periods ago significantly influences the present length of the communications queue. The presence of statistically significant estimates at lags 8, 9 and 13 can also be taken as a signal of non-stationarity in the transfer function itself. What is observed here is likely a reflection of the non-stationary behavior discovered in Chapter 4 for q_t at 150%ρ.

In studying the transfer function problem associating n_t, C_t and Q_t, the following analogue system provides a convenient image. Consider the three connected water tanks displayed in Figure 5.10. The water level in the first is analogous to aircraft loading, and the amount of water being injected into the system is analogous to aircraft arrivals (in our case, the arrival stream forms a Poisson process). We note that the amount of water entering the first tank can be varied. The second tank, which represents channel utilization, is bounded by a solid cover and has a volume equal to or less than 1.0 (the actual ceiling on C_t in the real world forces the volume to be less than .90). When the water level in the second tank is low, water from the first tank passes through the valve between the tanks, which determines the speed of transfer, and goes directly into the second tank where it is immediately discharged, with little concern for the third tank (waiting in a communications queue). As the amount of water arriving in Tank 1 increases, the level in the second tank rises and approaches its ceiling. Two events now occur: the water level in the third tank gets progressively higher, and the force exerted on the water leaving the second tank increases. When the water level in the third tank overflows, the system is declared out of control.

5.3 Studies of Air Traffic Control Network Capacities

Once a simulation model has been developed and tested for a single ATC sector, it is natural to consider how that model might be extended to simulate a group of interrelated sectors. In framing the problem, it is convenient to think of the ATC system in terms of a transporation network. The sectors to be modeled form a set of nodes which are connected by arcs representing passage between adjacent sectors. An example of such a representation is shown in Figure 5.11, which represents the most frequently observed movements of aircraft among the sectors at LaGuardia Airport during a two-hour period. The diagram gives an intuitively attractive physical picture of the system, showing the general geographical and functional relationships among the sectors. Similar diagrams at other airports and for enroute traffic were presented in Chapter 7 of Volume II.

Examination of the network in Figure 5.11 shows the usual arrival and departure sector sequences. A typical arriving aircraft passes through two arrival control sectors (AR), or alternatively a radar advisory (RA), moving then to the local controller (LC) and finally to the ground controller

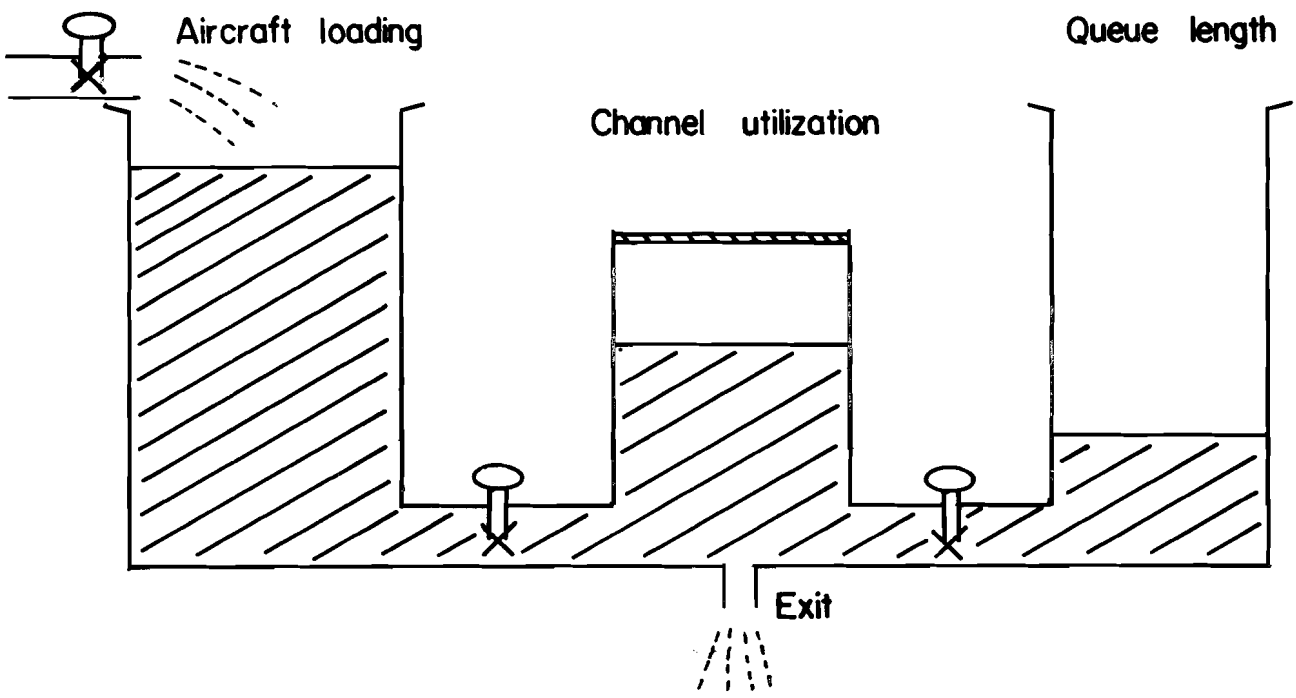

Figure 5.10 A Heuristic Model for Communication Responses Using a Triple-Tank Water System

LaGuardia

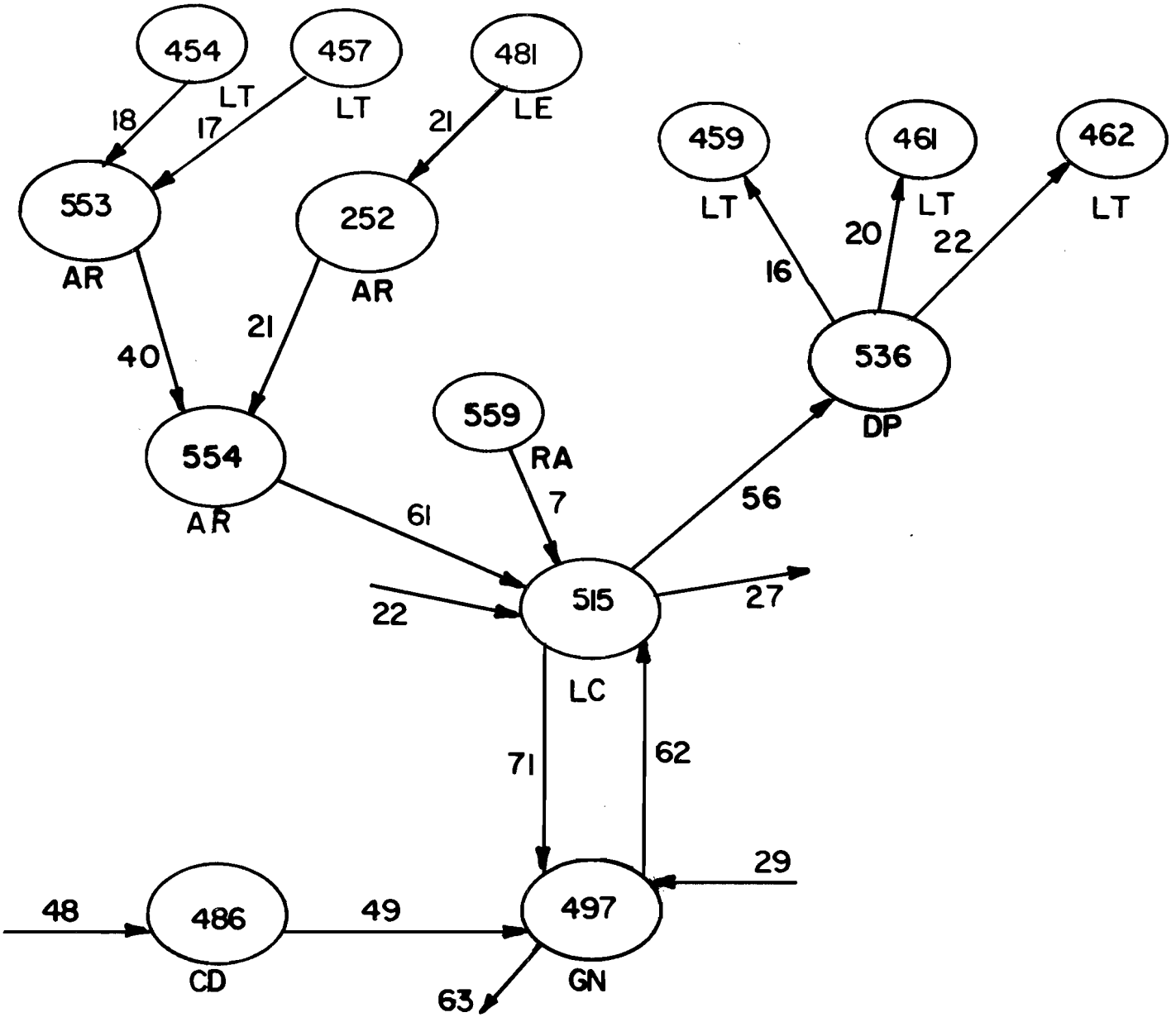

Figure 5.11 ATC Network at LaGuardia Airport

(GN). A typical departing aircraft begins at clearance delivery (CD) or ground control (GN), moving to the local controller (LC), and finally leaving the system through a departure control sector (DP). A small amount of traffic other than arrivals and departures is observed passing through the local control sector (LC).

In Figure 5.11, the number of aircraft which moved between all pairs of sectors during the sample period is indicated on the associated arcs. Since the number of aircraft within a given sector will not in general be the same at both ends of the sample period, the number of aircraft shown entering the sector may differ from the number of aircraft leaving. Such an effect becomes less important as the length of the sample period increases.

A convenient way to describe the movement patterns of aircraft through such a network is to construct a transition matrix $T(n \times n)$, where n is the number of sectors and element t_{ij} is the proportion of aircraft leaving sector i which move next to sector j. While not preserving the full arrival and departure sequences, the transition matrix is useful in describing the relative movement between pairs of sectors. Under certain assumptions which will be discussed in detail later, this matrix can be used to make inferences about the total system flow. The transition matrix for the network in Figure 5.11 is given in Table 5.4 along with a listing of the individual airport sector parameters.

This formulation of the ATC system as a network of sectors is similar to the procedures used in analyzing ground transportation systems. In typical highway networks, the major roads are coded as arcs and the important intersections as nodes. In contrast to highway networks, however, the transit time for aircraft moving through the ATC system is associated with the nodes rather than with the arcs. The transition time between sectors is small, typically less than fifteen seconds, and is not critical in the calculation of system capacity.

An important variable affecting total system flow is thus the time which an aircraft spends within a given sector. It was shown in Volume II that the distribution of these so-called "transit times" is not easily characterized, since the time for a single aircraft is a function of its velocity, its vector through the sector, the proximity of other aircraft, and other factors peculiar to that aircraft and sector. In particular, congestion in the communications system can affect the ability of pilots and controllers to relay required information quickly and, particularly in sectors around the terminal, can increase the length of time which aircraft spend in each sector.

Detailed consideration of flow through the ATC system must then consider the interaction of voice communications and sector transit times. Modeling the communications-flow network relationships in a dynamic framework is yet to be studied. However, it is possible to make statements about average system flow over a long period of time using the network formulation just developed.

In the discussion which follows, we determine the maximum feasible

Table 5.4 ATC Sector Parameters for Network Analysis

AIR TRAFFIC CONTROL NETWORK FLOW ANALYSIS
PRINCETON UNIVERSITY TRANSPORTATION PROGRAM

TABLE OF ATC SECTOR PARAMETERS

SECTOR IDENTIFICATION		MEAN TRANSIT TIME (MINUTES)	CAPACITY CONSTRAINT	NUMBER OF AIRCRAFT	MAX. FEASIBLE AIRCRAFT PER HR.
1	454 LT	9.16	MEAN	4.00	26.20
2	457 LT	7.81	MEAN	4.00	30.73
3	459 LT	7.76	MEAN	4.00	30.93
4	461 LT	4.44	MEAN	4.00	54.05
5	462 LT	4.27	MEAN	4.00	56.21
6	481 LE	7.71	MEAN	4.00	31.13
7	486 CD	2.76	MEAN	4.00	86.96
8	497 GN	5.59	MEAN	4.00	42.93
9	515 LC	5.31	MEAN	4.00	45.20
10	536 DP	3.61	MEAN	4.00	66.48
11	552 AR	6.69	MEAN	4.00	35.87
12	553 AR	11.03	MEAN	4.00	21.76
13	554 AR	3.52	MEAN	4.00	68.18
14	559 RA	7.95	MEAN	4.00	30.19

TRANSITION MATRIX

FROM/TO	1	2	3	4	5	6	7
1	0.0	0.0	0.0	0.0	0.0	0.0	0.0
2	0.0	0.0	0.0	0.0	0.0	0.0	0.0
3	0.0	0.0	0.0	0.0	0.0	0.0	0.0
4	0.0	0.0	0.0	0.0	0.0	0.0	0.0
5	0.0	0.0	0.0	0.0	0.0	0.0	0.0
6	0.0	0.0	0.0	0.0	0.0	0.0	0.0
7	0.0	0.0	0.0	0.0	0.0	0.0	0.0
8	0.0	0.0	0.0	0.0	0.0	0.0	0.0
9	0.0	0.0	0.0	0.0	0.0	0.0	0.0
10	0.0	0.0	0.28	0.34	0.38	0.0	0.0
11	0.0	0.0	0.0	0.0	0.0	0.0	0.0
12	0.0	0.0	0.0	0.0	0.0	0.0	0.0
13	0.0	0.0	0.0	0.0	0.0	0.0	0.0
14	0.0	0.0	0.0	0.0	0.0	0.0	0.0

FROM/TO	8	9	10	11	12	13	14
1	0.0	0.0	0.0	0.0	1.00	0.0	0.0
2	0.0	0.0	0.0	0.0	1.00	0.0	0.0
3	0.0	0.0	0.0	0.0	0.0	0.0	0.0
4	0.0	0.0	0.0	0.0	0.0	0.0	0.0
5	0.0	0.0	0.0	0.0	0.0	0.0	0.0
6	0.0	0.0	0.0	1.00	0.0	0.0	0.0
7	1.00	0.0	0.0	0.0	0.0	0.0	0.0
8	0.0	0.50	0.0	0.0	0.0	0.0	0.0
9	0.46	0.0	0.36	0.0	0.0	0.0	0.0
10	0.0	0.0	0.0	0.0	0.0	0.0	0.0
11	0.0	0.0	0.0	0.0	0.0	1.00	0.0
12	0.0	0.0	0.0	0.0	0.0	1.00	0.0
13	0.0	1.00	0.0	0.0	0.0	0.0	0.0
14	0.0	1.00	0.0	0.0	0.0	0.0	0.0

flow through an ATC network by first specifying the capacity of each sector. Assume that the maximum average flow in aircraft per unit time over a specified network of sectors is desired, where that average is to be computed over a sufficiently long length of time as to make the variance of sector transit times small in comparison. Then the specification of the mean transit times through each sector would be sufficient to determine the average number of aircraft in the sector for any specified arrival rate. In particular, if the mean transit time is μ hours and the arrival rate is λ aircraft per hour, then the expected number of aircraft in the sector at any given time is $\lambda\mu$. For the network in Figure 5.11, the mean transit time for each sector has been estimated from the historical data, and the resulting estimates are tabulated in Table 5.4.

For the purpose of determining maximum feasible flow over the network, it is also necessary to specify sector capacities. This is a complicated question and depends on the dynamic relationship of flow and communications. Such detailed study remains to be accomplished, but for purposes of illustration, it will be assumed that the capacity of a sector can be specified in arrivals per unit time, and that this capacity has been calculated from knowledge of the amount of traffic which a sector can handle. For instance, if it is desired that the expected number of aircraft in the sector not exceed n aircraft, then the capacity in arrivals per hour c is given by $c = k/\mu$. In Table 5.4, the maximum feasible number of aircraft per hour for each sector has been determined such that the expected number of aircraft will not exceed four.

Given the resulting air traffic control network and sector capacities, it is useful to consider the effect that individual sectors have on the total system flow. With some modification, standard maximum flow algorithms can be applied to the ATC network, and the sectors which are most likely to restrict system flow can be determined.

This problem will be analyzed under two sets of conditions. The first set are termed "free-flow" conditions, implying that aircraft are free to move from origin to destination through any feasible sequence of sectors. The second set of conditions are more restrictive and refer to a "constrained-flow" network. The added restriction is that the transition matrix obtained from the actual network operations must be preserved under maximum flow. These two sets of conditions are useful for answering different types of questions and will be discussed separately.

The determination of maximum feasible flow over a network with finite capacity under <u>free-flow</u> conditions is a fundamental problem in network analysis, since many questions can be reduced to consideration of maximum flow. A straightforward but important algorithm is available to determine the maximum flow between a single origin and a single destination given a network with arc capacities. While calculating the value of the maximum flow, the algorithm also determines an assignment of flow to the network which will realize that maximum.

The formulation of the air traffic control network must be modified

slightly to fit the conditions of the algorithm. First, the node capacities must be converted to arc capacities, which is easily accomplished by dividing each node in two, the first gathering only those arcs directed into the original node and the second gathering all arcs directed outward. An artificial arc is then constructed between the two new nodes, which represents movement of aircraft within the sector. The flow capacity which was originally assigned to the sector can now be assigned to this arc, while all the original arcs are considered to have infinite capacity.

The maximum flow algorithm can then be applied directly to determine the maximum flow between any two sectors, one as the origin and the other as the destination. However, it is of greater interest to consider the multiple origins and destinations in the network simultaneously. The procedure for doing so depends upon the questions to be answered, but a number of tricks are common.

First, consider Figure 5.11 once again. Aircraft arriving at LaGuardia normally enter the ATC system through one of four sectors: 454 (LT), 457 (LT), 481 (LE), and 559 (RA). All arrivals move to a single destination, sector 497 (GN). To determine the maximum number of arriving aircraft which can be handled per unit time (assuming no departures), a "super-source" can be constructed with arcs of infinite capacity directed to each of the four origins, as shown in Figure 5.12. All aircraft arriving at LaGuardia are then considered to originate at the super-source, making the single origin, single destination algorithm appropriate.

This same procedure is also applicable for considering the maximum number of departing aircraft per unit time (assuming no arrivals), since a super-source can be constructed with arcs directed into sectors 486 (CD) and 497 (GN), both origins of departing aircraft. Since departures from LaGuardia also have three possible destinations, 459 (LT), 461 (LT), and 462 (LT), a "super-sink" must also be constructed with arcs directed from each of the destinations. The standard algorithm can then be applied to the resulting single super-source, single super-sink network.

Considering arrivals and departures simultaneously is somewhat more difficult. While it is feasible to construct a super-source directed to each of the six possible origins and a super-sink for the four destinations, such a formulation has a major drawback. The simple construction of a super-sink and super-source would make no distinction between arriving and departing aircraft and thus would not ensure that aircraft entering at an arrival origin would move to an arrival destination. In particular, since sector 497 (GN) is both an origin (for departures) and a destination (for arrivals), the algorithm could quite likely assign a given aircraft this sector as both origin and destination, since such an assignment would cause no congestion in other parts of the network.

In order to preserve the proper arrival and departure sequences, it is necessary to move to a "multi-commodity flow" formulation. In such a formulation, arrivals and departures are treated as separate commodities, each with a distinct set of legitimate origins and destinations. The problem is

LaGuardia

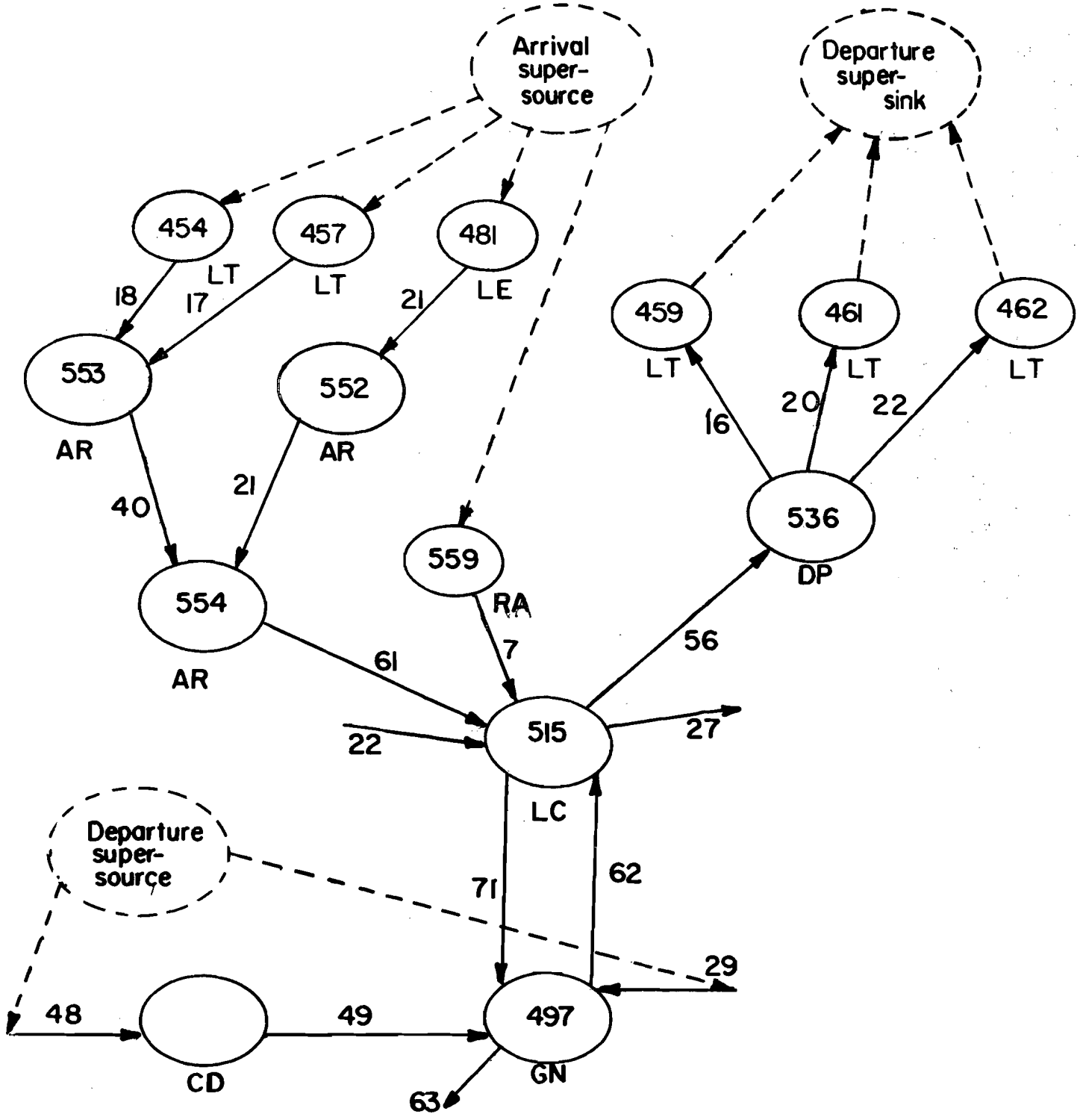

Figure 5.12 Modified ATC Network

then reduced to maximizing the sum of the flow of the two commodities, a linear programming problem.

Applying the maximum flow algorithm to the ATC network at LaGuardia illustrates the type of analysis which is possible. First, whether arrivals and departures are considered separately or simultaneously does not affect the maximum value of flow over the system, which is determined by the capacity of the ground controller, sector 497 (GN). Table 5.5 shows one possible assignment of this maximum flow to the network, restricted so that the number of arriving aircraft is equal to the number of departures. Second, the flow through the local controller, sector 515 (LC), is also near capacity. If some additional amount of through flow (neither arrival nor departure) was applied to sector 515 as observed in the empirical data, it would most likely become the critical sector in restricting total flow.

Several further points should be considered when analyzing a network under free-flow conditions. First, the assignment of flow to the sectors is not unique, even when the number of arrivals is required to equal the number of departures. Second, while the value of the maximum flow obtained is always unique, the identification of critical sectors may not be. It is often useful to increase the capacity of sectors which are critical in the initial run and to repeat the algorithm. Such a tactic will indicate how sensitive the maximum flow value is to the particular set of critical sectors selected. Third, the assumption that aircraft are free to choose any sequence of sectors between origin and destination is not very realistic, but it does provide an upper bound on the maximum feasible flow. More realistic assumptions can be imposed in constrained-flow analysis, but the added transition restrictions make the analysis more subject to the particular sample period from which the network is constructed.

In analyzing maximum system flow under <u>constrained-flow</u> conditions, the transition matrix discussed earlier plays a central role. It will be recalled that the matrix $\underset{\sim}{T}$ is of dimension (n x n) where n is the number of sectors in the system and that the element in the i'th row and the j'th column is

t_{ij} = the proportion of aircraft in sector i which move next to sector j.

It is instructive to note that for all sectors i not a destination, the sum of the elements in the i'th row equals one.

The solution of the maximum feasible flow problem under constrained-flow conditions proceeds as follows. Let

p_i = the proportion of total aircraft entering the system for which sector i is the origin;

f_j = the proportion of total system flow which passes through sector j; and

Table 5.5 Assignment of Maximum Feasible Flow to Free-Flow Network

MAXIMUM FEASIBLE FLOW ASSIGNMENT - FREE FLOW NETWORK

SECTOR IDENTIFICATION	MAX. FEASIBLE ARRIVAL RATE	ASSIGNED ARRIVAL RATE	CRITICAL SECTORS
1 454 LT	26.20	0.0	
2 457 LT	30.73	0.0	
3 459 LT	30.93	21.46	
4 461 LT	54.05	0.0	
5 462 LT	56.21	0.0	
6 481 LE	31.13	21.47	
7 486 CD	86.96	0.0	
8 497 GN	42.93	42.93	*
9 515 LC	45.20	42.93	
10 536 DP	66.48	21.46	
11 552 AR	35.87	21.47	
12 553 AR	21.76	0.0	
13 554 AR	68.18	21.47	
14 559 RA	30.19	0.0	

FROM/TO	1	2	3	4	5	6	7
1	0.0	0.0	0.0	0.0	0.0	0.0	0.0
2	0.0	0.0	0.0	0.0	0.0	0.0	0.0
3	0.0	0.0	0.0	0.0	0.0	0.0	0.0
4	0.0	0.0	0.0	0.0	0.0	0.0	0.0
5	0.0	0.0	0.0	0.0	0.0	0.0	0.0
6	0.0	0.0	0.0	0.0	0.0	0.0	0.0
7	0.0	0.0	0.0	0.0	0.0	0.0	0.0
8	0.0	0.0	0.0	0.0	0.0	0.0	0.0
9	0.0	0.0	0.0	0.0	0.0	0.0	0.0
10	0.0	0.0	21.46	0.0	0.0	0.0	0.0
11	0.0	0.0	0.0	0.0	0.0	0.0	0.0
12	0.0	0.0	0.0	0.0	0.0	0.0	0.0
13	0.0	0.0	0.0	0.0	0.0	0.0	0.0
14	0.0	0.0	0.0	0.0	0.0	0.0	0.0

FROM/TO	8	9	10	11	12	13	14
1	0.0	0.0	0.0	0.0	0.0	0.0	0.0
2	0.0	0.0	0.0	0.0	0.0	0.0	0.0
3	0.0	0.0	0.0	0.0	0.0	0.0	0.0
4	0.0	0.0	0.0	0.0	0.0	0.0	0.0
5	0.0	0.0	0.0	0.0	0.0	0.0	0.0
6	0.0	0.0	0.0	21.47	0.0	0.0	0.0
7	0.0	0.0	0.0	0.0	0.0	0.0	0.0
8	0.0	21.46	0.0	0.0	0.0	0.0	0.0
9	21.47	0.0	21.46	0.0	0.0	0.0	0.0
10	0.0	0.0	0.0	0.0	0.0	0.0	0.0
11	0.0	0.0	0.0	0.0	0.0	21.47	0.0
12	0.0	0.0	0.0	0.0	0.0	0.0	0.0
13	0.0	21.47	0.0	0.0	0.0	0.0	0.0
14	0.0	0.0	0.0	0.0	0.0	0.0	0.0

MAXIMUM FLOW = 42.93 AIRCRAFT PER HOUR.

t_{ij} (m) = the proportion of flow from sector i which reaches sector j in m-1 transitions. This is the element in the i'th row and j'th column of the m'th power of the one-step transition matrix $\underset{\sim}{T}$.

Then

$$f_j = p_j + \sum_{i=1}^{n} p_i \, t_{ij} \, (1) + \sum_{i=1}^{n} p_i \, t_{ij} \, (2) + \ldots =$$

$$p_j + \sum_{m=1}^{\infty} \sum_{i=1}^{n} p_i \, t_{ij} \, (m) \text{ for all sectors } j. \qquad (5.4)$$

If no circulation exists (i.e. no flow can pass through a given sector more than once), then the summation over m need only be taken to m=n-1, by which point all flow will have reached a destination. In general, the calculation of f_j terminates at an m such that all but a negligible proportion of total flow has reached a destination.

In evaluating the maximum flow on the network, the capacities computed earlier are now employed. Let

c_j = the capacity of sector j in arrivals per unit time, and define

r_j = the constraint which sector j imposes on total system flow in aircraft per unit time.

The for all $f_j > 0$, $r_j = c_j/f_j$. For all $f_j = 0$, $r_j = \infty$. (5.5)

The maximum system flow F is then equal to the smallest constraint among all the sectors in the system ($F = \min r_j$), since any larger flow would violate the capacity of at least one sector. The total flow through any sector j equals $F \times f_j$.

In the above analysis, it was assumed that the proportion of aircraft entering the system at each of the possible origins is given. If the p_i's are not specified, the value of the maximum flow is not so easily derivable. For the case of two origins, an algorithm has been developed determining p_1 and p_2 such that the total system flow is maximized.

Table 5.6 shows the maximum flow assignment obtained for the LaGuardia ATC system when analyzed under constrained-flow conditions based on the sample period in April, 1969. The critical sector in determining maximum system flow is the local controller, sector 515 (LC). The ground controller, sector 497 (GN), is also near its capacity. While the total system flow obtained is greater than under free-flow conditions, the total number of arriving and departing aircraft is actually less (39.61). This is due to the imposition of additional through traffic on sector 515 (LC), which was not considered in the free-flow case.

Table 5.6 Assignment of Maximum Feasible Flow to Constrained-Flow Network

MAXIMUM FEASIBLE FLOW ASSIGNMENT - CONSTRAINED FLOW NETWORK

SECTOR IDENTIFICATION	MAX. FEASIBLE ARRIVAL RATE	ASSIGNED ARRIVAL RATE	CRITICAL SECTORS
1 454 LT	26.20	5.09	
2 457 LT	30.73	4.81	
3 459 LT	30.93	4.54	
4 461 LT	54.05	5.68	
5 462 LT	56.21	6.23	
6 481 LE	31.13	5.94	
7 486 CD	86.96	13.58	
8 497 GN	42.93	42.63	
9 515 LC	45.20	45.20	*
10 536 DP	66.48	16.45	
11 552 AR	35.87	5.94	
12 553 AR	21.76	9.91	
13 554 AR	68.18	15.85	
14 559 RA	30.19	1.98	

FROM/TO	1	2	3	4	5	6	7
1	0.0	0.0	0.0	0.0	0.0	0.0	0.0
2	0.0	0.0	0.0	0.0	0.0	0.0	0.0
3	0.0	0.0	0.0	0.0	0.0	0.0	0.0
4	0.0	0.0	0.0	0.0	0.0	0.0	0.0
5	0.0	0.0	0.0	0.0	0.0	0.0	0.0
6	0.0	0.0	0.0	0.0	0.0	0.0	0.0
7	0.0	0.0	0.0	0.0	0.0	0.0	0.0
8	0.0	0.0	0.0	0.0	0.0	0.0	0.0
9	0.0	0.0	0.0	0.0	0.0	0.0	0.0
10	0.0	0.0	4.54	5.68	6.23	0.0	0.0
11	0.0	0.0	0.0	0.0	0.0	0.0	0.0
12	0.0	0.0	0.0	0.0	0.0	0.0	0.0
13	0.0	0.0	0.0	0.0	0.0	0.0	0.0
14	0.0	0.0	0.0	0.0	0.0	0.0	0.0

FROM/TO	8	9	10	11	12	13	14
1	0.0	0.0	0.0	0.0	5.09	0.0	0.0
2	0.0	0.0	0.0	0.0	4.81	0.0	0.0
3	0.0	0.0	0.0	0.0	0.0	0.0	0.0
4	0.0	0.0	0.0	0.0	0.0	0.0	0.0
5	0.0	0.0	0.0	0.0	0.0	0.0	0.0
6	0.0	0.0	0.0	5.94	0.0	0.0	0.0
7	13.58	0.0	0.0	0.0	0.0	0.0	0.0
8	0.0	21.14	0.0	0.0	0.0	0.0	0.0
9	20.84	0.0	16.45	0.0	0.0	0.0	0.0
10	0.0	0.0	0.0	0.0	0.0	0.0	0.0
11	0.0	0.0	0.0	0.0	0.0	5.94	0.0
12	0.0	0.0	0.0	0.0	0.0	9.91	0.0
13	0.0	15.85	0.0	0.0	0.0	0.0	0.0
14	0.0	1.98	0.0	0.0	0.0	0.0	0.0

MAXIMUM FLOW = 45.85 AIRCRAFT PER HOUR.

One additional point to notice is that, since the one-step transition matrix was calculated from empirical data in which the total number of entries into a sector did not always equal the total number of exits, some 'leakage' or misdirection of flow can occur. For example, the ratio of aircraft entering sector 497 (GN) on arrival patterns to those entering on departure patterns is 0.91, while the corresponding ratio upon leaving the sector is 1.01. Thus in the calculation of system flow, a small amount of flow which enters that sector through a departure transition will leave through an arrival transition. The effect of this misdirection on the calculations for the LaGuardia system is to increase the maximum flow by about 1.5 per cent above what it actually should be. To eliminate this type of leakage, the transition proportions could be adjusted such that the ratio of arrivals to departures is the same for both entry and exit of a given sector.

While the use of the one-step transition matrix does not assign full arrival and departure patterns, it does provide an assignment of maximum flow which preserves the general patterns observed in the data sample. The selection of free-flow or constrained-flow conditions depends upon the nature of the network being modeled and the questions to be answered.

In conclusion, consideration of the ATC system as a network of sectors provides the formulation necessary to consider a group of sectors simultaneously. The concepts of sector transit time and transitions between sectors make consideration of multiple-sector flow possible. Under certain assumptions regarding sector capacity, the maximum feasible flow over the system and the likely bottlenecks can be determined. Other techniques of network analysis could also be applied to determine the minimum path between given sectors in terms of expected time in the system, or to allocate routes so as to minimize system congestion.

It must be recognized, however, that the traffic intensity which a given sector can handle is really flow-dependent. While a specific pattern of arrivals might yield an acceptable long-term average loading on the system, the short-term effects might be entirely unacceptable. It is thus essential to consider the dynamic relationship between communications and flow and to specify sector capacity in another manner. The framework of the system as a network provides a means for handling the problem in a compact form and for using the results to determine total system flow.

5.4 The Sequential Structure of Intercommunication Gap Lengths

In all previous studies of the simulation of intercommunication gap lengths, the assumption was made that the sequential ordering of the gaps did not affect the time length of the gaps. But up to this date no evidence to either support or reject this hypothesis has been discussed. In this study, statistics are presented, extracted from the observed data of gap lengths, that help resolve this question.

Considerable data analysis was required, and a test of the hypothesis that the length of the first gap was equal to that of the remaining gaps was constructed taking advantage of rank order statistics. A summary of the probability level of the overall test for each sector and sector function is given in Table 5.7. A fairly general statement can be made. For the LT, LE and HI sectors the first gap lengths are shorter, while for the LC and AR sectors they are longer than the remaining gaps. Other sector functions seem to have equal length for all gaps. Tables of various statistics essential for comparing gap length at different locations are available for each sector and sector function on computer print-outs. Summary tables for the twelve sector functions are displayed in Tables 5.8 ∿ 5.19. The structure and interpretation of these sector function tables can be described as follows:

(i) The top line of each sector function table indicates the number of gaps. Summary statistics for aircraft which have made the same number of gaps are listed beneath. These statistics form a triangular table.

(ii) The first column contains the number of aircraft (upper entry) associated with a specific number of gaps and the average of the total gap lengths per aircraft (lower entry).

(iii) The top entry in the second column is the relative rank statistic $r_k/[(k + 1)/2]$ (for the construction of this statistic see the next section) for the first gap length. The second entry gives the probability of the observed relative rank under the hypothesis that the first gap length is not different from the remaining gap lengths. Unusually low or unusually high probabilities force the rejection of the hypothesis.

(iv) The upper entry of the elements in the triangular portion of the table is the ratio of the gap length of the specific order to the average gap length averaged over the appropriate aircraft. Under the hypothesis, all these upper entries would equal 1.0000. The lower entry of the pair is the standard deviation of the ratio in question divided by the number of gaps per aircraft. This lower entry is used to indicate the variation of the ratios over appropriate aircraft.

Table 5.7 Results of the Rank Test

Sector ID	Probability Level	Average Ratio	Sector ID	Probability Level	Average Ratio
451 LT	0.0048	0.7199	488 GN	0.4500	0.9817
453 LT	0.2143	0.8396	489 GN	0.9514	1.1795
454 LT	0.1696	0.9821	490 GN	0.9759	1.1031
455 LT	0.5343	0.9987	492 GN	0.6386	0.9913
456 LT	0.0202	0.6267	494 GN	0.2919	0.8932
457 LT	0.5000	1.2696	495 GN	0.3339	0.9600
458 LT	0.0006	0.6573	496 GN	0.1284	0.9317
459 LT	0.0	0.5738	497 GN	0.0954	0.8879
460 LT	0.0223	0.8242	498 GN	0.9584	1.6018
461 LT	0.3420	0.9117	501 GN	0.6841	1.0080
462 LT	0.0254	0.7374	502 GN	0.5610	1.1066
463 LT	0.0274	0.7887	503 GN	0.5000	1.0000
			504 GN	0.8286	0.9782
LT	0.0	0.8201			
			GN	0.5655	0.9889
464 LE	0.1363	0.8209			
465 LE	0.3274	0.9694	506 LC	0.0478	0.7715
466 LE	0.0013	0.5742	507 LC	0.9854	1.2028
467 LE	0.0277	0.7382	508 LC	0.9964	1.1372
468 LE	0.1578	0.8865	509 LC	0.8358	1.1364
469 LE	0.0226	0.6626	510 LC	0.9860	1.3363
470 LE	0.0245	0.8207	511 LC	0.6193	0.9930
471 LE	0.3268	0.9099	512 LC	1.0000	1.5648
472 LE	0.1006	0.8845	513 LC	0.6408	0.9491
473 LE	0.0497	0.8759	514 LC	0.9596	1.0858
474 LE	0.7035	1.0062	515 LC	0.9973	1.2337
			516 LC	0.8363	1.1420
LE	0.0000	0.8277	517 LC	0.4000	1.0766
			519 LC	0.9887	1.3230
475 HI	0.1516	0.8473	520 LC	0.9768	1.0297
476 HI	0.0016	0.6055	521 LC	0.8210	1.1128
477 HI	0.3782	0.9246	522 LC	1.0000	1.4017
478 HI	0.0030	0.5969			
479 HI	0.1986	0.8603	LC	1.0000	1.2074
480 HI	0.0001	0.6866			
481 HI	0.9916	1.1557	524 LG	0.1171	0.8321
482 HI	0.4611	1.2868	525 LG	0.0	0.8010
483 HI	0.7929	0.9064	526 LG	0.6473	0.9938
			527 LG	0.9652	0.2842
HI	0.0001	0.8505	528 LG	0.3500	0.9243
			LG	0.8448	1.0246
484 CD	0.9676	1.1861			
485 CD	0.0174	0.8935	529 AP	0.6810	1.0391
486 CD	0.7929	0.9522	530 AP	0.1300	0.8690
487 CD	0.0899	0.8539	531 AP	0.4500	1.1753
			532 AP	0.9000	1.3593
CD	0.5549	0.9926			
			AP	0.7437	1.0854

Table 5.7 Results of the Rank Test (continued)

Sector ID	Probability Level	Average Ratio
533 DP	0.5613	1.0381
534 DP	0.9998	1.2352
535 DP	0.4616	0.9975
536 DP	0.0005	0.6829
537 DP	0.9668	1.1193
538 DP	0.1284	0.9029
DP	0.7431	0.9864
539 AD	0.6500	1.0232
540 AD	0.6726	0.9613
541 AD	0.6300	1.1012
542 AD	0.7929	1.2204
543 AD	0.3946	0.8734
544 AD	0.7301	0.9833
AD	0.6912	1.0113
545 AR	0.2071	0.9135
546 AR	0.8807	1.2687
547 AR	0.6641	1.0514
548 AR	0.4438	0.9409
549 AR	0.8145	1.8754
550 AR	0.7617	1.6145
551 AR	0.9983	1.2009
552 AR	0.5699	1.0401
553 AR	0.7110	1.1723
554 AR	0.9975	1.2715
555 AR	0.5470	1.0643
556 AR	0.7214	0.8795
AR	0.9972	1.2143
557 RA	0.5820	1.0485
558 RA	0.0013	0.7507
559 RA	0.0786	0.9521
RA	0.2422	0.9195

Table 5.8 Intercommunication Gap Length Statistics for Sector Function CT

STATISTICS OF INTER-COMMUNICATION GAPS BY # OF GAPS AND LOCATION OF GAP.
RUN : LT

N GAPS	RANK PROB	1	2	3	4	5	6	7	8	9	10	11	12	13	14	15
59	1.00	1.0000														
219.8	0.0	0.0033														
84	0.91	0.7619	1.2381													
274.1	0.0082	0.2690	0.2690													
96	0.91	0.8692	0.9888	1.1419												
303.6	0.0122	0.2297	0.2184	0.2309												
82	0.85	0.8156	1.0966	1.0430	1.0448											
361.0	0.0015	0.1834	0.1868	0.1916	0.1855											
54	0.81	0.7299	1.1625	0.9931	1.0301	1.0844										
380.0	0.0019	0.1255	0.1477	0.1279	0.1389	0.1634										
42	0.91	1.0365	1.1251	1.0705	0.9243	0.7915	1.0521									
458.0	0.1201	0.1869	0.1243	0.1181	0.1599	0.0928	0.1136									
32	0.80	0.6986	1.1176	1.1502	0.9141	1.1201	0.8847	1.1146								
554.8	0.0136	0.0831	0.1517	0.1180	0.1277	0.0949	0.0873	0.1229								
21	0.79	0.6996	1.3440	1.2166	1.4606	0.9353	0.8211	0.6285	0.8943							
576.1	0.0316	0.0807	0.1353	0.0957	0.1387	0.1192	0.0536	0.0465	0.0752							
13	0.89	0.6977	0.8395	0.8557	1.4197	2.0160	0.7583	1.0083	0.7735	0.6312						
1266.2	0.2260	0.0584	0.0781	0.0745	0.1659	0.1911	0.0558	0.1208	0.0704	0.0695						
8	0.84	0.8524	0.9377	1.2699	0.8616	0.9762	1.6040	1.4916	0.9203	0.6130	0.4733					
1012.1	0.1944	0.0904	0.0466	0.0484	0.0634	0.0599	0.1113	0.1464	0.0461	0.0431	0.0293					
2	0.50	0.4238	0.4158	0.8489	0.9572	1.0611	1.8704	0.7790	1.4943	1.3597	0.5289	1.2610				
891.5	0.0899	0.0249	0.0266	0.0312	0.0298	0.0232	0.0126	0.0447	0.0070	0.0081	0.0389	0.0543				
8	0.54	0.5135	1.0563	1.4829	0.7521	1.5142	0.6932	1.1484	1.2218	1.2007	0.9403	0.7800	0.6966			
985.3	0.0070	0.0221	0.0568	0.0558	0.0428	0.0651	0.0269	0.0503	0.0901	0.0593	0.0378	0.0367	0.0381			
7	0.78	0.6056	0.9082	1.3579	1.1291	0.9331	1.0461	1.1200	1.3865	1.2708	0.8620	0.8930	0.7082	0.7794		
1113.4	0.1332	0.0462	0.0669	0.0553	0.1251	0.0448	0.0604	0.0367	0.0481	0.0336	0.0466	0.0424	0.0169	0.0490		
4	0.37	0.2472	0.6968	0.5446	0.6193	1.1182	0.6052	0.2959	0.5795	1.8950	3.4177	0.9603	1.2087	0.8781	0.9336	
1465.3	0.0092	0.0188	0.0384	0.0215	0.0305	0.0501	0.0302	0.0107	0.0254	0.0821	0.2445	0.0381	0.0453	0.0332	0.0245	
3	1.21	1.0005	1.4408	0.3779	0.6053	0.7655	0.7477	1.8201	0.8353	1.1807	2.2855	0.9718	1.1907	0.6131	0.6536	0.5114
1093.7	0.7480	0.0305	0.0239	0.0218	0.0131	0.0335	0.0194	0.0185	0.0172	0.0531	0.1152	0.0407	0.0704	0.0268	0.0277	0.0262
TOTALS		515	456	372	276	194	140	98	66	45	32	24	22	14	7	3
		0.8201	1.1053	1.0853	1.0345	1.0765	0.9550	1.0116	0.9620	1.0100	1.2165	0.9071	0.8608	0.7720	0.8136	0.5114

LEVEL OF OVERALL TEST IS 0.0

Table 5.9 Intercommunication Gap Length Statistics for Sector Function LE

STATISTICS OF INTER-COMMUNICATION GAPS BY # OF GAPS AND LOCATION OF GAP.
RUN : LE

N GAPS	RANK PROB	1	2	3	4	5	6	7	8	9	10	11	12	13	14	15
90	1.00	1.0000														
424.5	0.0	0.0035														
101	0.90	0.7612	1.2388													
537.6	0.0010	0.2976	0.2976													
82	0.90	0.8138	1.0451	1.1411												
508.5	0.0107	0.2437	0.2560	0.2665												
74	0.90	0.7787	1.0739	1.0975	1.0499											
563.8	0.0241	0.1697	0.2039	0.1825	0.1891											
53	0.86	0.8109	1.2285	0.8792	1.1316	0.9497										
556.8	0.0127	0.1450	0.1971	0.1420	0.1679	0.1459										
34	0.98	0.9540	0.9808	1.1200	1.1283	0.6978	1.1192									
574.0	0.4204	0.1304	0.1440	0.1741	0.1575	0.0946	0.1311									
21	0.79	0.7052	1.5063	1.1686	0.8439	0.9791	0.8950	0.9018								
744.5	0.0248	0.0998	0.1864	0.1520	0.0831	0.1205	0.0833	0.1499								
23	0.87	0.7794	1.3240	1.4600	1.0211	0.7821	0.8129	0.8925	0.9281							
860.0	0.1096	0.0919	0.1427	0.1403	0.0764	0.0653	0.0968	0.1060	0.0863							
7	0.86	0.9909	0.8600	1.6535	0.8670	0.8422	0.8795	1.0827	0.9732	0.8509						
1029.1	0.2321	0.1457	0.1069	0.1246	0.0561	0.1050	0.1035	0.1013	0.1789	0.0558						
7	0.62	0.5131	1.4986	0.8323	0.6790	1.0489	0.9951	1.2464	0.9535	0.6480	1.5852					
694.1	0.0282	0.0610	0.1239	0.0412	0.0851	0.0808	0.0880	0.0837	0.0665	0.0476	0.1153					
2	0.75	0.6299	0.7311	0.8215	0.1978	2.5883	1.2059	1.3837	1.5428	0.8811	0.5677	0.4502				
727.0	0.2512	0.0258	0.0617	0.0022	0.0101	0.0387	0.0022	0.0049	0.0221	0.0569	0.0107	0.0299				
1	0.62	0.1997	4.1573	1.2526	0.4539	0.0908	0.8714	0.5446	2.5416	0.1815	0.5991	0.9440	0.1634			
661.0	0.2345	0.0	0.0	0.0	0.0	0.0	0.0	0.0	0.0	0.0	0.0	0.0	0.0			
0	0.0	0.0	0.0	0.0	0.0	0.0	0.0	0.0	0.0	0.0	0.0	0.0	0.0	0.0		
0.0	0.0	0.0	0.0	0.0	0.0	0.0	0.0	0.0	0.0	0.0	0.0	0.0	0.0	0.0		
2	0.60	0.3544	0.1787	0.6854	0.1569	0.1831	3.7092	0.6407	0.0971	0.6720	0.5858	0.5114	0.9867	1.1510	4.0874	
1319.5	0.1463	0.0194	0.0115	0.0464	0.0023	0.0061	0.2598	0.0194	0.0044	0.0388	0.0041	0.0069	0.0317	0.0736	0.1244	
1	0.38	0.1433	0.1911	0.0358	0.9793	3.3320	0.9554	0.8002	1.1584	1.0271	3.2723	1.2420	0.1433	0.6330	0.7882	0.2986
1256.0	0.1236	0.0	0.0	0.0	0.0	0.0	0.0	0.0	0.0	0.0	0.0	0.0	0.0	0.0	0.0	0.0
TOTALS		498	408	307	225	151	98	64	43	20	13	6	4	3	3	1
		0.8277	1.1605	1.1051	1.0231	0.8928	1.0237	0.9557	0.9724	0.7404	1.3288	0.6849	0.5700	0.9783	2.9877	0.2986

LEVEL OF OVERALL TEST IS 0.0000

Table 5.10 Intercommunication Gap Length Statistics for Sector Function HI

STATISTICS OF INTER-COMMUNICATION GAPS BY # OF GAPS AND LOCATION OF GAP.
RUN : HI

N GAPS	RANK PROB	1	2	3	4	5	6	7	8	9	10	11	12	13	14	15
42	1.00	1.0000														
339.3	0.0	0.0031														
74	0.95	0.8078	1.1922													
428.2	0.1225	0.2764	0.2764													
77	0.97	0.8505	0.9815	1.1679												
437.6	0.2426	0.2074	0.2104	0.2187												
64	0.88	0.7892	0.8587	1.1223	1.2298											
466.2	0.0168	0.1992	0.1814	0.2117	0.2094											
47	0.84	0.7230	1.1166	0.8616	1.0649	1.2339										
593.3	0.0088	0.1474	0.1665	0.1282	0.1438	0.1990										
26	0.82	0.7397	1.0410	1.2095	0.9460	0.8962	1.1675									
641.3	0.0331	0.1077	0.1369	0.1380	0.0771	0.1320	0.1016									
20	0.88	1.0997	1.1674	0.9874	0.9123	0.9038	0.7614	1.1679								
685.3	0.1318	0.1967	0.1747	0.1154	0.0812	0.0907	0.0652	0.1219								
16	0.90	0.8150	1.1239	1.1643	1.4149	0.9137	0.8236	0.5449	1.1997							
773.8	0.2225	0.0849	0.1404	0.1138	0.1466	0.0863	0.0591	0.0463	0.1313							
6	0.87	0.8984	1.2782	1.1403	1.4436	0.9318	0.9304	0.6624	0.7957	0.9192						
910.2	0.2635	0.0960	0.0806	0.0992	0.1413	0.0987	0.0910	0.0268	0.0463	0.0482						
3	0.55	0.4688	1.4231	1.1710	1.8430	0.6316	0.4355	0.4790	0.9097	0.7668	1.8715					
1016.3	0.0658	0.0271	0.1089	0.0485	0.0420	0.0455	0.0112	0.0337	0.0260	0.0490	0.0939					
3	1.11	2.1446	0.8433	0.6343	0.8362	0.9948	0.6463	1.0660	2.0855	0.6331	0.6706	0.4453				
774.3	0.6425	0.2016	0.0623	0.0584	0.0453	0.0860	0.0311	0.0452	0.1525	0.0413	0.0396	0.0184				
1	0.31	0.0979	0.6405	0.2758	0.3469	0.0623	2.7576	0.5515	1.8503	2.7042	0.6850	1.7880	0.2402			
1349.0	0.0962	0.0	0.0	0.0	0.0	0.0	0.0	0.0	0.0	0.0	0.0	0.0	0.0			
1	1.86	4.7915	0.4914	1.0059	0.8677	0.7602	1.2516	0.5759	0.2304	1.1441	0.8216	0.3993	0.3379	0.3225		
1693.0	0.9456	0.0	0.0	0.0	0.0	0.0	0.0	0.0	0.0	0.0	0.0	0.0	0.0	0.0		
0	0.0	0.0	0.0	0.0	0.0	0.0	0.0	0.0	0.0	0.0	0.0	0.0	0.0	0.0	0.0	
0.0	0.0	0.0	0.0	0.0	0.0	0.0	0.0	0.0	0.0	0.0	0.0	0.0	0.0	0.0	0.0	
4	1.13	0.6198	0.7884	0.8184	0.5676	0.6437	0.5255	1.1189	0.6789	0.4433	1.7743	1.1513	0.5319	1.6386	0.5664	1.2642
1585.8	0.6783	0.0213	0.0266	0.0444	0.0250	0.0552	0.0219	0.0500	0.0153	0.0092	0.1544	0.0944	0.0256	0.0816	0.0212	0.1190
TOTALS		384	342	268	191	127	80	54	34	18	12	9	6	5	4	4
		0.8505	1.0479	1.0779	1.1226	1.0067	0.9212	0.8572	1.1103	0.8520	1.3525	0.9032	0.4509	1.3753	0.5664	1.2642

LEVEL OF OVERALL TEST IS 0.0001

Table5.11 Intercommunication Gap Length Statistics for Sector Function CD

STATISTICS OF INTER-COMMUNICATION GAPS BY # OF GAPS AND LOCATION OF GAP.

RUN : CD

N GAPS	RANK PROB	1	2	3	4	5	6	7	8	9	10	11	12	13	14	15
80	1.00	1.0000														
382.4	0.0	0.0035														
33	0.99	0.9164	1.0836													
553.7	0.4309	0.3566	0.3566													
11	1.05	1.1535	1.4770	0.3695												
470.1	0.6440	0.3350	0.3195	0.0773												
4	0.80	0.7012	1.6291	1.3333	0.3364											
747.0	0.1855	0.2158	0.2212	0.3264	0.0951											
3	1.33	1.4326	1.0064	1.6874	0.4305	0.4431										
859.7	0.8897	0.0993	0.1226	0.2252	0.0638	0.1085										
0	0.0	0.0	0.0	0.0	0.0	0.0	0.0									
0.0	0.0	0.0	0.0	0.0	0.0	0.0	0.0									
0	0.0	0.0	0.0	0.0	0.0	0.0	0.0	0.0								
0.0	0.0	0.0	0.0	0.0	0.0	0.0	0.0	0.0								
0	0.0	0.0	0.0	0.0	0.0	0.0	0.0	0.0	0.0							
0.0	0.0	0.0	0.0	0.0	0.0	0.0	0.0	0.0	0.0							
0	0.0	0.0	0.0	0.0	0.0	0.0	0.0	0.0	0.0	0.0						
0.0	0.0	0.0	0.0	0.0	0.0	0.0	0.0	0.0	0.0	0.0						
0	0.0	0.0	0.0	0.0	0.0	0.0	0.0	0.0	0.0	0.0	0.0					
0.0	0.0	0.0	0.0	0.0	0.0	0.0	0.0	0.0	0.0	0.0	0.0					
0	0.0	0.0	0.0	0.0	0.0	0.0	0.0	0.0	0.0	0.0	0.0	0.0				
0.0	0.0	0.0	0.0	0.0	0.0	0.0	0.0	0.0	0.0	0.0	0.0	0.0				
0	0.0	0.0	0.0	0.0	0.0	0.0	0.0	0.0	0.0	0.0	0.0	0.0	0.0			
0.0	0.0	0.0	0.0	0.0	0.0	0.0	0.0	0.0	0.0	0.0	0.0	0.0	0.0			
0	0.0	0.0	0.0	0.0	0.0	0.0	0.0	0.0	0.0	0.0	0.0	0.0	0.0	0.0		
0.0	0.0	0.0	0.0	0.0	0.0	0.0	0.0	0.0	0.0	0.0	0.0	0.0	0.0	0.0		
0	0.0	0.0	0.0	0.0	0.0	0.0	0.0	0.0	0.0	0.0	0.0	0.0	0.0	0.0	0.0	
0.0	0.0	0.0	0.0	0.0	0.0	0.0	0.0	0.0	0.0	0.0	0.0	0.0	0.0	0.0	0.0	
0	0.0	0.0	0.0	0.0	0.0	0.0	0.0	0.0	0.0	0.0	0.0	0.0	0.0	0.0	0.0	0.0
0.0	0.0	0.0	0.0	0.0	0.0	0.0	0.0	0.0	0.0	0.0	0.0	0.0	0.0	0.0	0.0	0.0
TOTALS		131	51	18	7	3	0	0	0	0	0	0	0	0	0	0
		0.9926	1.2067	0.8033	0.3767	0.4431	0.0	0.0	0.0	0.0	0.0	0.0	0.0	0.0	0.0	0.0

LEVEL OF OVERALL TEST IS 0.5549

Table 5.12 Intercommunication Gap Length Statistics for Sector Function GN

STATISTICS OF INTER-COMMUNICATION GAPS BY # OF GAPS AND LOCATION OF GAP.
RUN : GN

N GAPS	RANK PROB	1	2	3	4	5	6	7	8	9	10	11	12	13	14	15
219	1.00	1.0000														
135.2	0.0	0.0036														
120	1.03	1.0287	0.9713													
264.7	0.8633	0.2887	0.2887													
66	0.99	0.9961	0.9871	1.0168												
397.8	0.4401	0.2418	0.2569	0.2222												
45	1.00	0.9250	0.8179	1.0885	1.1686											
571.9	0.5266	0.1891	0.1944	0.2078	0.2489											
16	1.08	1.2153	0.9777	0.6810	1.5075	0.6185										
1060.1	0.7603	0.2610	0.2474	0.1468	0.2687	0.1167										
14	1.00	0.9039	0.9265	0.8596	1.1294	1.1798	1.0008									
839.8	0.5000	0.1537	0.1592	0.1600	0.1758	0.1141	0.1564									
10	1.07	0.7566	0.5066	0.9245	1.6071	1.4753	0.8821	0.8478								
763.5	0.6824	0.1005	0.0602	0.1729	0.1827	0.1901	0.1066	0.0929								
2	0.44	0.1812	0.8028	1.6472	3.5683	1.0715	0.0267	0.2293	0.4730							
1914.0	0.0614	0.0206	0.0130	0.0131	0.1427	0.0822	0.0012	0.0202	0.0351							
7	0.66	0.6570	1.7660	0.7077	0.7719	0.4830	0.7688	2.0738	0.9052	0.8667						
751.3	0.0395	0.0718	0.1324	0.0421	0.0709	0.0457	0.0576	0.2337	0.0877	0.0940						
3	0.97	0.8392	0.6278	1.2574	0.6609	1.0721	0.3246	2.2430	2.1538	0.0974	0.7237					
1425.0	0.4600	0.0569	0.0291	0.0820	0.0418	0.1178	0.0242	0.0884	0.1825	0.0024	0.0738					
0	0.0	0.0	0.0	0.0	0.0	0.0	0.0	0.0	0.0	0.0	0.0	0.0				
0.0	0.0	0.0	0.0	0.0	0.0	0.0	0.0	0.0	0.0	0.0	0.0	0.0				
1	0.15	0.1060	1.3981	0.1359	0.5827	0.1843	3.0058	0.3800	0.9167	0.1750	0.8752	3.3835	0.8568			
5210.0	0.0556	0.0	0.0	0.0	0.0	0.0	0.0	0.0	0.0	0.0	0.0	0.0	0.0			
0	0.0	0.0	0.0	0.0	0.0	0.0	0.0	0.0	0.0	0.0	0.0	0.0	0.0	0.0		
0.0	0.0	0.0	0.0	0.0	0.0	0.0	0.0	0.0	0.0	0.0	0.0	0.0	0.0	0.0		
1	1.33	1.3990	0.5635	0.1846	3.0118	0.2720	0.1263	2.1957	1.7294	0.4178	0.8550	1.4476	0.5441	0.5732	0.6801	
1441.0	0.7324	0.0	0.0	0.0	0.0	0.0	0.0	0.0	0.0	0.0	0.0	0.0	0.0	0.0	0.0	
0	0.0	0.0	0.0	0.0	0.0	0.0	0.0	0.0	0.0	0.0	0.0	0.0	0.0	0.0	0.0	0.0
0.0	0.0	0.0	0.0	0.0	0.0	0.0	0.0	0.0	0.0	0.0	0.0	0.0	0.0	0.0	0.0	0.0
TOTALS		504	285	165	99	54	38	24	14	12	5	2	2	1	1	0
		0.9889	0.9473	0.9734	1.2799	0.9326	0.8519	1.3649	1.1707	0.5793	0.7803	2.4155	0.7004	0.5732	0.6801	0.0

LEVEL OF OVERALL TEST IS 0.5655

Table 5.13 Intercommunication Gap Length Statistics for Sector Function LC

STATISTICS OF INTER-COMMUNICATION GAPS BY # OF GAPS AND LOCATION OF GAP.
RUN : LC

N GAPS	RANK PROB	1	2	3	4	5	6	7	8	9	10	11	12	13	14	15
125	1.00	1.0000														
99.3	0.0	0.0036														
296	1.07	1.0362	0.9637													
176.8	0.9996	0.2134	0.2134													
240	1.13	1.2218	0.8421	0.9361												
279.0	1.0000	0.2347	0.1884	0.1846												
135	1.22	1.5294	0.8216	0.9062	0.7426											
360.1	1.0000	0.2383	0.1819	0.1431	0.1397											
70	1.16	1.4470	0.9853	0.9975	0.7722	0.7980										
432.1	0.9974	0.2332	0.1990	0.1534	0.1374	0.1127										
35	1.14	1.5003	1.1696	0.8665	0.8025	0.7524	0.9087									
601.1	0.9584	0.2248	0.1963	0.1351	0.0896	0.0967	0.1603									
9	1.03	1.1017	1.4880	1.2645	0.9501	0.5808	0.8742	0.7407								
588.9	0.5662	0.1379	0.2080	0.2530	0.1237	0.0611	0.1094	0.0619								
8	0.92	0.7218	1.6582	1.0913	1.0078	0.7971	1.1088	0.9383	0.6767							
722.6	0.3217	0.0893	0.1787	0.1079	0.0611	0.0724	0.2092	0.0787	0.0813							
11	1.42	1.9721	1.5229	0.8695	1.0015	1.0269	0.5368	0.5383	0.8227	0.7093						
837.4	0.9964	0.1606	0.0816	0.0571	0.1412	0.1238	0.0488	0.0640	0.0833	0.0344						
5	0.80	0.6519	0.6255	0.9292	0.6349	1.1278	0.9652	1.6693	1.0741	1.2609	1.0612					
988.2	0.1959	0.0260	0.0467	0.0695	0.0600	0.0388	0.0592	0.0854	0.0624	0.0908	0.0482					
4	1.63	1.8523	2.1095	1.1750	0.4719	1.2575	0.8610	1.2626	0.5417	0.4671	0.3317	0.6697				
1238.5	0.9911	0.0428	0.1427	0.0898	0.0222	0.0612	0.0551	0.0623	0.0173	0.0611	0.0139	0.0284				
4	1.35	2.4223	0.8610	0.5068	1.1900	0.7425	1.0033	0.6606	0.7502	1.1140	0.7375	1.2537	0.7581			
964.8	0.9038	0.1695	0.0581	0.0306	0.0526	0.0591	0.0426	0.0794	0.0369	0.0603	0.0428	0.0598	0.0284			
2	1.57	2.1764	2.2281	0.3424	0.4275	0.3659	1.4013	0.8092	1.5014	0.3752	2.3394	0.4060	0.4359	0.1912		
1749.5	0.9347	0.0754	0.1663	0.0256	0.0113	0.0243	0.0831	0.0326	0.0908	0.0133	0.1007	0.0182	0.0262	0.0069		
1	1.20	1.3792	0.0945	0.5951	1.5209	0.1795	0.6329	0.8596	1.6343	0.4818	1.4642	0.6613	1.5870	1.9933	0.9163	
1482.0	0.6451	0.0	0.0	0.0	0.0	0.0	0.0	0.0	0.0	0.0	0.0	0.0	0.0	0.0	0.0	
19	0.99	0.8049	0.6549	0.6750	0.7284	0.6279	0.7199	0.8091	0.9516	0.7215	0.7650	0.7208	0.8030	0.7199	0.7151	0.5500
2344.2	0.4577	0.0555	0.0425	0.0398	0.0333	0.0427	0.0329	0.0507	0.0403	0.0337	0.0325	0.0292	0.0391	0.0371	0.0415	0.0229
TOTALS		964	839	543	303	168	98	63	54	46	35	30	26	22	20	19
		1.2074	0.9339	0.9250	0.7791	0.7832	0.8555	0.8569	0.8837	0.7689	0.8646	0.7621	0.7980	0.7297	0.7252	0.5500

LEVEL OF OVERALL TEST IS 1.0000

Table 5.14 Intercommunication Gap Length Statistics for Sector Function LG

STATISTICS OF INTER-COMMUNICATION GAPS BY # OF GAPS AND LOCATION OF GAP.
RUN : LG

N GAPS	RANK PROB	1	2	3	4	5	6	7	8	9	10	11	12	13	14	15
26	1.00	1.0000														
165.3	0.0	0.0023														
27	1.04	1.0724	0.9276													
212.6	0.7181	0.2563	0.2563													
25	1.06	1.1406	0.9131	0.9464												
316.4	0.7688	0.2492	0.2391	0.2121												
13	0.98	1.0102	0.7968	1.2414	0.9516											
360.3	0.4506	0.1876	0.1681	0.2151	0.1310											
16	0.90	0.7462	1.6011	1.0733	0.6302	0.9493										
578.8	0.1884	0.1376	0.2166	0.1613	0.1069	0.1117										
5	1.43	1.8931	0.7891	0.7077	1.6164	0.3896	0.6041									
871.0	0.9752	0.2224	0.0796	0.1714	0.3141	0.0613	0.0911									
2	0.50	0.3329	0.6726	2.2251	1.8948	0.6957	0.3320	0.8469								
1003.5	0.0786	0.0145	0.0465	0.1892	0.2587	0.0323	0.0070	0.0307								
4	0.94	0.9106	1.0599	0.6875	0.9478	1.1102	1.2843	0.9938	1.0059							
769.3	0.4136	0.0653	0.0719	0.0771	0.0597	0.0571	0.1457	0.0915	0.0610							
2	0.90	1.1901	0.5781	0.2211	3.1251	0.6173	1.2797	0.3468	0.2653	1.3765						
995.0	0.3921	0.1221	0.0393	0.0158	0.0518	0.0661	0.1322	0.0086	0.0017	0.0865						
1	1.64	1.6139	0.6023	0.2471	1.8301	0.8031	0.5019	1.1892	1.3050	1.4981	0.4093					
1295.0	0.8885	0.0	0.0	0.0	0.0	0.0	0.0	0.0	0.0	0.0	0.0					
0	0.0	0.0	0.0	0.0	0.0	0.0	0.0	0.0	0.0	0.0	0.0	0.0				
0.0	0.0	0.0	0.0	0.0	0.0	0.0	0.0	0.0	0.0	0.0	0.0	0.0				
1	0.15	0.1407	0.3719	0.4724	0.2613	0.9849	0.9548	3.8291	0.9447	0.2513	1.7688	0.7035	1.3166			
1194.0	0.0556	0.0	0.0	0.0	0.0	0.0	0.0	0.0	0.0	0.0	0.0	0.0	0.0			
1	1.71	1.3451	0.3269	0.3737	1.1988	1.0120	1.1116	0.0218	1.2922	0.5760	4.9260	0.3550	0.1059	0.3550		
4175.0	0.9093	0.0	0.0	0.0	0.0	0.0	0.0	0.0	0.0	0.0	0.0	0.0	0.0	0.0		
0	0.0	0.0	0.0	0.0	0.0	0.0	0.0	0.0	0.0	0.0	0.0	0.0	0.0	0.0	0.0	
0.0	0.0	0.0	0.0	0.0	0.0	0.0	0.0	0.0	0.0	0.0	0.0	0.0	0.0	0.0	0.0	
2	0.38	0.1387	0.1584	0.8932	0.8194	1.3646	0.6455	0.5845	0.0700	0.3589	0.2714	0.8365	0.4853	0.9588	2.1193	1.3587
2856.0	0.0509	0.0078	0.0065	0.0514	0.0318	0.0156	0.0334	0.0163	0.0003	0.0065	0.0050	0.0313	0.0276	0.0220	0.1308	0.0076
TOTALS		125	99	72	47	34	18	13	11	7	5	4	4	3	2	2
		1.0246	0.9712	0.9865	1.0488	0.8745	0.8467	0.9671	0.7487	0.8280	1.5294	0.6829	0.5983	0.7575	2.1193	1.3587

LEVEL OF OVERALL TEST IS 0.8448

Table 5.15 Intercommunication Gap Length Statistics for Sector Function AP

STATISTICS OF INTER-COMMUNICATION GAPS BY # OF GAPS AND LOCATION OF GAP.
RUN : AP

N GAPS	RANK PROB	1	2	3	4	5	6	7	8	9	10	11	12	13	14	15
15	1.00	1.0000														
139.4	0.0	0.0009														
8	1.00	1.0547	0.9453													
237.9	0.5000	0.2569	0.2569													
7	1.14	1.1735	0.7865	1.0400												
377.6	0.8227	0.2011	0.1208	0.2167												
2	1.20	1.1155	0.9662	1.2042	0.7141											
176.0	0.7365	0.0141	0.1625	0.2404	0.0639											
0	0.0	0.0	0.0	0.0	0.0	0.0										
0.0	0.0	0.0	0.0	0.0	0.0	0.0										
1	0.86	0.4651	2.2326	1.5814	0.1860	1.3953	0.1395									
129.0	0.3848	0.0	0.0	0.0	0.0	0.0	0.0									
1	1.75	2.5564	0.0515	0.0858	0.1716	1.6642	1.8015	0.6691								
408.0	0.9332	0.0	0.0	0.0	0.0	0.0	0.0	0.0								
0	0.0	0.0	0.0	0.0	0.0	0.0	0.0	0.0	0.0							
0.0	0.0	0.0	0.0	0.0	0.0	0.0	0.0	0.0	0.0							
0	0.0	0.0	0.0	0.0	0.0	0.0	0.0	0.0	0.0	0.0						
0.0	0.0	0.0	0.0	0.0	0.0	0.0	0.0	0.0	0.0	0.0						
0	0.0	0.0	0.0	0.0	0.0	0.0	0.0	0.0	0.0	0.0	0.0					
0.0	0.0	0.0	0.0	0.0	0.0	0.0	0.0	0.0	0.0	0.0	0.0					
0	0.0	0.0	0.0	0.0	0.0	0.0	0.0	0.0	0.0	0.0	0.0	0.0				
0.0	0.0	0.0	0.0	0.0	0.0	0.0	0.0	0.0	0.0	0.0	0.0	0.0				
0	0.0	0.0	0.0	0.0	0.0	0.0	0.0	0.0	0.0	0.0	0.0	0.0	0.0			
0.0	0.0	0.0	0.0	0.0	0.0	0.0	0.0	0.0	0.0	0.0	0.0	0.0	0.0			
0	0.0	0.0	0.0	0.0	0.0	0.0	0.0	0.0	0.0	0.0	0.0	0.0	0.0	0.0		
0.0	0.0	0.0	0.0	0.0	0.0	0.0	0.0	0.0	0.0	0.0	0.0	0.0	0.0	0.0		
0	0.0	0.0	0.0	0.0	0.0	0.0	0.0	0.0	0.0	0.0	0.0	0.0	0.0	0.0	0.0	
0.0	0.0	0.0	0.0	0.0	0.0	0.0	0.0	0.0	0.0	0.0	0.0	0.0	0.0	0.0	0.0	
0	0.0	0.0	0.0	0.0	0.0	0.0	0.0	0.0	0.0	0.0	0.0	0.0	0.0	0.0	0.0	0.0
0.0	0.0	0.0	0.0	0.0	0.0	0.0	0.0	0.0	0.0	0.0	0.0	0.0	0.0	0.0	0.0	0.0
TOTALS		34	19	11	4	2	2	1	0	0	0	0	0	0	0	0
		1.0854	0.9097	1.0323	0.4465	1.5298	0.9705	0.6691	0.0	0.0	0.0	0.0	0.0	0.0	0.0	0.0

LEVEL OF OVERALL TEST IS 0.7437

Table 5.16 Intercommunication Gap Length Statistics for Sector Function DP

STATISTICS OF INTER-COMMUNICATION GAPS BY # OF GAPS AND LOCATION OF GAP.
RUN : DP

N GAPS	RANK PROB	1	2	3	4	5	6	7	8	9	10	11	12	13	14	15
12	1.00	1.0000														
98.5	0.0	0.0009														
35	1.10	1.0774	0.9226													
103.3	0.9685	0.2209	0.2209													
51	1.04	1.0398	1.0271	0.9332												
185.7	0.7536	0.1713	0.1728	0.1614												
50	0.98	0.9222	0.8922	1.1577	1.0278											
224.1	0.4001	0.1341	0.1470	0.1614	0.1462											
35	0.90	0.8889	0.9472	0.9288	1.1476	1.0875										
243.1	0.1160	0.1354	0.1374	0.1148	0.1306	0.1536										
14	1.08	1.0374	1.0329	0.7686	1.4199	0.7398	1.0015									
306.4	0.7343	0.1108	0.1005	0.1012	0.1710	0.0944	0.1140									
12	0.96	0.9494	0.7772	1.1374	0.9815	0.7143	0.7630	1.6771								
379.4	0.3864	0.0794	0.0673	0.0887	0.1008	0.0676	0.0620	0.1768								
5	1.07	0.9719	0.5629	1.1167	0.7193	1.0421	1.8757	1.0254	0.6859							
401.6	0.6152	0.0333	0.0352	0.0571	0.1144	0.0756	0.1135	0.0485	0.0429							
3	0.93	0.7332	1.0004	0.6703	0.8125	1.0288	0.8105	1.5463	0.5081	1.8899						
500.3	0.4115	0.0320	0.0816	0.0478	0.0521	0.0473	0.0195	0.0871	0.0387	0.1149						
1	0.36	0.5085	0.5650	1.3842	0.8475	0.5085	0.7062	0.8757	1.3559	1.6949	1.5537					
354.0	0.1115	0.0	0.0	0.0	0.0	0.0	0.0	0.0	0.0	0.0	0.0					
0	0.0	0.0	0.0	0.0	0.0	0.0	0.0	0.0	0.0	0.0	0.0	0.0				
0.0	0.0	0.0	0.0	0.0	0.0	0.0	0.0	0.0	0.0	0.0	0.0	0.0				
1	0.46	0.2303	1.8952	2.1697	2.0369	0.9033	0.2923	1.8155	1.1601	0.2125	0.2303	0.3454	0.7085			
1355.0	0.1553	0.0	0.0	0.0	0.0	0.0	0.0	0.0	0.0	0.0	0.0	0.0	0.0			
0	0.0	0.0	0.0	0.0	0.0	0.0	0.0	0.0	0.0	0.0	0.0	0.0	0.0	0.0		
0.0	0.0	0.0	0.0	0.0	0.0	0.0	0.0	0.0	0.0	0.0	0.0	0.0	0.0	0.0		
0	0.0	0.0	0.0	0.0	0.0	0.0	0.0	0.0	0.0	0.0	0.0	0.0	0.0	0.0	0.0	
0.0	0.0	0.0	0.0	0.0	0.0	0.0	0.0	0.0	0.0	0.0	0.0	0.0	0.0	0.0	0.0	
1	1.88	3.3381	0.2384	0.3251	0.4118	0.8020	1.3439	0.1734	0.3685	0.5419	1.3439	0.6503	0.2384	1.1488	0.6503	1.6257
692.0	0.9474	0.0	0.0	0.0	0.0	0.0	0.0	0.0	0.0	0.0	0.0	0.0	0.0	0.0	0.0	0.0
TOTALS		220	208	173	122	72	37	23	11	6	3	2	2	1	1	1
		0.9864	0.9362	1.0050	1.0864	0.9375	1.0089	1.4242	0.7126	1.3532	1.0426	0.4978	0.4735	1.1488	0.6503	1.6257

LEVEL OF OVERALL TEST IS 0.7431

Table 5.17 Intercommunication Gap Length Statistics for Sector Function AD

STATISTICS OF INTER-COMMUNICATION GAPS BY # OF GAPS AND LOCATION OF GAP.
RUN : AD

N GAPS	RANK PROB	1	2	3	4	5	6	7	8	9	10	11	12	13	14	15
14	1.00	1.0000														
77.0	0.0	0.0009														
17	1.02	1.1655	0.8345													
220.2	0.5958	0.2376	0.2376													
12	0.88	0.7548	0.9824	1.2628												
257.8	0.1444	0.1791	0.2070	0.2175												
9	1.07	0.9802	0.6438	1.5255	0.8505											
272.0	0.6726	0.1509	0.1255	0.1913	0.1436											
12	1.11	1.0847	0.6496	1.0350	1.2222	1.0084										
311.3	0.7929	0.1380	0.0689	0.1630	0.1554	0.1315										
3	0.86	0.5343	1.4487	1.6934	1.0358	0.5234	0.7645									
475.0	0.3060	0.0440	0.1995	0.2653	0.0732	0.0568	0.0328									
5	1.15	1.0481	0.7277	0.4929	1.4437	1.1972	1.3407	0.7498								
266.6	0.7488	0.0726	0.0612	0.0470	0.0734	0.0934	0.1020	0.0798								
3	1.19	1.3184	1.0750	1.2466	1.1258	1.1068	0.7381	0.5075	0.8818							
451.3	0.7356	0.0750	0.0420	0.0541	0.0626	0.0649	0.0680	0.0153	0.1050							
3	0.80	0.5454	0.9994	0.7855	1.1917	1.0339	0.8715	1.5104	1.0997	0.9625						
1313.3	0.2512	0.0308	0.1026	0.0545	0.1108	0.1408	0.0705	0.0524	0.1181	0.1108						
0	0.0	0.0	0.0	0.0	0.0	0.0	0.0	0.0	0.0	0.0	0.0					
0.0	0.0	0.0	0.0	0.0	0.0	0.0	0.0	0.0	0.0	0.0	0.0					
1	1.83	4.0845	0.7670	0.1122	0.0748	0.0811	3.9722	0.1684	0.2619	0.6111	0.1497	0.7171				
1764.0	0.9431	0.0	0.0	0.0	0.0	0.0	0.0	0.0	0.0	0.0	0.0	0.0				
0	0.0	0.0	0.0	0.0	0.0	0.0	0.0	0.0	0.0	0.0	0.0	0.0	0.0			
0.0	0.0	0.0	0.0	0.0	0.0	0.0	0.0	0.0	0.0	0.0	0.0	0.0	0.0			
2	0.57	0.3453	0.4185	0.8328	1.2674	2.0621	0.3973	1.0859	0.3039	1.0592	1.0089	0.3973	0.4013	3.4201		
877.5	0.1284	0.0138	0.0224	0.0476	0.0450	0.0992	0.0193	0.0432	0.0099	0.0340	0.0063	0.0051	0.0024	0.0172		
0	0.0	0.0	0.0	0.0	0.0	0.0	0.0	0.0	0.0	0.0	0.0	0.0	0.0	0.0	0.0	
0.0	0.0	0.0	0.0	0.0	0.0	0.0	0.0	0.0	0.0	0.0	0.0	0.0	0.0	0.0	0.0	
0	0.0	0.0	0.0	0.0	0.0	0.0	0.0	0.0	0.0	0.0	0.0	0.0	0.0	0.0	0.0	0.0
0.0	0.0	0.0	0.0	0.0	0.0	0.0	0.0	0.0	0.0	0.0	0.0	0.0	0.0	0.0	0.0	0.0
TOTALS		81	67	50	38	29	17	14	9	6	3	3	2	2	0	0
		1.0113	0.8265	1.1344	1.1108	1.0443	1.0937	0.8673	0.7571	0.9362	0.7225	0.5039	0.4013	3.4201	0.0	0.0

LEVEL OF OVERALL TEST IS 0.6912

Table 5.18 Intercommunication Gap Length Statistics for Sector Function AR

STATISTICS OF INTER-COMMUNICATION GAPS BY # OF GAPS AND LOCATION OF GAP.
RUN : AR

N GAPS	RANK PROB	1	2	3	4	5	6	7	8	9	10	11	12	13	14	15
24	1.00	1.0000														
105.9	0.0	0.0023														
30	0.96	0.9806	1.0194													
155.8	0.2326	0.2616	0.2616													
48	1.04	1.0757	1.0285	0.8958												
218.1	0.7602	0.1897	0.1848	0.1696												
43	1.22	1.2675	0.9376	0.8586	0.9363											
248.1	0.9993	0.1585	0.1587	0.1217	0.1470											
52	1.10	1.1373	0.9114	1.0892	0.8417	1.0204										
275.3	0.9293	0.1451	0.1022	0.1349	0.0967	0.1384										
43	1.06	1.0834	1.0347	1.1842	0.9938	0.9803	0.7235									
374.6	0.7761	0.1333	0.0960	0.1297	0.1208	0.1196	0.0786									
34	1.08	1.4025	0.9785	1.1910	1.0211	0.8441	0.8145	0.7485								
500.7	0.8272	0.2031	0.0863	0.1254	0.0993	0.0910	0.0745	0.0926								
25	1.24	1.4623	1.1655	0.8917	1.0639	0.7803	0.7508	0.9996	0.8859							
527.2	0.9918	0.1270	0.1162	0.0722	0.1091	0.0682	0.0642	0.0876	0.0801							
23	0.97	1.1136	1.4984	0.8965	1.0230	0.9216	1.0374	0.8333	0.6591	1.0170						
588.4	0.4043	0.1112	0.1513	0.0737	0.0838	0.0962	0.1050	0.0750	0.0363	0.0818						
24	1.10	1.5466	1.1020	0.6784	1.3729	1.1587	0.5301	0.8877	0.9581	0.7875	0.9779					
607.6	0.8222	0.1826	0.1091	0.0417	0.1068	0.0910	0.0315	0.0577	0.0678	0.0761	0.0862					
10	1.07	1.1460	0.7212	1.0416	1.6343	1.0324	1.5659	0.9569	0.7091	0.7126	0.7975	0.6823				
760.1	0.6554	0.0874	0.0458	0.0392	0.1566	0.0649	0.1381	0.0672	0.0420	0.0403	0.0468	0.0325				
13	0.88	1.2129	1.8539	1.0419	1.5612	0.6494	1.4857	0.8410	0.5468	0.4809	0.7621	0.8882	0.6761			
1019.4	0.1994	0.1534	0.1657	0.1157	0.1430	0.0425	0.1250	0.0912	0.0374	0.0250	0.0816	0.0451	0.0511			
7	1.04	0.8940	1.7106	0.8884	0.9744	0.8515	0.8117	0.7780	1.6481	1.1129	1.0773	0.8588	0.3922	1.0021		
932.9	0.5801	0.0400	0.1277	0.0321	0.1044	0.0367	0.0211	0.0233	0.1343	0.0897	0.0566	0.0419	0.0104	0.0667		
7	0.82	0.9719	0.9108	2.0385	1.6594	0.8652	0.7466	0.6030	1.3641	1.4654	0.7188	0.6692	0.5444	0.7322	0.7104	
918.4	0.1865	0.0860	0.0403	0.1586	0.1541	0.0362	0.0600	0.0285	0.1026	0.1266	0.0339	0.0231	0.0259	0.0243	0.0249	
6	1.46	3.3089	1.6507	0.7605	1.3229	1.6723	0.4340	0.4768	0.4608	0.4185	0.4195	0.3755	0.9256	0.5571	0.4272	0.4802
1490.8	0.9812	0.2333	0.1442	0.0220	0.1210	0.1778	0.0224	0.0136	0.0136	0.0210	0.0171	0.0120	0.0689	0.0228	0.0165	0.0164
TOTALS		389	365	335	287	244	192	149	115	90	67	43	33	20	13	6
		1.2143	1.0822	1.0035	1.0717	0.9559	0.8471	0.8318	0.8552	0.8470	0.8424	0.7283	0.6333	0.7741	0.5797	0.4802

LEVEL OF OVERALL TEST IS 0.9972

Table 5.19 Intercommunication Gap Length Statistics for Sector Function RA

STATISTICS OF INTER-COMMUNICATION GAPS BY # OF GAPS AND LOCATION OF GAP.
RUN : RA

N GAPS	RANK PROB	1	2	3	4	5	6	7	8	9	10	11	12	13	14	15
14	1.00	1.0000														
155.2	0.0	0.0009														
21	0.86	0.7913	1.2087													
267.7	0.0248	0.2011	0.2011													
9	1.00	0.9355	0.6333	1.4312												
272.0	0.5000	0.1069	0.1635	0.2398												
12	0.87	0.9850	0.9525	1.0166	1.0459											
372.0	0.1508	0.2057	0.1138	0.1682	0.1565											
6	1.22	1.4095	1.1989	1.1544	0.5310	0.7061										
441.8	0.8759	0.2017	0.0983	0.1171	0.0586	0.0915										
6	0.76	0.7829	1.7372	0.8918	1.0765	1.0803	0.4313									
479.8	0.1160	0.1603	0.2208	0.0723	0.1660	0.1543	0.0651									
5	1.20	1.2169	0.8278	1.6844	0.9630	0.2215	0.8931	1.1932								
630.4	0.8145	0.0974	0.0661	0.0914	0.1182	0.0152	0.0986	0.1153								
5	1.07	0.8858	0.6422	0.8886	1.1400	1.4131	0.8585	0.8317	1.3402							
562.2	0.6152	0.0607	0.0698	0.1021	0.0947	0.1158	0.0913	0.0763	0.1132							
1	0.60	0.2871	0.2026	0.5741	0.4559	1.3846	0.3377	2.1445	0.1857	3.4278						
533.0	0.2193	0.0	0.0	0.0	0.0	0.0	0.0	0.0	0.0	0.0						
2	0.64	0.3212	0.6112	0.4271	0.9622	0.8968	1.5850	0.2037	1.1712	2.0563	1.7653					
744.5	0.1624	0.0159	0.0087	0.0209	0.0758	0.0737	0.0173	0.0029	0.0749	0.1146	0.1204					
1	0.17	0.1026	0.6978	0.4310	0.6567	1.2108	0.6054	3.3554	0.5541	1.9907	0.1129	1.2826				
1072.0	0.0569	0.0	0.0	0.0	0.0	0.0	0.0	0.0	0.0	0.0	0.0	0.0				
1	0.77	0.2072	0.2072	0.2826	3.7111	0.6028	2.7504	0.3956	2.5432	0.1695	0.1884	0.8100	0.1319			
637.0	0.3320	0.0	0.0	0.0	0.0	0.0	0.0	0.0	0.0	0.0	0.0	0.0	0.0			
0	0.0	0.0	0.0	0.0	0.0	0.0	0.0	0.0	0.0	0.0	0.0	0.0	0.0	0.0		
0.0	0.0	0.0	0.0	0.0	0.0	0.0	0.0	0.0	0.0	0.0	0.0	0.0	0.0	0.0		
0	0.0	0.0	0.0	0.0	0.0	0.0	0.0	0.0	0.0	0.0	0.0	0.0	0.0	0.0	0.0	
0.0	0.0	0.0	0.0	0.0	0.0	0.0	0.0	0.0	0.0	0.0	0.0	0.0	0.0	0.0	0.0	
1	1.88	1.4730	0.2455	0.6383	1.4730	0.6874	0.2455	0.5155	0.5892	0.4173	0.6137	0.5401	0.5155	0.7365	0.4910	0.5155
611.0	0.9474	0.0	0.0	0.0	0.0	0.0	0.0	0.0	0.0	0.0	0.0	0.0	0.0	0.0	0.0	0.0
TOTALS		84	70	49	40	28	22	16	11	6	5	3	2	1	1	1
		0.9195	1.0008	1.0817	1.0233	0.8775	0.8389	1.0589	1.1741	1.6863	0.8891	0.8776	0.3237	0.7365	0.4910	0.5155

LEVEL OF OVERALL TEST IS 0.2422

(v) The bottom line of the table gives the number of observations and the average value of the upper entries in the appropriate column. The cumulative probability related to the overall testing statistic is presented on the last line of each table. A small probability, say 0.01, indicates that the first gap length is shorter than the remaining gaps, while the high probability indicates the opposite.

Consider the difficulty which was encountered in constructing an appropriate test statistic. The number of aircraft responsible for the gaps, k = 1, 2, ..., varied, of course, along with the frequency of each gap. An approximate test was finally constructed taking advantage of order statistics. Let $r_{i,k}$ indicate the rank of the first gap length among the gap lengths provided by the ith aircraft which made k gaps. Under the assumption that the first gap length is not different from the remaining, $r_{i,k}$ should be uniformly distributed among 1, 2, ..., k given the i. According to the central limit theorem, the statistic $r_k = \sum_{i=1}^{n_k} (r_{i,k})/n_k$ should thus be distributed as a normal variable with mean equal to (k+1)/2 and variance equal to $(k^2 - 1)/12n_k$, where n_k is the number of aircraft which have made k gaps. The value $r_k/[(k+1)/2]$ is then called the relative rank statistic and has been listed on the second extra column on the left of the tables on the computer print-out. The figure beneath it is the theoretical probability level cumulated up to the observed value of r_k. The probability level for the overall testing statistic was obtained by finding the appropriate distribution of $k = \sum_{2}^{15} r_k/\text{s.d.}(r_k)$.

5.5 A Basic Queuing Theory Model

Because of the importance of communications queuing, a separate sub-project was set up to examine some aspects of this problem using queuing theory. The project formed part of the independent work of a senior student, Linda J. Lamort, in the Statistics Department of Princeton University.

For the purpose of this discussion, a queue is said to form only when an aircraft, wishing to communicate with the controller in a sector, has to wait while the controller is busy with another aircraft. This situation can be expressed in terms of a standard queuing process in which the aircraft is the "customer" and the controller is the "server." The communications process in this form lends itself to the application of classical queuing theory (see "Queues" by Cox and Smith; Methuen, London, 1961). In actual practice, communications queuing occurs when either the aircraft, or the controller, waits until the communications channel is free.

The type of queue examined here is a single server queue. The customers are assumed to arrive according to a Poisson process, so that the times t between successive arrivals are independent random variables with exponential probability density function

$$f(t) = \rho e^{-\rho t}; \qquad 0 \leq t < \infty \tag{5.6}$$

where ρ is the arrival rate, i.e., the number of aircraft arriving per unit time.

The distribution of service time, i.e., time taken for a communications transaction (CT), was developed from the analyses of the New York ARTCC communications data. The data analyses, described in Volume II and summarized in Chapter 1 of this report, showed that the distribution of the time t taken for a transmission (TR) could be adequately represented by a gamma distribution, with probability density function (p.d.f.)

$$f(t) = \frac{1}{\lambda^{\alpha}\Gamma(\alpha)} t^{\alpha-1} e^{-t/\lambda}; \qquad 0 \leq t < \infty, \quad \alpha > 0,\ \lambda > 0 \tag{5.7}$$

where λ and α are parameters to be estimated from the data. If the number of TR's in a given CT is x, then the time taken for the CT is the sum of x gamma distribution variates which itself has a gamma distribution with p.d.f. given by

$$f(t) = \frac{1}{\lambda^{\alpha x}\Gamma(\alpha)} t^{\alpha x-1} e^{-t/\lambda}; \qquad 0 \leq t < \infty. \tag{5.8}$$

A special investigation has been made of the distribution of the random variable x, the number of TR's per CT, and is described in the next section. For this study, the results of the earlier data analyses were used, in which it was found that the distribution of the number of TR's per CT would be fitted fairly well by a truncated negative binomial distribution

$$f(x) = \frac{1}{1-(1+\theta)^{-n}} \binom{n+x-1}{n-1} \left(\frac{\theta}{1+\theta}\right)^{x} \left(1 - \frac{\theta}{1+\theta}\right)^{n}; \quad x = 1, 2, \ldots \tag{5.9}$$

where n and θ are parameters estimated from the data. Thus, the service time (i.e. CT length) was regarded as a random variable from a gamma distribution given by Equation (5.8) compounded with a truncated negative

binomial distribution given by Equation (5.9).

The inter-arrival time distribution and the service time distribution define the model for the queuing process. The mathematical complexity of the service time distribution suggested that the properties of the queuing process could best be examined by a simulation. The service times (CT lengths) were therefore obtained by generating random variates from the distributions given by Equations (5.8) and (5.9), while the interarrival times were generated from the exponential distribution given by Equation (5.6).

A schematic diagram of the arrivals and service times of customers is shown in Figure 5.13. The variables shown are defined as follows:

t_i = inter-arrival time of ith customer

s_i = service time of ith customer

w_i = waiting time of ith customer

where the waiting time is defined as the time between arrival in queue and start of service. It can be seen from Figure 5.13 that if the server is busy when the ith customer arrives, his waiting time is $w_i = w_{i-1}+s_{i-1}-t_i$. A flow chart for a simulation of the basic queuing system is given in Figure 5.14 showing the calculation of one of the main quantities of interest, the waiting time. Other important responses are the number of customers in the queue (i.e., the queue length) and the probability that a customer does not have to wait.

The average waiting time to be served, the standard deviation of waiting time, and the queue length are given in Figures 5.15, 5.16 and 5.17 respectively, for different arrival rates, using the service time distribution parameters obtained from the data on the LT sector function. All three quantities show an exponential type increase with arrival rate. Figure 5.18 shows the probability of zero waiting time, which decreases linearly with increasing arrival rate. It should be noted that "arrival rate" in this model of a simple queue is the arrival rate of customers wishing to be served. Thus, in the ATC communications system, this is equivalent to the arrival rate of CT's within a sector, not the arrival rate of aircraft in a sector. Here the "customers" include those aircraft already in a sector, wishing to communicate for the second, third, fourth... time, etc., as well as the aircraft entering the sector. Furthermore, no distinction is made between CT's which are initiated by the pilot and those initiated by the controller. A more complex queuing theory model is needed to distinguish between the first CT and subsequent CT's of an aircraft, and to distinguish between pilot-initiated and controller-initiated CT's.

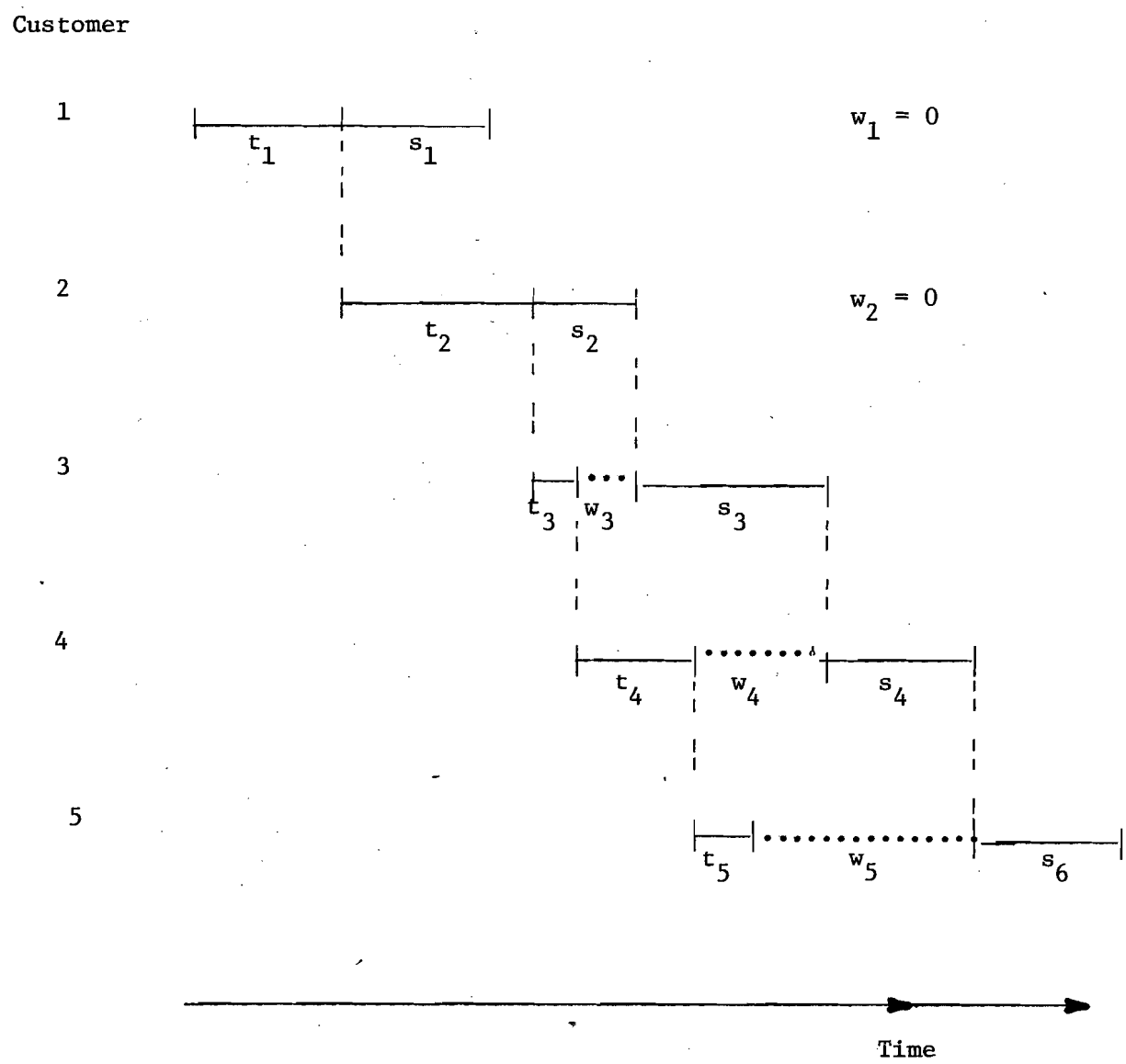

Figure 5.13 Schematic Diagram of Customers' Arrivals and Service Times

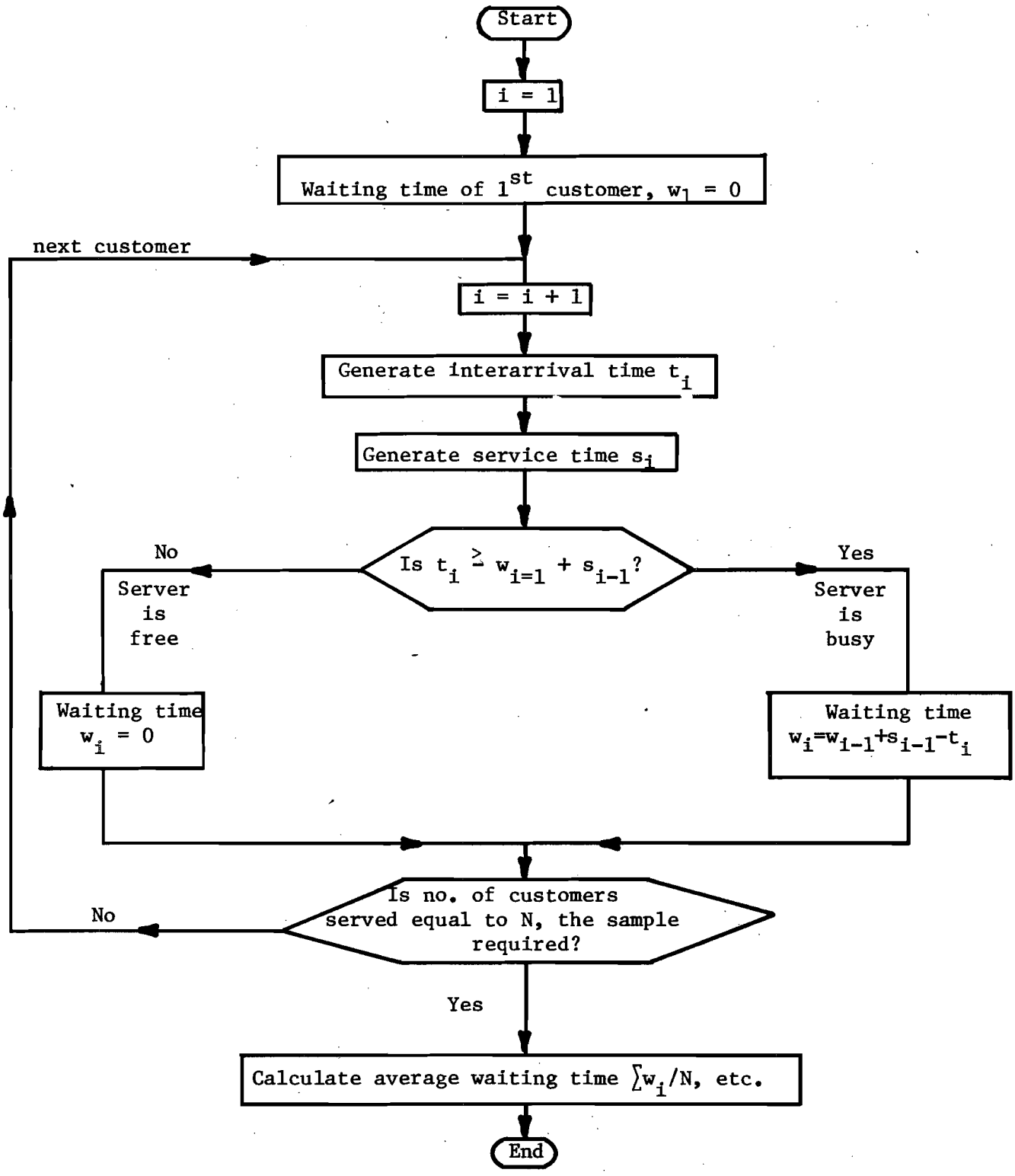

Figure 5.14 Flow Chart for Simulation of a Simple Queue

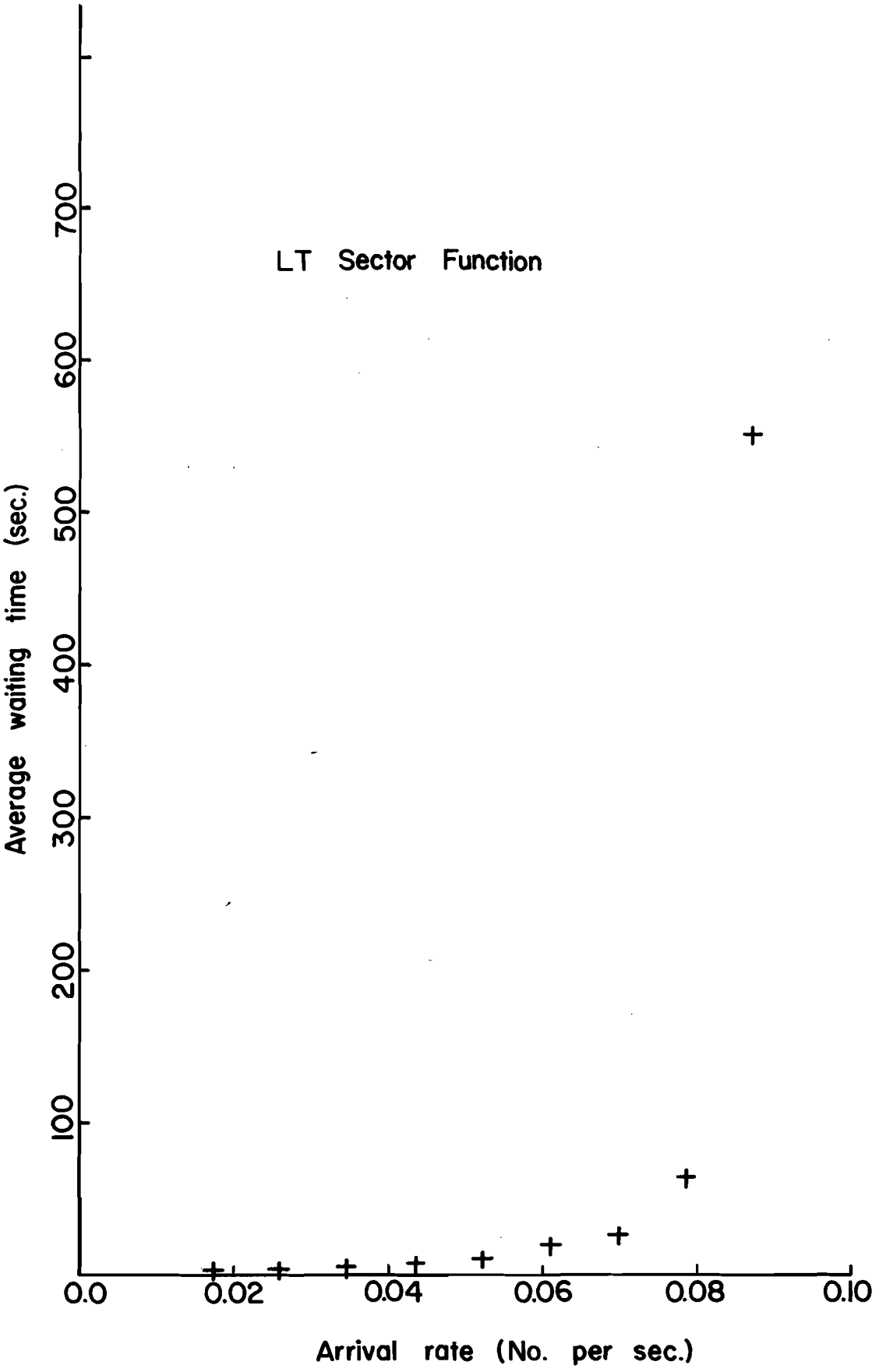

Figure 5.15 Average Waiting Time as a Function of Arrival Rate

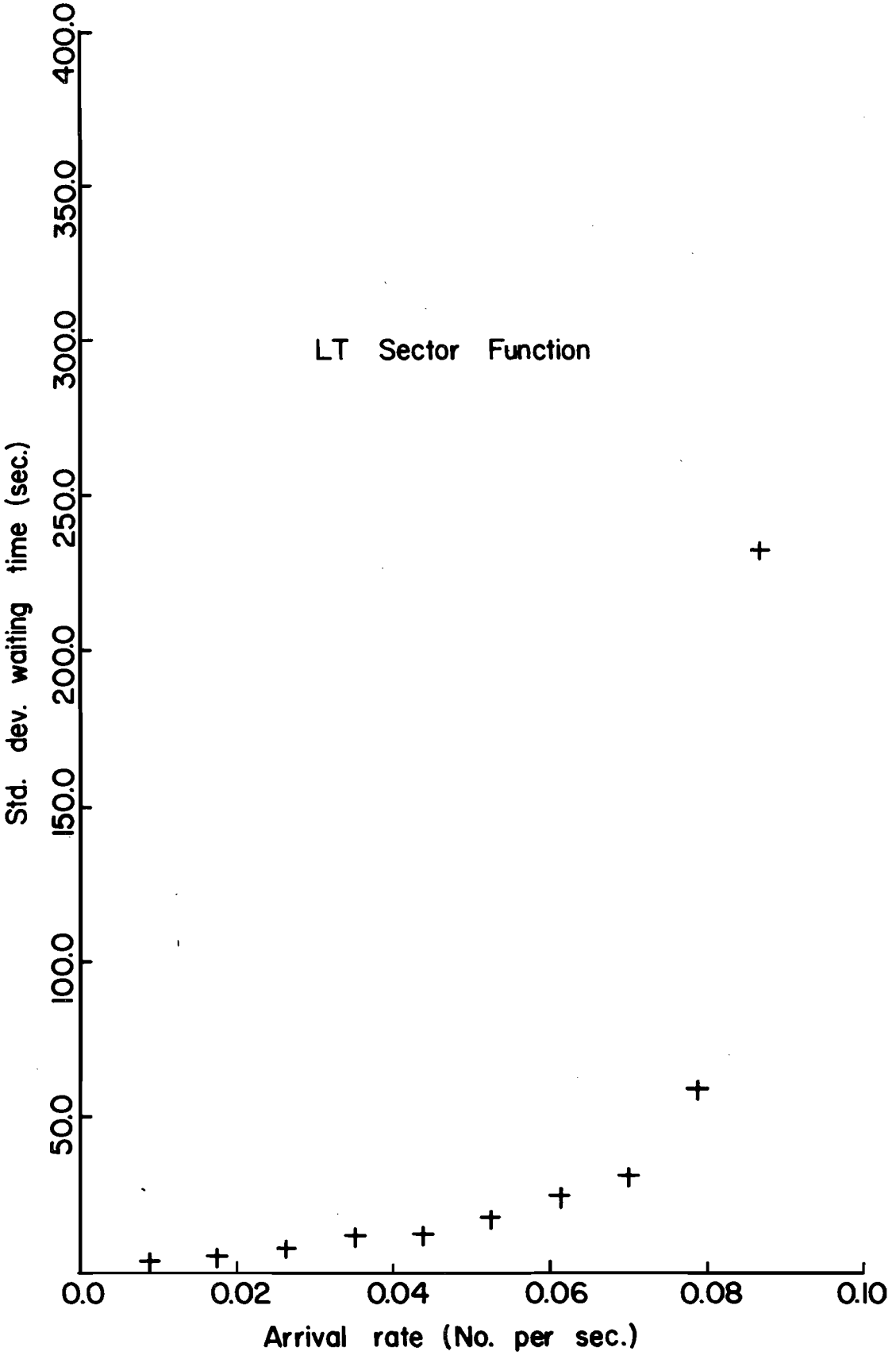

Figure 5.16 Standard Deviation of Waiting Time as a Function of Arrival Rate

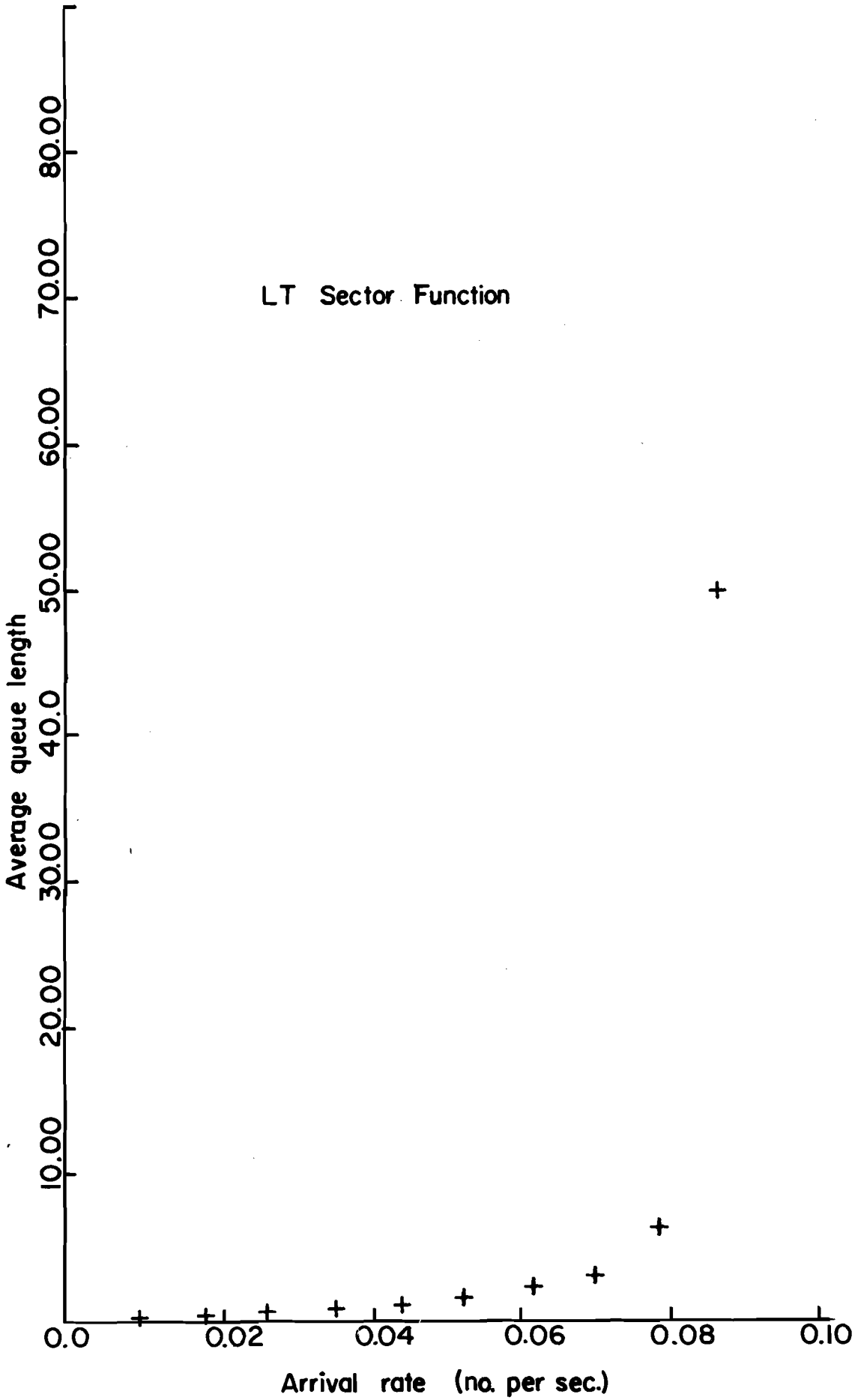

Figure 5.17 Average Queue Length as a Function of Arrival Rate

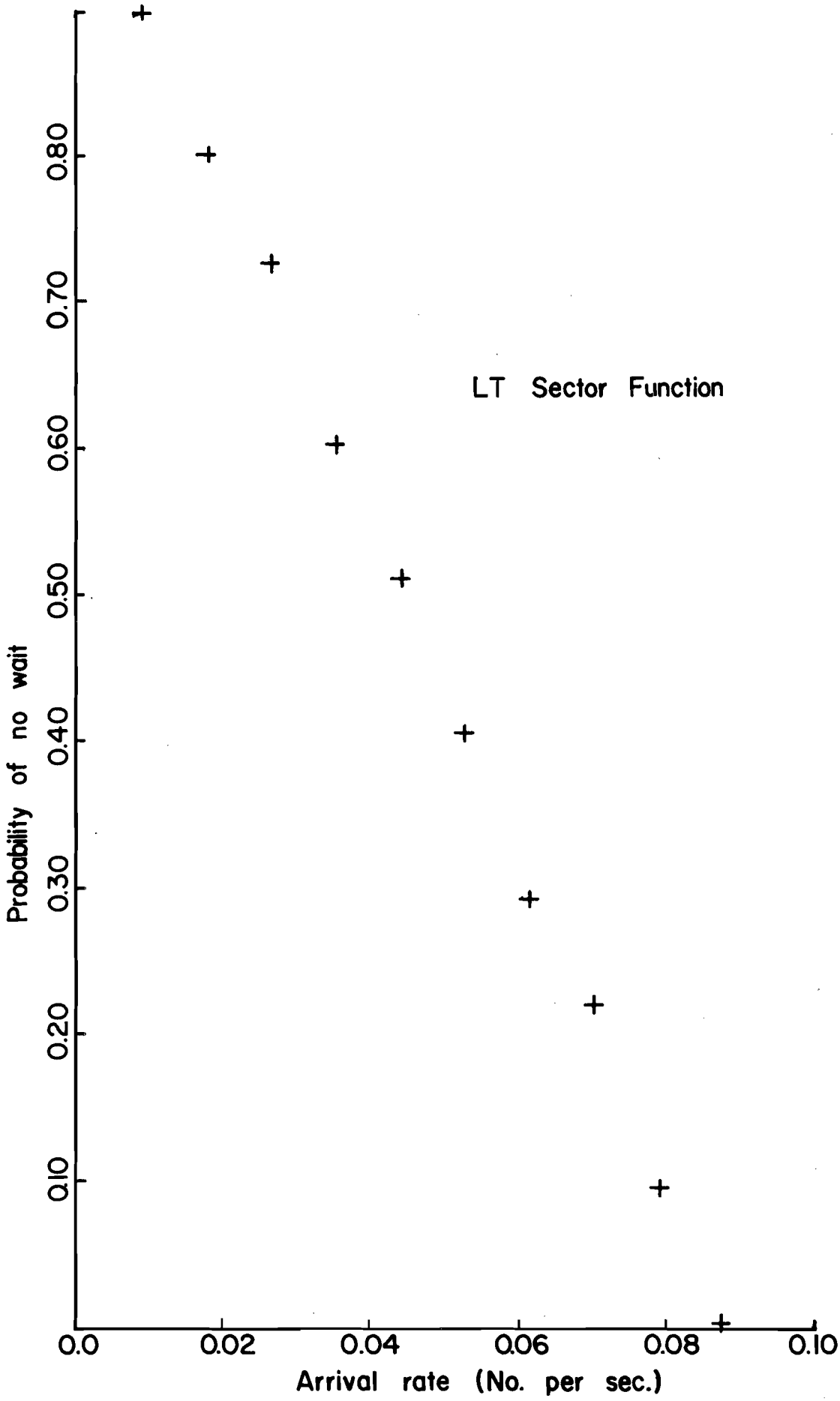

Figure 5.18 Probability of No Wait as a Function of Arrival Rate

Since the ATC communications data were originally obtained from tape recordings of communications, there is no record of the actual arrival times of aircraft into a sector. Data on each aircraft could start to be collected only at the beginning of the first CT. Thus, the data provide the distribution of "inter-beginning-of-first-CT" times or "inter-enter" times and not the true distribution of inter-arrival times of aircraft into a sector. A problem which requires a special study is to determine the inter-arrival time distribution or to find a relationship between the distributions of inter-arrival times and inter-enter times.

A preliminary examination of this problem was made using the model of a simple customer-service queue described above. In the simulation of the model, the times of the beginning of each service were recorded, and hence the distribution of inter-beginning-of-service times was obtained. This distribution was compared with the inter-arrival times, assumed in this model to have an exponential distribution. The distribution of inter-beginning-of-service times obtained from the simulation is shown in Figure 5.19 using arrival and service time distribution parameter values for the LT sector function. In this case, the distribution does not differ much from the exponential distribution with the same mean, since the service times are short in comparison to the inter-arrival times. For a busier sector the service time distribution will have a larger influence and cause a greater deviation of the inter-beginning-of-service time distribution from the exponential distribution.

5.6 Further Distributions for Number of TR per CT

Analyses of the New York ATC communications data showed that the distribution of x, the number of TR's per CT in a sector or sector function, could be represented by a truncated negative binomial distribution given by Equation (5.9) in the previous section. Although the agreement to the data was close for some sectors, a study of all sectors indicated the need for a better representation of the observed distributions. The problem of finding suitable probability distributions for the number of TR's per CT was the subject of a second independent work project by a senior student, Graham A. Harrison, in the Statistics Department of Princeton University.

A characteristic of the empirical distributions of numbers of TR's per CT is the long tail to the right, indicating the existence of CT's with relatively large numbers of TR's. A class of long-tailed probability distributions has been developed by H. S. Sichel in a paper "On a Family of Discrete Distributions Particularly Suited to Represent Long-tailed Frequency Data", Special Report, Council for Scientific and Industrial Research, Pretoria, South Africa (1971). These distributions were

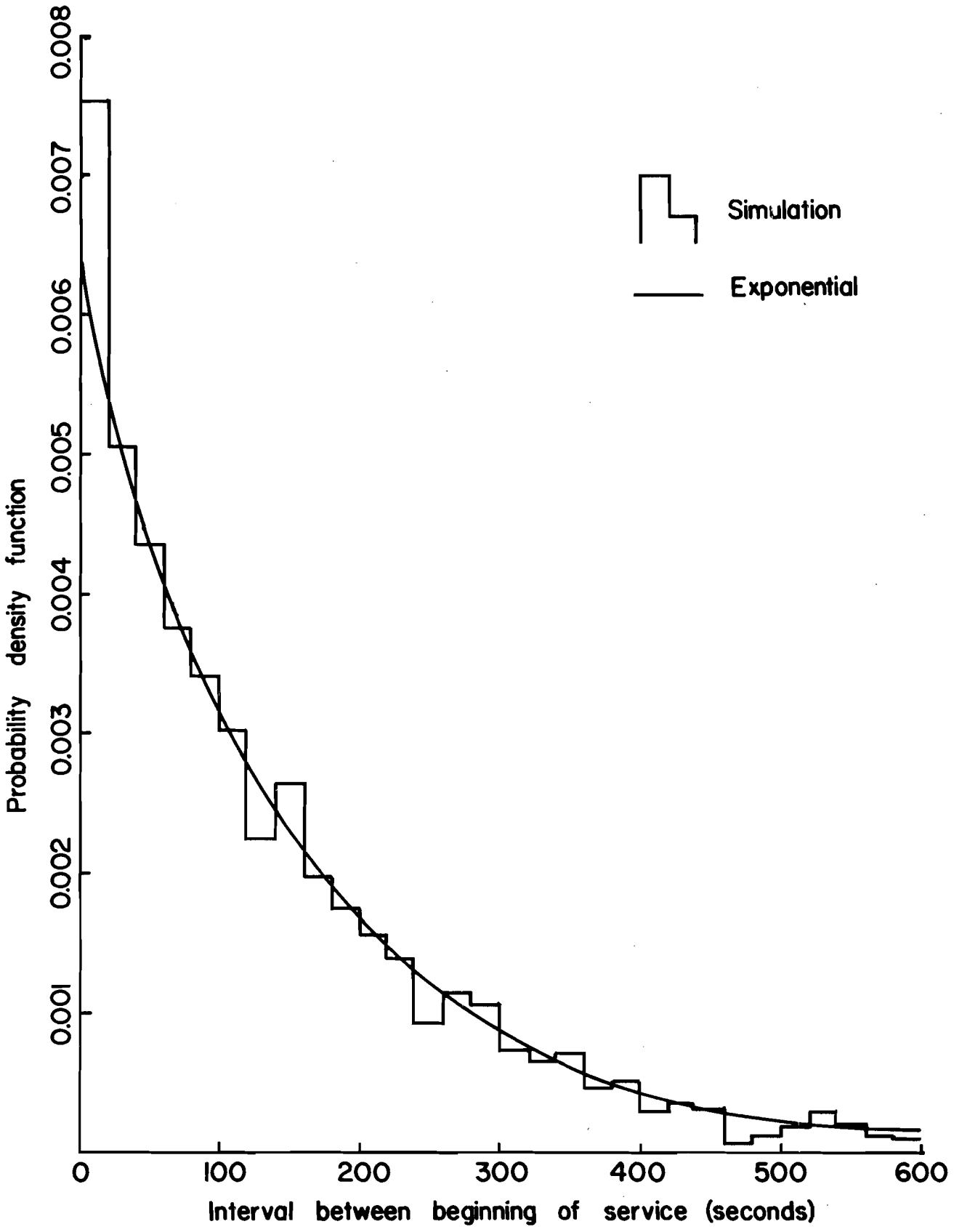

Figure 5.19 Distribution of Interval between Beginning of Service

examined for the data on x, the number of TR's per CT. Sichel developed his probability distribution $\phi(x)$ from a Poisson distribution $f(x|\lambda)$ in which the parameter λ was itself regarded as a random variable from a continuous distribution $g(\lambda)$, so that

$$\phi(x) = \int_0^\infty f(x|\lambda)g(\lambda)\, d\lambda. \tag{5.10}$$

The "mixing function" $g(\lambda)$ used by Sichel is

$$g(\lambda) = \kappa\lambda^{a-1} \exp\left(-\frac{b^2\lambda}{2} - \frac{c^2}{2\lambda}\right) \tag{5.11}$$

where a, b, c are parameters such that $-\infty < a < \infty$, $0 < b < \infty$, $0 < c < \infty$, and κ is a normalizing constant. For much of his analysis Sichel took $a = -1/2$.

As for most discrete distributions, Sichel's probability distribution $\phi(x)$ is defined for $x = 0$ as well as for $x = 1, 2, 3, \ldots$ etc. Since it is impossible for a CT to have zero TR's, the discrete distributions considered for this purpose had to be truncated so as to be defined only for the positive integers 1, 2, ..., etc. A truncated version of Sichel's distribution was obtained by repeating his derivation for a truncated Poisson distribution $f_T(x|\lambda)$ given by

$$f_T(x|\lambda) = \frac{1}{(1 - e^{-\lambda})} \frac{e^{-\lambda}\lambda^x}{x!}\ ;\ x = 1, 2, \ldots \tag{5.12}$$

where $(1 - e^{-\lambda})^{-1}$ is the truncation factor. For the case $a = -1/2$, the resulting truncated Sichel distribution is given by

$$\phi(x) = \frac{1}{2e^{-(bc + \alpha)}} \frac{\beta^x}{x!} \sum_{k=0}^{x-1} \frac{(x - 1 + k)!}{k!(x - 1 - k)!(2\alpha)^k} \qquad x = 1, 2, \ldots \tag{5.13}$$

where $\alpha = c(b^2 + 2)^{1/2}$, $\beta = c/(b^2 + 2)^{1/2}$.

The theoretical distributions given by the truncated negative binomial distribution in Equation (5.9) and the truncated Sichel distribution in Equation (5.13) were calculated for the parameter values obtained from the data on each sector function. A comparison of the observed frequencies of number of TR's per CT with those predicted by the truncated negative binomial distribution is given in Table 5.20 and with those predicted by the truncated Sichel distribution in Table 5.21. In almost all the sector functions, the truncated Sichel distribution provided a closer agreement to the data than the truncated negative binomial distribution.

Table 5.20 Results of Fitting the Truncated Negative Binomial Distribution to the Observed Number of TR per CT for the 12 Sector Functions

O - Observed frequency
P - Predicted frequency

# of TR/CT	LT		LE		HI		CD		GN		LC	
	O	P	O	P	O	P	O	P	O	P	O	P
1	266	396	261	360	209	317	51	38	280	393	615	1022
2	644	587	580	514	544	443	49	60	544	453	2126	1311
3	938	623	763	529	608	450	63	70	621	412	1213	1153
4	442	530	343	439	345	373	57	70	257	324	525	782
5	319	383	233	312	187	265	50	61	183	231	253	435
6	164	245	176	197	152	169	68	49	117	153	131	208
7	127	142	104	113	69	99	56	37	69	96	75	87
8	66	76	53	60	42	54	33	26	47	58	47	33
9	38	38	21	30	29	27	15	17	24	34	26	11
10	18	17	13	14	12	13	9	11	14	19	12	4
11	8	8	15	6	10	6	9	7	13	11	10	1
12	10	3	6	3	5	3	3	4	9	6	9	0
13	7	1	4	1	3	1	3	3	5	3	5	0
14	2	1	1	0	1	1	0	2	2	2	0	0
15	2	0	1	0	1	0	0	1	3	1	0	0
16	2	0	1	0	2	0	0	0	4	0	1	0
17	1	0	0	0	2	0	0	0	1	0	1	0
18	1	0	0	0	0	0	0	0	1	0	1	0
19	0	0	1	0	0	0	0	0	0	0	0	0
20	0	0	0	0	1	0	1	0	2	0	0	0
$\hat{\theta}$	1.28		1.30		1.35		1.73		1.72		1.08	
$\hat{n}$	12.54		11.27		9.86		6.40		4.49		34.09	
χ^2(13d.f.)	430.31		245.78		342.86		33.48		274.98		9034.23	

Table 5.20 Results of Fitting the Truncated Negative Binomial Distribution to the Observed Number of TR per CT for the 12 Sector Functions (continued)

O = Observed frequency

P = Predicted frequency

# of TR/CT	LG		AP		DP		AD		AR		RA	
	O	P	O	P	O	P	O	P	O	P	O	P
1	71	103	20	16	69	167	50	70	175	480	38	53
2	164	136	6	20	328	226	102	77	1153	641	77	67
3	173	133	26	21	369	229	93	72	806	633	110	70
4	118	107	25	19	137	192	53	61	345	514	45	65
5	54	75	14	16	117	142	44	49	241	363	49	56
6	28	47	12	13	52	95	38	38	157	232	49	47
7	17	27	13	10	37	59	19	28	114	136	27	37
8	11	15	5	7	25	34	15	21	62	75	26	28
9	8	8	4	5	14	19	13	15	27	39	24	21
10	5	4	3	4	12	10	12	10	31	19	12	16
11	2	2	3	3	9	5	11	7	8	9	11	11
12	5	1	2	2	3	3	4	5	8	4	7	8
13	1	0	3	1	2	1	2	3	7	2	7	6
14	0	0	1	1	3	1	0	2	4	1	8	4
15	0	0	0	0	3	0	2	2	5	0	2	3
16	0	0	1	0	1	0	1	1	0	0	1	2
17	1	0	0	0	1	0	0	1	2	0	2	1
18	0	0	0	0	0	0	1	0	2	0	0	1
19	0	0	0	0	0	0	1	0	1	0	2	1
20	0	0	0	0	1	0	2	0	1	0	1	0
$\hat{\theta}$	1.39		2.34		1.49		2.55		1.41		2.54	
$\hat{n}$	8.49		3.40		7.25		2.62		8.26		3.15	
χ^2(13d.f.)	92.44		20.10		315.42		34.14		1004.02		45.23	

Table 5.21 Results of Fitting the Truncated Sichel Distribution to the Observed No. of TR per CT for the 12 Sector Functions

O = Observed frequency

P = Predicted frequency

# of TR/CT	LT		LE		HI		CD		GN		LC	
	O	P	O	P	O	P	O	P	O	P	O	P
1	266	427	261	384	209	366	51	32	280	422	615	1184
2	644	608	580	530	544	462	49	56	544	476	2126	1336
3	938	622	763	527	608	435	63	71	621	414	1213	1080
4	442	513	343	426	345	342	57	73	257	311	525	703
5	319	364	233	297	187	240	50	65	183	213	253	393
6	164	232	176	186	152	155	68	52	117	138	131	196
7	127	135	104	108	69	94	56	38	69	86	75	90
8	66	74	58	58	42	55	33	27	47	53	47	38
9	38	38	21	30	29	31	15	18	24	34	26	15
10	18	19	13	15	12	17	9	11	14	19	12	6
11	8	9	15	7	10	9	9	7	13	11	10	2
12	10	4	6	3	5	5	3	4	9	6	9	1
13	7	2	4	1	3	2	3	2	5	3	5	0
14	2	1	1	1	1	1	0	1	2	2	0	0
15	2	0	1	0	1	1	0	1	3	1	0	0
16	2	0	1	0	2	0	0	1	4	1	1	0
17	1	0	0	0	2	0	0	0	1	0	1	0
18	1	0	0	0	0	0	0	0	1	0	1	0
19	0	0	1	0	0	0	0	0	0	0	0	0
20	0	0	0	0	1	0	1	0	2	0	0	0
$\hat{\alpha}$	12.7760		12.0048		8.3961		11.4554		6.2690		13.2685	
$\hat{\beta}$	2.6382		2.5461		2.2574		3.2002		1.9449		2.0981	
χ^2 (13d.f.)	332.06		209.84		194.94		37.14		209.49		1554.16	

Table 5.21 Results of Fitting the Truncated Sichel Distribution to the Observed No. of TR per CT for the 12 Sector Functions (continued)

O = Observed frequency

P = Predicted frequency

# of TR/CT	LG		AP		DP		AD		AR		RA	
	O	P	O	P	O	P	O	P	O	P	O	P
1	71	111	20	13	69	193	50	74	175	583	38	51
2	164	141	6	19	328	242	102	82	1153	687	77	70
3	173	132	26	21	369	228	93	74	806	612	110	74
4	118	102	25	19	137	180	53	59	345	463	45	67
5	54	70	14	16	117	127	44	45	241	315	49	56
6	28	43	12	13	52	83	38	33	157	200	49	45
7	14	25	13	9	37	52	19	24	114	121	27	34
8	11	14	5	7	25	31	15	18	62	71	26	26
9	8	7	4	5	14	18	13	13	27	41	24	19
10	5	4	3	3	12	10	12	9	31	23	12	14
11	2	2	3	2	9	5	11	7	8	13	11	10
12	5	1	2	1	3	3	4	5	8	7	7	7
13	1	1	3	1	2	1	2	3	7	3	7	5
14	0	0	1	1	3	1	0	2	4	2	8	4
15	0	0	0	1	3	1	2	2	5	1	2	2
16	0	0	1	0	1	0	1	1	0	1	1	2
17	1	0	0	0	1	0	0	1	2	0	2	1
18	0	0	0	0	0	0	1	1	2	0	0	1
19	0	0	0	0	0	0	1	1	1	0	2	1
20	0	0	0	0	1	0	2	0	1	0	1	1
$\hat{\alpha}$	9.4044		7.2837		7.8694		4.5265		7.2903		6.1098	
$\hat{\beta}$	2.2969		2.5644		2.2238		1.8104		2.0709		2.2379	
χ^2(13d.f.)	68.57		21.03		251.86		27.53		762.57		38.41	

Both distributions, however, tend to underestimate the observed frequency at the mode.

In addition to the two discrete distributions examined above, two continuous distributions were also considered: the gamma distribution and the log-Normal distribution. The gamma distribution is given by

$$f(x) = \frac{1}{\lambda^{\alpha}\Gamma(\lambda)} x^{\alpha-1} e^{-x/\lambda} \tag{5.14}$$

where α and λ are parameters, and the log-Normal distribution is given by

$$f(x) = \frac{1}{(\sqrt{2\pi})\ \sigma x} \exp\{-(\ln x - \mu)^2/2\sigma^2\} \tag{5.15}$$

where μ and σ are parameters. For the continuous distributions, x is defined for $0 \leq x < \infty$ and the probability that x lies between 0 and 1 is taken to be equivalent to the probability that x = 1 for the discrete distributions. Similarly, $P_r(1 \leq x < 2)$ for the unknown distributions is taken as equivalent to $P_r(x = 2)$ for the discrete distributions, and so on.

The log-Normal distribution has a sharp mode and long tail, and was found to fit the data somewhat better than the gamma distribution, although in both distributions the mode is too far to the left ,i.e., at too low a value of x, the number of TR's per CT. Examples of the fit of the gamma distribution are given in Table 5.22 and in Figure 5.20 and the log-Normal distribution in Table 5.23 and in Figure 5.21.

Of the four distributions examined, the truncated Sichel distribution gave the closest agreement to the observed frequencies of numbers of TR's per CT. The fit of this distribution could be improved by using the three-parameter version instead of fixing the parameter a equal to -1/2, but the mathematical expression for the distribution would be very involved and the estimation of the parameters very awkward.

Table 5.22 Results of Fitting the Gamma Distribution to the Observed Number of TR per CT for the HI and RA Sector Functions

O - Observed frequency

P - Predicted frequency

# of TR/CT	HI O	HI P	RA O	RA P
1	209	463	38	67
2	544	549	77	79
3	608	439	110	74
4	345	299	45	63
5	187	186	49	50
6	152	110	49	39
7	69	62	27	30
8	42	34	26	23
9	29	19	24	17
10	12	10	12	12
11	10	5	11	9
12	5	3	7	6
13	3	1	7	5
14	1	1	8	3
15	1	0	2	2
16	2	0	1	2
17	2	0	2	1
18	0	0	0	1
19	0	0	2	1
20	1	0	1	1
$\hat{\alpha}$	2.3676		1.7965	
$\hat{\lambda}$	1.2852		2.5384	
χ^2 (13d.f.)	311.28		51.07	

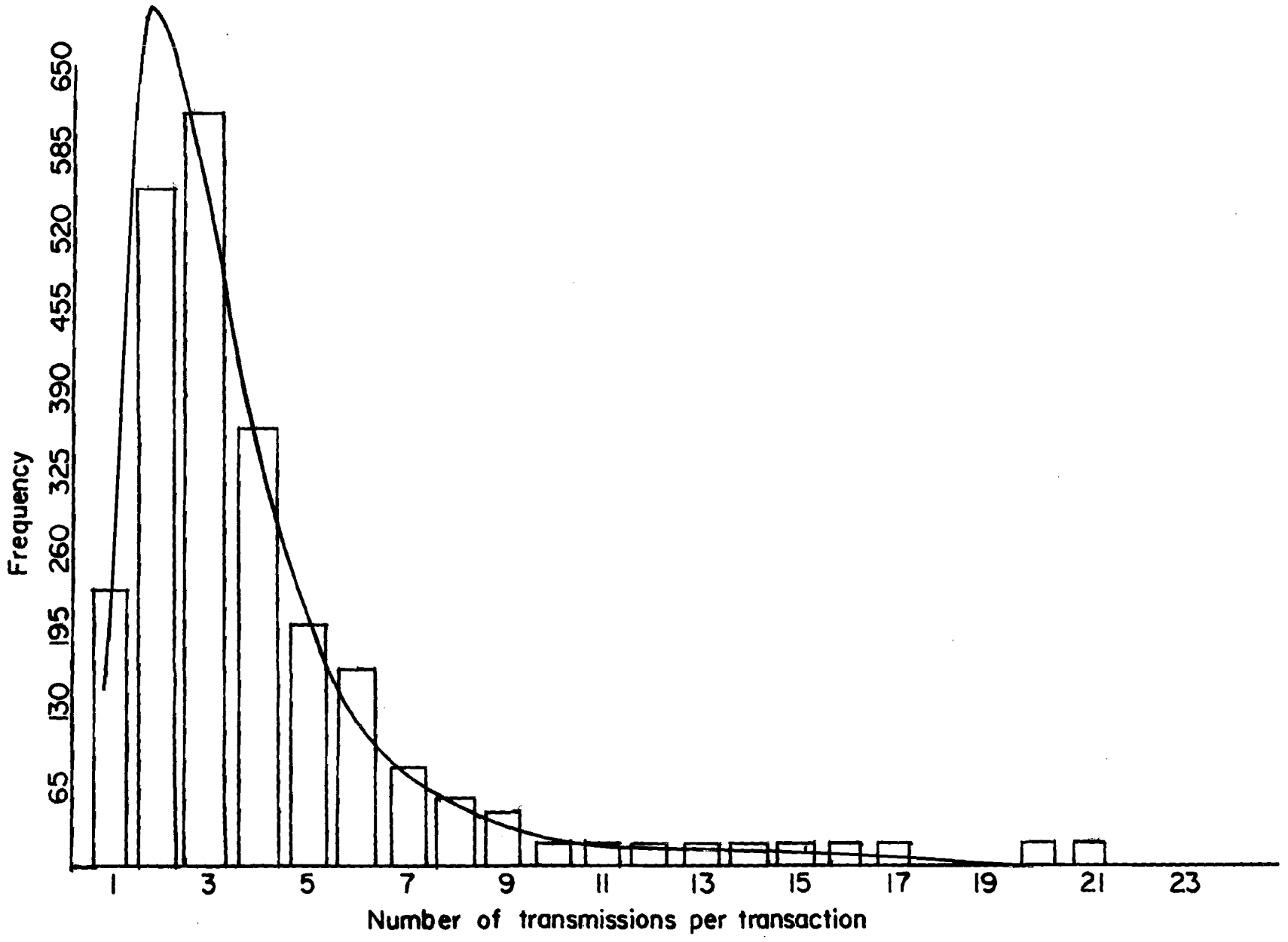

Figure 5.21 Fitting the Lognormal Distribution to the Observed Number of Transmissions per Transactions for Sector Function HI